

**HEAVY FERMIONS
AND
MAGNETIC ORDER.**

**A Thesis presented for the degree
of Doctor of Philosophy
of the University of London
and the Diploma of Imperial College,**

**by
Susan Goodbody.**

ACKNOWLEDGEMENTS.

I wish to thank my supervisor, Professor David Edwards. Without his patience and guidance this work would not have been possible. Also a further thanks goes to Professor Edwards for making it possible for me to spend a year in research institutes abroad.

Thanks to all my friends inside and outside university. In particular Nic, Gillian, Ric and Roma for their support and encouragement and Panaghis for his tormenting and his motorbike. Also Fiona and Tricia for much appreciated help at difficult times, and Susan for forcing me outside college occasionally. A huge amount of gratitude goes to Jan, Tom and Maree who helped in every way possible: listening to endless moans and worries, housing me, feeding me, telling me when to get a haircut... I cannot thank them enough. Thanks again to Jan and Tom for the typing assistance.

Finally Mum Dad and Anne for everything, with a special thankyou to Anne for all the waiting.

To Mum Dad and Anne.

TABLE OF CONTENTS.

<u>ABSTRACT.</u>	7.
<u>LIST OF FIGURES.</u>	9.
<u>1. INTRODUCTION.</u>	12.
1.1. PLAN OF ACTION.	12.
1.2. HISTORY AND DEFINITIONS.	17.
1.2.1. Kondo Impurity.	17.
1.2.2. Kondo Lattice.	19.
1.2.3. The Anderson Hamiltonian.	20.
1.2.4. Intermediate Valence.	21.
1.2.5. The Total Picture.	22.
1.3. EXPERIMENT.	24.
1.3.1. Specific Heat.	24.
1.3.2. Magnetic Susceptibility.	27.
1.3.3. Resistivity.	29.
1.4. THEORIES OF HEAVY FERMIONS.	31.
1.4.1. Quasi Particle Bands and Fermi Liquid Pictures.	32.
1.4.2. Other Techniques.	42.
<u>2. THE ALLOY ANALOGY.</u>	45.
2.1. THE ADVANTAGES AND DISADVANTAGES.	45.
2.2. THE TIME DEPENDENT ALLOY ANALOGY.	47.

2.3. THE PERTURBATION IN U OF HORVATIĆ AND ŽLATICĀ.	54.
2.3.1. The Method.	54.
2.3.2. The Self Energy and Impurity Density of States.	57.
2.4. A TIME DEPENDENT ALLOY ANALOGY.	64.
2.5. DISCUSSION.	67.
<u>3. THE SPIN ONLY CASE.</u>	68.
3.1. INTRODUCTION.	68.
3.2. THE F ELECTRON GREEN FUNCTION.	70.
3.2.1. The Model.	70.
3.2.2. The Ground State.	71.
3.2.3. The f Down Spin Wavefunction.	73.
3.3. RESULTS.	86.
3.3.1. The Effective Kondo Temperature.	86.
3.3.2. The Mass Enhancement.	89.
3.3.3. The Fermi Wavevector.	92.
3.3.4. The f Down Spin Density of States.	93.
3.3.5. Discussion.	96.
3.4. THE EXCHANGE INTERACTION IN HEAVY FERMION SYSTEMS.	99.
3.4.1. Introduction.	99.
3.4.2. A Schrieffer - Wolff Transformation.	100.
3.4.3. The f Electron Green Function.	105.
3.4.4. Properties of the Solution.	113.
3.4.5. Conclusion.	117.
<u>4. THE WEAKLY MAGNETIC PROBLEM.</u>	119.
4.1. INTRODUCTION.	119.
4.2. THE STRONGLY MAGNETIC CASE.	121.
4.2.1. The Variational Calculation.	121.
4.2.2. Results.	128.
4.2.3. The Self Energy Diagrams For The Strongly Magnetic Case.	

	134.
4.3. THE WEAKLY MAGNETIC CASE. _____	141.
4.3.1. The Self Energy Diagrams For The Weakly Magnetic Case. _____	141.
4.3.2. The Magnetisation in a Magnetic Field. _____	149.
4.3.3. Conclusion. _____	159.
<u>5. CRYSTAL FIELDS.</u> _____	160.
5.1. INTRODUCTION. _____	160.
5.2. A GENERAL THEORY. _____	164.
5.2.1. The Hamiltonian. _____	164.
5.2.2. The Hartree Fock Ground State For U Infinite. -	169.
5.2.3. A Variational Wavefunction. _____	173.
5.2.4. The Prototype System $CeSi_x$ _____	177.
5.2.5. The Mass Enhancement. _____	180.
5.2.6. The Hartree Fock Ground State For U Finite. —	182.
5.3. MAGNETIC ANISOTROPY IN THE LARGE CRYSTAL FIELD LIMIT. _____	185.
5.3.1. Symmetry Considerations. _____	185.
5.3.2. A Three Band Hamiltonian. _____	190.
5.3.3. A Self Consistent magnon. _____	194.
5.3.4. Conclusions and Further Work. _____	197.
APPENDIX A. _____	199.
APPENDIX B. _____	205.
APPENDIX C. _____	212.
REFERENCES. _____	221.

ABSTRACT

The heavy fermion (HF) systems such as superconducting CeCu_2Si_2 , magnetic NpBe_{13} and materials with no ordering such as CeAl_3 , are so named because at low temperatures they behave as very heavy Fermi liquids. This low temperature Fermi liquid state is characterised by flat f like quasi particle bands near the Fermi level which give rise to a much enhanced effective mass $m^*/m \cong 200$, enormous zero temperature specific heat γ and low temperature magnetic susceptibility values, and maxima in the resistivity at low temperatures.

In Chapter 1 the unusual low temperature behaviour of, and various theoretical models for, the HFs are discussed. In Chapter 2 an attempt is made to treat the paramagnetic HF impurity cerium systems as an alloy of occupied and unoccupied impurity sites in which the occupation of the impurity site has a time dependence. This time dependent alloy analogy idea proves difficult to implement. However a self energy is obtained which is exact in the atomic limit. This result is an improvement over the self energy of Horvatic' and Zlatic' (1982) which is only exact in the atomic limit for the symmetric case.

The remainder of the thesis is concerned with modelling the build up of HF behaviour in the ferromagnetic cerium systems as well as modelling the HF system CeSi_x . In Chapter 3 the spin degenerate periodic Anderson model is used to model a system with a strongly ferromagnetic ground state. The f electron Green function is calculated via a variational treatment. The numerical calculations of the f density of states, mass enhancement and Fermi wave vector show the build up of HF behaviour and the breakdown of the magnetic state with increasing hybridisation. An effective Kondo temperature is obtained which differs from the Bethe ansatz impurity Kondo temperature by a factor of two in the exponent.

The calculation is repeated including an exchange interaction in order to model systems like CeSi_x , $1.7 < x < 1.83$ in which

exchange and hybridisation compete. For certain magnitudes of the exchange coupling, it is found that the exchange and hybridisation add as an effective exchange interaction in agreement with the result of a Schrieffer-Wolff transformation for the Anderson impurity hamiltonian plus exchange interaction. In general though the hybridisation and exchange interaction affect the system in different ways. It is seen that the exchange interaction, favouring a magnetic ground state, could contribute to the mass enhancement. For $V \rightarrow 0$, the effective Kondo temperature agrees with the Bethe ansatz impurity result.

In Chapter 4, the error in the exponent of the lattice effective Kondo temperature is shown to be a fault of the variational approach via an analogous calculation for the impurity. The fault is identified as the unrealistic assumption that in the magnetic ground state there is no minority f spin occupation. The model is then pushed to the weakly magnetic regime to allow for some small minority f spin occupation and improve the effective Kondo temperature. The dominant self energy diagrams are identified. The calculated magnetisation shows good agreement with Bethe ansatz results. The Kondo temperature is identified and shown to be an improvement over the effective Kondo temperature of the strongly magnetic model.

In Chapter 5 the model is extended to include crystal field and spin orbit effects in order to describe magnetic anisotropy. It is shown that the two band model of a band of Γ_7 doublet states hybridising with a single conduction band in a lattice with inversion symmetry cannot describe magnetic anisotropy, contrary to the results of Thyamballi and Cooper (1985). It is concluded that the magnetic anisotropy arises as a result of the hybridisation between the Γ_7 doublet band and all the conduction bands. The existence of magnetic anisotropy is shown for a three band model of Γ_7 band and two conduction bands.

LIST OF FIGURES.

Figure 1.1. The variation from trivalence to tetravalence with f level energy.

Figure 1.2. The C/T (mJ/molK^2) versus T^2 behaviour for some typical heavy fermion systems.

Figure 1.3. A typical susceptibility versus temperature plot for the heavy fermion systems.

Figure 1.4. A typical resistivity versus temperature plot for the heavy fermion systems.

Figure 3.1. A schematic ground state band picture for the spin degenerate periodic Anderson model in the limit $U \rightarrow \infty$.

Figure 3.2a. A schematic f density of states for the spin degenerate periodic Anderson model in the limit $U \rightarrow \infty$.

Figure 3.2b. A schematic density of states for the Hubbard model.

Figure 3.3. The corrections to the Hartree Fock self energy for the spin degenerate periodic Anderson model.

Figure 3.4. The f down spin resonance energy for the spin degenerate periodic Anderson model.

Figure 3.5. A schematic picture of the f down spin quasi particle bands for the spin degenerate periodic Anderson model.

Figure 3.6. A schematic f density of states for the spin degenerate periodic Anderson model for finite U .

Figure 3.7. The mass enhancement versus hybridisation for $0 < V < 1.0\text{eV}$

Figure 3.8. The mass enhancement versus hybridisation for $0 < V < 1.5\text{eV}$.

Figure 3.9. The Fermi wavevector versus hybridisation for $0 < V < 1.0\text{eV}$.

Figure 3.10. The Fermi wavevector versus hybridisation for $0 < V < 1.5\text{eV}$.

Figure 3.11. The f down spin band density of states for $V = 0.35\text{eV}$.

Figure 3.12. The variation from magnetic to non magnetic ground state in the Rare Earths.

Figure 3.13. The self energy diagrams, other than Hartree Fock, in the down spin f electron self energy of the variational calculation for the spin degenerate periodic Anderson model plus exchange interaction.

Figure 3.14. The diagrams in $\Sigma_{cf\downarrow}(k,E)$ of the variational calculation for the spin degenerate periodic Anderson model plus exchange interaction.

Figure 3.15. The self energy diagrams, other than Hartree Fock, in the down spin conduction electron self energy $\Sigma_{cc\downarrow}(k,E)$ of the variational calculation for the spin degenerate periodic Anderson hamiltonian plus exchange interaction.

Figure 3.16. The f resonance energy for the spin degenerate periodic Anderson model plus exchange interaction.

Figure 3.17. The $\gamma(\text{mJ/molK}^2)$ versus silicon concentration in CeSi_x

Figure 4.1. A schematic impurity f density of states in the U infinite Hartree Fock ground state.

Figure 4.3. The f down spin impurity density of states for $V = 0.75\text{eV}$.

Figure 4.4. A schematic impurity f density of states in the U finite Hartree Fock ground state.

Figure 4.5. $1/4\langle n_{f\downarrow} \rangle$ versus $\ln|\hat{H}|$ for $\Delta = 0.005\text{eV}$.

Figure 4.6. $1/4\langle n_{f\downarrow} \rangle$ versus $\ln|\hat{H}|$ for $\Delta = 0.01\text{eV}$.

Figure 4.7. $1/4\langle n_{f\downarrow} \rangle$ versus $\ln|\hat{H}|$ for $\Delta = 0.04\text{eV}$.

Figure 4.8. $1/4\langle n_{f\downarrow} \rangle$ versus $\ln|\hat{H}|$ for $\Delta = 0.045\text{eV}$.

Figure 4.9. $1/4\langle n_{f\downarrow} \rangle - \ln|\hat{H}|$ versus $|\epsilon_f|\pi/\Delta$ for $\mu_B H = 0.01\text{ eV}$.

Figure 4.10. $1/4\langle n_{f\downarrow} \rangle - \ln|\hat{H}|$ versus $|\epsilon_f|\pi/\Delta$ for $\mu_B H = 0.1\text{ eV}$.

Figure 5.1. The magnetic excitation spectrum in CeSi_x .

Figure 5.2. A schematic ground state band picture for the periodic Anderson model with spin orbit and crystal field effects included.

Figure 5.3. The mass enhancement versus hybridisation.

Figure C.1. Nearest neighbour silicon atoms of a cerium in a model tetragonal lattice.

CHAPTER 1.

INTRODUCTION.

1.1. PLAN OF ACTION.

The subject of the present work is a model for heavy fermion (HF) cerium systems, a problem tackled by many theorists and experimentalists since the discovery of HF CeAl₃ in 1975 and the subject of countless publications. HF systems are metals with either magnetic (NpBe₁₃, UZn₁₂, UCd₁₁ and CeSi_{1.8}), non magnetic (CeAl₃ and CeCu₂), or superconducting (CeCu₂Si₂, UBe₁₃ and UPt₃) ground states in which the interactions of the system result in unusual low temperature behaviour generally accepted as that of a very heavy Fermi liquid. The heavy Fermi liquid state occurs for very low temperatures of order 10⁻³ times the degeneracy temperature of normal metals and is characterised by the temperature dependent Kondo resonance in the f density of states thought to arise from flat quasi particle bands of f character around the Fermi level. The enormous mass enhancement, huge low temperature susceptibility and specific heat which identify the HF systems can all be explained in terms of the temperature dependent Kondo resonance above the Fermi level. The unusual low temperature thermodynamic behaviour of the HFs is discussed in Section 1.3.

In all HF systems, one of the elements of the unit cell is a magnetic rare earth, usually cerium, or an actinide, usually uranium, and has inner shell electrons, 4f for cerium and 5f for uranium. However not all compounds involving magnetic materials with inner shell electrons are HF. Transition metals have inner shell 4d electrons but these electrons are mainly itinerant and therefore are usually non heavy. At the other extreme, gadolinium has highly localised 4f electrons and no f weight at the Fermi level so is also non heavy. The HF along with the closely related intermediate valence (IV) materials lie somewhere between the two,

in that the moment carrying electrons are partially localised and partially itinerant so that neither an itinerant nor localised theory will suffice.

In both the HF and IV systems, the dominant interactions are considered to be the hybridisation of the flat f band (or d band for some IV systems) with the conduction electrons as well as a coulomb repulsion between f electrons on the same site (see Section 1.4 for particular models). In HF systems, the position of the f level is far below the Fermi level and the hybridisation between f and conduction states is small. The interactions in the system result in a very narrow resonance of f character around the Fermi level, mass enhancement and other general Fermi liquid behaviour. Most of the f weight remains around the unhybridised f level position, so that the f electron is only slightly delocalised and the system is almost integral valent. In the intermediate valence system, the unhybridised f level position is much closer to the Fermi level so that in the interacting system the hybridisation reduces the f occupation considerably and the system is said to be intermediate valent. The two types of system are classified according to a schematic f density of states picture in Figure 1.1. The two types of system, HF and IV, are closely related and similar models are used to describe them. The aim of any theory must ultimately be to describe the full range of materials from the itinerant transition metals through the IV and HF systems to gadolinium.

In the bulk of the work of the thesis, the systems described are assumed to have magnetic ground states in contrast to the situation in very heavy cerium systems like CeAl_3 which have non magnetic ground states. The majority of work on HF cerium systems has concentrated on modelling the paramagnetic state of these very heavy systems, as we do in Chapter 2. However any complete model must be able to describe the transition from the very heavy non magnetic to the normal magnetic rare earth system. It seems reasonable therefore to build a model for magnetic cerium systems and study how, or if, it predicts the build up of HF behaviour. The theory, therefore, aims to describe the build up of HF behaviour in normal magnetic cerium compounds as well as modelling the fully fledged magnetic HF, $\text{CeSi}_{1.8}$. The development of a model for the magnetic systems is useful since the standard HF theories are not

able to deal with magnetic order. Most authors concentrate on the non magnetic systems.

The present work includes a model for HF paramagnetic systems in Chapter 2. The model is based on the alloy analogy and attempts to take better account of coulomb correlation site by introducing a time dependence to the f occupation of the impurity site. This time dependent alloy analogy idea proves difficult to implement. However a self energy is obtained which is exact in the atomic limit. This result is an improvement over the self energy of Horvatic' and Zlatic' (1982) which is only exact in the atomic limit for the symmetric case.

In Chapters 3 to 5 the magnetic cerium systems are treated. The starting point is a variational approach for the spin degenerate Anderson model. The treatment predicts that the magnetic state breaks down and the mass enhancement builds up as the hybridisation increases, in accord with the observation that all very HF cerium systems are non magnetic. However the calculated effective Kondo temperature has a factor of two wrong in the exponent. The question of the form of the competition between the R.K.K.Y. interaction and hybridisation in these HF materials is addressed. Why is it that the long range R.K.K.Y. interaction which leads to the magnetic ground states in the transition metals, as well as rare earths themselves is so apparently ineffectual in the HFs. The variational calculation is repeated including an exchange interaction in order to model systems like CeSi_x $1.7 < x < 1.83$ in which exchange and hybridisation compete. For certain magnitudes of the exchange coupling, it is found that the exchange and hybridisation add as an effective exchange interaction in agreement with the result of a Schrieffer-Wolff transformation for the Anderson impurity hamiltonian plus exchange interaction. In general though the hybridisation and exchange interaction affect the system in different ways. It is seen that the exchange interaction, favouring a magnetic ground state, could contribute to the mass enhancement. For $V \rightarrow 0$, the effective Kondo temperature agrees with the Bethe ansatz impurity result.

In Chapter 4, the error in the exponent of the lattice effective Kondo temperature is shown to be a fault of the model via an analogous calculation for the impurity. The fault is identified

as the unrealistic assumption, that in the magnetic ground state there is no minority f spin occupation. The model is then pushed to the weakly magnetic regime to allow for some small minority f spin occupation, as a test case for the extension of the lattice calculation to the weakly ferromagnetic regime. The dominant self energy diagrams are identified. The calculated magnetisation shows good agreement with Bethe ansatz results. The Kondo temperature is identified and shown to be an improvement over the effective Kondo temperature of the strongly magnetic model.

In Chapter 5 the model is extended to include crystal field and spin orbit effects in order to describe magnetic anisotropy. It is shown that the two band model of a band of Γ_7 doublet states hybridising with a single conduction band in a lattice with inversion symmetry cannot describe magnetic anisotropy contrary to the results of Thyamballi and Cooper (1985). It is concluded that the magnetic anisotropy arises as a result of the hybridisation between the Γ_7 doublet band and all the conduction bands. The existence of magnetic anisotropy is shown for a three band model of Γ_7 band and two conduction bands. As an introduction to the HF problem, a general description of the more popular or successful HF theories is presented (see Section 1.4) highlighting their relationship to, and expanding on those which allow most comparison with, the work of the thesis. Before any structured account of the theories can be presented, some of the vocabulary of the HF literature must be defined. Since no theory is needed before experimental discovery, the experimentally determined thermodynamic behaviour typical of HF systems is described. To cover all these areas in a logical manner, the remainder of the introduction is divided into three areas of discussion headed: History and Definitions, Experiment, and Theory.

Within the History and Definition section some popular terms of the literature namely: Kondo impurity, Kondo lattice, Anderson hamiltonian and intermediate valence, are introduced and defined and their role in the HF scenario is described. Under Experiment, the experimentally determined temperature dependence of specific heat, magnetic susceptibility, and resistivity of a few HF systems is reported. Under Theory, some of the better known theories are presented and a general picture unifying these and the results of

the present approach is described. More detailed discussion is reserved for those theories which permit most detailed comparison with the work of the thesis. In particular, we concentrate on those which permit the definition of a criterion for magnetism as they can be compared with the present work on the magnetic cerium systems.

1.2. HISTORY AND DEFINITIONS.

1.2.1. Kondo Impurity.

1975, the year CeAl_3 was identified, is recognised as the birth of the HF problem but in fact much earlier studies of local moments in $\text{La}_{1-x}\text{Ce}_x\text{Al}_2$ for $x < 1$, what is now referred to as a dilute HF system, revealed specific heats per impurity as large as those for concentrated systems. This and other similarities between the thermodynamic properties of the dilute and concentrated systems led to the hope that the concentrated system could be modelled as a lattice of impurities, the interactions between these f electron impurities being negligible. This hope was fuelled by the fact that the impurity problem had been under investigation for some years and to a large extent had been solved. For these studies of the impurity problem the reader is referred to publications such as: Krishnamurthy et al (1980), Andrei et al (1983), Tsvetick and Wiegmann (1983) and references therein.

Dilute magnetic alloys in which the magnetic impurity contains inner shell electrons were originally modelled by the s-d hamiltonian. The hamiltonian models the interaction between the conduction band of s type electrons and the single localised magnetic impurity f or d electron level lying a few electron volts below the Fermi level. The model assumes that the dominant interaction is an exchange interaction between the localised impurity spin, \underline{S} , and the spin of conduction electrons in its vicinity, $\sigma(0)$, so that

$$H_{s-d} = \sum_{k\sigma} \epsilon_k c_{k\sigma}^\dagger c_{k\sigma} - J \underline{S} \cdot \underline{\sigma}(0) . \quad (1.2.1)$$

where $c_{k\sigma}^\dagger$ creates an electron in the free electron state with momentum k and energy ϵ_k . The first term in equation (1.2.1) just describes a band of conduction electrons. In 1964, J. Kondo (Kondo (1964)) used the s-d model to describe magnetic impurity alloys exhibiting both a resistance minimum and evidence of local impurity moment behaviour. Kondo concluded that the concurrence of these

phenomena implied the resistance minimum was due to the interaction of the spins of the localised and conduction electrons and showed that this behaviour could be described using the s-d model of equation (1.2.1) with J negative. The negative J makes it more energetically favourable to align conduction and impurity spins antiparallel in these systems and is the origin of their non magnetic ground state. The description of systems of magnetic impurities in non magnetic metals which exhibit these thermodynamic properties, that is, a resistance minimum and Kondo screening of the moment in the ground state, has become known as the Kondo impurity problem. Also the s-d hamiltonian with J negative is known as the Kondo hamiltonian.

The Kondo problem has been studied by many authors. However the most successful treatments of the model have been made using the Bethe ansatz approach (Tsvetick and Wiegmann (1983), Andrei et al (1983)). The temperature dependence of the susceptibility, magnetisation and specific heat have all been determined. At high temperatures; the thermodynamic quantities behave as though the impurity moment is free and localised. At low temperatures, there is a cross over to a strong coupling or Fermi liquid regime where thermodynamic properties scale with a characteristic temperature T_0 (similar to the Kondo temperature T_K) and which features the famous Kondo, or Abrikosov Suhl, resonance in the f density of states. The characteristic temperature, T_0 , plays the role of a degeneracy temperature where $T_0 \ll T_F$ and T_F is the degeneracy temperature of normal metals. The very narrow Kondo resonance near the Fermi level implies some small delocalisation of the f electrons and consequently the number of f electrons in the interacting system is slightly less than integral. This limit of near integral valence is known as the Kondo limit.

All of the above impurity problem properties: the strong coupling Fermi liquid regime for $T < T_0$, the resistance minimum, $\langle n_f \rangle \cong 1$, where $\langle n_f \rangle$ is the f occupation and the Kondo resonance in the f electron density of states have come to be known as Kondo behaviour. The concentrated systems or HF systems which show similar behaviour are said to be 'Kondoesque'.

1.2.2. Kondo Lattice.

The term Kondo lattice is used to label concentrated f atom systems which exhibit similar thermodynamic behaviour to the dilute or impurity systems. These are the 'Kondoesque' systems mentioned in the previous section. In these concentrated systems a flat band of magnetic impurities lying a few volts below the Fermi level, instead of the single impurity of before, is interacting with the conduction band. For example CeAl_3 is termed a Kondo lattice system because it has a screened moment at low temperatures, a Curie Weiss susceptibility at high temperatures, a low temperature resistance minimum, and Kondo resonance in the f electron density of states near the Fermi level, all of which are similar to recognised impurity properties. There are however differences between the lattice and impurity systems as is evident via the resistance behaviour. The resistance of impurity systems saturates at low temperatures to a finite value, while in the concentrated systems it drops sharply to a very small zero temperature value. The low temperature resistance behaviour of the concentrated systems is attributed to the development of coherence between the f impurity electrons (see Figure 1.4 of Section 1.3).

Throughout the work of the thesis, the terms Kondo lattice and HF are considered as essentially synonymous. However which of the Kondo lattice systems merit the title 'heavy' depends on the individual's definition of 'heavy'. For example, YbCuAl (Mattens et al (1980)) is a Kondo lattice system but with a γ of 135 mJ/molK^2 (see Section 1.3.1) it is light compared to the very heavy systems like CeAl_3 where $\gamma = 1620 \text{ mJ/molK}^2$. Both systems exhibit Kondo like behaviour of thermodynamic quantities, and have a sharp resonance in the f density of states around the Fermi level and so some mass enhancement. In both cases, the large density of states around the Fermi level and the resulting mass enhancement are due to the same mechanism. The description of this mechanism is the root of the HF problem. It seems reasonable therefore to group together all the systems in which the heaviness occurs as the result of Kondo type behaviour instead of splitting them up according to degrees of heaviness. By this reasoning Kondo Lattice implies HF in what follows.

1.2.3. The Anderson Hamiltonian.

In 1961 P.W. Anderson proposed his famous hamiltonian to model a single spin 1/2 magnetic impurity in a metal (Anderson (1961)) :

$$H_{imp}^A = \sum_{k\sigma} \epsilon_k c_{k\sigma}^\dagger c_{k\sigma} + \sum_{\sigma} \epsilon_f f_{\sigma}^\dagger f_{\sigma} + \sum_{k\sigma} (V_{kf} c_{k\sigma}^\dagger f_{\sigma} + \text{h.c.}) + U f_{\uparrow}^\dagger f_{\uparrow} f_{\downarrow}^\dagger f_{\downarrow}, \quad (1.2.2)$$

where $c_{k\sigma}^\dagger$ creates a conduction electron in the free electron state of momentum k and energy ϵ_k and f_{σ}^\dagger creates an f electron with spin σ and energy ϵ_f on the impurity site. Term by term, the hamiltonian includes a single band of conduction electrons, a single spin degenerate f electron impurity level at ϵ_f , hybridisation between conduction electrons and the impurity of a strength V_{fk} and a coulomb repulsion between f electrons on the impurity site.

This Hamiltonian is ideally suited to the description of cerium systems since ionic cerium has one f electron but within any material the f occupation is between one and zero. In its application to cerium, the energy ϵ_f is a many body energy corresponding to an excitation from a $4f^1(5d6s)$ configuration to a $4f^0(5d6s\epsilon)$, where ϵ denotes a state at the Fermi level. In the case of uranium systems, the most likely relevant configurations of the uranium are f^2 and f^3 so that the form of the hamiltonian for uranium is not certain. Anderson developed his hamiltonian to describe magnetic impurity systems in which the impurity has inner shell electrons, that is those also described by the Kondo hamiltonian. In fact, in this the spin 1/2 case, the Anderson impurity hamiltonian transforms under the Schrieffer-Wolff transformation (Schrieffer and Wolff (1966)) to the Kondo hamiltonian of equation (1.2.1) with

$$J = - \frac{2V^2}{|\epsilon_f|}. \quad (1.2.3)$$

The term Anderson hamiltonian has become a group heading for a

number of hamiltonians with the same basic components as those of equation (1.2.2). When the full f electron degeneracy is included, it becomes the orbitally degenerate Anderson impurity hamiltonian. When the f impurity is replaced with a flat band of f electrons, it becomes the periodic Anderson hamiltonian and inclusion of spin orbit coupling and crystal field effects modifies it again. All of these different improvements to the original model are important in different limits.

Like the Kondo hamiltonian the Anderson impurity hamiltonian has been studied extensively. The most renowned techniques and results for the Anderson impurity hamiltonian are: the renormalisation group approach (Krishnamurthy et al (1980)), large N_f (where N_f is the degeneracy of the impurity orbital) approaches (Coleman (1983), Read and Newns (1983)), and the Bethe ansatz method (Tsvelick and Wiegmann (1983) and references therein). These theories predict the observed high temperature local moment behaviour of the HF impurity systems as well as the crossover at low temperature to the strong coupling or Fermi liquid regime. In this low temperature regime, all properties scale with T_k and are said to show Kondo behaviour. The results are in agreement with those for the Kondo Hamiltonian.

Other well known approximate methods of solving the impurity problem which compare well with Bethe ansatz results shall be described later in their generalisation to the lattice case.

1.2.4. Intermediate Valence.

Intermediate valence systems (IV) are generally rare earth systems where the proximity of the f level to the Fermi level results in instability of the valence (Lawrence et al (1981)). In these materials the bonding states $4f^n(5d6s)^m$ and $4f^{n-1}(5d6s)^{m+1}$ are nearly degenerate so that the valence is intermediate between the values of these two configurations. In the HF systems, the f electron level is sufficiently far below the Fermi level to render the system almost integral valent. In the IV systems both configurations are present and charge fluctuations between the two occur on a timescale T_{vf} . Experiments which probe the system on a

timescale less than T_{vf} , see both configurations, and greater than T_{vf} see the intermediate valence. In terms of a schematic density of states picture (see Figure 1.1), the hybridisation of the f band with the conduction band results in incomplete filling of the f resonance and thus intermediate valence.

1.2.5. The Total Picture.

In ordinary rare earth materials, the picture is of highly localised 4f electrons having well defined moments and Curie Weiss susceptibility. The hybridisation with conduction electrons is described by an s-f exchange interaction leading to an indirect R.K.K.Y. interaction between the f's and a magnetic ground state. In HF and IV systems the high temperature behaviour is again that of local moments. However the very important difference between these and the normal rare earth systems is the crossover at low temperatures to the strong coupling or Fermi liquid regime where the f electrons appear to exhibit both a localised and itinerant nature. This behaviour is reflected in the low temperature resistivity, specific heat and magnetic susceptibility (see Figures 1.2 to 1.4). The differences between the HF and IV systems is the near integral valence, Kondo resonance and resulting large mass enhancement of the HF not shown by the IVs. Also the non magnetic ground state of the IV systems is due to the quenching of the Ce^{3+} ion moments by valence fluctuations. However in HF systems like $CeAl_3$ it is thought that direct valence fluctuations cannot be responsible for the non magnetic ground state; rather spin fluctuations arising from *virtual* charge fluctuations are responsible, that is an f hops to the conduction band and then back with a change of spin.

In short HF systems are 4f rare earth or 5f uranium, samarium systems with almost integral valence often called Kondo lattice systems. They have possible magnetic, non magnetic or superconducting ground states. At high temperatures they have the thermodynamic behaviour of normal rare earths but at low temperatures there is a crossover to a strong coupling regime where the behaviour is described as Kondo-like. The low temperature Kondo-like behaviour for $T < T_0$ is similar to the impurity behaviour

with the additional development of coherence manifesting itself in the resistivity behaviour.

Any theory of Heavy Fermion systems must describe the transition from normal rare earth through to the almost integral valent HF systems, the intermediate valence and on to transition metals as the f electron level moves nearer to the Fermi level and the hybridisation takes over from exchange in the R.K.K.Y interaction.

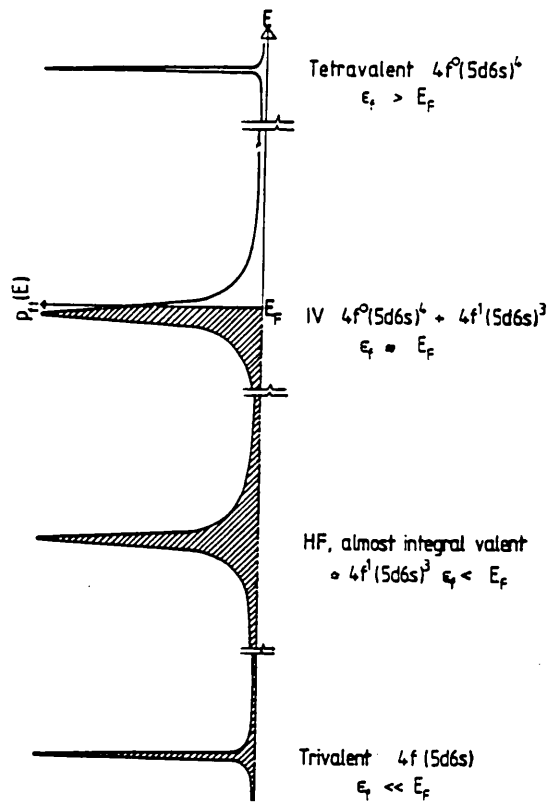


Figure 1.1. The variation from trivalence to tetravalence with f level energy ϵ_f . The hatched areas denote occupied density of states below the Fermi level E_F . The intermediate valence of the materials with $\epsilon_f \approx E_F$ is reflected in the incomplete filling of the f resonance. The near integral valence of the HFs where $\epsilon_f < E_F$ is reflected in an almost completely filled f resonance.

1.3. EXPERIMENT.

1.3.1. Specific Heat.

In a normal metal at temperatures $T < \Theta/50K$, Θ the Debye temperature, the specific heat varies with temperature as:

$$C = \gamma T + \beta T^3, \quad (1.3.1)$$

where $\gamma \propto N(0)(1+\lambda)$, $N(0)$ being the band density of states at the Fermi energy and $(1+\lambda)$ an enhancement factor due to phonons and possibly spin fluctuations. A plot of C/T versus T^2 has a constant gradient of β and a C/T intercept of γ . At low temperatures the specific heat behaviour of a HF system differs significantly from that of a normal metal. For $T < 10K$ the specific heat variation with temperature of HF systems has so far been seen to exhibit three main types of behaviour:

a) As in a normal metal but with a highly temperature dependent γ and enormous $\gamma(T=0)$ values:

$$C = \gamma(T)T + \beta T^3, \quad (1.3.2)$$

where for $T < 10K$, γ increases rapidly with decreasing temperature. The resulting enormous low temperature γ values have been attributed to a highly temperature dependent dressed density of states at the Fermi level (Stewart (1984a)). This type of low temperature, $T < 10K$, behaviour is displayed in the following compounds: superconducting $CeCu_2Si_2$ above the superconducting transition temperature $T_c = 0.6K$ (Steglich et al (1979), Stewart et al (1983)), superconducting UBe_{13} above the superconducting transition temperature $T_c = 0.97K$ (Ott et al (1984b), Stewart et al (1984b)), magnetic $NpBe_{13}$ above the magnetic transition temperature $T_m = 3.4K$ (Stewart et al (1984c)), nonmagnetic $CeAl_3$ (Ott et al (1984c), Berton et al (1977), Benoit et al (1981), Andres et al (1975)) and nonmagnetic $CeCu_6$ (Stewart et al (1984d)).

A plot of C/T versus T^2 (see Figure 1.2) shows very similar behaviour for each of the systems. The specific heats of the

superconducting and magnetic systems do of course have sharp peaks at the transition temperatures, so that for temperatures less than the transition temperatures the C/T behaviour is extrapolated from the behaviour above the transition temperatures. A plot of C versus T for each of the five systems listed shows low temperature peaks, distinct from those due to transitions in the superconducting and magnetic systems, of differing height and widths for each of these systems. Attempts have been made to identify the entropy under these peaks with the $k_B \ln(2S+1)$ per spin associated with the quenching of the moments in the impurity problem. In the lattice case the analogous quantity of entropy would be $R \ln(2S+1)$ (Stewart (1984a)). The peak in the specific heat of superconducting CeCu_2Si_2 around 3.5K (Steglich et al (1979)) corresponds to $R \ln 2$ entropy consistent with 'Kondo-like' behaviour. Less entropy is associated with the peak at 2K for UBe_{13} (Ott et al (1984b)). In CeAl_3 there are small peaks containing much less than $R \ln(2S+1)$ entropy at 0.35K, 2.5K and 6K (Berton et al. (1977)). The peak at 0.35K correlates well with anomalies in other properties. In conclusion, although comparison of C versus T behaviour between the systems shows good qualitative agreement the low temperature details do not compare well and have yet to be explained.

b) As for a normal metal but with an additional $T^3 \ln T$ term and again enormous values of γ :

$$C = \gamma T + \beta T^3 + \delta T^3 \ln T. \quad (1.3.3)$$

The above behaviour is shown by the superconductor UPt_3 above the superconducting transition temperature, $T_c = 0.54\text{K}$, up to 15K with $\gamma = 452 \text{ mJ/molK}^2$ (Stewart et al (1984e)). This behaviour is qualitatively similar to that of the non heavy spin fluctuator UAl_2 (Trainor et al (1975)). Doniach and Engelsberg (1966) and Brinkman and Engelsberg (1968) predicted that long range spin fluctuations would produce such a $T^3 \ln T$ term.

c) Identical at low temperatures, $T < 10\text{K}$, to normal metal behaviour:

$$C = \gamma T + \beta T^3, \quad (1.3.4.)$$

but as in cases a) and b) with unusually large γ values. Behaviour of this type is shown by U_2Zn_{17} above the transition temperature, $T_m = 9.7K$, up to 13K (Ott et al (1984a)), and UCd_{11} above the transition temperature $T_m = 5.0K$ (Fisk et al (1984)). The data for U_2Zn_{17} and UCd_{11} are consistent with $\gamma = 535 \text{ mJ/molK}^2$ and 840 mJ/molK^2 respectively, after extrapolation to zero.

In all three cases a,b and c the low temperature behaviour is dramatically different from that of normal metals consistent with enormous $\gamma(T=0)$ of around $400 \text{ mJ/mol}^\circ K$. When we compare the large $\gamma(0)$ values with the free electron type formula:

$$\gamma(0) = \frac{m^* k_F k_B^2}{\pi^2 \hbar^2 3}, \quad (1.3.5)$$

where m^* is the effective mass, k_F the Fermi wavevector, k_B the Boltzman constant it is seen that the large $\gamma(0)$ values of the HFs can imply large effective masses of order 10^3 for these systems. Also when the specific heat is interpreted in terms of the fraction of electrons in the band that are thermally excited (Lee et al. (1986)) a characteristic bandwidth temperature T_0 of around 10K is deduced. Both the enormous mass and characteristic temperature T_0 which is 10^{-3} of a typical Fermi temperature are consistent with the picture that HF systems are very heavy Fermi liquids at very low temperatures $T < T_0$.

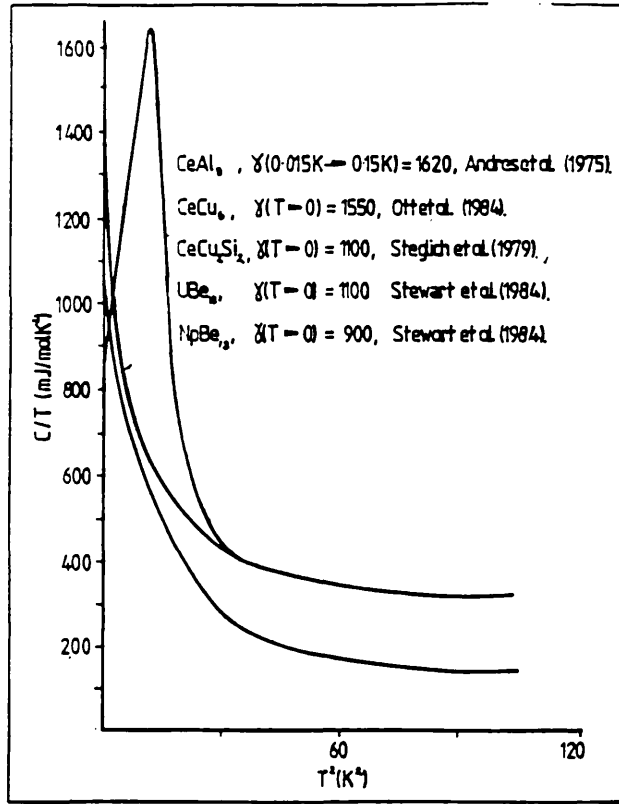


Figure 1.2. The C/T versus T^2 behaviour for some typical HF systems.

1.3.2. Magnetic Susceptibility.

Many studies have been made of the variation with temperature of the magnetic susceptibilities of HF systems such as: CeCuSi₂ (Sales and Viswanathan (1976)), UBe₁₃ (Troc et al (1971), Ott et al (1984b)), NpBe₁₃ (Stewart et al (1984c), U₂Zn₁₇ (Ott et al (1984a)), UCd₁₁ (Fisk et al (1984)), CeAl₃ (Edelstein et al (1974)), CeCu₆ (Stewart et al (1984d)) and UPt₃ (Frings et al. (1983)). The $\chi(T)$ versus T plots for the different systems show many similarities, in particular: a large temperature dependence having Curie Weiss behaviour at high temperature

$$\chi(T) \propto \frac{1}{T+\Theta}, \quad (1.3.6)$$

large effective moments $\mu_{\text{Beff}} > 2\mu_{\text{B}}$ (where $\mu_{\text{Beff}}^2 = g^2 \mu_{\text{B}}^2 J(J+1)$, μ_{B} is the Bohr magneton, J is the total angular momentum of, and g the Lande g -factor of either the free Ce^{3+} ions or U^{3+} or U^{4+} ions), and extremely large low temperature susceptibility $\chi(T)$ often described as enhanced Pauli paramagnetic. In fact for CeCu_2Si_2 $\chi(T=0) = 8 \times 10^{-3} \text{ emu/mol}$ (Sales and Viswanathan (1976)) and UBe_{13} $\chi(T=0) = 13.5 \times 10^{-3} \text{ emu/mol}$ (Troc et al (1971)) are seen to be truly enormous when compared to $\chi(T=0) = 0.5 \times 10^{-3}$ of Pu (Smith and Fisk (1982)) the nearest 5f electron element to being magnetic. The susceptibility behaviour described above is typical of HF systems and is suggestive of local moment behaviour at high temperatures crossing over at low temperatures to Fermi liquid behaviour (see Figure 1.3)

It appears that a typical HF $C(T)$ and $\chi(T)$ have been identified and attempts have been made to establish some correlation between the two. A popular method of examining any correlation is to calculate the Wilson Ratio:

$$R = \frac{\pi^2 k_{\text{B}}^2 \chi(T=0)}{g \mu_{\text{B}}^2 \gamma J(J+1)}, \quad (1.3.7)$$

The calculation of R poses the problem of determining the effective moment μ_{eff} . At high temperatures $\chi(T)$ does not follow the Curie Weiss behaviour expected of simple f^1 or f^2 (+ f^3 for uranium) while at low temperatures some mechanism destroys the Curie Weiss behaviour making it difficult to choose an effective moment. Using an approximate μ_{eff} (Stewart (1984a)) finds R to increase through the systems from superconducting to non magnetic to magnetic. R remains finite throughout indicating that the mechanism which screens the low temperature moment enhances both $\gamma(0)$ and $\chi(0)$.

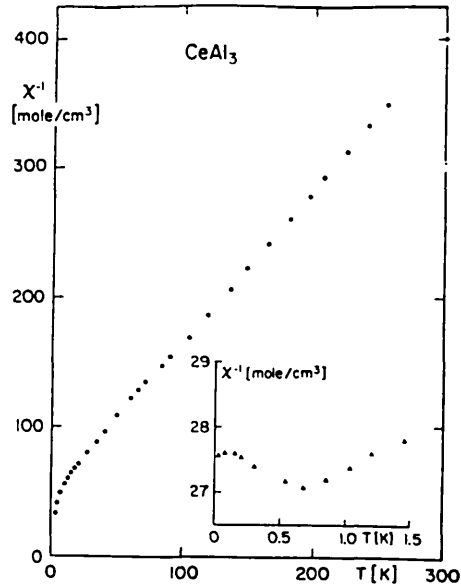


Figure 1.3. A typical inverse susceptibility plot for the HF systems. The data shown is for CeAl_3 (Andres et al (1975)). The insert shows the low temperature behaviour on an expanded scale.

1.3.3. Resistivity.

Studies of resistivity behaviour with temperature have been made for: CeCu_2Si_2 (Stewart et al (1983)), UBe_{13} (Ott et al (1983)), UPt_3 (Stewart et al (1984e)), NpBe_{13} (Stewart et al (1984c)), U_2Zn_{17} (Ott et al (1984a)), UCd_{11} (Fisk et al (1984)), CeAl_3 (Ott et al (1984c)) and CeCu_6 (Stewart et al (1984d)). With the exception of UPt_3 which has normal superconductor $\rho(T)$ behaviour, the HF systems have similar $\rho(T)$ behaviour with a large maximum in $\rho(T)$ at low temperatures, $\rho_{\text{max}}(T) \cong 120\mu\Omega\text{cm}$ to $250\mu\Omega\text{cm}$, and a decrease in $\rho(T)$ at low temperatures due to the development of coherence. In some of these systems for example CeAl_3 (Andres et al (1975)) and CeCu_2Si_2 (Lieke et al (1982)), the expected $\rho(T) \propto AT^2$ low temperature

behaviour of a Fermi liquid has been seen.

In particular the $\rho(T)$ versus T behaviour of CeCu_2Si_2 and UBe_{13} are very similar with peaks at low temperature and shoulders at higher temperatures. The three magnetic systems are again similar with a flat temperature dependence for $T > 100^\circ\text{K}$ and sharp falls below critical temperatures. The resistivities of CeAl_3 , CeCu_8 , show maxima at low temperatures and flat temperature dependence above 100°K . Figure 1.4 shows a typical HF resistivity variation with temperature.

Magnetoresistance measurements for UBe_{13} (Stewart et al (1984b)) show large negative values increasing in magnitude with decreasing temperature and increasing field. The temperature dependence of $\Delta R/R$ is similar to that of C/T and the authors conclude that the same mechanism causes the low temperature $\gamma(T)$ and $\rho(T)$ behaviour.

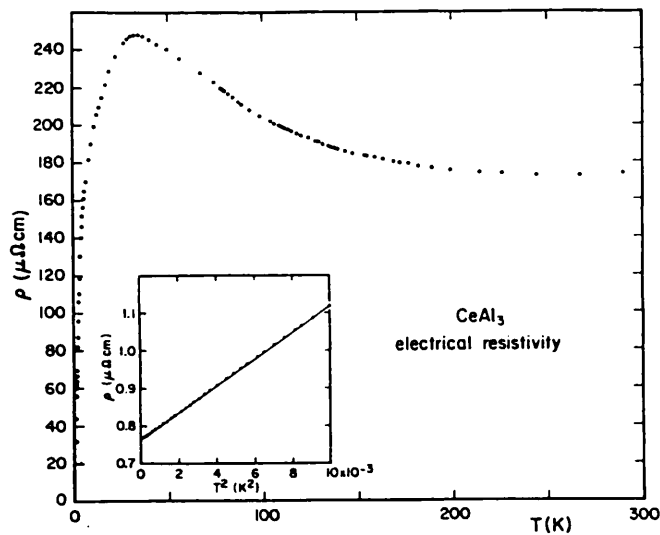


Figure 1.4. A typical resistivity versus temperature plot for the HF systems. The data shown is for CeAl_3 (Ott et al (1984c) and Andres et al (1975)).

1.4. THEORIES OF HEAVY FERMIONS.

Many theories have been proposed to describe HF systems, often based on impurity problem approaches, but so far the lattice problem has remained unsolved. The aim of any theory is to describe the high temperature local moment behaviour as well as the crossover at low temperatures to the strong coupling or Fermi liquid regime. In low temperature regime the thermodynamic behaviour of the lattice is similar to the low temperature behaviour of the impurity. However there is the additional problem in the lattice case of the development of coherence. The coherence manifests itself in the resistivity behaviour.

There are in general two main starting points in any treatment of the problem: either to work with a model hamiltonian, usually the periodic Anderson hamiltonian for cerium systems, or to attempt a self consistent band calculation for each system. The results of the two approaches for cerium compounds can be compared via their prediction for the f electron density of states. The band calculations, despite yielding good Fermi surfaces, predict a narrow f band of width around 1eV with its lower end pinned to the Fermi level. Although the band is narrow it is still far too broad to be the Kondo resonance of the low temperature Fermi liquid. Also the density of states arising from this band at the Fermi level is not in agreement with the results of X.P.S. and B.I.S. experiments which measure f weight at ϵ_f and $\epsilon_f + U$ where ϵ_f is the f level energy. The f weight around these energies as well as the Kondo resonance around the Fermi level can be understood on the basis of the Anderson hamiltonian (Gunnerson and Schönhammer (1983)). The problem of resolving the two approaches remains and is discussed in Section 1.4.1.

In the following section some account is given of a few of the better known attacks on the HF problem, concentrating on those treatments which allow most comparison with the work of the thesis. Most workers have concentrated on the HF cerium systems modelling these by either the periodic Anderson model or a lattice generalisation of the Kondo hamiltonian. From these two starting points several approaches have led to an effective hamiltonian describing a band of non interacting f electrons at renormalised f

level energy hybridising via a renormalised hybridisation with a conduction band. This effective hamiltonian describes quasi particle bands near the Fermi level, much narrower than those of the band calculations, and is consistent with a low temperature Fermi liquid description. All of these approaches are therefore grouped together for discussion in Section 1.4.1 along with a mention of band calculations. Other treatments such as perturbation methods, the alloy analogy and, for the impurity, the large N_f treatment of Gunnarson and Schönhammer are discussed separately. In all cases an attempt is made to point out the successes and weaknesses of each theory as well as the relationship to the present work.

1.4.1. Quasi Particle Bands and Fermi Liquid Pictures.

Throughout the introduction the HF systems have been referred to as Fermi liquids at low temperatures. In Landau Fermi liquid theory a strongly interacting system is viewed as a system of quasi particles having a distribution function equal to that of a non interacting system. The quasi particles are characterised by an effective mass, enhanced over the free electron mass, and an effective interaction parameterised by an infinite set of molecular fields quantified by Landau parameters. At temperatures less than the degeneracy temperature, T_F , a normal metal can be described as a Fermi liquid. It is now generally accepted that HF systems are also Fermi liquids with degeneracy temperature, T_0 , a couple of orders of magnitude smaller than those for ordinary metals that is $T_0 \approx 10\text{K}$ to 100K .

Suppose we choose our model hamiltonian as the periodic Anderson hamiltonian. The hamiltonian is suited to the description of HF cerium systems since ionic Ce^{3+} has one f electron per cerium but in compounds the hybridisation with the conduction band allows the possibility of $\langle n_f \rangle$, the f occupation of a site, less than one. From a general diagrammatic derivation of the f electron Green function for the periodic Anderson model we can show that if the HF are very heavy Fermi liquids then in the ground state they must have quasi particle bands around the Fermi level and therefore a resonance in the density of states near the Fermi level.

The spin degenerate periodic Anderson hamiltonian is written:

$$\begin{aligned}
H_{\text{latt}}^A = & \sum_{\mathbf{k}\sigma} \epsilon_{\mathbf{k}} c_{\mathbf{k}\sigma}^\dagger c_{\mathbf{k}\sigma} + \sum_{\mathbf{k}\sigma} \epsilon_f f_{\mathbf{k}\sigma}^\dagger f_{\mathbf{k}\sigma} + \sum_{\mathbf{k}\sigma} V (c_{\mathbf{k}\sigma}^\dagger f_{\mathbf{k}\sigma} + f_{\mathbf{k}\sigma}^\dagger c_{\mathbf{k}\sigma}) \\
& + \sum_i U f_i^\dagger f_{i\uparrow} f_{i\uparrow}^\dagger f_{i\downarrow}. \quad (1.4.1)
\end{aligned}$$

where $c_{\mathbf{k}\sigma}^\dagger$ and $f_{\mathbf{k}\sigma}^\dagger$ create a conduction electron and an f electron in a state of momentum \mathbf{k} and energy $\epsilon_{\mathbf{k}}$ and ϵ_f , respectively. Term by term the hamiltonian H_{latt}^A includes a conduction band with dispersion $\epsilon_{\mathbf{k}}$, a flat band of f electrons energy ϵ_f , a hybridisation term allowing hopping between conduction electron and f electron states and a strong on site coulomb repulsion between f electrons which makes double occupancy of an f site unfavourable. In the hamiltonian H_{latt}^A the hybridisation, V , is assumed real and momentum independent as usual. Also the orbital angular momentum of the f level is neglected so that N_f , the f level degeneracy is just the spin degeneracy of two. In reality crystal field and spin orbital coupling effects, which are not included here, split the degeneracy of the f level. However in cerium compounds the lowest energy f states in the ground state are a Γ_7 doublet so that treating the f level degeneracy as two is not unreasonable.

If both the coulomb interaction and hybridisation are treated as perturbations then a completely general diagrammatic derivation of the single particle Green function gives:

$$G_{ff\sigma}(k, E) = \frac{1}{E - \epsilon_f - \frac{V^2}{E - \epsilon_{\mathbf{k}}} - \Sigma_{ff\sigma}(k, E)_{\text{ex}}}, \quad (1.4.2)$$

where everything that is unknown about the interactions in the system is stored in the proper self energy $\Sigma_{ff\sigma}(k, E)_{\text{ex}}$. If the HF metals can be described by the periodic Anderson hamiltonian H_{latt}^A , and if they are heavy Fermi liquids at low temperature then they must have a Fermi surface and therefore the imaginary part of the self energy $\Sigma_{ff\sigma}(k, E)_{\text{ex}}$ must be zero at the Fermi energy. Therefore around the Fermi energy the self energy can be expanded in a Taylors expansion about the Fermi energy to give a Dyson equation for the quasi particle energies E . Here the \mathbf{k} dependence of the self energy

near the Fermi energy is neglected in favour of the energy dependence so that:

$$(E - \tilde{\epsilon}_f)(E - \epsilon_k) = \tilde{V}^2, \quad (1.4.3)$$

where

$$\tilde{\epsilon}_f = \frac{\epsilon_f + \Sigma_{ff\sigma}(0)_{ex}}{1 - \Sigma'_{ff\sigma}(0)_{ex}} \quad \text{and} \quad \Sigma'_{ff\sigma}(0)_{ex} = \left. \frac{d\Sigma_{ff\sigma}(E)_{ex}}{dE} \right|_{E=0} \quad (1.4.4)$$

and

$$\tilde{V}^2 = \frac{V^2}{1 - \Sigma'_{ff\sigma}(0)_{ex}}. \quad (1.4.5)$$

Equation (1.4.3) implies that near the Fermi level the quasi particle bands are those of an f level of renormalised energy $\tilde{\epsilon}_f$ hybridising via renormalised hybridisation \tilde{V} with the conduction band. A completely general derivation of this form shows how a self energy which has the correct properties for a Fermi liquid can give rise to quasi particle bands around the Fermi level.

There are several different methods which start from a periodic Anderson hamiltonian and lead to a renormalised non interacting Anderson hamiltonian which for spin degeneracy only has the form:

$$H_{eff} = \sum_{k\sigma} \epsilon_k c_{k\sigma}^\dagger c_{k\sigma} + \sum_{k\sigma} \tilde{\epsilon}_f f_{k\sigma}^\dagger f_{k\sigma} + \sum_{k\sigma} \tilde{V} (c_{k\sigma}^\dagger f_{k\sigma} + f_{k\sigma}^\dagger c_{k\sigma}). \quad (1.4.6)$$

The eigenfunctions of this effective hamiltonian form the quasi particle bands near the Fermi level of equation (1.4.3). The model is therefore consistent with a Fermi liquid picture. The methods which lead to an effective hamiltonian H_{eff} include the Gutzwiller variational approach to the orbitally degenerate periodic Anderson model by Rice and Ueda (1985), the functional integral approach for the lattice generalisation of the Kondo model by Read, Newns and

Doniach (1984), and the slave boson approach of Coleman (1984). The size of mass enhancement predicted by these models and width of the resonance depends on the actual behaviour of the real part of the model self energy around the Fermi level. The corresponding self energy of the band calculation deals with the Fermi surface very well but does not have enough energy dependence to flatten the bands sufficiently for a Kondo type resonance.

a) The Gutzwiller variational method (Gutzwiller (1965)), originally applied to the Hubbard model, is extended by Rice and Ueda (1985) to treat the two band orbitally degenerate Anderson model in the Kondo limit. The method amounts to proposing a variational ground state wavefunction for the system which contains an operator projecting out doubly occupied f electron configurations, and another fixing the number of f electrons. The energy of the ground state is then minimised. The main difficulty of the Anderson or Hubbard hamiltonian, that of taking adequate account of the many body coulomb correlation, is treated here via the projection operator which makes it unfavourable to have many doubly occupied f orbitals in the ground state. The orbitally degenerate Anderson hamiltonian is written:

$$\begin{aligned}
 H^{\text{gut}} = & \sum_{k\sigma} \epsilon_k c_{k\sigma}^\dagger c_{k\sigma} + \sum_{k1\sigma} \epsilon_f f_{k1\sigma}^\dagger f_{k1\sigma} + \sum_{k1\sigma} V_{k1} (c_{k\sigma}^\dagger f_{k1\sigma} + f_{k1\sigma}^\dagger c_{k\sigma}) \\
 & + \frac{U}{2} \sum_{i, 1\sigma \neq 1'\sigma'} n_{i1\sigma} n_{i1'\sigma'} \quad ,
 \end{aligned}
 \tag{1.4.7}$$

where $c_{k\sigma}^\dagger$ creates an electron in conduction state of momentum k spin σ and $f_{k1\sigma}^\dagger$ creates an electron in f state of momentum k and energy ϵ_f which is a bloch sum over sites i of f states with z component of orbital angular momentum l around the site i. The variational wavefunction is written as:

$$|\psi\rangle = P_{nf} P |\psi_0\rangle \tag{1.4.8}$$

where P and P_{nf} are operators which remove double occupancy and fix

the number of f electrons respectively. The operator P is treated by renormalising all hopping processes by a factor $q(n_f, L)$ where $N_f = 2L$ is the degeneracy of the f electron orbital. Since a hopping process involves a factor of V_{k1}^2 then the hybridisation, V_{k1} , is renormalised by $q^{1/2}$. In the U infinite limit, q is given by the ratio of occupation number factors for the correlated and uncorrelated wavefunctions. In the correlated wavefunction an $f_{l\sigma}$ electron can hop onto a site only if there are no f electrons on the site whereas in the uncorrelated wavefunction there need only be no $l\sigma$ electrons on the site. Therefore

$$q = \frac{1 - n_f}{1 - n_{ls}}, \quad (1.4.9)$$

where n_f is the number of f electrons and n_{ls} is the occupation of f electron state with z component of orbital angular momentum l and spin s. The operator P_{nf} which fixes the number of f electrons is treated by introducing a chemical potential μ_σ so that the energy to be minimised is that of the effective hamiltonian:

$$H_{eff}^{gut} = \sum_{k\sigma} \epsilon_k c_k^\dagger c_{k\sigma} + \sum_{k1\sigma} (\epsilon_f - \mu_\sigma) f_{k1\sigma}^\dagger f_{k1\sigma} + \sum_{k1\sigma} \tilde{V}_{k1} (c_{k\sigma}^\dagger f_{k1\sigma} + f_{k1\sigma}^\dagger c_{k\sigma})$$

where $\tilde{V}_{k1} = q^{1/2}(n_f, L)V_{k1}$.

(1.4.10)

It is easily seen that when only spin degeneracy is included, that is $L = 1$, the effective hamiltonian H_{eff}^{gut} is of the form of H_{eff} of equation (1.4.6) and is consistent with the low temperature Fermi liquid picture of quasi particle bands around the Fermi level.

For $L \neq 1$ the authors diagonalise H_{eff}^{gut} by assuming V_{k1} to be a constant. However within this approximation l is not conserved in the hopping processes and only the symmetric combination of orbitals is hybridised and effectively $L = 1$. The authors calculate a characteristic energy which has a form similar to the characteristic energy, the Kondo temperature, of the impurity problem:

$$(1-n_f) \propto e^{-\frac{(2L-1)(\epsilon_{k_F} - \epsilon_f - 1)}{2L^2V^2}}, \quad (1.4.11)$$

where n_f is the number of f electrons and $(\epsilon_{k_F} - \epsilon_f - 1)$ the depth of the bare f level from the Fermi level. For $L = 1$, that is spin degeneracy only, the exponent differs from that of the Bethe ansatz Kondo temperature by a factor of two. However as the degeneracy tends to infinity it agrees with the Kondo temperature of Bethe ansatz results.

The authors also calculate the magnetic susceptibility and find that for $L = 1$ the paramagnetic state is unstable towards magnetic order. Only in the mixed valence regime, that is large hybridisation, or for large degeneracy and not too small hybridisation is their paramagnetic state stable. The criterion for the stability of the paramagnetic state is:

$$2L \geq \frac{(\epsilon_{k_F} - \epsilon_f - 1)}{LV^2} \quad (1.4.12)$$

The result agrees with the criterion for paramagnetism of Read et al (1984) and Coleman (1983) only in the respect that large orbital degeneracy stabilises the paramagnetic state. The result is too crude to be applied to real systems.

The Gutzwiller treatment of the orbitally degenerate periodic Anderson hamiltonian, then, gives quasi particle bands near the Fermi level and a Kondo temperature but a criterion for magnetism which disagrees with that of Read et al (1984) and Coleman (1983) (see (b) and (c) of this section). The Gutzwiller treatment helps clarify the relationship between the HF Fermi liquid description and that of the prototype Fermi liquid ^3He . In the Gutzwiller approach to the periodic U infinite Anderson hamiltonian doubly occupied f configurations are projected out while keeping the f occupation close to one. The model is analogous to the almost localised Fermi liquid model for ^3He of Vollhardt (1984) where there is a small number of doubly occupied and empty sites. When ^3He is studied using Landau theory the observed divergence of the static

susceptibility can support the claim of Stoner theory that the system is near a ferromagnetic transition. However this divergence in the susceptibility can also mean that m^*/m is diverging indicating that the spin carrying systems are becoming localised. By applying the Gutzwiller variational method to ^3He Vollhardt (1984) finds solutions which indicate ^3He is almost localised rather than almost magnetic and that spin fluctuations are important but are a result of approaching localisation. The claim is that the HF's and ^3He are almost localised Fermi liquids. However comparisons between the two systems should be made with care due to the lack of Galilean invariance in the HF's as well as the presence of the heavy electron charge.

b) The functional integral approach of Read et al (1984) to the lattice generalisation of the Kondo model also results in an effective hamiltonian of the form of equation (1.4.6). The starting point is the SU(N) Kondo model (Coqblin and Schrieffer (1969)) extended to the lattice:

$$H_{CS} = \sum_{\mathbf{k}} \varepsilon_{\mathbf{k}} c_{\mathbf{k}}^{\dagger} c_{\mathbf{k}} + \frac{J_0}{N_f} \sum_{i11'} c_{i1}^{\dagger} c_{i1'} f_{i1}^{\dagger} f_{i1'}, \quad (1.4.13)$$

where $c_{\mathbf{k}}^{\dagger}$ creates a conduction electron in a free electron state of momentum \mathbf{k} and $f_{i1}^{\dagger}, c_{i1}^{\dagger}$ creates an f or conduction electron respectively at site i with z component of orbital angular momentum l . The authors neglect the spin of the electrons for simplicity. To find the large N_f limit in the non magnetic regime the properties of the ground state are calculated via the partition function as in the analogous impurity calculation (Read and Newns (1983)). The resultant effective hamiltonian appearing in the partition function definition is a one body hamiltonian. Within the static approximation this effective hamiltonian is, once again, a zero correlation periodic Anderson hamiltonian with renormalised hybridisation and f level energy as in equations (1.4.10) and (1.4.6). The renormalising parameters are determined self consistently to minimise the free energy and fix the number of electrons in the conduction band, as in the Gutzwiller treatment of Rice and Ueda (1985).

In the limit $N_f \rightarrow \infty$ the authors find that the system behaves as a lattice of impurities with intersite effects coming in at order $1/N_f$. For this large N_f they calculate a Kondo temperature equal to that of the impurity case:

$$T_K^{\text{fun}} = D \exp \left[- \frac{1}{\rho_0 J_0} \right], \quad (1.4.14)$$

where ρ_0 is the conduction band density of states and D is the energy difference between the chemical potential and the effective bottom of the band. To determine the stability of the non magnetic Kondo ground state the energy of this ground state is compared with that of a ground state fully magnetised via the R.K.K.Y. interaction. The Kondo ground state is considered stable provided its energy is less than the corresponding magnetic ground state, that is provided

$$\exp \left[- \frac{1}{\rho_0 J_0} \right] > A \frac{(\rho_0 J_0)^2}{N_f^2}, \quad (1.4.15)$$

where A is a constant of proportionality which depends on the band structure and the type of magnetic order. The criterion for non magnetic Kondo ground state of equation (1.4.15) agrees with that derived by Coleman (1983) and shows that for finite N_f the stability of the nonmagnetic ground state is greatest for large J_0 . Also the critical coupling, J_0 , for a non magnetic ground state tends to zero as the degeneracy tends to infinity, in agreement with the result of Rice and Ueda (1985).

Since both exchange and hybridisation can polarise the conduction band then both these interactions contribute to the exchange interaction of equation (1.4.13). In Chapter 3 the competition between these two interactions and their effect on the criterion for magnetism is examined.

c) The slave boson technique is another large N_f treatment of the Anderson hamiltonian in which the end result is an effective one body hamiltonian of the form of equation (1.4.10). The

thermodynamic properties are calculated as a series in $1/N_f$ and then the limit as N_f tends to infinity is taken. The starting point is the orbitally degenerate Anderson hamiltonian in the U infinite limit. In the $U \rightarrow \infty$ limit, double occupancy of any impurity site is strictly forbidden by placing a slave boson on each f site so that the hybridisation term becomes:

$$H_{fc} = \frac{1}{\sqrt{N_f}} \sum_{ikm} V_{im}(k) (c_{imk}^\dagger b_i^\dagger f_{im} + \text{h.c.}), \quad (1.4.16)$$

where c_{imk} creates a conduction electron in a state of energy ϵ_k on a site i with z component of angular momentum m , about this site and f_{im} creates an f electron in a state of energy ϵ_f on site i with z component of angular momentum m , about this site. The mixing term H_{fc} of equation (1.4.16) only includes hybridisation between conduction and f impurity electrons of the same angular momentum, an approximation necessary for the method. The restriction to hybridisation between electrons of the same angular momentum means that intersite effects arising from an f hopping onto the conduction band and back with a change of angular momentum are neglected. This approximation is possibly one of the reasons that the lattice appears to be equivalent to a lattice of impurities to leading order in $1/N_f$.

The next step is to conserve the operator

$$Q_i = b_i^\dagger b_i + n_{fi}. \quad (1.4.17)$$

When Q_i is set equal to one, the conservation of Q_i ensures that n_{fi} , the number of f electrons on site i , is less than one as required. The condition $Q_i = 1$ is implemented in different ways by Coleman (1984) and Read and Newns (1984) for the impurity problem. Coleman calculates the temperature dependence of $\chi(T)$ and $C(T)$ and the f spectral function. He obtains the development of a Kondo resonance with small spectral weight above the Fermi level however the approximations of the method produce spurious results at low temperatures. Read and Newns (1984) impose the condition $Q_i = 1$ by introducing a mean field for the boson and using functional integral techniques. They obtain a finite theory at low temperatures. The

method is equivalent to replacing the operator b of equation (1.4.17) by a constant, b_0 , which renormalises the hybridisation so that $\tilde{V}(k) = b_0 V(K)$. The constraint $Q_j = 1$ is expressed as an integral and in the mean field is evaluated at its saddle point. This brings in a second parameter which plays the role of a lagrange multiplier and shifts ϵ_f to $\tilde{\epsilon}_f$. In the mean field theory it is shown that the limit $N_f \rightarrow \infty$ must be taken firstly maintaining Q/N_f constant, and then setting $Q/N_f = 1/N_f$ at the end of the calculation. When this process is carried out the mean field theory produces finite zero temperature χ and γ as well as the correct exponent in the Kondo temperature.

The mean field approximation has been applied to the lattice by Read and Newns (1984) and results in a renormalised U infinite Anderson hamiltonian with

$$V \rightarrow b_0 V \quad b_0^2 = 1 - n_f \quad \text{and} \quad \epsilon_f \rightarrow \tilde{\epsilon}_f \quad (1.4.18)$$

a result equivalent to large N_f Gutzwiller and functional integral results.

All of the effective hamiltonians resulting from the Gutzwiller method, functional integral techniques and the slave boson approach are equivalent and yield narrow f quasi particle bands near the Fermi level which are consistent with a low temperature Fermi liquid description.

The alternative approach to the use of a model hamiltonian is to attempt a self consistent band calculation for a particular system using the local density approximation. Band calculations have been used successfully to determine the ground state properties of transition metals and give reasonable cross sections, effective masses and band structures. There have been many calculations of this type performed for HF systems. Calculations for CeCuSi_2 (Jarlborg et al (1983)), UBe_{13} (Takegahara et al (1985) and CeSn_3 (Koelling (1982)) give good Fermi surfaces all of which are in good agreement with one another, the main feature being a "wide" ($\cong 1\text{eV}$) f band around ϵ_f . These results do not, however, agree with the results of photo emission or inverse photo emission experiments for cerium compounds which show peaks in the f density of states at ϵ_f and $\epsilon_f + U$ as well as a very narrow resonance (of width $\ll 1\text{eV}$)

around the Fermi energy. These density of states features at ϵ_f and $\epsilon_f + U$ are built into the Anderson model and their absence in the band calculation results is attributed to the linear density approximation not accounting well enough for the strong f electron correlation, a prominent feature of the Anderson model. It would be comforting if the differences between these results could be resolved allowing the band calculations to take their proper place as a basis for many body calculations.

1.4.2. Other Techniques.

There are many other techniques used to tackle the Anderson hamiltonian. However we choose to discuss only the perturbation in U treatment developed by Yoshida and Yamada and the application of this method by Horvatic' and Zlatic', as well as the alloy analogy approach and the variational method of Gunnarson and Schönhammer. The alloy analogy and perturbation in U treatments are discussed in Chapter 2 in the context of the work of the thesis. The method of Gunnarson and Schönhammer is used to treat the impurity Anderson model for dilute cerium systems but a short description of the method is included here because of its success in fitting XPS and BIS measurements of concentrated systems.

The method of Gunnarson and Schönhammer relies on the degeneracy of the impurity orbital N_f being large and gives exact results in the limit N_f infinite. However even for N_f as small as six the results are in very good agreement with the $N_f \rightarrow \infty$ results. The Anderson impurity hamiltonian is written with angular momentum as a good quantum number. Here the problem of generalising to the lattice hamiltonian is the same as for the slave boson technique, that is, only hybridiation between conduction and impurity states of the same z component of angular momentum can be included.

$$H_{GS} = \sum_{\nu=1}^{N_f} \left[\int \epsilon \psi_{\epsilon\nu}^\dagger \psi_{\epsilon\nu} d\epsilon + \epsilon_f \psi_{\nu}^\dagger \psi_{\nu} + \int (V(\epsilon) \psi_{\nu}^\dagger \psi_{\epsilon\nu} + \text{h.c.}) d\epsilon + U \sum_{\nu < \mu} n_{\nu} n_{\mu} \right], \quad (1.4.19)$$

with

$$\sum_{\mathbf{k}} V_{\mathbf{k}m}^* V_{\mathbf{k}m'} \delta(\varepsilon - \varepsilon_{\mathbf{k}}) = \sum_{\mathbf{k}} |V_{\mathbf{k}}|^2 \delta(\varepsilon - \varepsilon_{\mathbf{k}}) \delta_{mm'} \equiv |V(\varepsilon)|^2 \delta_{mm'} , \quad (1.4.20)$$

where $\psi_{\varepsilon\nu}^\dagger$ creates an electron in a state of energy ε and angular momentum ν , about the impurity site, and ψ_ν^\dagger creates an f electron with energy ε_f and angular momentum ν . Here $\nu = (m, \sigma)$ is the combined index for orbital and spin degeneracies since these degeneracies are equivalent when the model assumption of equation (1.4.20) is made.

To compare with BIS results the single particle f electron Green function for $E > 0$, defined as:

$$g^>(z) = \langle \phi_0 | \psi_\nu \frac{1}{z + E_0(N) - H} \psi_\nu^\dagger | \phi_0 \rangle , \quad (1.4.21)$$

is calculated. Here $|\phi_0\rangle$ and $E_0(0)$ are the exact ground state and ground state energy of the system respectively. The authors calculate this ground state, ground state energy and Green function via an approximation which is exact in the N_f infinite limit. By acting on the vacuum repeatedly with H_{GS} new states are formed. The ground state is chosen as a linear combination of those which have a non zero coupling to the ground state in the limit N_f infinite. The N_f infinite limit is taken so that $N_f V$ remains finite. In this way the variationally determined ground state is ensured of being an eigenstate at least for $N_f \rightarrow \infty$. To calculate the Green function of equation (1.4.21) a complete set of basis states is inserted on either side of the operator so that

$$g^>(z) = \sum_{ij} \langle \phi_0^1 | \psi_\nu | i \rangle \langle i | \frac{1}{z + E_0^1(N) - H} | j \rangle \langle j | \psi_\nu^\dagger | \phi_0^1 \rangle , \quad (1.4.22)$$

where $|\phi_0^1\rangle$ and $E_0^1(N)$ are the approximate ground state and ground state energies calculated in the N_f infinite limit. Normally a very large basis set $\{|i\rangle\}$ is required to evaluate $g^>(z)$ but in the N_f infinite limit the basis set is small. This basis set is determined by repeatedly acting on $\psi_\nu^\dagger |\phi_0^1\rangle$ with H_{GS} to form new basis states

and then keeping only those which have a non vanishing coupling to $\psi_U^\dagger |\phi_o^1\rangle$ in the N_f infinite limit. In this first order calculation, the problem reduces to the inversion of a simple matrix. However in more accurate calculations where wavefunctions coupling with $O(1/N_f)$ are included in the basis set the inversion must be done numerically.

The authors have calculated f electron density of states showing peaks around ϵ_f and $\epsilon_f + U$ as well as a narrow Kondo resonance which are in very good agreement with experiment. They are also able to calculate XPS core spectrum and found that $\langle n_f \rangle > 0.7$ and $\Delta \cong 0.1\text{eV}$ for cerium systems such as CeNi_2 and CePd_3 .

CHAPTER 2.

THE ALLOY ANALOGY.

2.1. THE ADVANTAGES AND DISADVANTAGES.

The alloy analogy (AA) treatment of the the Anderson hamiltonian is generally used as a model for the IV systems. However the basic AA idea can equally well be applied to the almost integral valent HF cerium systems. The system is treated as an alloy of $4f^1$ and $4f^0$ ions. Each site is either occupied by one or zero f electrons in analogy with an AB alloy which has either an A or B atom on each site. Consider an up spin f electron in the system. It sees an atomic potential of ϵ_f , where ϵ_f is the f level energy, at site i if this site is empty or $\epsilon_f + U$ if the site is occupied by a down spin f . Within the AA approximation the up spin f electron is described as moving in a *static* random potential taking values of ϵ_f with probability $(1 - \langle n_{f\downarrow} \rangle)$ and $\epsilon_f + U$ with probability $\langle n_{f\downarrow} \rangle$.

The AA approximation has several advantages and disadvantages. It is exact in both trivially soluble atomic, $V = 0$, and zero coulomb correlation limits. Also it has been applied to the periodic Anderson hamiltonian as a model for IV systems and the resulting magnetic susceptibility and specific heat are in very good agreement with experiment (Leder and Czychołł (1979), Seki (1980), Czychołł (1982), Czychołł and Leder (1981), (1982)). The AA therefore seems to be a good starting point for a model of the almost integral valent HF systems in which the hybridisation is known to be small. Unfortunately the AA cannot describe a Fermi liquid, there is no Fermi surface. Also its treatment of the coulomb correlation is not sophisticated enough to allow the description of the many body Kondo resonance of the HF systems. The lack of a Fermi surface in the AA treatment is a problem for both the IV and HF systems. However the correct treatment of the coulomb

correlation is more important in the HF systems since the many body Kondo resonance is the origin of all the strange HF low temperature behaviour. In the IV materials the Kondo resonance, and hence its effect, is swamped by the resonance at ϵ_f (see Figure 1.1).

The treatment of the coulomb correlation is lacking in the AA because the model does not account for the fact that the 'type of atom' is not fixed for all time as in a genuine alloy, but can in fact change with time as an f hops off into the conduction band. In the following section an attempt is made to deal with this failing via a time dependent AA (TDAA). Within the new TDAA the f electron spins are not frozen. The f electron occupation of any site has a time dependence and the static approximation of the AA is lifted. With the introduction of this time dependence it is proposed that the coulomb correlation can be more adequately treated.

2.2. THE TIME DEPENDENT ALLOY ANALOGY.

In this section a prescription for a TDAA is discussed. The treatment is applied here to the Anderson impurity hamiltonian and results in a modification of the straightforward AA self energy. The ideas can equally well be applied for a treatment of the periodic Anderson model where an analogous self energy is found when the single site approximation is made. The original aim of the present calculation was to determine the form of the modified self energy for the impurity and study its success via comparisons with the exact Bethe ansatz impurity results. If the comparison was good, the analogous self energy of the lattice case could then be calculated with a certain amount of conviction. In the present chapter a TDAA impurity self energy is found which has the attractive feature of the exact atomic limit. This self energy is the origin of a sharp resonance near the Fermi level in the f electron density of states and reduces to the result of Horvatic' and Zlatic' for the symmetric Anderson model. Unfortunately the derivation of this self energy is not rigorous, so that we resolve simply to highlight its advantages of over the perturbation theory result of Horvatic' and Zlatic'(1980) (1982).

The spin degenerate Anderson impurity hamiltonian is written:

$$H_{\text{imp}}^A = \sum_{k\sigma} \epsilon_k c_{k\sigma}^\dagger c_{k\sigma} + \sum_{\sigma} \epsilon_f f_{\sigma}^\dagger f_{\sigma} + \sum_{k\sigma} (V_k c_{k\sigma}^\dagger f_{\sigma} + \text{h.c.}) + U f_{\uparrow}^\dagger f_{\uparrow} f_{\downarrow}^\dagger f_{\downarrow} \quad (2.2.1)$$

where $c_{k\sigma}^\dagger$ creates a conduction electron in a state of energy ϵ_k , momentum k , and spin σ and f_{σ}^\dagger creates an f electron in a state of energy ϵ_f and spin σ on the impurity site. In the following the hybridisation is assumed to be real and independent of momentum. In this chapter the discussion concentrates on the proper f electron retarded self energy $\Sigma_{ff\sigma}(E)$ which is defined in the Dyson equation:

$$G_{ff\sigma}(E) = G_{ff\sigma}^{\circ}(E) + G_{ff\sigma}^{\circ}(E) \Sigma_{ff\sigma}(E) G_{ff\sigma}(E), \quad (2.2.2)$$

where $G_{ff\sigma}(E)$ is the f_{σ} electron propagator and $G_{ff\sigma}^{\circ}(E)$ is the unperturbed f_{σ} electron propagator when the unperturbed hamiltonian

is the zero correlation hamiltonian. From equation of motion methods

$$G_{ff\sigma}^{\circ}(E) = \frac{1}{E - \varepsilon_f - \Lambda(E) + i\Delta(E)}, \quad (2.2.3)$$

where

$$\Lambda(E) - i\Delta(E) = \sum_k \frac{V^2}{(E - \varepsilon_k)}. \quad (2.2.4)$$

In the following, a constant unperturbed conduction band density of states is assumed so that $\Delta(E)$ is independent of E . Also the contribution of Λ is neglected since this just produces a small shift in the f resonance position.

From equation of motion methods the retarded f_{σ} electron Green function can be written:

$$G_{ff\sigma}(t) = G_{ff\sigma}^{\circ}(t) + U \int_{-\infty}^{\infty} dt' G_{ff\sigma}^{\circ}(t-t') \langle f_{\sigma}(t') n_{f-\sigma}(t') : f_{\sigma}^{\dagger} \rangle, \quad (2.2.5)$$

where $n_{f-\sigma}(t') = f_{-\sigma}^{\dagger}(t') f_{-\sigma}(t')$. Within the straightforward time independent AA of Section 2.1 this equation is decoupled as:

$$\langle f_{\sigma}(t') n_{f-\sigma}(t') : f_{\sigma}^{\dagger} \rangle = N_{f-\sigma} \langle f_{\sigma}(t') : f_{\sigma}^{\dagger} \rangle, \quad (2.2.6)$$

so that

$$G_{ff\sigma}^{\wedge\wedge}(t) = G_{ff\sigma}^{\circ}(t) + U N_{f-\sigma} \int_{-\infty}^{\infty} dt' G_{ff\sigma}^{\circ}(t-t') G_{ff\sigma}^{\wedge\wedge}(t'), \quad (2.2.7)$$

where $N_{f-\sigma} = 1$ or 0 with probabilities $(1 - \langle n_{f-\sigma} \rangle)$ and $\langle n_{f-\sigma} \rangle$ respectively. Within the new TDAA, equation (2.2.5) is decoupled so as to retain the time dependence of the $f_{-\sigma}$ occupation using:

$$\langle f_{\sigma}(t') n_{f-\sigma}(t') : f_{\sigma}^{\dagger} \rangle = V_{-\sigma}(t') \langle f_{\sigma}(t') : f_{\sigma}^{\dagger} \rangle, \quad (2.2.8)$$

so that

$$G_{ff\sigma}^{TDAA}(t) = G_{ff\sigma}^{\circ}(t) + \int_{-\infty}^{\infty} dt' V_{-\sigma}(t') G_{ff\sigma}^{\circ}(t-t') G_{ff\sigma}^{TDAA}(t'), \quad (2.2.9)$$

with

$$V_{-\sigma}(t') = UN_{f-\sigma}(t'), \quad (2.2.10)$$

where now $N_{f-\sigma}(t') = 0$ or 1 at time t' . The $f_{-\sigma}$ Green function of the TDAA (equation (2.2.9)) is then expanded as:

$$\begin{aligned} G_{ff\sigma}^{TDAA}(t) = & G_{ff\sigma}^{\circ}(t) + \int_{-\infty}^{\infty} dt_1 G_{ff\sigma}^{\circ}(t-t_1) V_{-\sigma}(t_1) G_{ff\sigma}^{\circ}(t_1) \\ & + \int_{-\infty}^{\infty} dt_1 \int_{-\infty}^{\infty} dt_2 G_{ff\sigma}^{\circ}(t-t_1) V_{-\sigma}(t_1) G_{ff\sigma}^{\circ}(t_1-t_2) V_{-\sigma}(t_2) G_{ff\sigma}^{\circ}(t_2) \dots \end{aligned} \quad (2.2.11)$$

In order to evaluate equation (2.2.11) we write

$$\begin{aligned} V_{-\sigma}(t_1) V_{-\sigma}(t_2) V_{-\sigma}(t_3) \dots V_{-\sigma}(t_n) = \\ U^n \langle n_{f-\sigma} \rangle P_{-\sigma}(t_2, t_1) P_{-\sigma}(t_3, t_2) \dots P_{-\sigma}(t_n, t_{n-1}), \end{aligned} \quad (2.2.12)$$

where $P_{-\sigma}(t_n, t_{n-1})$ is the probability that if $N_{f-\sigma}(t)$ is unity at time t (that is the impurity site is occupied by an $f_{-\sigma}$ at time t) where t is the earlier of times t_n and t_{n-1} , then it is still unity at the later of times t_n and t_{n-1} . In the straightforward AA, this probability has no time dependence and is equal to unity for all time. In the TDAA, the static approximation is lifted and this probability can deviate from unity as time evolves. In the HF systems, which we hope to model, the hybridisation between conduction and f electron states is small, so that the likelihood of an f hopping off the impurity site is also small. Therefore we

expect that in the HF systems the probability $P_{-\sigma}(t_n, t_{n-1})$ is close to unity for all time. The function $P_{-\sigma}(t_n, t_{n-1})$ must reflect the behaviour of the $f_{-\sigma}$ occupation of the impurity site and is identified with the charge density function:

$$P_{-\sigma}(t_n, t_{n-1}) = \frac{\langle T[n_{f-\sigma}(t_n) n_{f-\sigma}(t_{n-1})] \rangle - \langle n_{f-\sigma} \rangle^2}{\langle n_{f-\sigma} \rangle (1 - \langle n_{f-\sigma} \rangle)}, \quad (2.2.13)$$

which has the property that


$$P_{-\sigma}(t_n, t_n) = 1, \quad (2.2.14)$$

as it must, and which ensures that the TDAA reduces to the AA when the time dependence of $P_{-\sigma}(t_n, t_{n-1})$ is lifted. Also

$$\langle T[n_{f-\sigma}(t_n) n_{f-\sigma}(t_{n-1})] \rangle - \langle n_{f-\sigma} \rangle^2 = -i \chi_{-\sigma}(t_n - t_{n-1}) \quad (2.2.15)$$

where

$$\chi_{-\sigma}(t_n - t_{n-1}) = \text{Diagram} \quad , \quad (2.2.16)$$

where the full lines represent the $f_{-\sigma}$ propagators and  represents all the interactions between these $f_{-\sigma}$ electrons. Hence

$$P_{-\sigma}(t_n, t_{n-1}) = -i \frac{\chi_{-\sigma}(t_n - t_{n-1})}{\langle n_{f-\sigma} \rangle (1 - \langle n_{f-\sigma} \rangle)}. \quad (2.2.17)$$

Now when we substitute equation (2.2.12) into equation (2.2.11) then

*

From here on we choose to work with an approximation to the self energy of equation (2.2.22) which arises when we convolute the unperturbed Green function, $G_{ff\sigma}^0(E)$, in the denominator of equation (2.2.22) to give $\tilde{G}_{ff\sigma}^0(E)$. The time dependent alloy analogy therefore becomes:

$$\Sigma_{ff\sigma}^{\text{T D A A}}(E) = \frac{U\langle n_{f-\sigma} \rangle}{1 - U\tilde{G}_{ff\sigma}^0(E)(1 - U\langle n_{f-\sigma} \rangle)} . \quad (2.2.23b)$$

This self energy is exact to second order and is also in agreement with the second order self energy of Horvatic' and Zlatic' in the symmetric case (see sections 2.3 and 2.4).

$$\begin{aligned}
G_{ff\sigma}^{TDAA}(t) &= G_{ff\sigma}^{\circ}(t) + U\langle n_{f-\sigma} \rangle \int_{-\infty}^{\infty} dt_1 G_{ff\sigma}^{\circ}(t-t_1) G_{ff\sigma}^{\circ}(t_1) \\
&+ U\langle n_{f-\sigma} \rangle \int_{-\infty}^{\infty} dt_1 \int_{-\infty}^{\infty} dt_2 G_{ff\sigma}^{\circ}(t-t_1) \tilde{G}_{ff\sigma}^{\circ}(t_1-t_2) G_{ff\sigma}^{\circ}(t_2) \dots
\end{aligned} \tag{2.2.18}$$

where

$$\tilde{G}_{ff\sigma}^{\circ}(t_{n-1} - t_n) = G_{ff\sigma}^{\circ}(t_{n-1} - t_n) P_{-\sigma}(t_n, t_{n-1}). \tag{2.2.19}$$

When we take the Fourier transform of equation (2.2.18) we find:

$$\begin{aligned}
G_{ff\sigma}^{TDAA}(E) &= G_{ff\sigma}^{\circ}(E) + U\langle n_{f-\sigma} \rangle G_{ff\sigma}^{\circ}(E) G_{ff\sigma}^{\circ}(E) \\
&+ U\langle n_{f-\sigma} \rangle G_{ff\sigma}^{\circ}(E) \tilde{G}_{ff\sigma}^{\circ}(E) G_{ff\sigma}^{\circ}(E) \dots,
\end{aligned} \tag{2.2.20}$$

or, after summing the series in equation (2.2.20),

$$G_{ff\sigma}^{TDAA}(E) = G_{ff\sigma}^{\circ}(E) + U\langle n_{f-\sigma} \rangle G_{ff\sigma}^{\circ}(E) \frac{1}{1 - U \tilde{G}_{ff\sigma}^{\circ}(E)} G_{ff\sigma}^{\circ}(E), \tag{2.2.21}$$

Equation (2.2.21) is a T matrix equation for the TDAA f_{σ} electron Green function. The corresponding self energy is:

$$\Sigma_{ff\sigma}^{TDAA}(E) = \frac{U\langle n_{f-\sigma} \rangle}{1 - U \tilde{G}_{ff\sigma}^{\circ}(E) + U G_{ff\sigma}^{\circ}(E) \langle n_{f-\sigma} \rangle}, \tag{2.2.22}$$

where, after substituting equation (2.2.17) into (2.2.19) and taking the Fourier transform we find:

$$\tilde{G}_{ff\sigma}^{\circ}(E) = \frac{1}{2\pi i} \int dE' G_{ff\sigma}^{\circ}(E') \frac{\chi_{-\sigma}(E - E')}{\langle n_{f-\sigma} \rangle (1 - \langle n_{f-\sigma} \rangle)}. \tag{2.2.23}$$

*

This TDAA result reduces to the straightforward AA result when

either the time dependence is neglected, or the hybridisation is zero, since in each of these cases

$$P_{-\sigma}(t_n, t_{n-1}) = 1, \quad (2.2.24)$$

and hence

$$\tilde{G}_{ff\sigma}^0(E) = G_{ff\sigma}^0(E), \quad (2.2.25)$$

so that

$$\Sigma_{ff\sigma}^{TDAA}(E) = \Sigma_{ff\sigma}^{AA}(E) = \frac{U \langle n_{f-\sigma} \rangle}{1 - U G_{ff\sigma}^0(E) (1 - \langle n_{f-\sigma} \rangle)}. \quad (2.2.26)$$

The f electron Green function therefore reduces to its AA expression:

$$G_{ff\sigma}^{AA}(E) = \frac{(1 - \langle n_{f-\sigma} \rangle)}{(E - \epsilon_f + i\Delta)} + \frac{\langle n_{f-\sigma} \rangle}{(E - \epsilon_f - U + i\Delta)}. \quad (2.2.27)$$

This reduction to the straightforward AA expression for $V \rightarrow 0$ ensures that the TDAA like the AA is exact in the atomic limit.

The form of the convoluting charge susceptibility $\chi_{-\sigma}(E - E')$ in equation (2.2.23) remains a problem. If we suppose that for small hybridisation the addition of time dependence just produces a small fluctuation in $P_{-\sigma}(t_n, t_{n-1})$, then the corresponding charge susceptibility $\chi_{-\sigma}(E)$ has poles at the Fermi energy and at small energies on either side of the Fermi energy. These poles at small finite energies are difficult to identify with any real excitation and lead to sharp resonances in the f_{σ} electron density of states just above and just below the Fermi level. This unrealistic result arises because the decoupling described in equation (2.2.12) is only good if the times t_n to t_1 are already time ordered, that is $t_n > t_{n-1} > \dots > t_2 > t_1$. However this is not in fact the case.

The decoupling described and hence the self energy of equation (2.2.22) are suspect. However the idea that the time dependence can be introduced by convoluting some Green function with a charge susceptibility seems reasonable. In order to find a better

prescription for a TDAA, we compare the straightforward AA self energy with that of Horvatic' and Zlatic' (Horvatic' and Zlatic' (1980), (1982)). These authors treat the Anderson impurity hamiltonian for general asymmetry using the perturbation in U techniques of Yosida and Yamada (Yosida and Yamada (1970), (1975), Yamada (1975a), (1975b) Yamada (1976)). The origin of the success of the second order self energy of Horvatic' and Zlatic' is identified as due to the fact that, for the symmetric case, it is exact in the atomic limit for any correlation. A modification of the straightforward AA is proposed which retains the exact atomic limit not only for the symmetric case of Horvatic' and Zlatic' but for any asymmetry.

2.3. THE PERTURBATION IN U OF HORVATIC AND ZLATIC.

2.3.1. The Method.

The perturbation in coulomb correlation energy approach was first developed to treat the symmetric Anderson impurity hamiltonian where the virtual bound state accommodates one half of the impurity electron of each spin (Yosida and Yamada (1970)). In fact it relies on the presence of electron hole symmetry for the expansions in U to be tractable. In their series of papers Yosida and Yamada concentrate on the symmetric Anderson impurity model and choose the unperturbed hamiltonian as the zero correlation hamiltonian. For this starting point, the expansions in $u = U/\pi\Delta$, where Δ is the half width of the virtual bound state, are good for small correlation, that is $u < 1$. The reader is referred to Yosida and Yamada (1970) for details of the expansions. The essential point about the expansion around the zero correlation result is that the odd order terms vanish because the unperturbed f electron Green functions have the property $G_{ff}^{\circ}(\tau) = -G_{ff}^{\circ}(-\tau)$. The even order terms are given as imaginary time integrals of determinants built from the impurity electron Green functions, $G_{ff}^{\circ}(\tau)$, of the unperturbed hamiltonian.

The perturbation expansions, in $u = U/\pi\Delta$, for the macroscopic quantities are found to be rapidly convergent up to $u = 4$. The magnetic susceptibility, specific heat, entropy and resistivity are calculated to fourth order in u (Yamada (1975a) and Yamada (1976)). The results are consistent with those of Krishnamurthy et al (1975). Also the perturbation terms are calculated for general order (Yosida and Yamada (1975)) to investigate the relations between the specific heat, susceptibility and scattering t matrix. The results are consistent with the phenomenological Fermi liquid theory of Nozières (Nozières (1974)).

The same authors also formulate the perturbation expansion in terms of deviations from Hartree Fock for general asymmetry in order to treat the strong correlation regime (Yosida and Yamada (1970)). However without the electron hole symmetry the odd order terms do not vanish and the expansions become extremely complicated. The authors calculate the second order deviation from the Hartree Fock ground state and find it to be of order Δ/U . However they concede

that this does not mean that the higher order terms will also be small for large U and conclude that each term in the expansion must be calculated and examined individually.

In the first of a series of papers on the subject, Horvatic' and Zlatic' study the low temperature properties of the asymmetric Anderson impurity hamiltonian using the perturbation methods of Yosida and Yamada to expand around the Hartree Fock results (Horvatic' and Zlatic' (1980)). For this the asymmetric case the determinantal expressions of Yosida and Yamada become extremely complicated. However Horvatic' and Zlatic' (1980) propose that in the limit of not too large correlation and small asymmetry the perturbation expansion of Yosida and Yamada must retain its rapid convergence. The authors also claim that in the dilute alloy region where $U/\pi\Delta \approx 1$, the correlation effects are significant for the nearly symmetric ground state only and that only the first few terms are necessary in an expansion in U about the Hartree Fock solution. They therefore apply the method of Yosida and Yamada to the asymmetric non degenerate Anderson impurity hamiltonian and calculate the corrections to the Hartree Fock f electron self energy to second order in U . The difference between the expansion for the self energy of Horvatic' and Zlatic' (1980), (1982) for the asymmetric case and that of Yamada (1975) for the symmetric case is that the odd order terms in the expansion for the asymmetric case are non zero.

In the notation of Horvatic' and Zlatic' the symmetric Anderson hamiltonian is identified by $E_d = 0$ where $E_d = \varepsilon_d + (U/2)\langle n_d \rangle$, ε_d is the d level energy and $\langle n_d \rangle / 2 = \langle n_{d\sigma} \rangle = \langle n_{d-\sigma} \rangle$ is the d electron occupation of either spin. The authors choose to drop the spin index since the spins are equivalent in the paramagnetic case. Therefore E_d can be used as a measure of the asymmetry of the model. We note here that the model was originally developed to model magnetic impurity systems where the impurity has inner shell d electrons. Hence the subscript d in E_d and ε_d . Later the results of Horvatic' and Zlatic' are discussed in their application to the HF systems where the magnetic impurity has inner shell f electrons and E_d becomes E_f .

The second order correction to the Hartree Fock self energy is:

$$\Sigma_{dd}^{(2)}(\omega_m) = \frac{U^2}{\beta} \sum_{\omega_B} G_{dd}^{HF}(\omega_m - \omega_B) \chi_o(\omega_B) \quad (2.3.1)$$

where

$$\chi_o(\omega_B) = -\frac{1}{\beta} \sum_{\omega_F} G_{dd}^{HF}(\omega_F) G_{dd}^{HF}(\omega_F + \omega_B) \quad (2.3.2)$$

and $G_{dd}^{HF}(\omega_n)$ is the d electron propagator within the Hartree Fock approximation:

$$G_{dd}^{HF}(\omega_n) = \frac{1}{i\omega - E_f + \frac{i\Delta\omega_n}{|\omega_n|}}, \quad \omega_n = \frac{\pi}{\beta}(2n + 1) \quad (2.3.3)$$

where $\omega_F = (\pi/\beta)(2n + 1)$ and $\omega_B = (\pi/\beta)2n$ are the Fermi and Bose frequencies respectively. An analytical expression for the second order retarded self energy $\Sigma_{dd}^{(2)}(\omega_n)$ is found for $k_B T/\Delta$, ω/Δ and E_d/Δ all $\ll 1$ (Horvatic' and Zlatic' (1980)). The imaginary part of the self energy is zero at the Fermi energy so that the self energy has the correct behaviour for a Fermi liquid. The results are good for dilute alloys with nearly half filled virtual bound state such as AlMn. Also, for $E_d = 0$, the results coincide with those of Yamada (1975), as they must. In Horvatic' and Zlatic' (1982) the second order self energy is recalculated as a function of E_d/Δ and the effect of asymmetry on the macroscopic quantities is examined. For the moment we concentrate on the effect of asymmetry and correlation on the impurity electron density of states. When the authors calculate the $T = 0$ (where T is temperature) impurity electron density of states using their second order self energy they find two types of behaviour. For $u = U/(\pi\Delta) < 1$ the impurity density of states has a single narrow peak around the Fermi level. However for $u = U/(\pi\Delta) > 2$ it has narrow resonance around the Fermi level as well as two broader peaks around ϵ_f and $\epsilon_f + U$, as seen by Yamada (1975) for the symmetric case. These impurity density of states features are reminiscent of the f electron density of states of the HF cerium systems.

2.3.2. The Self Energy and Impurity Density of States.

There are several comments to be made on the suitability of this second order self energy approximation in a model for the HF cerium systems. In these systems the correlation is strong and in general $E_f \neq 0$. Consider the $T = 0$ d electron Green function of Horvatic' and Zlatic' (1980), (1982), in which the self energy is approximated by its second order term:

$$G_{dd}(E) = \frac{1}{E - E_d - \text{Re} \Sigma_{dd}^{(2)}(E) + i\Delta - i\text{Im} \Sigma_{dd}^{(2)}(E)}, \quad (2.3.4)$$

where $E_d = \varepsilon_d + U/2\langle n_d \rangle$ includes the Hartree Fock term of the self energy. Here the prefixes Re and Im denote real and imaginary parts. For energies near the Fermi energy, $E_F = 0$, the real and imaginary parts of the second order self energy can be expanded in a Taylor series around $E = 0$. Also since

$$\text{Im} \Sigma_{dd}^{(2)}(0)^R = \left. \frac{d}{dE} \text{Im} \Sigma_{dd}^{(2)}(E) \right|_{E=0} = 0, \quad (2.3.5)$$

(Horvatic' and Zlatic' (1980)) then for energies near the Fermi energy the d electron density of states is given by:

$$\rho_{dd}(E) = \frac{\tilde{\Delta}}{\pi \Delta} \frac{\tilde{\Delta}}{(E - \tilde{E}_d)^2 + \tilde{\Delta}^2}, \quad (2.3.6)$$

where

$$\tilde{E}_d = \frac{\tilde{\Delta}}{\Delta} (E_d + \text{Re} \Sigma_{dd}^{(2)}(0)), \quad (2.3.7)$$

and

$$\tilde{\Delta} = \frac{1}{1 - \left. \frac{d}{dE} \text{Re} \Sigma_{dd}^{(2)}(E) \right|_{E=0}} \quad (2.3.8)$$

For $|x| = |\epsilon_d|/U > 1$, that is in the weak correlation regime where $U < |\epsilon_d|$:

$$\frac{\tilde{E}_d}{\tilde{\Delta}} = \frac{E_d}{\Delta} \left[1 - \frac{E_d}{\Delta} u^2 \left[\frac{\pi(1 - \ln 2)}{|x|^3} - \frac{1}{x^4} \dots \right] \right], \quad (2.3.9)$$

where $u = U/(\pi\Delta)$, (Horvatic' and Zlatic' (1982)) so that in this weak correlation regime, $(\tilde{E}_d / \tilde{\Delta}) \rightarrow E_d/\Delta$ with increasing asymmetry. Therefore, for energies near the Fermi energy, the impurity electron density of states is that of a renormalised resonance at \tilde{E}_d . For $E_d = 0$ this narrow resonance lies on the Fermi level, and provided the asymmetry, and hence E_d , is small, the resonance is always near the Fermi level in this the weak correlation regime. However in the strong correlation regime that is $|x| < 1$ or $U > |\epsilon_d|$

$$\frac{\tilde{E}_d}{\tilde{\Delta}} = \frac{E_d}{\Delta} \left[1 - \frac{E_d}{\Delta} u^2 \left[(\pi^2/4 - 2) - (\pi^2/4 - 17)x^2 \dots \right] \right], \quad (2.3.10)$$

(Horvatic' and Zlatic' (1982)). It is easily seen that even for small asymmetry the renormalised resonance will not lie on the Fermi level and will move far away from the Fermi level for large U . Therefore in the HF systems where the inner shell impurity electrons are f electrons and $u \approx 2$ or 3 , the second order self energy of Horvatic' and Zlatic' will only produce a narrow resonance (the Kondo resonance) near the Fermi energy, for extremely small asymmetry. In fact it can be shown that the three peaked structure in the impurity electron density of states (Horvatic' and Zlatic' (1980), (1982)) is entirely dependent on small asymmetry for two reasons. Firstly, it is seen that only for small asymmetry and small correlation will the renormalised f resonance lie near the Fermi level. Secondly, and perhaps more importantly is that provided $E_f = 0$ the second order self energy of Horvatic' and

Zlatic' is exact in the atomic limit for any size of correlation, a point which the authors do not make in any of their papers.

Consider the exact atomic limit self energy which is given by equation (2.2.26) with $\Delta = 0$. We write this self energy as the sum of Hartree Fock and all higher order terms as:

$$\Sigma_{ff\sigma}^{AL}(E)_{ex} = U\langle n_{f-\sigma} \rangle + \frac{U^2 \langle n_{f-\sigma} \rangle (1 - \langle n_{f-\sigma} \rangle) G_{ff\sigma}^{\circ}(E)}{1 - U(1 - \langle n_{f-\sigma} \rangle) G_{ff\sigma}^{\circ}(E)}, \quad (2.3.11)$$

where

$$G_{ff\sigma}^{\circ}(E) = \frac{1}{E - \varepsilon_f + i\delta}. \quad (2.3.12)$$

Here the superscript, AL, stands for atomic limit and the subscript, ex, denotes that this is the exact expression. The second term in equation (2.3.11) is re-expressed by multiplying top and bottom by $(G_{ff\sigma}^{\circ}(E))^{-1}$ and adding and subtracting a factor of $U\langle n_{f-\sigma} \rangle$ in the denominator so that

$$\Sigma_{ff\sigma}^{AL}(E)_{ex} = U\langle n_{f-\sigma} \rangle + \frac{U^2 \langle n_{f-\sigma} \rangle (1 - \langle n_{f-\sigma} \rangle) G_{ff\sigma}^{HF}(E)}{1 - U(1 - 2\langle n_{f-\sigma} \rangle) G_{ff\sigma}^{HF}(E)}, \quad (2.3.13)$$

where

$$G_{ff\sigma}^{HF}(E) = \frac{1}{E - \varepsilon_f - U\langle n_{f-\sigma} \rangle + i\delta}, \quad (2.3.14)$$

is the Hartree Fock f electron Green function in the atomic limit. It is now immediately obvious that in the symmetric case where $E_f = 0$ and $\langle n_{f\sigma} \rangle = \langle n_{f-\sigma} \rangle = 1/2$, that the exact atomic limit self energy has no terms higher than second order in U , that is

$$\Sigma_{ff\sigma}^{AL}(E)_{ex} = \frac{U}{2} + \frac{U^2}{4} G_{ff\sigma}^{HF}(E). \quad (2.3.15)$$

Now compare this exact atomic limit self energy for $E_f = 0$ with the self energy of Horvatic' and Zlatic' for $E_f = 0$ and $T = 0$:

$$\Sigma_{ff\sigma}^{Hz}(E) = \frac{U}{2} + \Sigma_{ff\sigma}^{(2)}(E) , \quad (2.3.16)$$

where a spin index has been added to the notation of Horvatic' and Zlatic' to allow easy comparison with the self energy of the TDAA self energy in the following section. In $\Sigma_{ff\sigma}^{Hz}(E)$ of equation (2.3.16) the first term is just the Hartree Fock term and the second term is the second order self energy of equation (2.3.1) at $T = 0$. Therefore

$$\Sigma_{ff\sigma}^{Hz}(E) = \frac{U}{2} + \frac{U^2}{2\pi i} \int dE' G_{ff\sigma}^{HF}(E') \chi_0(E - E') , \quad (2.3.17)$$

where $G_{ff\sigma}^{HF}(E)$ is the f_σ electron Green function in the Hartree Fock approximation of equation (2.3.14) and

$$\chi_0(E - E') = \frac{i}{2\pi} \int dE_p G_{ff\sigma}^{HF}(E_p - E) G_{ff\sigma}^{HF}(E_p - E') . \quad (2.3.18)$$

In order to perform the integrals over E' and E_p in equations (2.3.17) and (2.3.18) we express $G_{ff\sigma}^{HF}(E)$ and $\chi_0(E)$ in terms of spectral representations:

$$G_{ff\sigma}^{HF}(E) = \int_0^\infty \frac{A^+(\omega_1)}{\omega_1 - E - i\delta} d\omega_1 + \int_{-\infty}^0 \frac{A^-(-\omega_1)}{\omega_1 - E + i\delta} d\omega_1 , \quad (2.3.19)$$

where

$$A^+(E) = -\rho_{ff\sigma}^{HF}(E) \quad \text{for } E > E_f = 0 , \quad (2.3.20)$$

$$A^-(-E) = -\rho_{ff\sigma}^{HF}(E) \quad \text{for } E < E_f = 0 , \quad (2.3.21)$$

and similarly for $\chi_0(E)$ to find

$$\Sigma_{ff\sigma}^{(2)}(E) = U^2 \left[\int_0^\infty d\omega_1 \int_0^\infty d\omega_2 \frac{A^+(\omega_1) J^+(\omega_2)}{(\omega_1 + \omega_2 - E - i\delta)} - \int_{-\infty}^0 d\omega_1 \int_{-\infty}^0 d\omega_2 \frac{A^-(-\omega_1) J^-(-\omega_2)}{(\omega_1 + \omega_2 - E + i\delta)} \right], \quad (2.3.22)$$

where

$$\begin{aligned} J^+(E) &= \frac{1}{\pi} \text{Im } \chi_o(E) \\ &= \int_0^\infty d\omega_4 \int_{-\infty}^0 d\omega_3 \rho_{ff\sigma}^{\text{HF}}(\omega_3) \rho_{ff\sigma}^{\text{HF}}(\omega_4) \delta(\omega_4 - \omega_3 - E) \\ &\quad E > E_F = 0, \end{aligned} \quad (2.3.23)$$

and

$$\begin{aligned} J^-(-E) &= -\frac{1}{\pi} \text{Im } \chi_o(E) \\ &= -\int_0^\infty d\omega_3 \int_{-\infty}^0 d\omega_4 \rho_{ff\sigma}^{\text{HF}}(\omega_3) \rho_{ff\sigma}^{\text{HF}}(\omega_4) \delta(\omega_3 - \omega_4 + E) \\ &\quad E < E_F = 0. \end{aligned} \quad (2.3.24)$$

Here $\rho_{ff\sigma}^{\text{HF}}(E)$ are the f electron densities of states within the Hartree Fock approximation. Therefore in the limit $V \rightarrow 0$ there will only be contributions to $J^+(E)$ and $J^-(-E)$ when the Hartree Fock density of states are centred around the Fermi level, that is when $E_f = 0$. For $E_f = 0$,

$$J^+(E) = \frac{\delta(E)}{4} \quad \text{for } E > E_F = 0, \quad (2.3.25)$$

$$J^-(-E) = -\frac{\delta(E)}{4} \quad \text{for } E < E_F = 0, \quad (2.3.26)$$

and substituting equations (2.3.25) and (2.3.26) into equation

(2.3.22) gives:

$$\Sigma_{ff\sigma}^{(2)}(E) = \frac{U^2}{4} G_{ff\sigma}^{HF}(E) , \quad (2.3.27)$$

so that

$$\Sigma_{ff\sigma}^{Hz}(E) = \frac{U}{2} + \frac{U^2}{4} G_{ff\sigma}^{HF}(E) , \quad (2.3.28)$$

which is the exact atomic limit result of equation (2.3.15). From this comparison of the exact atomic limit self energy and that of Horvatic' and Zlatic' for $V \rightarrow 0$, it is easily seen that for $E_f \neq 0$, the accuracy of the second order perturbation result deteriorates on two counts. Firstly, for $E_f \neq 0$, the exact atomic limit self energy has terms of all orders in U so that the second order perturbation theory cannot hope to describe even the atomic limit for strong correlation. Secondly, for $E_f \neq 0$ the Hartree Fock densities of states are not centred on the Fermi level, so that as V tends to zero these functions will shrink to δ functions which are not centred on the Fermi level. Subsequently the integrals over these density of states in $\chi_o(E)$ (see equation 2.3.18) will not yield the correct result:

$$J^+(E) = \frac{1}{\pi} \text{Im } \chi_o(E) = \langle n_{f-\sigma} \rangle (1 - \langle n_{f-\sigma} \rangle) \delta(E) , \quad (2.3.29)$$

$$J^-(-E) = -\frac{1}{\pi} \text{Im } \chi_o(E) = - \langle n_{f-\sigma} \rangle (1 - \langle n_{f-\sigma} \rangle) \delta(E) , \quad (2.3.30)$$

of the atomic limit. Therefore when $E_f \neq 0$, even the second order term of Horvatic' and Zlatic' is no longer equal to the second order term in the exact atomic limit self energy. It would appear that the success of this type of second order perturbation theory result relies on the nearness of the parameter space in which $E_f \approx 0$ and the correlation is small to that where $E_f = 0$. In its application to the strong correlation HF systems, the second order self energy can only be good for $E_f = 0$.

To improve on the result of Horvatic' and Zlatic' we need a

prescription for a self energy which retains the atomic limit even for $E_f \neq 0$. In the following, the ideas of the TDAA are used to obtain a self energy which has this property. This self energy reduces to that of Horvatic' and Zlatic' for $E_f = 0$. However it is an improvement over the result of Horvatic' and Zlatic' since it retains the exact atomic limit for $E_f \neq 0$. This new self energy is not restricted to the small correlation regime for $E_f \neq 0$.

2.4. A TIME DEPENDENT ALLOY ANALOGY SELF ENERGY.

Let us rewrite the straightforward AA self energy of equation (2.2.26) as the sum of Hartree Fock and all higher order terms as:

$$\Sigma_{ff\sigma}^{\text{AA}}(E) = U\langle n_{f-\sigma} \rangle + \frac{U^2 \langle n_{f-\sigma} \rangle (1 - \langle n_{f-\sigma} \rangle) G_{ff\sigma}^1(E)}{1 - (U(1 - 2\langle n_{f-\sigma} \rangle) - \bar{\Sigma}_{ff\sigma}(0)) G_{ff\sigma}^1(E)}, \quad (2.4.1)$$

where

$$G_{ff\sigma}^1(E) = \frac{1}{E - \epsilon_f - U\langle n_{f-\sigma} \rangle - \bar{\Sigma}_{ff\sigma}(0) + i\Delta}, \quad (2.4.2)$$

and $\bar{\Sigma}_{ff\sigma}(0)$ is the exact self energy, minus the Hartree Fock term, evaluated at $E = E_f = 0$. This straightforward AA self energy is exact in the atomic limit. At this stage a lead is taken from the TDAA discussion of Section 2.2 so that the Green functions $G_{ff\sigma}^1(E)$ are convoluted with the Fourier transform of the charge susceptibility of equation (2.2.16). In equation (2.2.16) the lines now represent the propagators $G_{ff\sigma}^1(E)$ so that

$$\Sigma_{ff\sigma}^{\text{TDAA}}(E) = U\langle n_{f-\sigma} \rangle + \frac{U^2 \langle n_{f-\sigma} \rangle (1 - \langle n_{f-\sigma} \rangle) \tilde{G}_{ff\sigma}^1(E)}{1 - (U(1 - 2\langle n_{f-\sigma} \rangle) - \bar{\Sigma}_{ff\sigma}(0)) \tilde{G}_{ff\sigma}^1(E)}, \quad (2.4.3)$$

where

$$\tilde{G}_{ff\sigma}^1(E) = \frac{1}{2\pi i} \int dE' G_{ff\sigma}^1(E') \frac{\chi_{-\sigma}^1(E - E')}{\langle n_{f-\sigma} \rangle (1 - \langle n_{f-\sigma} \rangle)}. \quad (2.4.4)$$

Suppose that this function $\tilde{G}_{ff\sigma}^1(E)$ is evaluated by making the simplest approximation to $\chi_{-\sigma}^1(E - E')$ that is $\chi_o^1(E - E')$, where $\chi_o^1(E - E')$ is given by equation (2.3.18) with $G_{ff\sigma}^{\text{HF}}(E)$ replaced by

$G_{ff\sigma}^1(E)$. When $G_{ff\sigma}^1(E)$ and $\chi_o^1(E - E')$ are written in terms of spectral representations then

$$\tilde{G}_{ff\sigma}^1(E) = \left[\int_0^{\infty} d\omega_1 \int_0^{\infty} d\omega_2 \frac{A^{1+}(\omega_1) J^{1+}(\omega_2)}{(\omega_1 + \omega_2 - E - i\delta)} - \int_{-\infty}^0 d\omega_1 \int_{-\infty}^0 d\omega_2 \frac{A^{1-}(-\omega_1) J^{1-}(-\omega_2)}{(\omega_1 + \omega_2 - E + i\delta)} \right], \quad (2.4.5)$$

where

$$A^{1+}(E) = -\rho_{ff\sigma}^1(E) \quad \text{for } E > E_F = 0, \quad (2.4.6)$$

$$A^{1-}(-E) = -\rho_{ff\sigma}^1(E) \quad \text{for } E < E_F = 0, \quad (2.4.7)$$

and

$$\begin{aligned} J^{1+}(E) &= \frac{1}{\pi} \text{Im } \chi_o^1(E) \\ &= \int_0^{\infty} d\omega_4 \int_{-\infty}^0 d\omega_3 \rho_{ff\sigma}^1(\omega_3) \rho_{ff\sigma}^1(\omega_4) \delta(\omega_4 - \omega_3 - E) \\ &\quad E > E_F = 0, \end{aligned} \quad (2.4.8)$$

$$\begin{aligned} J^{1-}(-E) &= -\frac{1}{\pi} \text{Im } \chi_o^1(E) \\ &= -\int_0^{\infty} d\omega_3 \int_{-\infty}^0 d\omega_4 \rho_{ff\sigma}^1(\omega_3) \rho_{ff\sigma}^1(\omega_4) \delta(\omega_3 - \omega_4 + E) \\ &\quad E < E_F = 0. \end{aligned} \quad (2.4.9)$$

and

$$\rho_{ff\sigma}^1(E) = \frac{1}{\pi} \frac{\Delta}{(E - \varepsilon_f - U\langle n_{f-\sigma} \rangle - \bar{\Sigma}_{ff\sigma}(0))^2 + \Delta^2}. \quad (2.4.10)$$

As $V \rightarrow 0$ and hence $\Delta \rightarrow 0$ the lorentzian function $\rho_{ff\sigma}^1(E)$ shrinks to a delta function. Also since the Friedel sum rule can be expressed as:

$$\langle n_{f\sigma} \rangle = \frac{1}{\pi} \int \rho_{ff\sigma}^1(E) dE , \quad (2.4.11)$$

then as $V \rightarrow 0$ $\rho_{ff\sigma}^1(E)$ must shrink to a delta function at the Fermi level in order to obtain the correct f occupation $\langle n_{f\sigma} \rangle$. Therefore

$$J_{v \rightarrow 0}^{1+}(E) = \langle n_{f-\sigma} \rangle (1 - \langle n_{f-\sigma} \rangle) \delta(E) , \quad (2.4.12)$$

$$J_{v \rightarrow 0}^{1-}(-E) = - \langle n_{f-\sigma} \rangle (1 - \langle n_{f-\sigma} \rangle) \delta(E) , \quad (2.4.13)$$

and when equations (2.4.12) and (2.4.13) are substituted in equation (2.4.5) we find

$$\tilde{G}_{ff\sigma}^1(E) = G_{ff\sigma}^1(E) . \quad (2.4.14)$$

When equation (2.4.14) is substituted in equation (2.4.3) we see that the self energy $\Sigma_{ff\sigma}^{TDA}(E)$ has the exact atomic limit result of equation (2.4.1) even for $E_f \neq 0$.

2.5. DISCUSSION.

In the previous sections the success of the second order perturbation theory of Horvatic' and Zlatic', in its application to the impurity density of states calculations, is identified. The second order perturbation theory self energy of Horvatic' and Zlatic' is seen to yield impurity density of states at ϵ_d and $\epsilon_d + U$ for $E_d \approx 0$ and small correlation because it is exact in the atomic limit for $E_d = 0$. For $E_d \neq 0$ all terms in the exact atomic limit self energy of higher order than U^2 are multiplied by E_d . Therefore although these higher order terms vanish for $E_d = 0$, for $E_d \neq 0$ they will be large when the correlation is large. Therefore it is concluded that when the second order perturbation theory self energy is used in a model for the HF systems its validity must surely be restricted to $E_f = 0$.

A non rigorous TDAA derivation leads to a self energy which is an improvement over that of Horvatic' and Zlatic' since it retains the exact atomic limit for $E_d \neq 0$. This TDAA has terms of all orders in U and is therefore better suited to a description of the large correlation regime than that of Horvatic' and Zlatic'. Also for $E_f = 0$ it retains all the attractive features of the $E_f = 0$ self energy of Horvatic' and Zlatic'. This TDAA self energy would therefore appear to be a better prescription for the HF systems where the coulomb correlation is large and $E_f \neq 0$.

The TDAA model is not pushed any further since the derivation of the self energy is not rigorous. However we could take a further lead from Zlatic', Horvatic' and Šokčević (1985) and Horvatic' and Zlatic' (1985) and use this self energy along with exact definitions like the Friedel sum rule and the Wilson ration to calculate the charge and magnetic susceptibilities.

CHAPTER 3.

THE SPIN ONLY CASE.

3.1. INTRODUCTION.

In the following chapters the Anderson lattice hamiltonian is used to model cerium systems which have a ferromagnetic ground state. The periodic Anderson hamiltonian in its various forms is generally used to model the very heavy cerium systems which have non magnetic ground states. However in the limit of weak hybridisation it can describe the magnetic ground state of a normal rare earth metal. The present work approaches the problem from this magnetic end. The model predicts build up of HF behaviour and breakdown of the magnetic state with increasing hybridisation. As well as modelling the precursors of HF behaviour in the non heavy magnetic rare earth systems, the model can also be thought of as a starting point for a description of ferromagnetic HF systems such as $\text{CeSi}_{1.8}$. If pushed to the weakly ferromagnetic regime the model predicts build up of Kondo-like behaviour and breakdown of the magnetic state with increasing hybridisation and so offers some explanation of the variation between ferromagnetic CeSi_x , $1.7 < x < 1.83$, and nonmagnetic CeSi_x , $1.83 < x < 2.0$, which will be discussed in Chapter 5.

The early part of the present chapter serves as an introduction to the variational method of determining the f electron Green function which is used throughout the present work. The starting point is the spin degenerate periodic Anderson hamiltonian so that the calculation is referred to as the 'spin only case'. A preliminary calculation (Edwards (1987)) includes some unnecessary approximations which limit the validity of the results to the region of small hybridisation. The following calculation contains none of these approximations so that the expressions obtained for the single particle f down spin Green function, mass enhancement and Fermi

wavevector are better suited to the description of the larger hybridisation regime where the hybridisation starts to produce large mass enhancements.

In the the latter half of the present chapter the treatment of the spin only model is extended to the case where both exchange interactions and hybridisation are present. The treatment of exchange is usually neglected in work on HF's probably because most workers study the very heavy non magnetic cerium systems where the hybridisation is considered to be the dominant interaction. However in the rare earth metals themselves the exchange interaction dominates in the R.K.K.Y interaction and leads to magnetic order. This is particularly evident in gadolinium which is ferromagnetic with a saturation moment of $7.6\mu_B$ indicating a large conduction spin polarisation parallel to the f moment of $0.67\mu_B$. Hybridisation alone leads to antiparallel spin alignment. It is likely therefore that in some systems exchange and hybridisation are competing on an equal footing. The manner in which these interactions are competing is an important problem for any theory which hopes to treat the full range of rare earth systems from magnetic to non magnetic, normal to heavy.

To study the competition between exchange and hybridisation in the lattice systems a variational calculation of the single particle f down spin Green function is made for an assumed ferromagnetic system which is modelled by the spin degenerate periodic Anderson hamiltonian plus exchange interaction. The results of this variational calculation are examined for the form of competition between the hybridisation, favouring breakdown of the magnetic state, and an exchange interaction favouring stability of the magnetic state. The effect of these two interactions on the Kondo temperature of the model is examined in the light of the criterion for magnetism of Read et al (1984) and Coleman (1983) (see Section 1.4). The combined behaviour of hybridisation and exchange for the lattice system is compared with that predicted for the impurity by a Schrieffer Wolff transformation on the Anderson impurity hamiltonian plus exchange interaction.

3.2. THE F ELECTRON GREEN FUNCTION.

3.2.1. The Model.

In this section a variational calculation of the f electron Green function is made for a strongly ferromagnetic system described by the spin degenerate Anderson lattice hamiltonian. The breakdown of the magnetic state is examined to see if the classic features of the nonmagnetic HF appear such as an increase in the effective mass and Kondo resonance in the f electron density of states. It is found that the magnetic state breaks down as the hybridisation is increased there being a particular point, defined as the effective Kondo temperature of this model, at which the initial assumption of strong ferromagnetism collapses. The model succeeds in predicting reasonable build up of mass enhancement due to a build up of density of states at the Fermi level. This sharp density of states is considered to be a precursor of the HF Kondo resonance.

The calculated effective Kondo temperature differs from the impurity Kondo temperature of Bethe ansatz calculations by a factor of two in the exponent. This is not the same factor of two found by Rice and Ueda (1985). In Chapter 4 an analogous variational calculation for the impurity also leads to an effective Kondo temperature with the same factor of two missing in the exponent. We therefore conclude that the difference between the lattice effective Kondo temperature and the impurity Kondo temperature of the Bethe ansatz calculation is a failing of the variational method rather than a genuine difference between the lattice and impurity systems. In Chapter 4 the model is improved to predict a better Kondo temperature for the impurity.

The following calculation of the f down spin Green function for the strongly ferromagnetic case involves proposing a reasonable approximate ferromagnetic ground state, of no down spin occupation, for the system assuming it to be modelled by the spin one half Anderson lattice hamiltonian, and then postulating a variational wavefunction for a down spin f electron introduced into the system. The method leads to a Dyson equation for quasi particle energies greater than the Fermi level which yields a flat band of f like quasi particles very close to the Fermi level and thus a resonance

in the f density of states near the Fermi level. The picture of a flat band of f like quasi particles near the Fermi level is consistent with the Fermi liquid pictures described in the introduction (see Section 1.4).

The starting point, then, is the spin degenerate or spin one half periodic Anderson model:

$$H_{latt}^A = \sum_{k\sigma} \epsilon_k c_{k\sigma}^\dagger c_{k\sigma} + \sum_{k\sigma} \epsilon_f f_{k\sigma}^\dagger f_{k\sigma} + \sum_{k\sigma} V (c_{k\sigma}^\dagger f_{k\sigma} + f_{k\sigma}^\dagger c_{k\sigma}) + \sum_i U f_{i\uparrow}^\dagger f_{i\uparrow} f_{i\downarrow}^\dagger f_{i\downarrow}, \quad (3.2.1)$$

where $c_{k\sigma}^\dagger$ creates a conduction electron in a state of energy ϵ_k , momentum k and spin σ and $f_{k\sigma}^\dagger$ creates an f electron in a state of energy ϵ_f , momentum k and spin σ . Term by term the hamiltonian describes a conduction band of energies ϵ_k , a flat f band of energy ϵ_f , hybridisation between the f and conduction bands with a strength V assumed independent of k as is usual and finally a coulomb interaction between f electrons on the same site.

3.2.2. The Ground State.

An approximate strongly ferromagnetic ground state for the Anderson lattice hamiltonian is calculated using the Hartree Fock approximation to the coulomb interaction which puts the down spin f level up at energy $\epsilon_f + U\langle n_{f\uparrow} \rangle$ where $\langle n_{f\uparrow} \rangle$ is the up spin occupation in the ground state. U is taken to be large so that the hybridisation of this down spin f level with the conduction band is assumed to result in negligible down spin occupation. The ground state, then, is one of an unhybridised down spin conduction band, unhybridised flat f down spin band, so that $\langle n_{f\downarrow} \rangle = 0$, and two up spin bands resulting from the hybridisation of up spin f and up spin conduction electrons. The ground state bands are drawn schematically in Figure 3.1. The two up spin bands are labelled by n, the band index, equal to 1 or 2. The states in the up spin bands are created by eigenstate creation operators $a_{kn\uparrow}^\dagger$ and have energies ϵ_{kn} . The ground state is given by:

$$|0\rangle = \prod_{\substack{kn\uparrow \\ \text{occ}}} a_{kn\uparrow}^\dagger \prod_{k < k_F} c_{k\downarrow}^\dagger |V\rangle, \quad (3.2.2)$$

where $|V\rangle$ is the vacuum state, and the product in (3.2.2) is over wavevectors of occupied eigenstates. Also

$$a_{kn\uparrow}^\dagger = A_{kn\uparrow} f_{kn\uparrow}^\dagger + B_{kn\uparrow} c_{k\uparrow}^\dagger, \quad (3.2.3)$$

where $A_{kn\uparrow}^2$ is the f up spin electron weight, and $B_{kn\uparrow}^2$ the up spin conduction electron weight, in the state $a_{kn\uparrow}^\dagger |V\rangle$. It is easily shown that

$$A_{kn\uparrow} = \frac{V}{\sqrt{(\varepsilon_{kn} - \varepsilon_f)^2 + V^2}}, \quad (3.2.4)$$

$$B_{kn\uparrow} = \frac{(\varepsilon_{kn} - \varepsilon_f)}{\sqrt{(\varepsilon_{kn} - \varepsilon_f)^2 + V^2}}, \quad (3.2.5)$$

with energies ε_{kn} (see Figure 3.1) given by the two roots of

$$(\varepsilon_{kn} - \varepsilon_k)(\varepsilon_{kn} - \varepsilon_f) = V^2. \quad (3.2.6)$$

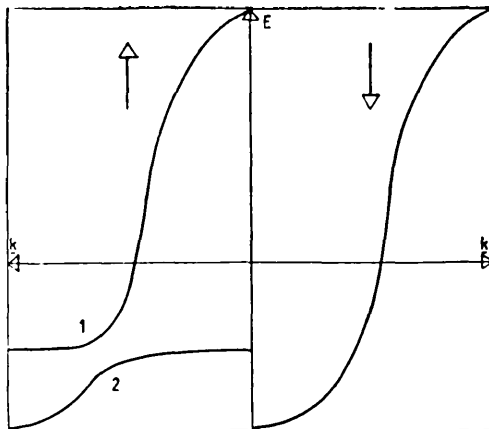


Figure 3.1. A schematic ground state band picture for the spin degenerate periodic Anderson model in the limit $U \rightarrow \infty$. The lower and upper up spin bands are labelled 2 and 1 respectively.

3.2.3. The f Down Spin Wavefunction.

Now that the ground state is established we postulate a variational wavefunction for an f down spin electron introduced into the system. The end result of this procedure is a Dyson equation with an identifiable down spin f electron self energy.

From a completely general diagrammatic expansion in which the hybridisation and the coulomb interaction are both treated as perturbations the f single particle Green function is given by:

$$\begin{aligned}
 \overline{\overline{G}}_{ff}(k,E) &= \overline{G}_{ff}^{\circ}(k,E) + \overline{G}_{ff}^{\circ}(k,E) \overline{G}_{cf}(k,E) + \overline{G}_{ff}^{\circ}(k,E) \left(\sum_{ff} (k,E) \right) \overline{G}_{ff}(k,E) \\
 & \hspace{15em} (3.2.7)
 \end{aligned}$$

$$\overline{\overline{G}}_{cf}(k,E) = \overline{G}_{cf}^{\circ}(k,E) + \overline{G}_{cf}^{\circ}(k,E) V \overline{G}_{ff}(k,E) \hspace{10em} (3.2.8)$$

so that

$$\begin{aligned}
 G_{ff\downarrow}(k,E) &= G_{ff\downarrow}^{\circ}(k,E) + G_{ff\downarrow}^{\circ}(k,E) V G_{cf\downarrow}(k,E) \\
 & \hspace{15em} G_{ff\downarrow}^{\circ}(k,E) \Sigma_{ff\downarrow}(k,E) G_{ff\downarrow}(k,E), \hspace{5em} (3.2.9)
 \end{aligned}$$

and

$$G_{cf\downarrow}(k,E) = G_{cf\downarrow}^{\circ}(k,E) V G_{ff\downarrow}(k,E), \hspace{10em} (3.2.10)$$

where $G_{f\downarrow}^0(k, E)$, $G_{ff\downarrow}(k, E)$ are the unperturbed and full down spin f electron propagators, $G_{c\downarrow}^0(k, E)$ is the unperturbed down spin conduction electron propagator and $G_{cf\downarrow}(k, E)$ is the Fourier transform of the propagator $\langle 0 | T [f_{k\downarrow}(t) , c_{k\downarrow}^\dagger(0)] | 0 \rangle$. Also everything that is unknown about the interactions of the system is stored in the $f\downarrow$ electron self energy, $\Sigma_{ff\downarrow}(k, E)_{ex}$. This contains all processes in which the $f\downarrow$ electron first interacts with the system via the coulomb interaction and after all subsequent interactions emerges finally as an $f\downarrow$ electron. From equations (3.2.9) and (3.2.10) we find

$$G_{ff\downarrow}(k, E) = \frac{1}{E - \varepsilon_f - \frac{V^2}{E - \varepsilon_k} - \Sigma_{ff\downarrow}(k, E)_{ex}}. \quad (3.2.11)$$

The full f down spin self energy

$$\Sigma_{ff\downarrow}^F(E) = \frac{V^2}{E - \varepsilon_k} + \Sigma_{ff\downarrow}(k, E)_{ex}. \quad (3.2.12)$$

However in the following text the term 'f electron self energy' is used to mean $\Sigma_{ff\downarrow}(k, E)_{ex}$. It is desired that any treatment of the Anderson hamiltonian give a Green function of the form of equation (3.2.11). Within the present approach a variational wavefunction is postulated for an f down spin electron of momentum k in the system as the sum of all the most likely processes which would occur if an f electron were added to the ground state. This approach yields a Green function of the form of equation (3.2.11) as required.

A down spin f electron entering the system can sample the f down spin state of momentum k , the down spin conduction state of momentum k , since it can hybridise with this state via V , and be involved in many other more exotic excitations all of which must be included for an exact self energy $\Sigma_{ff\downarrow}(k, E)_{ex}$. It is impossible to include the infinite set of possible processes in $\Sigma_{ff\downarrow}(k, E)_{ex}$, instead only the most important set are included. To identify the most important set of processes or diagrams in $\Sigma_{ff\downarrow}(k, E)_{ex}$ an

analogy is drawn between the present situation of ferromagnetic Hartree Fock ground state for the Anderson hamiltonian of equation (3.2.1) and the treatment of the Hubbard model (Hubbard (1963), (1964)) of Edwards (1968) where again the approximate ground state is ferromagnetic Hartree Fock. In the present model the approximate ground state is one of hybridised up spin bands and an unoccupied down spin f level at $\epsilon_f + U\langle n_{f\uparrow} \rangle$. The f density of states can be represented schematically as in Figure 3.2.a. The next stage is to write down the most likely processes occurring due to the coulomb correlation between f electrons in the ground state. In the treatment of the nearly half filled Hubbard model by Edwards (1968) the initial ground state is again calculated within Hartree Fock so that the f density of states is as in Figure 3.2b. As for the periodic Anderson model the next stage is to write down the most likely processes occurring due to the coulomb interaction between f electrons, the only electrons in this case.

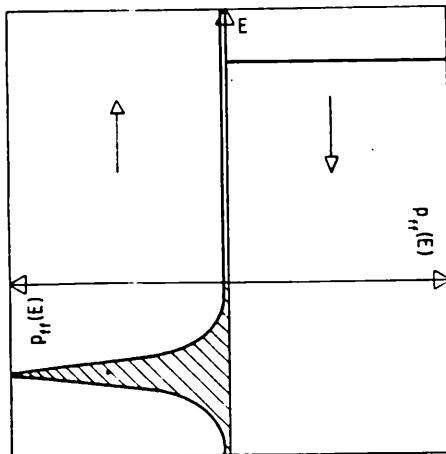


Figure 3.2a. A schematic f density of states for the spin degenerate periodic Anderson model in the limit $U \rightarrow \infty$. The hatched area denotes occupied density of states below the Fermi energy E_F .

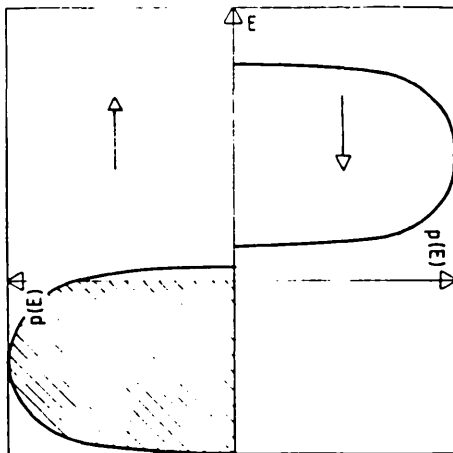


Figure 3.2b. A schematic density of states for the Hubbard model. The hatched area denotes occupied density of states below the Fermi energy E_F .

For both models the approximate ground state has no down spin f occupation and few numbers of up spin holes, or rather in the case of the present model, small up spin weight in the states above the Fermi level. The task of taking better account of the coulomb correlation by inclusion of diagrams other than just Hartree Fock is the same in both cases. Therefore the arguments of Edwards (1968) apply equally well to the present model if the up spin f electron propagators of the Hubbard model are replaced by the hybridised up spin f electron propagators of the Anderson model. The self energy diagrams with the least number of up spin electron lines will have the largest contribution since in the corresponding analytic expression each up spin electron line brings in a factor of the number of up spin states above the Fermi level. Therefore the smaller the number of up spin electron lines the larger the contribution. The dominant diagrams are represented schematically as in Figure 3.3.

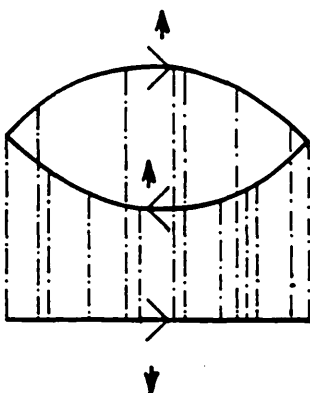


Figure 3.3. The corrections to the Hartree Fock self energy for the spin degenerate periodic Anderson model. The lines $\xrightarrow{\uparrow}$ and $\xrightarrow{\downarrow}$ represent the up and down spin f electron propagators respectively. The dotted lines represent scattering via the coulomb interaction.

The diagrams in Figure 3.3 describe a down spin f flipping to an up spin f and exciting a magnon as well as interactions between this magnon and the single particle excitations. The diagrams of Figure 3.3 are exact to order U^2 . The inclusion of the interactions between the magnon and single particle excitation brings in terms of all orders in U and is discussed in Chapter 4 where a diagrammatic treatment of the problem is given for the weakly magnetic impurity case.

For the moment we are concerned with identifying likely processes involving down spin f electrons for inclusion in a variational f down spin wavefunction. In the present chapter, then, the small number of unoccupied up spin states argument is used to postulate a variational wavefunction which includes a process in which the down spin f flips to an up and excites a magnon.

The variational wavefunction is written:

$$|\psi\rangle = \left[A_{\mathbf{k}} f_{\mathbf{k}\downarrow}^\dagger + F_{\mathbf{k}} c_{\mathbf{k}\downarrow}^\dagger + \sum_{\mathbf{k}'_1 > k_F} G_{\mathbf{k}'_1} a_{\mathbf{k}'_1\uparrow}^\dagger S_{\mathbf{k}-\mathbf{k}'}^- \right] |0\rangle, \quad (3.2.13)$$

where the subscript \mathbf{k}'_1 denotes an up spin quasi particle state of momentum \mathbf{k}' in band 1 of Figure 3.1 and $S_{\mathbf{k}-\mathbf{k}'}^-$ is an approximate magnon creation operator given by:

$$S_{k-k'}^- = \sum_p c_{(p-k')\downarrow}^\dagger c_{(p-k)\uparrow} + \sum_p f_{(p-k')\downarrow}^\dagger f_{(p-k)\uparrow}, \quad (3.2.14)$$

where $k-k'$ is the momentum of the magnon. If the down spin wavefunction is just written as a sum of the first two terms of (3.2.13) then the Dyson equation yields down spin bands of the same form as the up spin bands of Figure 3.1 but with the f down spin level position at $\varepsilon_f + U\langle n_{f\uparrow} \rangle$. The self energy for this case would just be the first, that is, Hartree Fock term of a perturbation expansion and would not yield a resonance at the Fermi level which arises from the many body character of the coulomb interaction. To improve on the Hartree Fock solution better account must be taken of the coulomb correlation, that is more diagrams must be summed in the self energy or, equivalently, more processes must be included in the variational wavefunction. In this limit of a small number of unoccupied up spin states the addition of the third term is considered to take account of the most important consequences of the coulomb correlation. In fact the third term in the variational wavefunction of equation (3.2.13) leads to a contribution to the down spin self energy, given by equation (3.2.18), which within certain approximations is in exact agreement with the analytical expression corresponding to Figure 3.3. This statement is discussed later in Section (3.4.3) for the periodic Anderson hamiltonian plus exchange interaction.

The coefficients A_k , F_k , and $G_{k'}$ in the variational wavefunction are sought by left multiplying the Schrodinger equation:

$$H|\psi\rangle = \varepsilon|\psi\rangle, \quad (3.2.15)$$

by $\langle 0|f_{k\downarrow}$, $\langle 0|c_{k\downarrow}$, and $\langle 0|S_{k-k'}^+ a_{k''}\uparrow$. Here ε is the energy of the state $|\psi\rangle$, and S_{-q}^+ is the hermitian conjugate of S_q^- . The three equations for the coefficients are solved to give F_k and $G_{k'}$ in terms of A_k so that

$$A_k \left[\varepsilon - E_0 - \varepsilon_f - \frac{V^2}{(\varepsilon - E_0 - \varepsilon_k)} - \Sigma_{ff\downarrow}(\varepsilon - E_0) \right] = 0$$

for $\varepsilon - E_0 > 0$, (3.2.16)

where E_0 is the ground state energy and ε the energy of the variational wave function describing the ground state plus one f down spin electron. The quantity $E = \varepsilon - E_0$ is identified as an excitation energy so that equation (3.2.16) corresponds to a Dyson equation for the particle excitation energies of the system. The Fermi energy is taken as $E = 0$ so that only solutions of the Dyson equation with $E > 0$ are significant, others being strictly inconsistent with the assumption of no down spin f occupation in the ground state. Since the excitation energies are by definition the poles of the f down spin Green function equation (3.2.16) is consistent with an f down spin Green function:

$$G_{ff\downarrow}(E, k) = \frac{1}{E - \varepsilon_f - \frac{V^2}{(E - \varepsilon_k)} - \Sigma_{ff\downarrow}(k, E)} \quad \text{for } E > 0,$$

(3.2.17)

which is of the correct form predicted by the general diagrammatic analysis of equations (3.2.7) to (3.2.11). The approximate f electron self energy $\Sigma_{ff\downarrow}(k, E)$ is calculated as:

$$\Sigma_{ff\downarrow}(k, E) = U\langle n_{f\uparrow} \rangle + \frac{\sum_{k' > k_F} \frac{U^2 A_{k',1}^2 \langle n_{f\uparrow} \rangle}{E - \epsilon_{k',1} - \hbar\omega_{k-k'}}}{1 - \sum_{k' > k_F} \frac{U A_{k',1}^2}{E - \epsilon_{k',1} - \hbar\omega_{k-k'}}}, \quad (3.2.18)$$

where the sums are over the up spin quasi particle wavevectors in band one such that the state of momentum k in band 1 is unoccupied. Also $\hbar\omega_{k-k'}$, is the magnon energy and is given by:

$$\hbar\omega_{k-k'} = \frac{\langle 0 | S_{k-k'}^+ H_{\text{latt}}^A S_{k-k'}^- | 0 \rangle}{\langle 0 | S_{k-k'}^+ S_{k-k'}^- | 0 \rangle}. \quad (3.2.19)$$

The operator $S_{k-k'}^-$, is only an approximation to the creation operator of the real magnon and within this approximation we find that the model magnon dispersion has a zero momentum, $k-k'=0$, magnon energy of zero in disagreement with the finite energy of the zero momentum magnetic excitation in a real system such as CeSi_x (M.Kohgi et al (1987)). The non zero magnon energy of the real world is a result of crystal field and spin orbit coupling effects which are not included in the spin degenerate periodic Anderson model. In the following, then, a lead is taken from experiment and a flat magnon dispersion is assumed (Kohgi et al (1987) and Figure 5.1). In Chapter 5 an attempt is made to remove the inconsistency, which is introduced here when we insert the magnon energy by hand, by improving the model to include crystal field and spin orbit coupling effects. Within the flat magnon dispersion approximation the self energy of equation (3.2.18) is k independent and is rewritten as:

$$\Sigma_{ff\downarrow}(E) = \frac{U\langle n_{f\uparrow} \rangle}{1 - \frac{U \hat{\Sigma}_{ff\downarrow}^0(E)}{\langle n_{f\uparrow} \rangle}}, \quad (3.2.20)$$

where

$$\hat{\Sigma}_{ff\downarrow}^0(E) = \sum_{k'_1 > k_F} \frac{A_{k'_1}^2 \langle n_{f\uparrow} \rangle}{E - \epsilon_{k'_1} - h\omega_{\text{mag}}}, \quad (3.2.21)$$

and $h\omega_{\text{mag}}$ is the now momentum independent magnon energy. To evaluate (3.2.21) a sum has to be performed over $A_{k'_1}^2$, the f up spin density of states above the Fermi level. If the model was entirely self consistent there would be some small down spin occupation so that the up spin Green function would also have self energy contributions due to the coulomb correlation. These would affect the down spin self energy via the sum over k'_1 . In the following chapter this self consistency is introduced for the impurity case by including non zero down and up spin f electron self energies in the model. However in the present strongly ferromagnetic case it is neglected.

From equation (3.2.6) we see that for small hybridisation the dispersion of quasi particle states for energies greater than the Fermi level is practically identical to that of the original unhybridised conduction band. The sum over the quasi particle wavevectors k'_1 in equation (3.2.21) can therefore be evaluated as an integral over the unhybridised band energies from the Fermi energy ($E_F = 0$) to the top of the band so that

$$\begin{aligned} \hat{\Sigma}_{ff\downarrow}^0(E) = & \frac{\langle n_{f\uparrow} \rangle V}{W} \left[\frac{B(E)}{2} \ln \left| \frac{(T_p - \epsilon_f)^2 + V^2}{\epsilon_f^2 + V^2} \right| - B(E) \ln \left| \frac{E - T_p - h\omega_{\text{mag}}}{E - h\omega_{\text{mag}}} \right| \right. \\ & \left. \frac{B(E)(E - \epsilon_f - h\omega_{\text{mag}})}{V} \left[\tan^{-1} \left[\frac{T_p - \epsilon_f}{V} \right] - \tan^{-1} \left[\frac{-\epsilon_f}{V} \right] \right] \right], \end{aligned} \quad (3.2.22)$$

where

$$B(E) = \frac{V}{(E - 2\varepsilon_f - \hbar\omega_{\text{mag}})(E - \hbar\omega_{\text{mag}}) + \varepsilon_f^2 + V^2}. \quad (3.2.23)$$

$\hat{\Sigma}_{ff\downarrow}^0(E)$ and hence $\Sigma_{ff\downarrow}(E)$ has no imaginary part for energies less than the magnon energy so that for energies greater than the Fermi energy and less than the magnon energy the Dyson equation can be solved for down spin quasi particle energies ε_{km} where

$$\varepsilon_{km} - \varepsilon_f - \frac{V^2}{\varepsilon_{km} - \varepsilon_k} - \Sigma_{ff\downarrow}(\varepsilon_{km}) = 0, \quad (3.2.24)$$

for $0 < \varepsilon_{km} < \hbar\omega_{\text{mag}}$

and m is an index labelling the possible multiple solutions of equation (3.2.24). As $E \rightarrow \hbar\omega_{\text{mag}}$ the logarithmic term in equation (3.2.22) diverges so that $\Sigma_{ff\downarrow}(E)$ tends to zero as the magnon energy is approached. Far away from the magnon energy $\Sigma_{ff\downarrow}(E)$ is dominated by the Hartree Fock term $U\langle n_{f\uparrow} \rangle$. From Figure 3.4

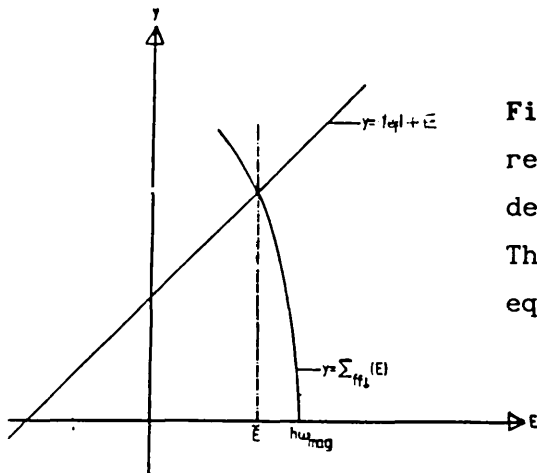


Figure. 3.4. The f down spin resonance energy for the spin degenerate periodic Anderson model. The figure shows the solution of equation (3.2.25).

we see that for some energy \tilde{E} very near the magnon energy

$$\tilde{E} - \varepsilon_f - \Sigma_{ff\downarrow}(\tilde{E}) = 0, \quad (3.2.25)$$

so that for energies very near \tilde{E} a Taylor expansion of the self energy around \tilde{E} is valid and the Dyson equation can be written:

$$(\epsilon_{km} - \tilde{E})(\epsilon_{km} - \epsilon_k) = \tilde{V}^2, \quad (3.2.26)$$

with

$$\tilde{E} = \epsilon_f + \Sigma_{ff\downarrow}(\tilde{E}) \quad (3.2.27)$$

and

$$\tilde{V}^2 = \frac{V^2}{1 - \Sigma_{ff\downarrow}'(\tilde{E})}, \quad \Sigma_{ff\downarrow}'(\tilde{E}) = \left. \frac{d\Sigma_{ff\downarrow}'(\epsilon_{km})}{d\epsilon_{km}} \right|_{\epsilon_{km} = \tilde{E}}. \quad (3.2.28)$$

When equation (3.2.26) for the down spin quasi particle energies is compared with equation (3.2.6) and Figure 3.1 for the up spin quasi particle energies it is easily seen that for energies $0 < \epsilon_{km} < h\omega_{\text{mag}}$ the down spin quasi particles form bands resulting from the hybridisation via renormalised hybridisation \tilde{V} of an f level at renormalised energy \tilde{E} with the conduction band. The quasi particle bands are sandwiched between the magnon energy and the Fermi energy and are represented schematically as in Figure 3.5.

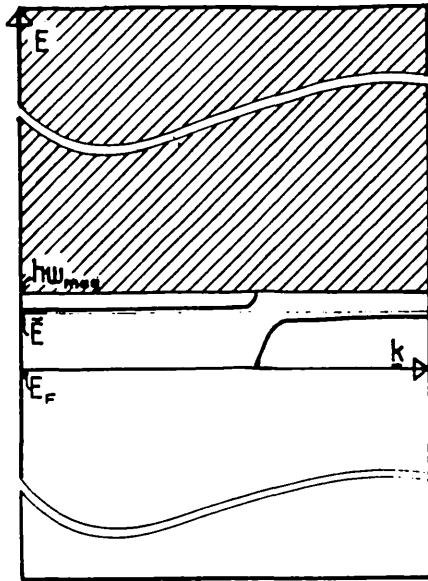


Figure 3.5. A schematic picture of the f down spin quasi particle bands for the spin degenerate periodic Anderson model. The bands are sandwiched in the narrow energy region between the Fermi level at $E_F = 0$ and the magnon energy $h\omega_{\text{mag}}$. In the hatched region $E > h\omega_{\text{mag}}$ there are no well defined bands. There is no f down spin weight below the Fermi level.

It should be noted that the self energy is varying rapidly in the region between the Fermi level and the magnon energy so that despite the narrowness of this energy region an expansion around \tilde{E} gives reasonable self energy values only very close to \tilde{E} . Equation (3.2.26) is therefore only useful for fixing the position of the resonance. When we calculate the mass enhancements and Fermi wavevector, both of which involve evaluating the self energy at the Fermi level, the expansion around \tilde{E} is not used.

The final picture of an f level of renormalised energy, \tilde{E} , hybridising via a renormalised hybridisation \tilde{V} to yield quasi bands at the Fermi level is consistent with the argument of Section 1.4 that flat quasi particle bands of this type must occur if the system is a Fermi liquid at zero temperature. The flat quasi particle bands of the present model result in a sharp resonance in the f down spin density of states above the Fermi level which we identify as the precursor of a Kondo resonance. For small hybridisations, ($\Delta = 0.02\text{eV}$), the resonance is extremely narrow and lies extremely close to the magnon energy so that the quasi particle density of states at the Fermi level is not much enhanced over the unhybridised density of states. As the hybridisation increases the renormalised f energy

\tilde{E} moves closer to the Fermi level and the quasi particle bands are pushed flatter at the Fermi level (see Figure 3.5). Hence the quasi particle density of states at the Fermi level and subsequently the mass enhancement increase (see Section 3.3). A limit to the model must be defined since as the hybridisation and the subsequent build up of density of states at the Fermi level increases, there is also a build up of down spin f density of states below the Fermi level in the tail of this resonance above the Fermi level. At some point the density of states below the Fermi level supports a non negligible down spin f occupation violating the basic assumption of the model of strong ferromagnetism. A limit is placed on the hybridisation in Section 3.3 for this the strongly ferromagnetic case. In Chapter 4 the model is pushed to the weakly magnetic regime for the impurity case, allowing an extension of the model to larger hybridisations.

3.3. RESULTS.

3.3.1. The Effective Kondo Temperature.

The Kondo temperature T_K of the impurity problem is defined in the Bethe ansatz expression for the high temperature susceptibility (Andrei (1983)). Below the Kondo temperature the conduction electrons screen the impurity moment so that T_K locates a point on an energy scale below which a screened moment is favoured over a free moment. For the lattice case the Kondo temperature also locates an energy dividing regions in which magnetic and non magnetic Kondo like ground states are stable (Doniach (1977), Read et al (1984) and Coleman (1983)).

The effective Kondo temperature of the present treatment of the spin degenerate lattice system is defined now as the magnon energy for which the postulated ferromagnetic state breaks down. When the resonance lies on the Fermi energy we assume the break down of the magnetic state is complete. Thus the magnon energy for which the model breaks down is given by equation (3.2.25) with \tilde{E} set to zero. It is considered that this definition locates an effective Kondo temperature which must at least be related to the real Kondo temperature. In fact in Section (3.4.4) we find that when an exchange interaction is included in the model, and the hybridisation tends to zero, the effective Kondo temperature is in agreement with the calculated Kondo temperature of Read, News and Doniach (1984) and Coleman (1983) as well as the exact Bethe ansatz result for the impurity.

For small hybridisation, \tilde{E} lies very close to the magnon energy so that for $\tilde{E} = 0$ the magnon energy must be very close to zero and in equation (3.2.22) $\hat{\Sigma}_{ff\downarrow}^0(0)$ is dominated by the $\ln|h\omega_{\text{mag}}|$ term so that

$$\hat{\Sigma}_{ff\downarrow}^0(0) \approx \frac{\langle n_{f\uparrow} \rangle V^2}{W\epsilon_f^2} \ln |h\omega_{\text{mag}}|. \quad (3.3.1)$$

When equation (3.3.1) is used in equation (3.2.25) with $\tilde{E} = 0$ we find that in the limit of large U the effective Kondo temperature of

the model is given as:

$$T_K^{eff} \propto e^{-\frac{\langle n_{f\uparrow} \rangle W |\epsilon_f|}{V^2}} \quad (3.3.2)$$

When the effective Kondo temperature of the model is compared with the Bethe ansatz result for the impurity, namely:

$$T_K \propto e^{-\frac{W |\epsilon_f|}{2V^2}}, \quad (3.3.3)$$

it is seen that the effective Kondo temperature of the model differs from the impurity Kondo temperature by a factor of two in the exponent. The factor of two is not the same factor of two of Rice and Ueda (1985) and appears to be a product of the model rather than a genuine difference between the lattice and impurity cases. The same error occurs in the effective impurity Kondo temperature of Chapter 4. Therefore the model yields an effective Kondo temperature which is too small or, equivalently, the postulated ferromagnetic ground state is too stable in contrast to the result of Rice and Ueda where the factor of two means that their non magnetic ground state is too stable.

A possible explanation for the error in the exponent of the effective Kondo temperature is that the up spin density of states at the Fermi level which enters the exponent as $V^2 / |\epsilon_f|^2$ is too small by a factor of two. The strictly ferromagnetic ground state is too rigid an approximation since for finite U , no matter how large, there will always be some down spin occupation due to hybridisation. A schematic f density of states picture in a more realistic U finite approximation is shown in Figure 3.6.

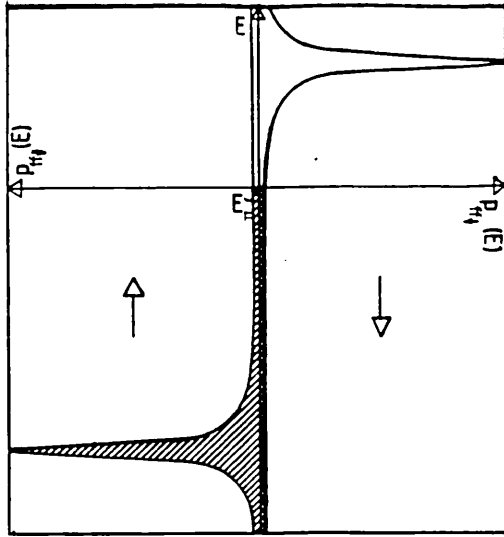


Figure 3.6. A schematic f density of states for the spin degenerate periodic Anderson model for U finite. The hatched areas denote occupied density of states below the Fermi energy E_F .

It is easily seen that, if a resonance is building up in the down spin density of states due to processes represented by the diagrams of Figure 3.3, then there must be analogous processes in which down spin hole lines play the part of up spin particle lines, giving rise to a resonance in the up spin density of states below the Fermi level. A completely self consistent calculation would therefore yield an up spin density of states at E_F larger than $V^2/|\epsilon_f|^2$ due to the extra contribution from the up spin resonance lying just below the Fermi level.

The build up of the resonance in the up spin density of states is consistent with an earlier breakdown of the ferromagnetic ground state. As the hybridisation increases both the up and down spin resonances move nearer the Fermi level. The up and down spin quasi bands are pushed flatter at the Fermi level and subsequently the up and down spin f electron density of states at the Fermi level increases. The increase in f electron density of states of both spins around the Fermi level means that more up spin electrons and down spin holes are available for excitations of the sort represented by the diagrams of Figure 3.3. Therefore more f electron density of states is built up around the Fermi level via these additional excitations. There is a kind of bootstrapping effect building up weight at E_F . In Chapter 4 the bootstrapping effect is studied in the impurity problem with a view to correcting

the effective Kondo temperature.

3.3.2. The Mass Enhancement.

The mass enhancement of the model is defined as the density of down spin quasi particle states at the Fermi level, $N(E)$, divided by the unhybridised conduction band density of states at the Fermi level, $N_0(E)$, so that

$$\frac{m^*}{m} = \frac{N(E)}{N_0(E)} \Big|_{E=0}, \quad (3.3.4)$$

where the Fermi energy $E_F = 0$. The general definition of the density of states for any dispersion relation is:

$$N(E) = \int_{s(E)} \frac{1}{|\nabla \epsilon_{\mathbf{k}}|} dS, \quad (3.3.5)$$

where the integral is over a surface of constant energy E . For both the new quasi particle bands and the unhybridised conduction bands the energy of the band states is assumed to be a function of $|\mathbf{k}|$. The Fermi surface for both the unperturbed and quasi particle bands is therefore a sphere of radius equal to the relevant Fermi wavevector. Therefore to evaluate the density of unhybridised conduction states or quasi particle states at the Fermi energy we integrate over the surface of a sphere of a radius equal to the relevant Fermi wavevector in equation (3.3.5). As a result the mass enhancement is given by:

$$\frac{m^*}{m} = \frac{\sum_m 4\pi k^2 \frac{dk}{d\epsilon_{k_m}} \Big|_{\epsilon_{k_m}=0, k=k_{Fm}}}{4\pi k^2 \frac{dk}{d\epsilon_k} \Big|_{\epsilon_k=0, k=k_F}}, \quad (3.3.6)$$

where ϵ_{k_m} are the quasi particle energies in band m , ϵ_k are the

unperturbed conduction band energies, k_{Fm} is the Fermi wavevector of the quasi particle band m and k_F is the Fermi wavevector of the unperturbed conduction band. The definition (3.3.6) allows for the possibility of more than one quasi particle band crossing the Fermi level and contributing to the mass enhancement. In the present case there is only one value of m for which $\epsilon_{km} = 0$, that is only one quasi band at the Fermi level. Schematically (see Figure 3.5) the treatment of the strong on site coulomb correlation via inclusion of the magnon excitations in the down spin wavefunction has resulted in a flat band of states at the Fermi level giving a large down spin density of states at the Fermi level. The quasi particle bands are pushed flat so that the value of the gradient in equation (3.3.5) is decreased over the corresponding value for the unperturbed conduction band to give the mass enhancement. The flat quasi bands describe quasi particle states which are more localised than the unperturbed conduction band states and therefore electrons in these states appear heavier.

To evaluate equation (3.3.6) a constant unhybridised conduction band density of states is assumed so that

$$N_o(E) = \frac{N}{W}, \quad (3.3.7)$$

where W is the width of the band and N the number of sites. The assumption of a constant unperturbed conduction band density of states means that

$$4\pi k^2 \frac{dk}{d\epsilon_k} \Big|_{\epsilon_k=0, k=k_F} = \frac{1}{W} = 4\pi k^2 \frac{dk}{d\epsilon_k} \Big|_{\epsilon_{km}=0, k=k_{Fm}}. \quad (3.3.8)$$

so that when this result is used in equation (3.6.6) we find:

$$\frac{m^*}{m} = \sum_m \frac{\frac{d\epsilon_k}{dk} \Big|_{\epsilon_k=0, k=k_F}}{\frac{d\epsilon_{km}}{dk} \Big|_{\epsilon_{km}=0, k=k_{Fm}}}. \quad (3.3.9)$$

An expression for the mass enhancement is found by differentiating the Dyson equation (3.2.24) with respect to k and solving for m^*/m in terms of the derivatives with respect to k of the quasi particle energies and unperturbed band energies as they appear in equation (3.3.9). Finally we need the value of the unperturbed conduction band energy $\epsilon_k = \epsilon_{k_{Fm}}$ for which $\epsilon_{km} = 0$ and $k = k_{Fm}$. That is the unperturbed conduction band energies for which the quasi particle bands cross the Fermi level. These are found from equation (3.2.24) with $\epsilon_{km} = 0$.

$$\epsilon_{k_{Fm}} = \frac{V^2}{\sum_{ff\downarrow}(0) + \epsilon_f}, \quad (3.3.10)$$

so that

$$\frac{m^*}{m} = 1 + V^2 \frac{1 - \sum_{ff\downarrow}(\epsilon_{km})}{d\epsilon} \Big|_{\epsilon_{km}=0, k=k_{Fm}} \frac{1}{\sum_{ff\downarrow}(0) + \epsilon_f} \quad (3.3.11)$$

Figures 3.7 and 3.8 show the mass enhancement versus hybridisation behaviour for coulomb correlation $U = 7\text{eV}$, conduction bandwidth $W = 10\text{eV}$ and f electron energy $\epsilon_f = -1.5\text{eV}$. These parameter values apply for all the Figures 3.7 through to 3.11 and are reasonable for typical HF materials. Figure 3.8 shows how the mass enhancement of the model increases rapidly for hybridisations greater than 1.3 eV. However for hybridisations as large as $V = 1.3\text{eV}$ the Fermi wave vector has deviated appreciably from the zero down spin occupation value of 0.0669eV (see Section 3.3.3) so that the initial assumption of no down spin occupation does not apply. The model therefore cannot be trusted for hybridisations greater than $V = 1.3\text{eV}$. In Chapter 4 an attempt is made to generalise the technique to the weakly magnetic case for the impurity and thus probe the larger hybridisation region. The model is extended for the impurity case, for which exact results are available as a test case for the

possible extension of the lattice model to the weakly ferromagnetic regime. Figure 3.7 shows in more detail the mass enhancement for hybridisations of magnitudes more consistent with the assumptions of the model. The figure shows mass enhancements of around 12 for hybridisations of 0.85eV ($\Delta = 0.2\text{eV}$). The model therefore predicts a build up of mass enhancement as the hybridisation increases and the magnetic state breaks down. It cannot, however, be pushed to the larger hybridisation regime where the truly very heavy masses occur.

3.3.3. The Fermi Wavevector.

For a constant unhybridised conduction band density of states and ϵ_k a function of $|k|$ the conduction band energies, ϵ_k , must vary as the cube of the wavevector. The expression

$$\epsilon_k = W \left[\frac{k}{k_{\max}} \right]^3 - W + T_p, \quad (3.3.12)$$

where T_p and W are the top of and width of the conduction band respectively, ensures that ϵ_k equals T_p for the maximum value of k and ϵ_k equals B_t , the bottom of the conduction band, when k equals zero. When we substitute the value of ϵ_k when k equals k_{Fm} from equation (3.3.10) into equation (3.3.12) we find:

$$\left[\frac{k}{k_{\max}} \right] = \left[\frac{1}{W} \left[\frac{v^2}{\Sigma(0) + \epsilon_f} - T_p + W \right] \right]^{\frac{1}{3}}. \quad (3.3.13)$$

The behaviour of the quasi band Fermi wavevector with increasing hybridisation is shown in Figures 3.9 and 3.10. As the hybridisation increases the Fermi wavevector and Fermi volume also increase consistent with an increase in down spin occupation.

Figure 3.9 shows that for $V = 0.75\text{eV}$ ($\Delta = 0.177\text{eV}$), the Fermi wavevector has increased in size by approximately 2% over the unperturbed Fermi wavevector of 0.0669eV , an amount considered large enough to determine the limit of the model's validity. Figure 3.10 is included for completeness and shows how the Fermi wavevector increases dramatically as the hybridisation is increased beyond about 0.85eV ($\Delta = 0.2\text{eV}$).

3.3.4. The f Down Spin Density of States.

The band density of states, $N(E)$, is defined as the sum of all the single particle density of states:

$$N(E) = - \frac{1}{\pi} \text{Im} \sum_{\mathbf{k}} G_{\downarrow}(E+i\delta, \mathbf{k}). \quad (3.3.14)$$

The model allows the calculation of the f down spin Green function for energies above the Fermi level:

$$G_{f\downarrow}(Z, \mathbf{k}) = \frac{1}{Z - \epsilon_f - \frac{V^2}{Z - \epsilon_{\mathbf{k}}} - \Sigma_{f\downarrow}(Z)} \quad E > 0, \quad (3.3.15)$$

and therefore we can calculate the f down band density of states above the Fermi level. The density of states can be divided into two energy regions. For energies less than the magnon energy the down spin f electron Green function has a quasi particle pole for each \mathbf{k} . The quasi particle pole occurs at energy $\epsilon_{\mathbf{k}m}$ given by the Dyson equation (3.2.24) where the index m allows for the possibility of more than one quasi particle for a given \mathbf{k} . In the energy region $0 < E < \hbar\omega_{\text{mag}}$ the f down spin density of states is given by the sum of the weights in the quasi particle poles for each \mathbf{k} . For energies $E \geq \hbar\omega_{\text{mag}}$, the continuum, the density of states is calculated without any approximation and is found to join continuously at the magnon energy with the density of states for $E < \hbar\omega_{\text{mag}}$.

For $E < \hbar\omega_{\text{mag}}$

$$G_{ff\downarrow}(E+i\delta, k) = \sum_m \frac{Z(\epsilon_{km})}{(E + i\delta - \epsilon_{km})}, \quad (3.3.16)$$

where $Z(\epsilon_{km})$ is the weight in the quasi particle pole. Thus

$$N(E) = \sum_{km} Z(\epsilon_{km}) \delta(E - \epsilon_{km}), \quad (3.3.17)$$

where km are the wavevectors of the quasi particle states in band m . The sum over km is as usual changed to an integral over energy from the bottom to the top of the band to find

$$N(E) = \frac{V^2}{W(E - \epsilon_f - \Sigma_{ff\downarrow}(E))^2}, \quad E < \hbar\omega_{\text{mag}}. \quad (3.3.18)$$

For energies greater than the magnon energy the density of states is calculated from equation (3.3.14). At the magnon energy the density of states is given exactly as:

$$N(E = \hbar\omega_{\text{mag}}) = -\frac{1}{\pi} \lim_{\delta \rightarrow 0} \text{Im} \left[\frac{1}{(\hbar\omega_{\text{mag}} - \epsilon_f + i\delta)} - \frac{1}{W(\hbar\omega_{\text{mag}} - \epsilon_f + i\delta) \int_{Bt}^{Tp} \frac{V^2}{(\hbar\omega_{\text{mag}} - \epsilon_f + i\delta)(\epsilon - \hbar\omega_{\text{mag}} - i\delta) + V^2} d\epsilon} \right] \quad (3.3.19)$$

where Tp and Bt are the top and bottom of the unhybridised conduction band respectively. Therefore

$$N(E = \hbar\omega_{\text{mag}}) = \frac{1}{\pi} \text{Im} \left[\frac{1}{(\hbar\omega_{\text{mag}} - \epsilon_f + i\delta)} - \frac{V^2}{W(\hbar\omega_{\text{mag}} - \epsilon_f + i\delta)^2} \int_{Bt}^{\text{Tp}} \frac{d\epsilon}{(\epsilon - \hbar\omega_{\text{mag}} + \frac{V^2}{(\hbar\omega_{\text{mag}} - \epsilon_f)} - i\delta)} \right], \quad (3.3.20)$$

and after taking the imaginary part in equation (3.2.20) we find that at the magnon energy the f down spin density of states is given as:

$$N(E = \hbar\omega_{\text{mag}}) = \frac{V^2}{W(\hbar\omega_{\text{mag}} - \epsilon_f)^2}, \quad (3.3.21)$$

which joins continuously with the density of states for $E = \hbar\omega_{\text{mag}} - \zeta$, where ζ is a small quantity, of equation (3.3.18).

The resulting f down spin electron density of states is shown in Figure 3.11 for $U = 7\text{eV}$, $W = 10\text{eV}$, $\epsilon_f = 5\text{eV}$, and $\hbar\omega_{\text{mag}} = 0.005\text{eV}$, as in the mass enhancement calculation, and $V = 0.35\text{eV}$.

The f down spin density of states exhibits the expected narrow resonance around energy at $\epsilon_f + U$ which is consistent with the picture of most of the f down spin weight still being around this energy. It also shows a very narrow resonance close to the spin wave energy of 0.005eV , which is identified as a precursor of the Kondo resonance.

3.3.5. Discussion.

The model is seen to predict build up of Kondo like behaviour of mass enhancement, density of states and Fermi wavevector with increasing hybridisation up to $V \cong 0.75\text{eV}$, if the model is only strictly trusted in the strongly ferromagnetic regime. To probe the larger hybridisation regime the restriction to no down spin

occupation must be lifted and is the subject of the following chapter. The model does succeed in predicting that the build up of HF behaviour is concurrent with breakdown of the magnetic state. However the wrong exponent in the effective Kondo temperature remains a problem. This error in the exponent is attributed to the up spin density of states used in the calculation being too small by a factor of two. An attempt to correct the exponent in the Kondo temperature is given in the following chapter for the impurity as a test for a possible way of improving the lattice effective Kondo temperature.

Figure 3.7.

The Mass Enhancement Versus Hybridisation

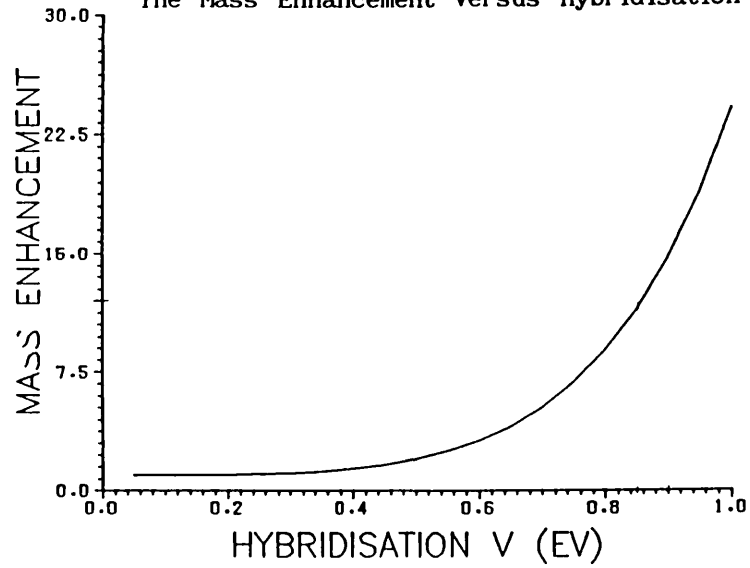


Figure 3.9.

The Fermi Wavevector Versus Hybridisation

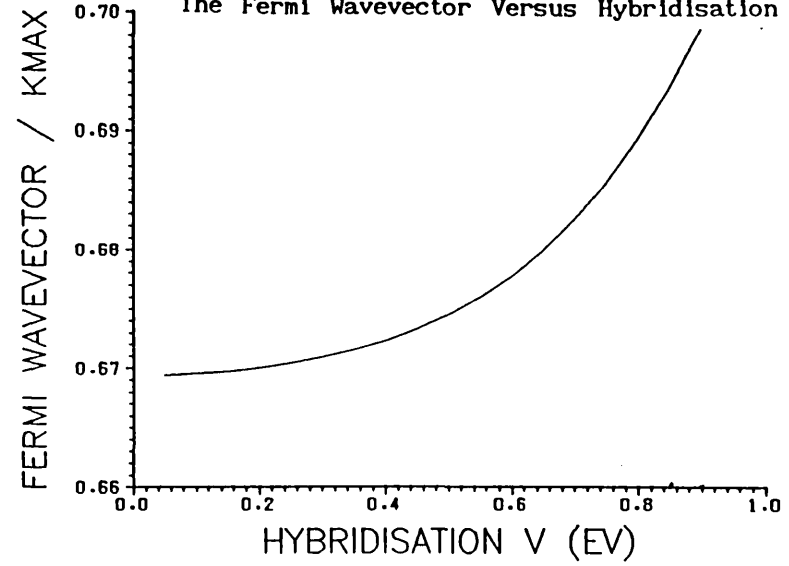


Figure 3.8.

The Mass Enhancement Versus Hybridisation

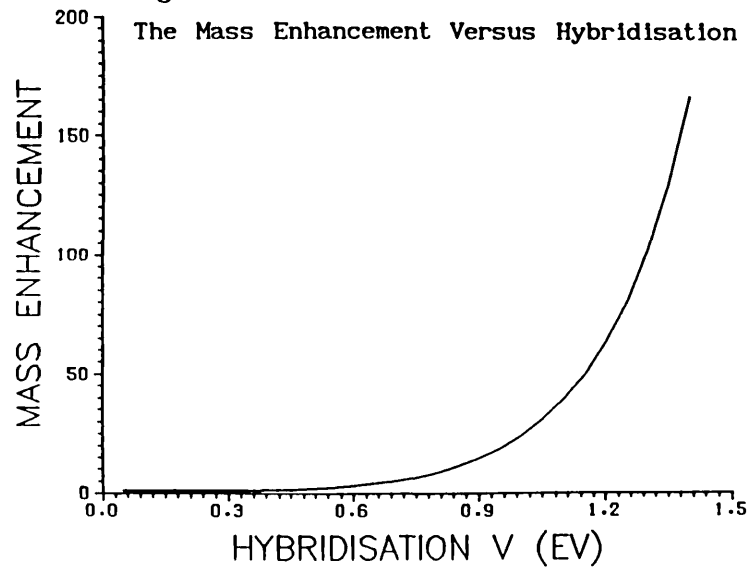


Figure 3.10.

The Fermi Wavevector Versus Hybridisation

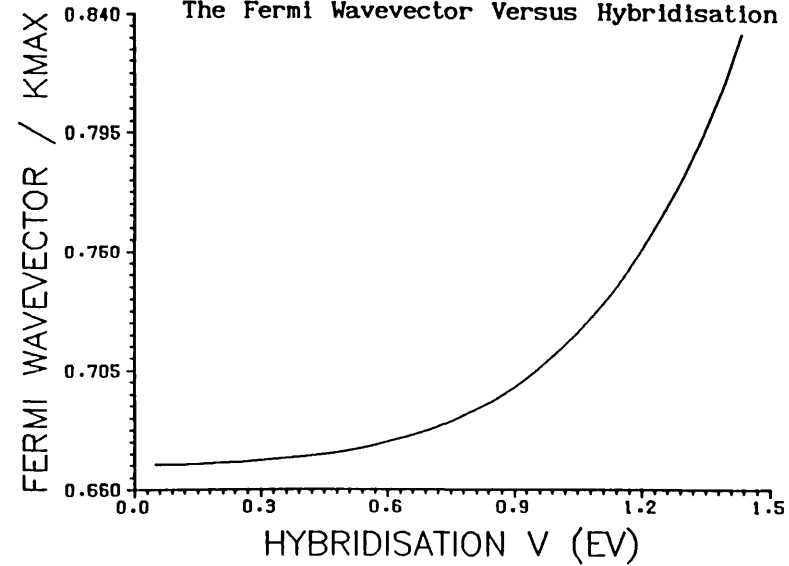
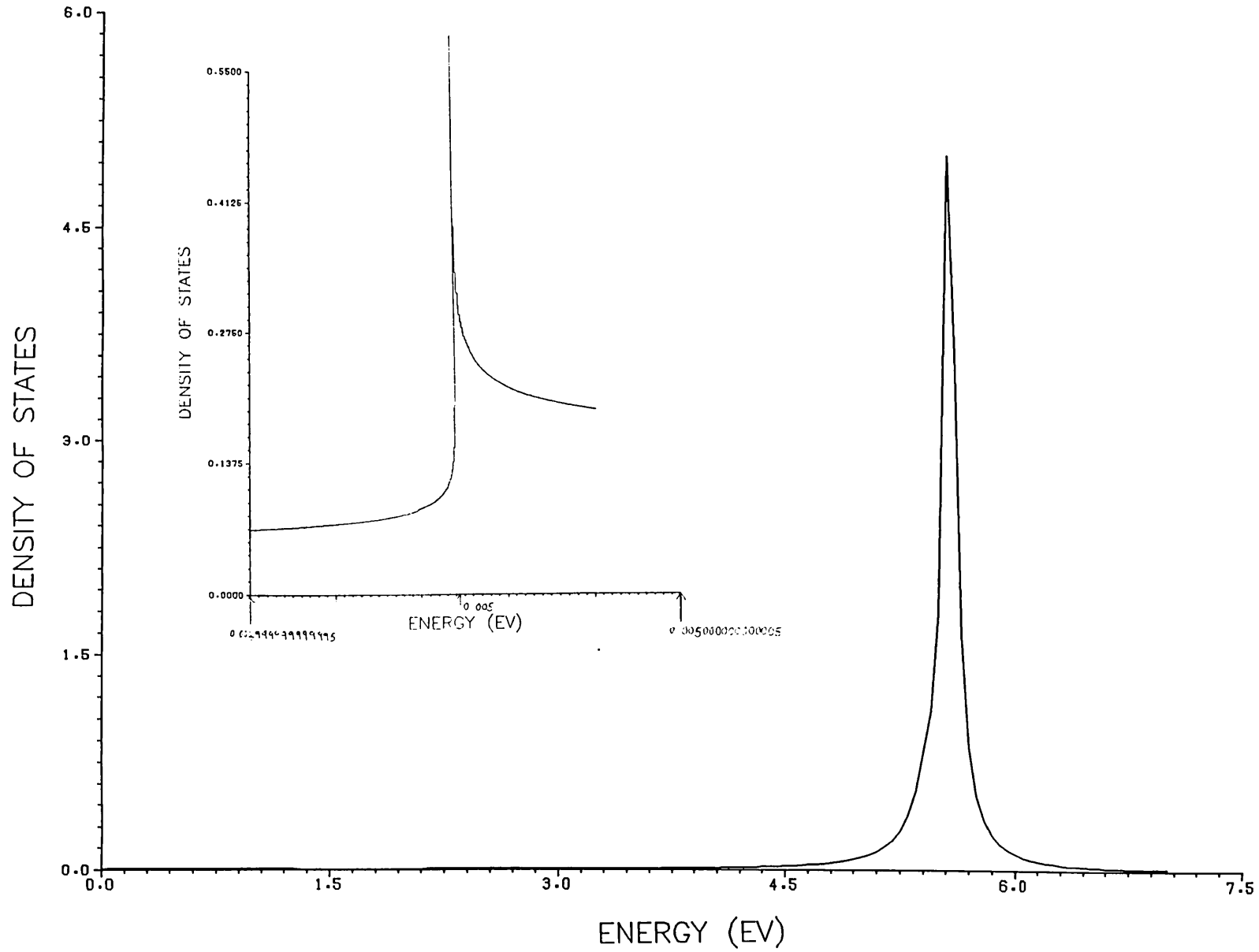


Figure 3.11. F DOWN SPIN DENSITY OF STATES FOR $V = 0.35\text{EV}$



3.4. THE EXCHANGE INTERACTION IN HEAVY FERMION SYSTEMS.

3.4.1. Introduction.

In normal rare earth metals the magnetism is a consequence of the exchange interaction:

$$I_{\text{ex}} = - J_{\text{ex}} \underline{S}_i \cdot \underline{\sigma}_i , \quad (3.4.1)$$

an on site interaction between the f spin (σ) and conduction electron spins (S) such that for J_{ex} positive it is energetically favourable to align these spins parallel. Via the conduction electrons a localised impurity spin on one site can interact indirectly with impurity spins on neighbouring sites tending to align them all parallel or antiparallel depending on the sign of J_{ex} . The conduction band is polarised via the exchange interaction. However it can also be polarised via hybridisation. Therefore the R.K.K.Y. interaction, that is the interaction between ions which results via conduction electron polarisation and governs the magnetism of a system, is built up via both exchange and hybridisation. The question of how the hybridisation and exchange interactions compete in the range of systems from the rare earth to the HF is the subject of the following sections.

We know that the hybridisation term of the Anderson impurity hamiltonian transforms under a Schrieffer-Wolff transformation (Schrieffer and Wolff (1966)) to an exchange interaction, as defined in equation (1.2.1), (or equivalently equation (3.4.1) where i is the impurity site) with a negative effective coupling constant $-2V^2/|\epsilon_f|$. The result is usually assumed to apply also to the lattice so that in a model for say gadolinium where the size of the ground state moment indicates that the total exchange coupling must be positive, the hybridisation is neglected. On the other hand in theories of the non magnetic HF systems the exchange interaction is generally neglected in favour of the hybridisation between the conduction and f electrons so that these systems are often modelled by a periodic Anderson hamiltonian. It is through this hybridisation that f electron weight is built up at the Fermi level resulting in the large mass enhancement and other hallmarks of the

HF systems. For the non magnetic HF systems, then, the hybridisation term seems to dominate the ground state properties, including the magnetism, and it seems reasonable to neglect any exchange interaction in its favour. As the f level energy moves deeper towards the normal rare earth regime and the hybridisation matrix decreases the exchange interaction takes over and dominates in the R.K.K.Y. interaction. Any treatment of the full class of rare earth systems must therefore include accounts of both these interactions in the intermediate regime where neither exchange nor hybridisation dominates.

From a Schrieffer-Wolff transformation for the Anderson impurity hamiltonian plus exchange interaction we find that in the Kondo limit, $V \ll |\epsilon_f|$, the exchange and hybridisation add as a new effective exchange interaction when $J_{ex} \ll 2V^2/|\epsilon_f|$ for J_{ex} positive or negative, and also for $J_{ex} \gg 2V^2/|\epsilon_f|$ when J_{ex} is positive. To study the competition between exchange and hybridisation in the lattice a variational calculation of the single particle f down spin Green function is made for an assumed ferromagnetic system which is modelled by the spin degenerate periodic Anderson hamiltonian plus exchange interaction with J_{ex} positive. A calculation of the effective Kondo temperature for this model shows that, for the effective Kondo temperature at least, exchange and hybridisation add as an effective exchange, as in the impurity case. Also as $V \rightarrow 0$ this effective Kondo temperature agrees exactly with the Bethe ansatz result. In the region $J_{ex} \approx 2V^2/|\epsilon_f|$ it is seen that, as in the impurity case, the exchange and hybridisation do not add simply as an effective exchange interaction. Also we find that in the region where J_{ex} is of order $2V^2/|\epsilon_f|$ the exchange interaction can have a non negligible effect on the mass enhancement. For HF systems like $CeSi_x$ in which the exchange and hybridisation are competing in the ground state we propose that exchange should be included in the model.

3.4.2. A Schrieffer - Wolff Transformation.

The Schrieffer-Wolff transformation is performed on the Anderson impurity hamiltonian:

$$H_{\text{imp}}^A = \sum_{\mathbf{k} \sigma} \varepsilon_{\mathbf{k}} c_{\mathbf{k}\sigma}^\dagger c_{\mathbf{k}\sigma} + \sum_{\sigma} \varepsilon_f f_{\sigma}^\dagger f_{\sigma} + U f_{\uparrow}^\dagger f_{\uparrow} f_{\downarrow}^\dagger f_{\downarrow} + \sum_{\mathbf{k}\sigma} V (c_{\mathbf{k}\sigma}^\dagger f_{\sigma} + f_{\sigma}^\dagger c_{\mathbf{k}\sigma}), \quad (3.4.2)$$

where $c_{\mathbf{k}\sigma}^\dagger$ creates a conduction electron in a state of energy $\varepsilon_{\mathbf{k}}$, momentum \mathbf{k} and spin σ and f_{σ}^\dagger creates an f electron in a state of energy ε_f and spin σ on the impurity site. The aim of the transformation is to project out operations which change the number of f electrons in a state. The transformation leads to a new hamiltonian:

$$H_{\text{eff}} = \frac{2V^2}{|\varepsilon_f|} \underline{S} \cdot \underline{\sigma} + H_0 + \bar{H}, \quad (3.4.3)$$

where

$$\underline{S} \cdot \underline{\sigma} = \sum_{\sigma \mathbf{k} \mathbf{k}'} \left[c_{\mathbf{k}'\sigma}^\dagger c_{\mathbf{k}-\sigma} f_{-\sigma}^\dagger f_{\sigma} + \sum_{\sigma'} \frac{\sigma \sigma'}{2} c_{\mathbf{k}'\sigma}^\dagger c_{\mathbf{k}\sigma} f_{\sigma'}^\dagger f_{\sigma'} \right]. \quad (3.4.4)$$

The term \bar{H} contains a direct spin independent interaction, a term which shifts the f electron energy and a term which changes the occupancy of the f orbital by two (Schrieffer and Wolff (1966)). In the new effective hamiltonian H_{eff} the important interaction is of the form of the exchange term of the s-d hamiltonian of equation (1.2.1). The exchange coupling strength, $-2V^2/|\varepsilon_f|$, of the effective exchange interaction is negative and is built entirely from hybridisation. The negative sign of the effective coupling constant means that it is energetically favourable to align the conduction and impurity spins antiparallel resulting in a quenching of the impurity moment. Therefore through the Schrieffer-Wolff transformation the non magnetic ground state and resistance minimum of the Anderson impurity hamiltonian can be viewed in terms of the Kondo type picture. When the exchange coupling constant of equation (1.2.1) is negative the s-d hamiltonian is normally referred to as the Kondo hamiltonian.

In the remainder of this section the results are quoted for a

Schrieffer-Wolff transformation on the Anderson impurity hamiltonian plus exchange interaction. The Anderson impurity hamiltonian of equation (3.4.2) with an added exchange interaction is written:

$$H_{imp}^{AI} = H_{imp}^A + I_{imp} \quad (3.4.5)$$

where

$$I_{imp} = - J_{ex} \underline{S} \cdot \underline{\sigma} \quad (3.4.6)$$

The hybridisation and exchange are both treated as perturbations and following Schrieffer and Wolff (1966) a canonical transformation is chosen to eliminate the hybridisation term of the impurity hamiltonian of equation (3.4.5) to first order. The two interactions, exchange and hybridisation, can only be compared if the orbital angular momentum of the impurity is neglected, since otherwise the hybridisation can result in a change of orbital angular momentum which the exchange interaction cannot.

We follow the method of Schrieffer and Wolff (1966) and take the limit U infinite to exclude intermediate states with double f occupancy. The transformed hamiltonian is given as:

$$H_{eff}^I = - \left[J_{ex} - \frac{2V^2}{|\epsilon_f|} \right] \underline{S} \cdot \underline{\sigma} + H_o + \bar{H}$$

$$- \sum_{\substack{k_1, k_2, k_3 \\ \sigma, \sigma'}} \frac{(\sigma\sigma')VJ_{ex}}{2(\epsilon_f - \epsilon_{k_1})} c_{k_1, \sigma'}^\dagger c_{k_2, \sigma}^\dagger c_{k_3, \sigma} f_{\sigma'}$$

$$- \sum_{\substack{k_1, k_2, k_3 \\ \sigma}} \frac{J_{ex} V}{(\epsilon_f - \epsilon_{k_1})} c_{k_1, -\sigma}^\dagger c_{k_2, \sigma}^\dagger c_{k_3, -\sigma} f_{\sigma} \quad (3.4.7)$$

where \bar{H} is as in equation (3.4.3). In the limits

$$U \rightarrow \infty, V \ll |\epsilon_f| \quad \text{and} \quad \left| J_{\text{ex}} - \frac{2V^2}{|\epsilon_f|} \right| \gg \left| \frac{J_{\text{ex}} V}{|\epsilon_f|} \right|,$$

or equivalently

$$V \ll |\epsilon_f| \left\{ \begin{array}{l} J_{\text{ex}} > 0 \quad \text{and} \quad J_{\text{ex}} \gg 2V^2/|\epsilon_f| \quad \text{or} \quad J_{\text{ex}} \ll 2V^2/|\epsilon_f| \\ J_{\text{ex}} < 0 \quad \text{and} \quad J_{\text{ex}} \ll 2V^2/|\epsilon_f| \end{array} \right. , \quad (3.4.8)$$

the hamiltonian H_{eff}^I reduces to

$$H_{\text{eff}}^I = - J \underline{S} \cdot \underline{\sigma} + H_0 + \bar{H}, \quad (3.4.9)$$

where

$$J = \left[J_{\text{ex}} - \frac{2V^2}{|\epsilon_f|} \right]. \quad (3.4.10)$$

Therefore within the limits defined in equation (3.4.8) the important term is again an exchange interaction with a new exchange coupling constant J . With J_{ex} negative the total coupling constant is negative and a non magnetic ground state is favoured. For J_{ex} positive the exchange interaction favours a magnetic ground state and will dominate for J_{ex} large enough to determine the sign of J . If this new impurity result is also true for the lattice then the criterion for a Kondo like non magnetic ground state of equation (1.4.15) becomes:

$$-\frac{1}{e(-J)\rho_0} > A \frac{(\rho_0 J)^2}{N_f^2}, \quad (3.4.11)$$

with J given by equation (3.4.10). The assumption that impurity results can be applied to the lattice is found to be not unreasonable by Read, Newns and Doniach (1984). The authors find that for large N_f , where N_f is the orbital degeneracy of the f

level, the concentrated system behaves as a lattice of impurities, intersite effects coming in at order $(1/N_f)$.

Consider the rare earth systems where J_{ex} is positive. For very small hybridisation, the criterion for magnetism of equation (3.4.11) predicts that the magnetic ground state is stable. The result therefore supports the treatment of the magnetic rare earth systems by an R.K.K.Y. interaction. At the other extreme of large hybridisation, $2V^2/|\epsilon_f| \gg J_{ex}$, the hybridisation dominates and the ground state is non magnetic. In this large hybridisation region the result supports the Anderson lattice treatment. In the intermediate regime where J_{ex} is of the order of $2V^2/|\epsilon_f|$ there can exist either a magnetic or a non magnetic ground state. In this intermediate regime the exchange and hybridisation do not simply couple as an effective exchange interaction.

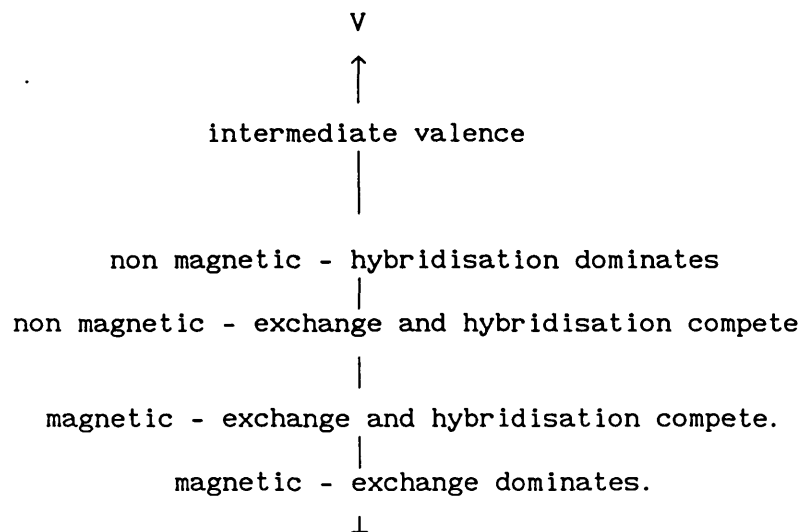


Figure 3.12. The variation from magnetic to non magnetic ground state in the rare earths with increasing hybridisation. We assume that J_{ex} remains fairly constant from system to system but that the hybridisation varies.

From Figure 3.12 where the arrow points in the direction of increasing hybridisation we see that the systems with a Kondo like ground state which are nearest to integral valence, that is, have the smallest hybridisation, are those in which the exchange interaction could play an important role. Some HF systems could

therefore fall into regime of non negligible exchange interaction implying that the exchange interaction should be included in their treatment. However it is possible that heaviness only occurs when $2V^2/|\epsilon_f| \gg J_{ex}$ so that the neglect of exchange in the treatment of HF systems is reasonable. In the following section we investigate the effect of exchange and hybridisation on the mass enhancement when J_{ex} is of the order of $2V^2/|\epsilon_f|$, via a variational calculation for the lattice.

3.4.3. The f Electron Green Function.

In the present section the variational calculation of Section (3.2) is reworked with an exchange interaction included in the hamiltonian. We treat the case where the exchange interaction favours parallel alignment of the conduction and impurity spins since this is the situation in the rare earth systems.

The system is again assumed strongly ferromagnetic with no down spin occupation in the ground state and is described by the Anderson lattice hamiltonian with an exchange interaction included:

$$H_{latt}^{AI} = H_{latt}^A + I_{latt}, \quad (3.4.12)$$

where H_{latt}^A is given by equation (3.2.1) and

$$I_{latt} = - \sum_{\sigma k' k q} J_{ex} \left[c_{k\sigma}^\dagger c_{k+q-\sigma} f_{k',-\sigma}^\dagger f_{k',-q\sigma} + \sum_{\sigma'} \frac{\sigma\sigma'}{2} c_{k\sigma}^\dagger c_{k+q\sigma} f_{k',\sigma'}^\dagger f_{k',-q\sigma'} \right], \quad (3.4.13)$$

with $J_{ex} > 0$. At this stage it is useful to determine the exact form of the f electron Green function as in Section (3.2.3). From a general diagrammatic expansion treating the coulomb, hybridisation and exchange interactions as perturbations the f down spin single particle Green function is written as:

$$\begin{aligned}
\overline{\overline{G_{ff}(k,E)}} &= \overline{G_{ff}^{\circ}(k,E)} + \overline{G_{ff}^{\circ}(k,E)} \overline{G_{cf}(k,E)} + \overline{G_{ff}^{\circ}(k,E)} \overline{\left(\sum_{ff}^I(k,E)\right)} \overline{G_{ff}(k,E)} \\
&\quad + \overline{G_{ff}^{\circ}(k,E)} \overline{\left(\sum_{cf}^I(k,E)\right)} \overline{G_{cf}(k,E)}
\end{aligned} \tag{3.4.14}$$

$$\begin{aligned}
\overline{\overline{G_{cf}(k,E)}} &= \overline{G_{cf}^{\circ}(k,E)} \overline{G_{ff}(k,E)} + \overline{G_{cf}^{\circ}(k,E)} \overline{\left(\sum_{cf}^I(k,E)\right)} \overline{G_{ff}(k,E)} \\
&\quad + \overline{G_{cf}^{\circ}(k,E)} \overline{\left(\sum_{cf}^I(k,E)\right)} \overline{G_{cf}(k,E)}
\end{aligned} \tag{3.4.15}$$

where $G_{ff\downarrow}^{\circ}(k,E)$ and $G_{ff\downarrow}(k,E)$ are the unperturbed and full down spin f electron Green functions respectively, $G_{cf}(k,E)$ is the fourier transform of the Green function $\langle 0 | T [c_{k\downarrow}^{fc\downarrow}(t) f_{k\downarrow}^{\dagger}(0)] | 0 \rangle$. Also $G_{cc\downarrow}^{\circ}(k,E)$ and $G_{cc\downarrow}(k,E)$ are the unperturbed and full down spin conduction electron Green functions respectively. Also $\sum_{ff\downarrow}^I(k,E)_{ex}$ is a proper down spin f electron self energy representing all processes in which the f down spin electron first interacts with the system via the coulomb interaction or the exchange interaction and after all subsequent interactions it emerges still as an f down. $\sum_{fc\downarrow}^I(k,E)_{ex}$ is another proper self energy in which the f down spin electron first interacts with the system via the coulomb or exchange interactions and after all subsequent interactions it emerges as a down spin conduction electron. Finally $\sum_{cc\downarrow}^I(k,E)_{ex}$ is another proper self energy in which a down spin conduction electron first interacts with the system via exchange and after all subsequent interactions it emerges as a down spin conduction electron. The f down single particle Green function is therefore given as:

$$\begin{aligned}
G_{ff\downarrow}(k, E) = & G_{ff\downarrow}^{\circ}(k, E) + G_{ff\downarrow}^{\circ}(k, E) V G_{cf\downarrow}(k, E) + \\
& G_{ff\downarrow}^{\circ}(k, E) \Sigma_{ff\downarrow}^I(k, E) G_{ff\downarrow}(k, E) + \\
& G_{ff\downarrow}^{\circ}(k, E) \Sigma_{fc\downarrow}(k, E) G_{cf\downarrow}(k, E),
\end{aligned}
\tag{3.4.16}$$

where

$$\begin{aligned}
G_{cf\downarrow}(k, E) = & G_{cc\downarrow}^{\circ}(k, E) V G_{ff\downarrow}(k, E) + G_{cc\downarrow}^{\circ}(k, E) \Sigma_{cf}(k, E) G_{ff\downarrow}(k, E) \\
& G_{cc\downarrow}^{\circ}(k, E) \Sigma_{cc\downarrow}(k, E) G_{cf\downarrow}(k, E),
\end{aligned}
\tag{3.4.17}$$

so that

$$G_{ff\downarrow}(k, E) = \frac{1}{E - \varepsilon_f - \frac{(V + \Sigma_{cf\downarrow}(k, E)_{ex})^2}{(E - \varepsilon_k - \Sigma_{cc\downarrow}(k, E)_{ex})} - \Sigma_{ff\downarrow}^I(k, E)_{ex}}.
\tag{3.4.18}$$

The subscripts, ex, denote that these are the exact quantities. The same notation will be used without the subscripts, ex, for the corresponding approximate quantities of the model. From the form of the exact f down spin electron Green function of equation (3.4.18) we see that including an exchange interaction in the model modifies the f electron self energy term, introduces a conduction electron self energy and an additional contribution $\Sigma_{cf\downarrow}(k, E)_{ex}$ to the hybridisation. The result is a similar f electron Green function to that of equation (3.2.11) where exchange is not included in the model, but now with a new effective energy dependent hybridisation:

$$V^I(E)_{ex} = (V + \Sigma_{cf\downarrow}(k, E)_{ex}).
\tag{3.4.19}$$

The analysis of Section 3.4.2 predicts that if the impurity result

can be generalised to the lattice then in any lattice solution the hybridisation strength V and exchange coupling J_{ex} must appear as in equation (3.4.10). Therefore in the variational calculation we expect that for $J_{\text{ex}} \gg 2V^2/|\epsilon_f|$ and $J_{\text{ex}} \ll 2V^2/|\epsilon_f|$ we will find an effective hybridisation matrix V_{eff} :

$$V_{\text{eff}} = V - \frac{|\epsilon_f| J_{\text{ex}}}{2}, \quad (3.4.20)$$

(at least near the Fermi level) as well as a new effective Kondo temperature:

$$T_K^{\text{eff I}} = e^{-\frac{1}{(-J) \rho_0}} \quad \text{where} \quad J = J_{\text{ex}} - \frac{2V^2}{|\epsilon_f|}. \quad (3.4.21)$$

However from the diagrammatic expansion it is obvious that in general exchange and hybridisation appear in the f electron Green function in quite different ways. The exchange interaction contributes to a conduction electron self energy $\Sigma_{c_c \downarrow}(k, E)_{\text{ex}}$ and an energy dependent hybridisation $\Sigma_{c_f \downarrow}(k, E)_{\text{ex}}$.

In the remainder of this section the variational calculation for the f down spin electron is made and the competition between J_{ex} and V examined. An approximate ground state is calculated by making the Hartree Fock approximation to both the exchange and coulomb interactions so that the many body periodic Anderson hamiltonian plus exchange interaction becomes two single particle up and down spin hamiltonians as before:

$$H_{\uparrow} = \sum_{\mathbf{k}} \epsilon_{\mathbf{k}\uparrow} c_{\mathbf{k}\uparrow}^{\dagger} c_{\mathbf{k}\uparrow} + \sum_{\mathbf{k}} \epsilon_{f\uparrow} f_{\mathbf{k}\uparrow}^{\dagger} f_{\mathbf{k}\uparrow} + \sum_{\mathbf{k}} V (c_{\mathbf{k}\uparrow}^{\dagger} f_{\mathbf{k}\uparrow} + f_{\mathbf{k}\uparrow}^{\dagger} c_{\mathbf{k}\uparrow}), \quad (3.4.22)$$

$$H_{\downarrow} = \sum_{\mathbf{k}} \epsilon_{\mathbf{k}\downarrow} c_{\mathbf{k}\downarrow}^{\dagger} c_{\mathbf{k}\downarrow}, \quad (3.4.23)$$

$$\epsilon_{\mathbf{k}\uparrow} = \epsilon_{\mathbf{k}} - \frac{J_{\text{ex}}}{2} \langle n_{f\uparrow} \rangle, \quad (3.4.24)$$

$$\varepsilon_{k\downarrow} = \varepsilon_k + \frac{J_{ex}}{2} \langle n_{f\uparrow} \rangle, \quad (3.4.25)$$

$$\varepsilon_{f\uparrow} = \varepsilon_f - \frac{J_{ex}}{2} \left[\langle n_{c\uparrow} \rangle - \langle n_{c\downarrow} \rangle \right], \quad (3.4.26)$$

where $\langle n_{c\uparrow} \rangle$ and $\langle n_{c\downarrow} \rangle$ are the up and down spin conduction electron occupation in the ground state and $\langle n_{f\uparrow} \rangle$ is the up spin f occupation in the ground state. Within the Hartree Fock approximation we solve the up spin problem for the ground state:

$$|0\rangle^i = \prod_{\substack{kn\uparrow \\ occ}} a_{kn\uparrow}^{i\dagger} \prod_{k < k_F} c_{k\downarrow}^\dagger |V\rangle \quad (3.4.27)$$

where the up spin eigenstates $a_{kn\uparrow}^{i\dagger} |V\rangle$ and energies ε_{kn}^i as well as the conduction and f electron amplitudes, B_{kn}^i and A_{kn}^i , in a state are given by equations (3.2.3) to (3.2.6) with ε_f replaced by $\varepsilon_{f\uparrow}$ and ε_k by $\varepsilon_{k\uparrow}$. In the ground state $|0\rangle^i$ the up and down spin bands are as in Figure (3.1) but with up spin bands shifted by $-J_{ex} \langle n_{f\uparrow} \rangle / 2$ and the down spin bands by $J_{ex} \langle n_{f\uparrow} \rangle / 2$ due to the exchange interaction.

With the approximate ground state established the steps of the variational calculation are repeated. Firstly a variational wavefunction is proposed for the f down spin electron. The variational wavefunction of the spin only calculation (see equation (3.2.13)) still represents the sum of the most likely processes occurring when a down spin electron enters the system, even with the addition of an exchange interaction. Once again the f down spin electron can access the level at $\varepsilon_{f\downarrow} + U \langle n_{f\uparrow} \rangle$ or, via the hybridisation any of the unoccupied conduction states. Also, since the f weight in the unoccupied up spin states is still small, the additional lowest energy excitations which are most likely are those in which a down spin f, or conduction electron, excites a particle hole pair in the opposite spin band and propagates with the hole as a magnon. The third process can now occur via the exchange or the coulomb interactions. The variational wavefunction is written:

$$|\psi\rangle^i = \left[D_k^i f_{k\downarrow}^\dagger + F_k^i c_{k\downarrow}^\dagger + \sum_{k' > k_F} G_{k',i}^i a_{k',i\uparrow}^\dagger S_{k-k'}^- \right] |0\rangle, \quad (3.4.28)$$

where $S_{k-k'}^-$ is the approximate magnon creation operator of equation (3.2.14). As in Section 3.2.3 we obtain equations for the coefficients D_k^i , F_k^i , $G_{k',i}^i$ by left multiplying the Schrodinger equation by each of the constituent elements of the variational wavefunction $|\psi\rangle^i$. The equations for the coefficients are solved for a Dyson equation in the limit of small hybridisation and $J_{ex} \ll U$. The Schrieffer-Wolff transformation of Section (3.4.2) for the impurity predicts that, for J_{ex} as defined in equation (3.4.8), the exchange and hybridisation just add in the ratios J_{ex} to $2V^2/|\epsilon_f|$ to give an effective exchange coupling, J , of equation (3.4.10). However it cannot describe the regime where J_{ex} is of the order of $2V^2/|\epsilon_f|$. In order to be able to study this regime, for the lattice, and take the limit of small hybridisation we work to order $V^2/|\epsilon_f|^2$ and $J_{ex}/|\epsilon_f|$. Also in this Kondo limit $V < |\epsilon_f|$ the up spin f density of states above the Fermi level is approximated by its value at the Fermi level. Within these approximations (see Appendix A) the Dyson equation becomes:

$$E - \epsilon_f - \frac{(V + \Sigma_{fc\downarrow}^I(k, E))^2}{(E - \epsilon_k - \Sigma_{cc\downarrow}^I(k, E))} - \Sigma_{ff\downarrow}^I(k, E) = 0, \quad (3.4.29)$$

which agrees exactly with the form predicted by the general diagrammatic expansion of equation (3.4.18) with $\Sigma_{ff\downarrow}^I(k, E)$ calculated within the model as:

$$\Sigma_{ff\downarrow}^I(k, E) = U \langle n_{f\uparrow} \rangle + \sum_{\sigma} \frac{J_{ex}}{2} \langle n_{c\sigma} \rangle + \hat{\Sigma}_{ff\downarrow}^I(k, E), \quad (3.4.30)$$

where the first two terms are just the Hartree Fock contributions due to the coulomb and exchange interactions and

$$\hat{\Sigma}_{ff\downarrow}^I(k, E) = \frac{\langle n_{f\uparrow} \rangle U^2 A_{k_F^1}^{I2}}{\sum_{occ}^{k_1'} [E - \epsilon_{k_1'}^I - \hbar\omega_{k-k'}]} , \quad (3.4.31)$$

$$1 - \frac{U A_{k_F^1}^{I2} + J_{ex} B_{k_F^1}^{I2}}{\sum_{occ}^{k_1'} [E - \epsilon_{k_1'}^I - \hbar\omega_{k-k'}]}$$

where

$$A_{k_F^1}^{I2} = \frac{V^2}{|\epsilon_f|^2} , \quad (3.4.32)$$

is the f up spin density of states at the Fermi level in the limit of small hybridisation. The superscript I distinguishes this f electron self energy from that of Section (3.2) where exchange is not included.

Also $\Sigma_{fc\downarrow}(k, E)$ is given by:

$$\Sigma_{fc\downarrow}(k, E) = - \frac{\hat{\Sigma}_{ff\downarrow}^I(k, E) J_{ex}}{U A_{k_F^1}^I} , \quad (3.4.33)$$

and $\Sigma_{cc\downarrow}(k, E)$ by:

$$\Sigma_{cc\downarrow}(k, E) = \frac{J_{ex}}{2} \langle n_{f\uparrow} \rangle + \hat{\Sigma}_{cc\downarrow}(k, E) , \quad (3.4.34)$$

where the first term of equation (3.4.34) is just the Hartree Fock term and

$$\hat{\Sigma}_{cc\downarrow}(k, E) = \frac{\hat{\Sigma}_{ff\downarrow}^I(k, E) J_{ex}^2}{U^2 A_{k_F^1}^{I2}} , \quad (3.4.35)$$

In each of these self energies $\hbar\omega_{k-k'}$, is the magnon energy which is

later approximated by a constant $\hbar\omega_{\text{mag}}$ as in Section (3.2.3). In Section (3.2.3) it was stated that the approximate self energy $\hat{\Sigma}_{ff\downarrow}(E)$ of equation (3.2.18), which results from a variational treatment of the spin only model, is given exactly by the contribution of diagrams of Figure 3.3. Within the present treatment of the periodic Anderson model plus exchange interaction the self energy terms $\hat{\Sigma}_{ff\downarrow}^I(k,E)$, $\Sigma_{cf\downarrow}(k,E)$ and $\Sigma_{cc\downarrow}(k,E)$ can also be identified with the contributions of particular diagrams. When we express the coulomb and exchange interactions of equation (3.4.12) in terms of the Hartree Fock basis operators, $a_{kn\uparrow}^\dagger$, $a_{kn\downarrow}$, $f_{k\downarrow}^\dagger$, $f_{k\downarrow}$, $c_{k\downarrow}^\dagger$, $c_{k\downarrow}$, $n = 1$ or 2 then we can show that, within certain approximations, the self energies of the variational calculation can be identified as those of Figures 3.13 to 3.15. These approximations are: the up spin propagators $\overrightarrow{\text{---}} \uparrow$ and the down spin conduction and f electron propagators $\overrightarrow{\text{---}}_{c\downarrow}$ and $\overrightarrow{\text{---}}_{f\downarrow}$ are all approximated by their Hartree Fock expressions, the hybridisation is small, the magnon pole approximation is made to the susceptibility and the scattering between the up spin electron and the magnon results in zero momentum transfer. In each of Figures 3.13. to 3.15 the broken lines $\text{---}\cdot\text{---}\cdot\text{---}$ represent scattering via the coulomb or exchange interactions while the dotted lines $\text{---}\cdot\text{---}\cdot\text{---}$ represent scattering via the exchange interaction alone.

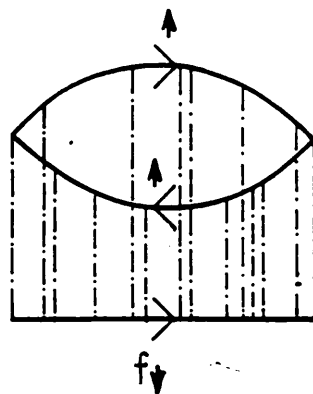


Figure 3.13. The self energy diagrams, other than Hartree Fock, in the down spin f electron self energy of the variational calculation for the spin degenerate periodic Anderson model plus exchange interaction. The broken lines represent scattering via both the coulomb correlation and exchange interaction.

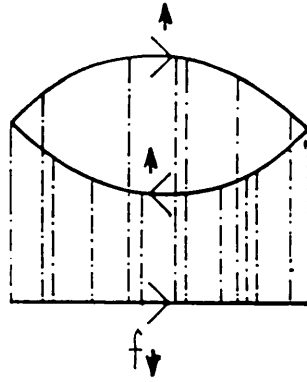


Figure 3.14. The diagrams in $\Sigma_{cf\downarrow}(k,E)$ of the variational calculation for the spin degenerate periodic Anderson model plus exchange interaction.

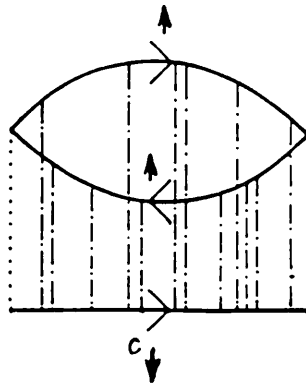


Figure 3.15. The diagrams, other than Hartree Fock, in the down spin f electron self energy $\Sigma_{cc\downarrow}(k,E)$ of the variational calculation for the spin degenerate periodic Anderson model plus exchange interaction.

3.4.4. Properties of The Solution.

With the approximation of a flat magnon dispersion, the self energies $\hat{\Sigma}_{ff\downarrow}^I(E)$, $\hat{\Sigma}_{cf\downarrow}(E)$ and $\hat{\Sigma}_{cc\downarrow}(E)$ are now momentum independent. These self energies are very similar to the f electron self energy of the spin only case and therefore have similar properties. For energies less than the magnon energy the imaginary part of any of the self energies is zero, and the Dyson equation (3.4.29) can be solved for quasi particle energies. Again near the magnon energy the f self energy $\Sigma_{ff\downarrow}^I(E)$ tends to zero so that for some energy \hat{E} very close to the magnon energy (see Figure 3.16)

$$\hat{E} - \varepsilon_f - \Sigma_{ff\downarrow}^I(\hat{E}) = 0 \quad (3.4.36)$$

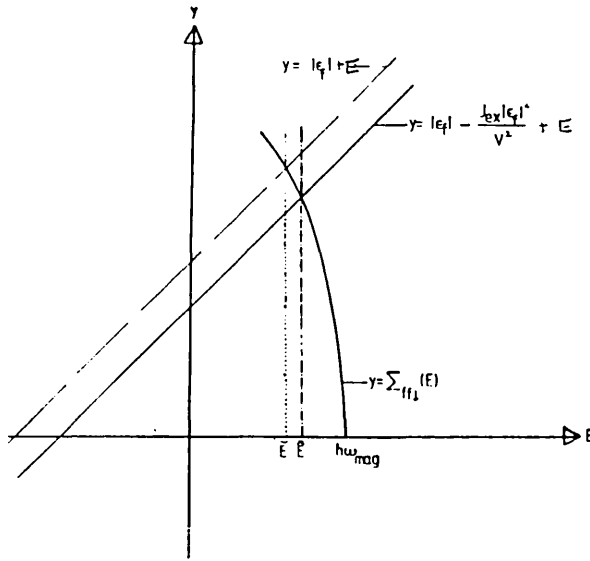


Figure 3.16. The f resonance energy for the spin degenerate periodic Anderson model plus exchange interaction. The figure illustrates the solution of equation (3.4.36).

When the self energy $\Sigma_{ff\downarrow}^I(\hat{E})$ is expanded in a Taylor series around \hat{E} then in the limit $U \rightarrow \infty$ the quasi particle energies very close to \hat{E} are given by:

$$(E - \hat{E})(E - \varepsilon_{k\downarrow}) = \frac{\hat{V}^2(\hat{E})}{1 - \Sigma'_{ff\downarrow}^I(\hat{E})}, \quad \Sigma'_{ff\downarrow}^I(\hat{E}) = \left. \frac{d\Sigma_{ff\downarrow}^I(E)}{dE} \right|_{E=\hat{E}} \quad (3.4.37)$$

where

$$\hat{E} = \varepsilon_f + \Sigma_{ff\downarrow}(\hat{E}) \quad (3.4.38)$$

and

$$\hat{V}^2(E) = (V + \Sigma_{cf}(\hat{E}))^2 \quad (3.4.39)$$

with $\Sigma_{cf}(\hat{E})$ given by equation (3.4.33). For energies close to \hat{E} the quasi particles form the bands of an f level of renormalised energy \hat{E} hybridising via a renormalised hybridisation with the conduction band. The quasi particle bands are drawn schematically as in Figure 3.5 with \tilde{E} replaced by \hat{E} .

As in the spin only case the magnetic state breaks down as the hybridisation increases and the resonance near the Fermi level accomodates non negligible down spin occupation. From Figure 3.16 we see that the inclusion of the exchange interaction shifts these quasi particle bands at the Fermi level relative to their positions in the spin only case so that the resonance position is shifted further away from the Fermi level. Therefore for any hybridisation the exchange interaction, with exchange coupling J_{ex} positive, stabilises the magnetic state in accord with the prediction of the criterion of magnetism of equation (3.4.11), where exchange and hybridisation are considered to add as an effective exchange interaction.

In the limit $U \rightarrow \infty$ we find using equation (3.4.36) to solve for $\hat{\Sigma}_{ff\downarrow}^{-1}(\hat{E})$ that

$$\hat{V}^2(\hat{E}) = v^2 \left[1 + \frac{J_{ex} |\epsilon_f|}{v^2} \right]^2, \quad (3.4.40)$$

If the the exchange and hybridisation do in fact combine as an effective exchange or effective hybridisation as in the impurity then we expect the hybridisation matrix to be given by equation (3.4.20). The disagreement between the expected result and the result of the variational calculation could be due to the fact that the variational wavefunction does not deal adequately with hybridisation, hence the wrong Kondo temperature in Section 3.3.1. However the implication that in general the hybridisation and exchange do not add as an effective hybridisation is the correct result, as is seen from the general diagramatic expansion.

The effective Kondo temperature of the model does however vindicate the idea that exchange and hybridisation add to give an an effective exchange interaction. The effective Kondo temperature of the model is defined as that magnon energy for which the ferromagnetic state breaks down. The breakdown is considered to occur when the resonance lies on the Fermi level, since then the down spin density of states below the Fermi level is holding non negligible down spin and the initial postulate of no down spin occupation is invalid. The resonance energy \hat{E} is defined in

equation (3.4.38) so that for $\hat{E} = 0$

$$-\epsilon_f - U\langle n_{f\uparrow} \rangle - \hat{\Sigma}_{ff\downarrow}^I(0) = 0 \quad (3.4.41)$$

and equation (3.4.41) can be solved for the magnon energy or effective Kondo temperature. The self energy term $\hat{\Sigma}_{ff\downarrow}^I(E)$ is considered to be well treated by the variational wavefunction of equation (3.4.28) so that we expect the calculated Kondo temperature to be a good test of whether exchange and hybridisation add as an effective exchange or not. In the limit of $U \rightarrow \infty$, the effective Kondo temperature is given by:

$$T_K^{eff} \propto e^{-W \left[\frac{V^2}{|\epsilon_f|} - J_{ex} \right]^{-1}} \quad (3.4.42)$$

For $J_{ex} = 0$ the effective Kondo temperature of the model reduces to the spin only result of equation (3.3.2) and is once again wrong by a factor of two in the exponent. This error is discussed in Section 3.3.1 and is treated in Chapter 4 for the impurity. However for $V \rightarrow 0$ the effective Kondo temperature agrees with the Kondo temperature of Read et al (1984) and Coleman (1983) where the system is modelled by the orbitally degenerate version of H_{latt}^{AI} (see equation (3.4.12)) with $V = 0$. The result for $V \rightarrow 0$ also agrees with exact Bethe Ansatz results for impurity. The agreement with exact results for $V \rightarrow 0$ vindicates the model definition of the effective Kondo temperature and shows that for $U \rightarrow \infty$ the variational ansatz treats the exchange interaction contribution to $\hat{\Sigma}_{ff\downarrow}^I(E)$ very well but, as in the spin only case, is lacking in the treatment of the hybridisation. We identify the origin of the error in the exponent of the Kondo temperature as due to the fact that even for large U there will be some down spin occupation in the ground state and subsequently some up spin self energy which is neglected in the $\langle n_{f\downarrow} \rangle = 0$ ground state. In Chapter 4 the effective Kondo temperature is improved for the impurity by treating the hybridisation of the up and down spins on an equal footing and

performing a self consistent calculation.

In equation (3.4.42) J_{ex} enters the exponent in the effective Kondo temperature as predicted by the Schrieffer Wolff transformation of Section (3.4.2) for the impurity, if we accept the missing factor of two in front of V^2 . The result is consistent with the postulate that for $V \ll |\epsilon_f|$ and $J_{ex} \ll 2V^2/|\epsilon_f|$ or $J_{ex} \gg 2V^2/|\epsilon_f|$ hybridisation and exchange can be thought of as simply adding to give a total exchange strength J of equation (3.4.10), favouring a magnetic or non magnetic ground state depending on the magnitude of J .

3.4.5. Conclusion.

From the variational treatment of the spin degenerate Anderson hamiltonian with exchange interaction we find that the magnetic state breaks down and the mass enhancement builds up with increasing hybridisation, as before. However we also find additional contributions to the down spin f electron self energy, $\hat{\Sigma}_{f\downarrow}(k,E)$, due to the exchange interaction which push the narrow down spin f resonance at the Fermi level nearer to $\hbar\omega_{mag}$ than for the $J_{ex} = 0$ case. If this were the only effect of exchange then the mass enhancement would be slightly decreased over that of the $J_{ex} = 0$ case for any hybridisation. However the exchange interaction also acts to increase the effective hybridisation (see equation (3.4.40)), so that for any hybridisation, V , the net result on the mass enhancement depends on which of the two competing effects of exchange is dominant.

The postulate that the exchange interaction and hybridisation present in rare earth systems combine as an effective exchange interaction for $J_{ex} \ll 2V^2/|\epsilon_f|$ or $J_{ex} \gg 2V^2/|\epsilon_f|$, with effective coupling constant J where

$$J = J_{ex} - \frac{2V^2}{|\epsilon_f|}, \quad (3.4.43)$$

as suggested by a Schrieffer Wolff transformation on the impurity is

vindicated by a lattice calculation of the effective Kondo temperature. In general, though, the variational calculation of the f down spin Green function shows that the hybridisation and exchange interactions affect the system in quite different ways. This result is in agreement with the predictions of the completely general diagrammatic expansion in which the exchange interaction leads to an energy dependent contribution, $\Sigma_{cf}(k,E)$, to the hybridisation as well as a conduction electron self energy, $\Sigma_{cc}(k,E)$. Therefore in general no simple addition of exchange and hybridisation is possible.

Consider the results and their application to rare earth systems where J_{ex} is positive. In gadolinium the f level is deep below the Fermi level, the hybridisation is small and the ground state is magnetic. As we move through the rare earth series the hybridisation changes. The magnetic ground state remains stable until the hybridisation is of such a magnitude that the criterion for a non magnetic ground state of equation (3.4.11) is satisfied. Some of these rare earth systems are heavy and are usually considered to be those in which the exchange interaction is negligible. In these systems the ground state is non magnetic and the hybridisation dominates in the mass enhancement. However there are other systems with possibly magnetic or non magnetic ground states where J_{ex} is of the order of $2V^2/|\epsilon_f|$. The variational calculation with the exchange interaction included shows how mass enhancement could build up via both exchange and hybridisation in these systems.

In their studies of $CeSi_x$ Sato et al (Preprint) claim that in this system exchange and hybridisation are competing for the hybridisations associated with $1.7 < x < 2.0$. In this HF system the magnetic state breaks down with increasing silicon concentration, or hybridisation. Therefore this system is an ideal candidate for comparison with the model. The authors postulate that magnetic $CeSi_{1.8}$ and non magnetic $CeSi_{1.9}$ flank very heavy systems (see Figure 3.17). Therefore for $CeSi_x$, at least, there may well be very heavy systems with $1.8 < x < 1.9$ in which the exchange interaction is not yet dominated by the hybridisation. These systems are suited to the description by the model developed here which shows how exchange could contribute to large mass enhancement.

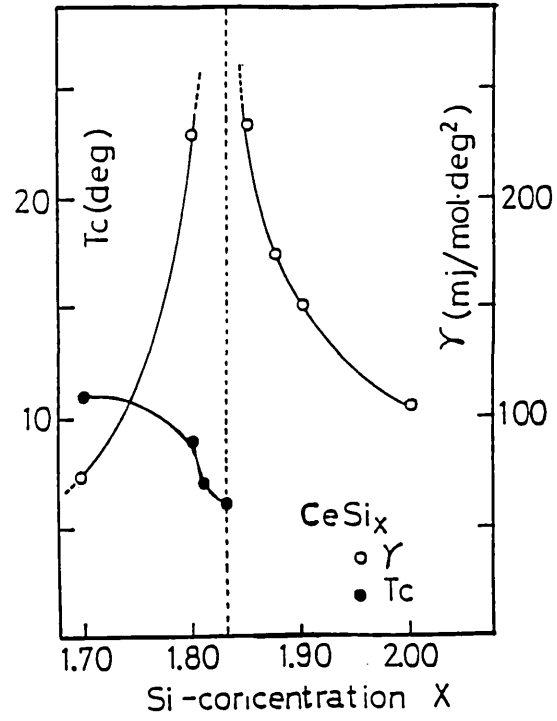


Figure 3.17. The γ (mJ/molK²) versus silicon concentration in CeSi_x (Sato et al (Preprint)).

CHAPTER 4.

THE WEAKLY MAGNETIC PROBLEM.

4.1. INTRODUCTION.

In Chapter 3 a model is developed for cerium systems to describe the breakdown of the strongly ferromagnetic state and the build up of HF behaviour with increasing hybridisation. The main limitation of the model is that the arguments on which it is based start to break down as soon as the hybridisation produces some non negligible down spin occupation. Therefore the next step must be to improve the model in order to describe the weakly ferromagnetic regime. Also the main possible problem result of the model of the previous chapter is the missing factor of two in the exponent of the effective Kondo temperature.

In the present chapter both the extension of the model to the weakly magnetic regime and the correction of the effective Kondo temperature are examined for the impurity. We initially model the strongly magnetic case to determine whether the discrepancy of two in the effective Kondo temperature of the previous chapter is a genuine difference between the lattice and impurity cases, or a defect in the variational method. The calculation is then extended to the weakly magnetic regime. The ultimate aim is to develop a model for the impurity in the weakly magnetic regime which gives reasonable agreement with Bethe ansatz and, via the lattice analogue, gives some insight on how to extend the lattice model to the weakly ferromagnetic regime.

The system under investigation is a dilute HF cerium system described by the Anderson impurity hamiltonian. It is assumed that a magnetic field acts on the impurity to ensure a magnetic ground state. First the variational method is used to calculate the f down spin Green function for the strongly magnetic case of no down spin f

occupation. The density of states is calculated and the effective Kondo temperature of the model is defined and evaluated for this strongly magnetic limit. As for the lattice calculation of Chapter 3 we find that the effective impurity Kondo temperature differs from the exact impurity result by a factor of two in the exponent. The self energy diagrams equivalent to the variationally calculated self energy are identified and found to be those of Edwards (1968). The model is next pushed into the weakly magnetic regime of non negligible down spin occupation which is analogous to the weakly ferromagnetic regime of the lattice problem. The self energies for both the up and down spin Green functions are postulated. Within certain approximations these are identical to the self energy of the variational calculation. The magnetisation is calculated as a function of magnetic field and is found to have the scaling behaviour predicted from Bethe ansatz results. The new Kondo temperature for the improved model is shown to be in better agreement with the exact Kondo temperature than that of the strongly magnetic model.

4.2. THE STRONGLY MAGNETIC CASE.

4.2.1. The Variational Calculation.

The spin degenerate Anderson impurity hamiltonian with magnetic field on the impurity is written:

$$H_{\text{imp}}^A = \sum_{\mathbf{k}\sigma} \varepsilon_{\mathbf{k}} \psi_{\mathbf{k}\sigma}^\dagger \psi_{\mathbf{k}\sigma} + \sum_{\sigma} \varepsilon_{f\sigma} \psi_{\sigma}^\dagger \psi_{\sigma} + \sum_{\mathbf{k}\sigma} (V_{\mathbf{k}} \psi_{\sigma}^\dagger \psi_{\mathbf{k}\sigma} + \text{h.c.}) + U \psi_{\sigma}^\dagger \psi_{\sigma} \psi_{-\sigma}^\dagger \psi_{-\sigma} , \quad (4.2.1)$$

where ψ_{σ}^\dagger creates an f electron on the impurity site with spin σ , and $\psi_{\mathbf{k}\sigma}^\dagger$ creates a conduction electron in a state of momentum \mathbf{k} , energy $\varepsilon_{\mathbf{k}}$ and spin σ . Also

$$\varepsilon_{f\sigma} = \varepsilon_f + (\sigma)\mu_B H, \quad (\sigma) = \begin{array}{l} + \text{ when the spin is down} \\ - \text{ when the spin is up} \end{array} , \quad (4.2.2)$$

so that the magnetic field only acts on the impurity. Following Gunnarson and Schönhammer (1983) we introduce the new one particle states:

$$\psi_{\varepsilon\sigma}^\dagger |V\rangle = \frac{1}{\tilde{V}(\varepsilon)} \sum_{\mathbf{k}} V_{\mathbf{k}}^* \delta(\varepsilon - \varepsilon_{\mathbf{k}}) \psi_{\mathbf{k}\sigma}^\dagger |V\rangle , \quad (4.2.3)$$

and make the model assumption

$$\sum_{\mathbf{k}} |V_{\mathbf{k}}|^2 \delta(\varepsilon - \varepsilon_{\mathbf{k}}) = |\tilde{V}(\varepsilon)|^2 , \quad (4.2.4)$$

so that within this new basis the hamiltonian can be rewritten as

$$H_{\text{imp}}^A = \int \sum_{\sigma} \varepsilon \psi_{\varepsilon\sigma}^\dagger \psi_{\varepsilon\sigma} d\varepsilon + \sum_{\sigma} \varepsilon_{f\sigma} \psi_{\sigma}^\dagger \psi_{\sigma} + \int \sum_{\sigma} (\tilde{V}(\varepsilon) \psi_{\sigma}^\dagger \psi_{\varepsilon\sigma} + \text{h.c.}) d\varepsilon + U \psi_{\sigma}^\dagger \psi_{\sigma} \psi_{-\sigma}^\dagger \psi_{-\sigma} + H_s . \quad (4.2.5)$$

The final term in the hamiltonian, H_s , just counts all the energies of those conduction electrons which do not hybridise with the impurity, that is those which have orbital angular momentum not

equal to three. This term will just give a constant energy shift of the total energy of these $l \neq 3$ non interacting electrons and will not contribute to the interesting physics. In the remainder of this chapter the unhybridised conduction band density of states is assumed to be a constant equal to the number of electron sites divided by the band width W . Therefore when we assume that the hybridisation V_k is real and momentum independent then

$$\sum_k |V|^2 \delta(\epsilon - \epsilon_k) = |\tilde{V}|^2, \quad (4.2.6)$$

$$\Rightarrow \tilde{V}^2 = \frac{V^2}{W} \quad (4.2.7)$$

As in the lattice case of Chapter 3 the first step in the variational calculation is to propose a ground state for the system described by the hamiltonian H_{imp}^A . Again we make the Hartree Fock approximation to the coulomb interaction. The coulomb interaction is assumed to be large so that the hybridisation of the down spin f level at energy $\epsilon_f + \mu_B H + U \langle n_{f\uparrow} \rangle$ produces negligible down spin f occupation. Therefore the approximate ground state has no down spin f electrons and consists of a filled Fermi sphere of down spin conduction electrons and a filled Fermi sphere of states resulting from the hybridisation of the up spin f electron level with the up spin conduction band. The ground state is written:

$$|0\rangle = \prod_{occ} \phi_{\epsilon_n}^\dagger \prod_{k < k_F} \psi_{k\downarrow}^\dagger \prod_{\substack{occ \\ l \neq 3}} \psi_{\epsilon_{l\uparrow}}^\dagger |V\rangle, \quad (4.2.8)$$

where $\phi_{\epsilon_n}^\dagger$ are the eigenstate creation operators for the states in the hybridised up spin bands. The operators $\phi_{\epsilon_n}^\dagger$ diagonalise the up spin hamiltonian:

$$H_{imp\uparrow}^A = \int \epsilon \psi_{\epsilon\uparrow}^\dagger \psi_{\epsilon\uparrow} d\epsilon + \epsilon_{f\uparrow} \psi_{f\uparrow}^\dagger \psi_{f\uparrow} + \int \tilde{V} (\psi_{f\uparrow}^\dagger \psi_{\epsilon\uparrow} + h.c.) d\epsilon, \quad (4.2.9)$$

where the energy integrals are from the bottom to the top of the unperturbed conduction band and

$$\phi_{E\uparrow}^\dagger = \int c(E, \varepsilon) \psi_{\varepsilon\uparrow}^\dagger d\varepsilon + d(E) \psi_{\uparrow}^\dagger. \quad (4.2.10)$$

$c^2(E, \varepsilon)$ is the weight of the up spin conduction state of energy ε in the new up spin eigenstate of energy E and $d^2(E)$ the f up spin weight in this eigenstate. Also

$$\int c^2(E, \varepsilon) d\varepsilon + d^2(E) = 1, \quad (4.2.11)$$

so that each new state can hold one electron and the operators $\phi_{E\uparrow}^\dagger$ $\phi_{E\uparrow}$ obey normal anticommutation relations. The coefficients $d(\varepsilon)$ are determined using the relations between the single particle up spin f electron Green function and the eigenstate Green function:

$$\langle\langle \psi_{\uparrow} \psi_{\uparrow}^\dagger \rangle\rangle_E = \int d^2(E) \langle\langle \phi_{E\uparrow} \phi_{E\uparrow}^\dagger \rangle\rangle_E dE, \quad (4.2.12)$$

$$\Rightarrow -\frac{1}{\pi} \text{Im} \langle\langle \psi_{\uparrow} \psi_{\uparrow}^\dagger \rangle\rangle_E = d^2(E). \quad (4.2.13)$$

From equation of motion methods the up spin f electron Green function in the Hartree Fock approximaton is:

$$\langle\langle \psi_{\uparrow} \psi_{\uparrow}^\dagger \rangle\rangle_E = \frac{1}{E + i\delta - \varepsilon_{f\uparrow} - \int_{Bt}^{Tp} \frac{\tilde{V}^2}{E + i\delta - \varepsilon} d\varepsilon}, \quad (4.2.14)$$

where Tp and Bt are the top and bottom of the unhybridised conduction band. To solve for $d^2(E)$ we take the imaginary part and use the usual definition:

$$\int_{Bt}^{Tp} \frac{\tilde{V}^2}{E + i\delta - \varepsilon} d\varepsilon = \Lambda(E) - i\Delta(E). \quad (4.2.15)$$

Since we have already assumed a constant unhybridised conduction band density of states of width W , we find that $\Delta(E)$ is a constant, $\Delta = \pi V^2/W$, independent of energy. Also the contribution of Λ is neglected as is usual in the literature since it just provides a small shift in the f level resonance position so that

$$d^2(E) = \frac{1}{\pi} \frac{\Delta}{(E - \epsilon_{f\uparrow})^2 + \Delta^2}, \quad (4.2.16)$$

is just the up spin f density of states. Therefore in any eigenstate of energy E , $d^2(E)$ gives a measure of the up spin f weight in that state. From equation (4.2.16) the up spin f weight in any up spin band eigenstate is seen to be small for all states of energy E except those for which $E \approx \epsilon_{f\uparrow}$. Similarly the up spin conduction electron weight in any eigenstate of energy E is:

$$c^2(E, \epsilon) = \delta(E - \epsilon) - \frac{\tilde{V}^2}{\pi} \text{Im} \left[\frac{1}{(E + i\delta - \epsilon)^2 (E - \epsilon_{f\uparrow} + i\Delta)} \right]. \quad (4.2.17)$$

For states with energy E far from $\epsilon_{f\uparrow}$ the up spin conduction weight in the state is practically unity. For states of energy E very close to $\epsilon_{f\uparrow}$ the second term in equation (4.2.17) is not negligible so that the up spin conduction weight in states of this energy is reduced and the eigenstate has more f character.

Within the Hartree Fock approximation, for $U \rightarrow \infty$, the up and down spin f densities of states in the ground state can be drawn schematically as in Figure 4.1

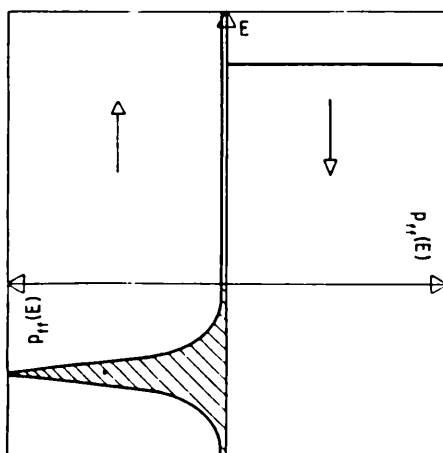


Figure 4.1. A schematic impurity density of states in the $U \rightarrow \infty$ Hartree Fock ground state. The hatched area denotes occupied density of states below the Fermi energy E_F .

The next stage in the calculation is to take better account of the coulomb correlation than the simple Hartree Fock approximation. From a general diagrammatic expansion in which both the coulomb interaction and the hybridisation are treated as perturbations the f down spin Green function can be written:

$$G_{ff\downarrow}(E) = \frac{1}{E - \varepsilon_{f\downarrow} - \int_{Bt}^{Tp} \frac{\tilde{V}^2}{(E-\varepsilon)} d\varepsilon - \Sigma_{ff\downarrow}(E)_{ex}}, \quad (4.2.18)$$

where everything that is unknown about the interactions of the system is stored in an exact self energy $\Sigma_{ff\downarrow}(E)_{ex}$. Within the Hartree Fock approximation the only contribution to this self energy is $U\langle n_{f\uparrow} \rangle$. The aim of the variational calculation is to take better account of the coulomb correlation and calculate further contributions to the exact self energy $\Sigma_{ff\downarrow}(E)_{ex}$. Correct account of the coulomb correlation is the basis of the impurity problem and a good treatment will yield the Kondo resonance in the f electron density of states and the resulting strange thermodynamic properties of these dilute HF systems.

As in the spin only lattice case a variational wavefunction is proposed for an f down spin electron entering this system described by the Anderson impurity hamiltonian H_{imp}^A . The wavefunction is written as the sum of all the lowest energy and most likely processes to occur if an f down spin electron were placed in the system. Once again an analogy can be drawn between the present situation and that of the nearly half filled Hubbard model with a ferromagnetic ground state (Edwards (1968)). Consider a schematic representation of the f weight in any state for the impurity ground state of equation (4.2.8) and Figure 4.1. When a down spin f electron enters the system described by hamiltonian H_{imp}^A , it can sample the unhybridised f down spin state at energy $E = \varepsilon_f + \mu_B H + U\langle n_{f\uparrow} \rangle$, any of the unoccupied down spin conduction electron states via hybridisation \tilde{V} , as well as an infinite number of other processes, all of which must be included for an exact self energy $\Sigma_{ff\downarrow}(E)_{ex}$. If only the first two possibilities are included, the

down spin eigenstates are given by equation (4.2.10) (with \uparrow replaced by \downarrow), in which $d^2(E)$ is now the down spin density of states, and we have the Hartree Fock solution. To improve on the Hartree Fock result we must take better account of the coulomb correlation by including more processes in the variational wavefunction. To determine the processes with the largest contribution to the f down spin self energy, other than the Hartree Fock contribution, an analogy is drawn between the present problem and that of the nearly half filled Hubbard model of Edwards (1968). There is only one type of electron in this problem and the coulomb correlation exists between any of these electrons on the same site. The density of states in the Hubbard model Hartree Fock ground state is as in Figure 3.2b. To improve on the Hubbard model Hartree Fock approximation we include diagrams with the smallest number of up spin electron lines since the up spin density of states above the Fermi level is small. Diagrams with the least number of electron lines involve the least number of integrations over this small up spin density of states above the Fermi level and have the largest contribution. Therefore in the Hubbard model self energy we include diagrams representing a down spin exciting a particle hole pair in the opposite spin band and then propagating with the up spin hole as a magnon and scattering off the up spin electron. The diagrams are represented schematically as in Figure 3.3 and are exact to second order for the strongly ferromagnetic case.

In the present Anderson impurity problem the coulomb correlation acts only between the f electrons on the impurity site so that processes involving the coulomb correlation will depend on the f weight in any state. From the schematic f density of states for the impurity of Figure 4.1 we see that up spin f weight in any state $\phi_{E\uparrow}^\dagger|V\rangle$ where E is greater than the Fermi level is small. Therefore from the analogy with the Hubbard model arguments we include processes in which the number of times we integrate over this density is small. The diagrams are therefore once again those of Figure 3.3 except that this time the up and down spin f electron propagators are those of the Anderson impurity problem. In the variational wavefunction we include processes where an f down spin excites a particle hole pair in the opposite spin band via the coulomb correlation. The variational wavefunction

$$|\Psi\rangle = \left[A\psi_{\downarrow}^{\dagger} + \int_0^{T_p} F(\epsilon)\psi_{\epsilon\downarrow}^{\dagger} + \int_0^{T_p} G(E)\phi_{E\uparrow}^{\dagger}S^{-} |0\rangle \right], \quad (4.2.19)$$

where

$$H_{imp}^A |\psi\rangle = E |\psi\rangle, \quad (4.2.20)$$

and the operator S^{-} is defined as:

$$S^{-} = f_{\downarrow}^{\dagger} f_{\uparrow}. \quad (4.2.21)$$

and creates a particle hole pair of opposite spin. The coefficient $G(E)$ of equation (4.2.19) will depend on the f weight in the up spin eigenstate created by $\phi_{E\uparrow}^{\dagger}$. As in the lattice case we solve for the coefficients A , $F(\epsilon)$ and $G(E)$ and find

$$E - \epsilon_{f\downarrow} - \int_0^{T_p} \frac{\tilde{V}^2}{(E-\epsilon)} d\epsilon - \Sigma_{ff\downarrow}(E) = 0 \quad \text{for } E > 0, \quad (4.2.22)$$

where

$$E = E - E_0, \quad E_0 \text{ is the ground state energy}, \quad (4.2.23)$$

and

$$\Sigma_{ff\downarrow}(E) = U\langle n_{f\uparrow} \rangle + \frac{\int_0^{T_p} \frac{U^2 d^2(\epsilon) \langle n_{f\uparrow} \rangle}{E - \epsilon - h\omega_0} d\epsilon}{1 - \int_0^{T_p} \frac{U d^2(\epsilon)}{E - \epsilon - h\omega_0} d\epsilon}. \quad E > 0. \quad (4.2.24)$$

Here $h\omega_0$ is the energy to flip an f electron spin and is defined by

$$E_o + h\omega_o = \frac{\langle 0 | S^+ H_{imp}^A S^- | 0 \rangle}{\langle 0 | S^+ S^- | 0 \rangle} \quad (4.2.25)$$

In order to arrive at equation (4.2.22) we require that there is no down spin occupation in the ground state. For this condition to be strictly true the bottom of the conduction band must lie on the Fermi level otherwise the hybridisation will always result in some down spin occupation. Therefore for the case of no down spin occupation the integrals over the band energies in equation (4.2.19) and equation (4.2.22) are necessarily from B_t to T_p where $B_t = 0$. A more realistic ground state is one in which the bottom of the conduction band lies below the Fermi level so that the hybridisation produces small but finite down spin occupation. For this more realistic situation the integrals in equations (4.2.19) and (4.2.22) are again from B_t to T_p but $B_t \neq 0$. We assume that the down spin occupation is infinitely small but non zero in the following. The energy E of equation (4.2.23) is identified as an excitation energy so that equation (4.2.22) is a Dyson equation consistent with a down spin f electron Green function

$$G_{ff\downarrow}(E) = \frac{1}{E - \epsilon_{f\downarrow} - \int_{B_t}^{T_p} \frac{\tilde{V}^2}{(E-\epsilon)} d\epsilon - \Sigma_{ff\downarrow}(E)} \quad E > 0. \quad (4.2.26)$$

We retain the restriction to energies greater than the Fermi level in equation (4.2.26) since solutions of energy $E < 0$ are inconsistent with the postulate of no down spin f occupation, and we are assuming that this occupation is negligibly small.

4.2.2. Results.

The form of the self energy of equation (4.2.24) has similar consequences for the impurity down spin f electron density of states as the analogous self energy of the spin only lattice model has for the f band density of states. The self energy, $\Sigma_{ff\downarrow}(E)$, has no

imaginary part for energies less than $\hbar\omega_0$, so that for energies greater than the Fermi energy and less than $\hbar\omega_0$ the Dyson equation becomes:

$$E - \varepsilon_{f\downarrow} + i\Delta - \Sigma_{ff\downarrow}(E) = 0, \quad 0 < E < \hbar\omega_0, \quad (4.2.27)$$

where equation (4.2.15) has been used, and the contribution of Λ has been neglected. The Dyson equation (4.2.27) can only yield finite lifetime quasi particle solutions since Δ is non zero for all energies. In analogy with the lattice case there is an energy \tilde{E} close to $\hbar\omega_0$ for which the real part of the Dyson equation is zero, implying that there is a finite lifetime quasi particle with this energy. For energies near \tilde{E} we can expand the self energy in a Taylor series around \tilde{E} so that

$$-\frac{1}{\pi} \text{Im } G_{ff\downarrow}(E) = \frac{1}{\pi\Delta} \frac{\tilde{\Delta}^2}{(E - \tilde{E})^2 + \tilde{\Delta}^2} \quad E \approx \tilde{E}, \quad (4.2.28)$$

where

$$\tilde{\Delta} = \frac{\Delta}{1 - \left. \frac{d\Sigma_{ff\downarrow}(E)}{dE} \right|_{\tilde{E}}}. \quad (4.2.29)$$

Therefore from equation (4.2.28) we see that for energies near \tilde{E} there is a sharp resonance in the f density states which is identified as a precursor of the Kondo resonance of the nonmagnetic HF impurity systems.

The effective Kondo temperature for the impurity case is, in analogy with the lattice calculation of Section (3.3.1), defined as the value of $\hbar\omega_0$ for which the resonance lies on the Fermi level and the strongly magnetic ground state has broken down. In the limit of very large U and $|\varepsilon_f| \gg \mu_B H$, the effective Kondo temperature for the impurity is given by:

$$T_K^{\text{eff}} \propto e^{-\frac{\langle n_{f\uparrow} \rangle W |\epsilon_f|}{V^2}} \quad (4.2.30)$$

The result is compared with the exact Kondo temperature of the Bethe ansatz (Andrei et al (1983)):

$$T_K \propto e^{-\frac{W |\epsilon_f|}{2 V^2}} \quad (4.2.31)$$

As for the lattice case the exponent is wrong by a factor of two suggesting that the up spin density of states at the Fermi energy, $V^2/|\epsilon_f|^2$, is too small by a factor of two. The variational approach leads to the same exponent in the effective Kondo temperature for both the lattice and the impurity cases. Therefore we conclude that the missing factor of two in the lattice effective Kondo temperature is a defect of the variational method rather than a genuine difference between the impurity and the lattice cases. In Section 4.3 we improve the model and hence the effective Kondo temperature for the impurity by solving the problem self consistently including the resonances in both the down and up spin densities of states, and thus raising the magnitude of the up spin density of states at the Fermi energy.

In Figures 4.2 and 4.3. the calculated f down spin density of states is plotted for $U = 7\text{eV}$, $W = 10\text{eV}$, $\epsilon_f = -1.5\text{eV}$ and a magnon energy of 0.005eV . In Figure 4.2, $V = 0.25\text{eV}$ and the f down spin density of states is seen to have a narrow resonance near the magnon energy which we identify as a precursor to the Kondo resonance. The resonance is extremely narrow and so close to the magnon energy that the computer cannot detect the difference between the two. The other density of states feature, the resonance at $\epsilon_f + U\langle n_{f\uparrow} \rangle$ supports most of the f weight. Figure 4.3 shows density of states for $V = 0.75\text{eV}$ where the two features are more obvious. The model is breaking down for this size of hybridisation. However the actual value is not unreasonable for HF systems. Gunnarson and Schönhammer (1983) calculate $\Delta \approx 0.1\text{eV}$ from their fits to XPS and BIS experiments for materials like CeNi_5 and CePd_3 using a

semi-elliptical conduction band. This corresponds to $V \approx 0.56\text{eV}$ when the conduction band is taken as a constant $1/W$, where W is the band width, and $W = 10\text{eV}$.

For both values of hybridisation the f down spin density of states agree qualitatively with the results of Gunnarson and Schönhammer (1983) as well as the results of XPS and BIS experiments for materials such as CeNi_5 and CePd_3 .

Figure 4.2. F DOWN SPIN DENSITY OF STATES $V=0.25\text{EV}$

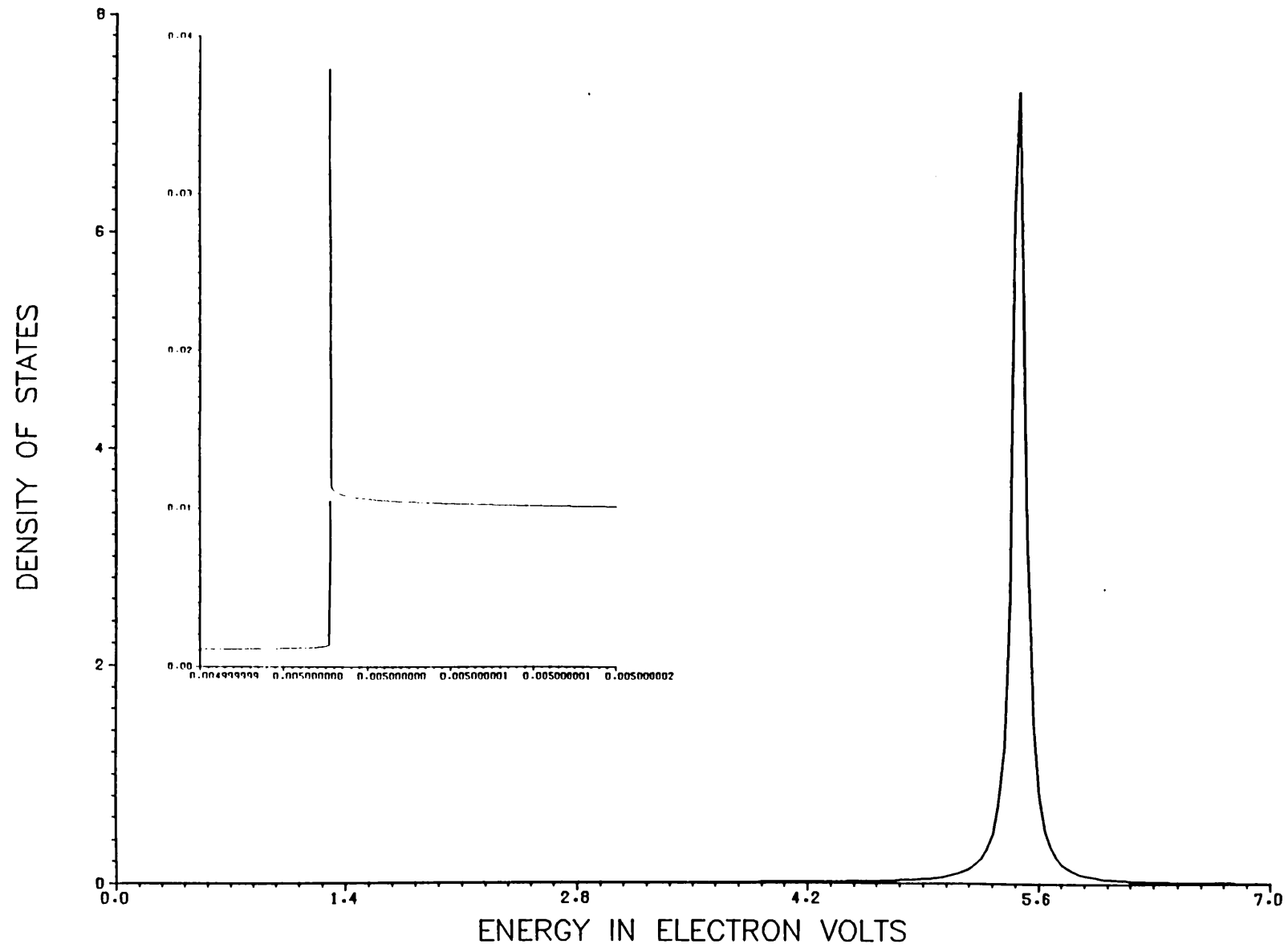
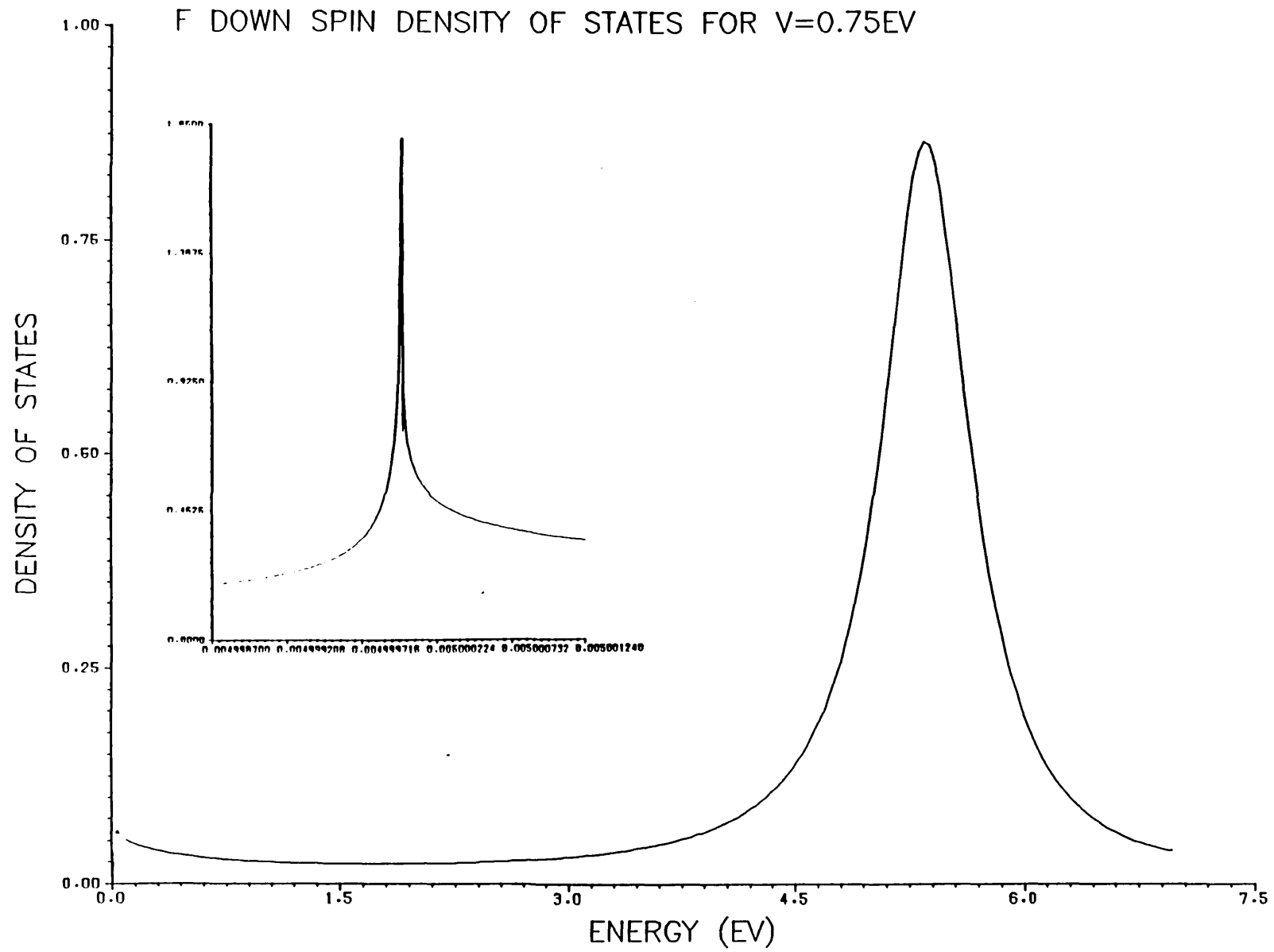


Figure 4.3.



4.2.3. The Self Energy Diagrams for the Strongly Magnetic Case.

As for the lattice case we can identify a particular class of self energy diagrams which within certain approximations correspond exactly to the self energy of the variational calculation (see equation (4.2.24)). In this section the diagrams for the strongly magnetic case of no down spin f occupation are identified. Later in Section 4.3 the model is pushed to the weakly magnetic regime using similar diagrams for both the up and down spin self energies.

The exact self energy is written as the sum of the Hartree Fock contribution plus all other contributions as:

$$\Sigma_{ff\downarrow}(E) = U\langle n_{f\uparrow} \rangle + \hat{\Sigma}_{ff\downarrow}(E), \quad (4.2.32)$$

where in this case of small up spin f weight above the Fermi level the dominant diagrams in $\hat{\Sigma}_{ff\downarrow}(E)$ are those with the smallest number of up spin electron lines (see Section 4.2.1). Therefore

$$\hat{\Sigma}_{ff\downarrow}(E) = \text{Diagram} \quad (4.2.33)$$

where the full lines now represent the full f electron propagators of the impurity problem and the dashed lines represent interactions via the coulomb interaction. Also the arrows label the spins of these f electron propagators. $\hat{\Sigma}_{ff\downarrow}(E)$ is a very difficult function to evaluate within a completely self consistent calculation. Therefore approximate solutions are sought which retain the important features of the problem. Consider first the self energy diagram:

$$U^2 \hat{\Sigma}_{ff\downarrow}^{\circ}(E) = \text{Diagram} \quad (4.2.34)$$

The corresponding analytical expression is :

$$U^2 \hat{\Sigma}_{ff\downarrow}^{\circ}(E) = \frac{U^2}{2\pi i} \int dE' G_{ff\uparrow}(E') \chi(E-E'), \quad (4.2.35)$$

and is exact when $G_{ff\uparrow}(E)$ is the full up spin f electron propagator and $\chi(E - E')$ is the exact susceptibility. Once again this analytical expression is extremely difficult to evaluate self consistently so that we approximate the up and down spin f electron propagators by their Hartree Fock expressions, $G_{ff\sigma}^{\circ}(E)$ and calculate the susceptibility within RPA. Within the Hartree Fock approximation for U tends to infinity, we assume that the hybridisation of the down spin f is negligible, therefore:

$$G_{ff\uparrow}^{\circ}(E) = \frac{1}{E - \varepsilon_{f\uparrow} + i\Delta}, \quad (4.2.36)$$

$$G_{ff\downarrow}^{\circ}(E) = \frac{1}{E - \varepsilon_{f\downarrow} - U\langle n_{f\uparrow} \rangle + i\delta}, \quad (4.2.37)$$

where we have used equation (4.2.15) and have neglected the contribution of Λ . Also the RPA susceptibility is:

$$\chi_{\text{RPA}}(E-E') = \frac{\chi_0(E-E')}{1 - U\chi_0(E-E')}, \quad (4.2.38)$$

where

$$\chi_o(E-E') = \frac{i}{2\pi} \int dE_p G_{ff\uparrow}^o(E_p - E) G_{ff\downarrow}^o(E_p - E'). \quad (4.2.39)$$

To evaluate the integral over E_p in equation (4.2.39) we write the Hartree Fock propagators in spectral representation:

$$G_{ff\uparrow}^o(E_p - E) = -\int_0^\infty \frac{d\omega \rho_{ff\uparrow}^o(\omega)}{(\omega - E_p + E - i\delta)} - \int_{-\infty}^0 \frac{d\omega \rho_{ff\uparrow}^o(\omega)}{(\omega - E_p + E + i\delta)}, \quad (4.2.40)$$

and

$$G_{ff\downarrow}^o(E_p - E') = -\int_0^\infty \frac{d\omega \rho_{ff\downarrow}^o(\omega)}{(\omega - E_p + E' - i\delta)}, \quad (4.2.41)$$

where $\rho_{ff\uparrow}^o(\omega)$, $\rho_{ff\downarrow}^o(\omega)$ are the up and down spin densities of states within the Hartree Fock approximation. When equations (4.2.40) and (4.2.41) are substituted into equation (4.2.39) then

$$\chi_o(E-E') = -\int_{-\infty}^0 d\omega_1 \int_0^\infty d\omega_2 \frac{\rho_{ff\uparrow}^o(\omega_1) \rho_{ff\downarrow}^o(\omega_2)}{(E - E' + \omega_1 - \omega_2 + i\delta)}, \quad (4.2.42)$$

so that after inserting the expressions for the Hartree Fock densities of states in equation (4.2.42) we find

$$\chi_o(E-E') = -\frac{1}{\pi} \int_{-\infty}^0 \left[\frac{\Delta}{(\omega_1 - \epsilon_f + \mu_B H)^2 + \Delta^2} \frac{1}{(E - E' + \omega_1 - \epsilon_f - \mu_B H - U\langle n_{f\uparrow} \rangle + i\delta)} \right] d\omega_1. \quad (4.2.43)$$

The analogous analysis for the strongly ferromagnetic ground state of the Hubbard model yields an expression for $\chi_{RPA}^{HUB}(k-k', E-E')$ (Edwards and Hertz and Hertz and Edwards (1973)) which has a low energy pole for positive energy $E-E'$ for which

$$1 - U\chi_{\text{RPA}}^{\text{HUB}}(\mathbf{k}-\mathbf{k}', E-E') = 0 \quad (4.2.44)$$

and corresponds to the excitation of a magnon where the magnon creation operator is given by:

$$S_{\mathbf{k}-\mathbf{k}'}^- = \sum_{\mathbf{p}} f_{(\mathbf{p}-\mathbf{k}')\downarrow}^\dagger f_{(\mathbf{p}-\mathbf{k})\uparrow} \quad (4.2.45)$$

The RPA susceptibility of the impurity problem, equation (4.2.38) is dominated by a similar but now finite lifetime excitation. From equation (4.3.43) the real and imaginary part of $\chi_0(E-E')$ in the limit of small hybridisation and large U are found to be:

$$\text{Re}\chi_0(E-E') \approx \frac{-\langle n_{f\uparrow} \rangle}{E - E' - 2\mu_B H - U\langle n_{f\uparrow} \rangle}, \quad (4.2.46)$$

$$\text{Im}\chi_0(E-E') = \frac{\Delta}{(E - E' - 2\mu_B H - U\langle n_{f\uparrow} \rangle)^2 + \Delta^2}. \quad (4.2.47)$$

Therefore although the denominator of equation (4.2.38) is never exactly zero there is positive energy $E-E' = \hbar\omega_0 \approx 2\mu_B H$ for which

$$1 - U\text{Re}\chi_0(\hbar\omega_0) = 0, \quad (4.2.48)$$

$$\text{Im}\chi_0(\hbar\omega_0) \approx 0, \quad (4.2.49)$$

so that there exists a slightly damped excitation with this energy. For low energies then, we can expand the RPA susceptibility in a Taylor series around its pole at $E-E' = \hbar\omega_0 \approx 2\mu_B H$ so that

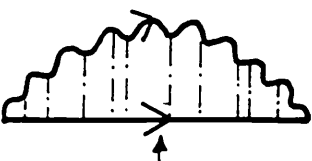
$$\chi_{\text{RPA}}(E-E') \approx \frac{1}{(E - E' - \hbar\omega_0)} \left[\frac{-1}{\chi_0(\hbar\omega_0)^2} \frac{d\chi_0(E-E')}{d(E-E')} \right]_{E-E'=\hbar\omega_0}^{-1}, \quad (4.2.50)$$


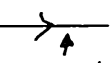
$$\chi_{\text{RPA}}(E-E') \approx \frac{-\langle n_{f\uparrow} \rangle}{(E - E' - \hbar\omega_0)} \quad (4.2.51)$$

At small energies the the impurity RPA susceptibility is dominated by an excitation, of energy $\hbar\omega_0 \approx 2\mu_B H$, with a small but finite lifetime. This excitation corresponds to a damped f electron spin flip. The amount of damping is small for small hybridisations. Therefore, for small hybridisation, it is reasonable to approximate the RPA susceptibility by its pole contribution and neglect the damping. When we substitute equation (4.2.51) into equation (4.2.35) and carry out the integral over E' we find:

$$U^2 \hat{\Sigma}_{ff\downarrow}^0(E) = U^2 \int_0^{T_p} \frac{\langle n_{f\uparrow} \rangle d^2(\epsilon)}{(E - \epsilon - 2\mu_B H + i\delta)} d\epsilon \quad (4.2.52)$$

Therefore the contribution to the self energy from the diagrams of equation (4.2.34) agrees exactly with the self energy of the variational calculation of equation (4.2.24) to order U^2 . So far no account has been taken of the interaction between the electron hole pair of opposite spin and the single particle excitations which are included in the self energy diagrams of equation (4.2.22). Within the spin flip pole approximation these diagrams can be redrawn as:

$$\hat{\Sigma}_{ff\downarrow}^0(E) = \text{Diagram} \quad E > E_F \quad (4.2.53)$$


where  is the positive energy spin flip excitation,  represents the up spin particle line and the broken lines represent interactions via the coulomb correlation. These diagrams can be expanded as:

$$\hat{\Sigma}_{ff\downarrow}(E) = U^2 \left[\begin{array}{c} \text{Diagram 1} + \text{Diagram 2} \\ \text{Diagram 3} \dots \dots \dots \end{array} \right]$$

$E > E_F$ (4.2.54)

which we write analytically as

$$\hat{\Sigma}_{ff\downarrow}(E) = U^2 \left\{ \frac{1}{2\pi i} \int dE' G_{ff\uparrow}^{\circ}(E') \chi(E-E') + \left[\frac{1}{2\pi i} \int dE'_1 G_{ff\uparrow}^{\circ}(E'_1) \chi(E-E'_1) \right] \frac{U}{\langle n_{f\uparrow} \rangle} \left[\frac{1}{2\pi i} \int dE'_2 G_{ff\uparrow}^{\circ}(E'_2) \chi(E-E'_2) \right] + \dots \right\}$$

(4.2.55)

and hence

$$\hat{\Sigma}_{ff\downarrow}(E) = \begin{cases} \frac{U^2 \hat{\Sigma}_{ff\downarrow}^{\circ}(E)}{1 - U \frac{\hat{\Sigma}_{ff\downarrow}^{\circ}(E)}{\langle n_{f\uparrow} \rangle}} & E > E_F \\ 0 & E \leq E_F \end{cases}$$

(4.2.56)

Equation (4.2.56) of the diagrammatic treatment is identical to equation (4.2.24) of the variational calculation. Therefore the variational method yields a self energy contribution which can be identified with the diagrams of equation (4.2.33) when the propagators are approximated by their Hartree Fock expressions and the spin flip pole approximation is made to the susceptibility.

4.3. THE WEAKLY MAGNETIC CASE.

4.3.1. The Self Energy Diagrams for the Weakly Magnetic Case.

In this section the model and ideas developed for the strongly magnetic case, where $\langle n_{f\downarrow} \rangle$ is constrained to be strictly zero, are extended to describe the more realistic finite U case where $\langle n_{f\downarrow} \rangle \approx 0$ and $\langle n_{f\uparrow} \rangle \approx 1$. In any real system there is always some down spin occupation due to hybridisation, therefore in any system there is also some up spin self energy due to coulomb correlation. In the $\langle n_{f\downarrow} \rangle = 0$ model the up spin self energy due to coulomb correlation is approximated as zero. The effective Kondo temperature for this $\langle n_{f\downarrow} \rangle = 0$ case is too small as a result of a missing factor of two in the exponent. A possible explanation for the error in the exponent is that the up spin density of states at the Fermi level for the $\langle n_{f\downarrow} \rangle = 0$ model is too small by a factor of two. The extension of the model to account for the fact that in a real system $\langle n_{f\downarrow} \rangle \approx 0$ results in an up spin self energy contribution and hence some extra up spin density of states, which could be the missing density of states of the $\langle n_{f\downarrow} \rangle = 0$ model. The motivation for the present calculation is therefore the possible improvement of the effective Kondo temperature of the $\langle n_{f\downarrow} \rangle = 0$ model. The calculation was also intended as a test case for the generalisation to $\langle n_{f\downarrow} \rangle \neq 0$ in the lattice.

In the following sections both up and down spin self energy diagrams are defined. They are essentially those of equation (4.2.33) where for the up spin self energies the up spin electron lines of equation (4.2.33) are replaced by down spin hole lines and vice versa. These self energies are the origin of a sharp resonance in the down spin density of states above Fermi level, as before, as well as a new similar resonance in the up spin density of states below the Fermi level. It is easily seen that up spin density of states at the Fermi level is now larger than for the $\langle n_{f\downarrow} \rangle = 0$ model and thus the effective Kondo temperature must be improved. In Section (4.3.2) a quantitative comparison of the Kondo temperature of the $\langle n_{f\downarrow} \rangle \approx 0$ model is made with the exact Bethe ansatz results (Andrei (1983)) to show the improvement over the effective Kondo temperature of the $\langle n_{f\downarrow} \rangle = 0$ model. Also the variation of the

magnetisation with magnetic field is calculated and shows good agreement with the exact Bethe ansatz results.

The system is once again modelled by the Anderson Impurity hamiltonian, H_{imp}^A , with a magnetic field acting on the impurity (see equation (4.2.1)). The starting point is again an approximate ground state in which the coulomb interaction is treated in the Hartree Fock approximation. For this finite U case the Hartree Fock propagators are:

$$G_{ff\uparrow}^o(E) = \frac{1}{E - \epsilon_{f\uparrow} - U\langle n_{f\downarrow} \rangle + i\Delta}, \quad (4.3.1)$$

and

$$G_{ff\downarrow}^o(E) = \frac{1}{E - \epsilon_{f\downarrow} - U\langle n_{f\uparrow} \rangle + i\Delta}. \quad (4.3.2)$$

Therefore the up and down spin f electron densities of states are lorentzians around $\epsilon_{f\uparrow} + U\langle n_{f\downarrow} \rangle$ and $\epsilon_{f\downarrow} + U\langle n_{f\uparrow} \rangle$ respectively and the hybridisation produces non negligible down spin occupation. At this stage it is more convenient to think in terms of self energy diagrams rather than variational wavefunctions. In the approximate ground state only the Hartree Fock term $U\langle n_{f-\sigma} \rangle$ is included in the exact self energy $\Sigma_{ff\sigma}^o(E)_{ex}$ (see equation (4.2.18) with $\downarrow = \sigma$). Once again we are faced with the problem of taking better account of the coulomb correlation via corrections to the Hartree Fock approximation.

From the schematic f electron density of states picture Figure (4.4)

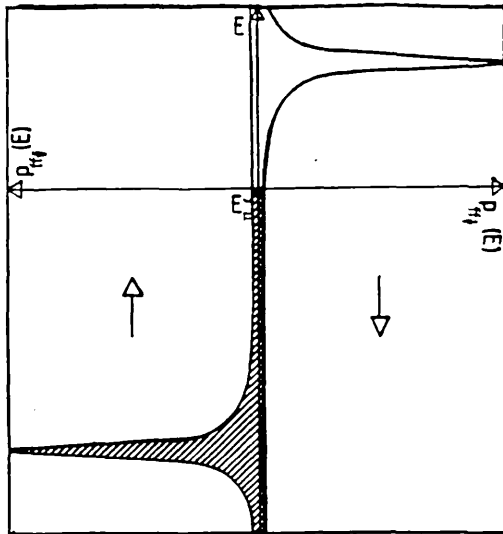


Figure 4.4. A schematic impurity f density of states in the U finite Hartree Fock ground state. The hatched areas denote occupied density of states below the Fermi energy E_F .

we notice that for finite U the number of unoccupied up spin states is of the same order of magnitude as the number of occupied down spin states, and is in fact identical for the symmetric Anderson model where $\epsilon_f = -U/2$. For $\langle n_{f\downarrow} \rangle \approx 0$ and $\langle n_{f\uparrow} \rangle \approx 1$ the number of unoccupied up spin states is still small and therefore the dominant down spin self energy diagrams will still be those of equation (4.2.33). Similarly the number of occupied down spin states is small. Hence by parallel arguments the up spin self energy, other than the Hartree Fock term, is dominated by diagrams with the smallest number of down spin hole lines so that

$$\Sigma_{ff\uparrow}(E) = U\langle n_{f\downarrow} \rangle + \hat{\Sigma}_{ff\uparrow}(E), \quad (4.3.3)$$

where the first term is just the Hartree Fock contribution and

$$\hat{\Sigma}_{ff\uparrow}(E) = \text{Diagram} \quad (4.3.4)$$

Here the full lines once again represent the full f electron

propagators and the broken lines represent interactions via the coulomb interaction. In the up spin self energy $\hat{\Sigma}_{ff\uparrow}^{\circ}(E)$ the down spin ^{particle} _{hole} lines play the part of the up spin ^{hole} _{particle} lines of the down spin self energy diagrams $\hat{\Sigma}_{ff\downarrow}^{\circ}(E)$. For the case of $\langle n_{f\downarrow} \rangle \approx 0$ and $\langle n_{f\uparrow} \rangle \approx 1$, $\hat{\Sigma}_{ff\downarrow}^{\circ}(E)$ and $\hat{\Sigma}_{ff\uparrow}^{\circ}(E)$ are given by the diagrams of equations (4.2.33) and (4.3.4) respectively. Within certain approximations these diagrams are equivalent to the variational self energy for the $\langle n_{f\downarrow} \rangle = 0$ case. To evaluate the contributions of the diagrams of equations (4.2.33) and (4.3.4) we treat firstly the contribution from diagrams:

$$U^2 \hat{\Sigma}_{ff\downarrow}^{\circ}(E) =$$

$$(4.3.5)$$

$$U^2 \hat{\Sigma}_{ff\uparrow}^{\circ}(E)$$

$$(4.3.6)$$

The interactions between the electron hole pair and the single particle excitations equation of (4.3.4) are treated later. For the moment we treat the problem of evaluating the analytical expressions corresponding to equation (4.3.5) and (4.3.6):

$$U^2 \hat{\Sigma}_{ff\sigma}^{\circ}(E) = \frac{U^2}{2\pi i} \int dE' G_{ff-\sigma}(E') \chi^{\sigma}(E-E'). \quad (4.3.7)$$

Once again this extremely complicated expression is evaluated within some reasonable approximations. As before the susceptibility is calculated within RPA so that:

$$\chi_{\text{RPA}}^{\sigma}(E-E') = \frac{\chi_0^{\sigma}(E-E')}{1 - U\chi_0^{\sigma}(E-E')}, \quad (4.3.8)$$

where

$$\chi_0^{\sigma}(E-E') = \frac{i}{2\pi} \int dE_p G_{ff-\sigma}^{\circ}(E_p - E) G_{ff\sigma}^{\circ}(E_p - E'). \quad (4.3.9)$$

and $G_{ff\sigma}^{\circ}(E)$ are the Hartree Fock propagators. When we substitute the spectral representations for the Hartree Fock propagators in equation (4.3.9) and perform the integral over E_p then

$$\chi_0^{\downarrow}(E-E') = \begin{cases} - \int_{-\infty}^0 d\omega_1 \int_0^{\infty} d\omega_2 \frac{\rho_{ff\uparrow}^{\circ}(\omega_1) \rho_{ff\downarrow}^{\circ}(\omega_2)}{(E - E' + \omega_1 - \omega_2 + i\delta)} & E-E' > E_F \\ O(\text{up spin } f \text{ weight at } E_F) \times \\ O(\text{down spin } f \text{ weight at } E_F) & E-E' \leq E_F \end{cases} \quad (4.3.10)$$

and

$$\chi_0^{\uparrow}(E-E') = \begin{cases} O(\text{up spin } f \text{ weight at } E_F) \\ O(\text{down spin } f \text{ weight at } E_F) & E-E' > E_F \\ \int_{-\infty}^0 d\omega_2 \int_0^{\infty} d\omega_1 \frac{\rho_{ff\downarrow}^{\circ}(\omega_1) \rho_{ff\uparrow}^{\circ}(\omega_2)}{(E - E' + \omega_1 - \omega_2 - i\delta)} & E-E' \leq E_F \end{cases} \quad (4.3.11)$$

where $E_F = 0$ is the Fermi energy and $\rho_{ff\sigma}^{\circ}(E)$ are the spin σ f electron density of states within the Hartree Fock approximation. As for the $\langle n_{f\downarrow} \rangle = 0$ model $\chi_{\text{RPA}}^{\sigma}(E-E')$ are dominated by finite lifetime excitations at positive energy $E-E' = \hbar\omega_{\downarrow} \approx 2\mu_B H$ for $\chi_{\text{RPA}}^{\downarrow}(E-E')$ and negative energy $E-E' = -\hbar\omega_{\uparrow} \approx -2\mu_B H$ for $\chi_{\text{RPA}}^{\uparrow}(E-E')$. Once again these excitations correspond to a damped f electron spin flip excitations. For small hybridisations the damping is small

since $\text{Im}\chi_{\text{RPA}}^{\downarrow}(E-E')$ is small for $E-E' \neq 2\mu_B + U(\langle n_{f\uparrow} \rangle - \langle n_{f\downarrow} \rangle)$ and $\text{Im}\chi_{\text{RPA}}^{\uparrow}(E-E')$ is small for $E-E' \neq -2\mu_B + U(\langle n_{f\uparrow} \rangle - \langle n_{f\downarrow} \rangle)$.

For small hybridisations the damping is neglected and the susceptibilities are written as expansions around their poles so that

$$\chi_{\text{RPA}}^{\downarrow}(E-E') \approx \begin{cases} - \frac{\langle n_{f\uparrow} \rangle (1 - \langle n_{f\downarrow} \rangle)}{(E - E' - \hbar\omega_{o\downarrow} + i\delta)} & E-E' > E_F \\ 0 & E-E' \leq E_F \end{cases} \quad (4.3.12)$$

and

$$\chi_{\text{RPA}}^{\uparrow}(E-E') \approx \begin{cases} 0 & E-E' > E_F \\ - \frac{\langle n_{f\uparrow} \rangle (1 - \langle n_{f\downarrow} \rangle)}{(E - E' + \hbar\omega_{o\uparrow} - i\delta)} & E-E' \leq E_F \end{cases} \quad (4.3.13)$$

When these pole approximations are used to calculate the self energy contributions of equations (4.3.5) and (4.3.6) then we find

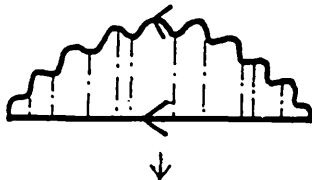
$$U^2 \hat{\Sigma}_{ff\downarrow}^o(E) \approx \begin{cases} \langle n_{f\uparrow} \rangle (1 - \langle n_{f\downarrow} \rangle) U^2 \int_0^{T_p} \frac{d_{\uparrow}^2(\varepsilon)}{(E - \varepsilon - \hbar\omega_{o\downarrow} + i\delta)} d\varepsilon & E \geq E_F \\ 0 & E < E_F \end{cases} \quad (4.3.14)$$

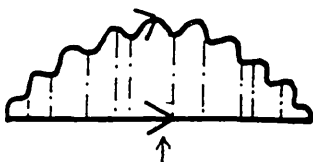
and



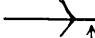
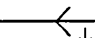
$$U^2 \hat{\Sigma}_{ff\uparrow}^{\circ}(E) = \begin{cases} 0 & E > E_F \\ \langle n_{f\uparrow} \rangle (1 - \langle n_{f\downarrow} \rangle) U^2 \int_0^{\infty} \frac{d_{\downarrow}^2(\epsilon)}{\text{Re} (E - \epsilon + h\omega_{o\uparrow} - i\delta)} & E \leq E_F \end{cases} \quad (4.3.15)$$

where for a completely self consistent calculation $d_{\uparrow}^2(\epsilon)$ and $d_{\downarrow}^2(\epsilon)$ are now the up and down spin f electron densities of states associated with the Green function which we are trying to calculate.

To calculate $\hat{\Sigma}_{ff\sigma}^{\circ}(E)$ of equations (4.3.4) and (4.2.33) we must include the interactions between the single particle excitations and the electron hole pair of opposite spin. For small hybridisations the diagrams are redrawn within the spin flip pole approximation. At this stage we assume the system is modelled by the symmetric Anderson model so that the accuracy of the pole approximation is the same for each spin and

$$\hat{\Sigma}_{ff\uparrow}^{\circ}(E) = \text{Diagram} \quad (4.3.16)$$


$$\hat{\Sigma}_{ff\downarrow}^{\circ}(E) = \text{Diagram} \quad (4.3.17)$$


where  represents a positive energy spin flip excitation and  a negative energy spin flip excitation,  an up spin particle line and  a down spin hole line. When equations (4.3 16) and (4.3 17) are expanded as in equation (4.2.54) then

$$\hat{\Sigma}_{ff\downarrow}(E) \approx \begin{cases} \frac{U^2 \hat{\Sigma}_{ff\downarrow}^o(E)}{1 - U\hat{\Sigma}_{ff\downarrow}^o(E)} & E > E_F \\ \frac{\langle n_{f\downarrow} \rangle}{\langle n_{f\downarrow} \rangle} & \\ 0 & E \leq E_F \end{cases} \quad (4.3.18)$$

and

$$\hat{\Sigma}_{ff\uparrow}(E) \approx \begin{cases} 0 & E > E_F \\ \frac{U^2 \hat{\Sigma}_{ff\uparrow}^o(E)}{1 + U\hat{\Sigma}_{ff\uparrow}^o(E)} & \\ \frac{\langle n_{f\uparrow} \rangle}{\langle n_{f\uparrow} \rangle} & E \leq E_F \end{cases} \quad (4.3.19)$$

with $U^2 \hat{\Sigma}_{ff\downarrow}^o(E)$ given by equation (4.3.14) and $U^2 \hat{\Sigma}_{ff\uparrow}^o(E)$ by equation (4.3.15) and $\hbar\omega_{o\downarrow} = -\hbar\omega_{o\uparrow} \approx 2\mu_B H$. Both the up and down spin self energies for this $\langle n_{f\downarrow} \rangle \approx 0$ and $\langle n_{f\uparrow} \rangle \approx 1$ model have similar properties to the self energy of the $\langle n_{f\downarrow} \rangle = 0$ model (see equation (4.2.24)). They are the origin of a sharp resonance in the down spin density of states above the Fermi level as well as a new similar (identical for $\varepsilon_f = U/2$) resonance in the up spin density of states just below the Fermi level.

Within the $\langle n_{f\downarrow} \rangle = 0$ model the magnetic state breaks down with increasing hybridisation as is expected. However the breakdown does

not occur quickly enough. The magnetic state is too stable or the Kondo temperature is too small. The breakdown of the magnetic state occurs as down spin density of states builds up around the Fermi level due to processes described by equation (4.2.33). As the hybridisation increases the up spin density of states above the Fermi level available for excitations of equation (4.2.33) increases and in turn the resonance near the Fermi level in the down spin density of states grows. Within the new $\langle n_{f\downarrow} \rangle \approx 0$ and $\langle n_{f\uparrow} \rangle \approx 1$ model there are resonances in both the up and down spin density of states around the Fermi level. Therefore there are more up spin states available for the processes of equation (4.2.33), the origin of the down spin resonance near the Fermi level. Similarly there are more occupied down spin states available for the excitations of equation (4.3.4) leading to a build up of the up spin density of states near the Fermi level. As hybridisation increases both these resonances grow each aiding the build up of the other, so that the magnetic state of the improved $\langle n_{f\downarrow} \rangle \approx 0$ and $\langle n_{f\uparrow} \rangle \approx 1$ model breaks down more quickly than for the $\langle n_{f\downarrow} \rangle = 0$ case. The extension of the model to describe $\langle n_{f\downarrow} \rangle \approx 0$ and $\langle n_{f\uparrow} \rangle \approx 1$ and subsequently an up spin self energy must therefore improve the exponent of the effective Kondo temperature.

In the following section the magnetisation is calculated as a function of field and the results compared with those of Bethe ansatz. The comparison shows that the extension of the model to account for the fact that $\langle n_{f\downarrow} \rangle \approx 0$ and $\langle n_{f\uparrow} \rangle \approx 1$ does indeed improve the effective Kondo temperature.

4.3.2. Magnetisation Versus Magnetic Field.

From the exact Bethe ansatz results for the impurity model (Andrei et al (1983)) the f electron magnetisation in a magnetic field is given as:

$$m = 1 - \frac{1}{2 \ln \left| \frac{H}{T_K} \right|}, \quad (4.3.20)$$

where H is a high field such that $H/T_K > 10^2$ and T_K is the Kondo temperature. In this section we calculate the magnetisation of the new weakly magnetic model as a function of magnetic field. The calculated magnetisation versus the magnetic field behaviour is found to be in good agreement with the exact Bethe ansatz behaviour of equation (4.3.20) so that a Kondo temperature for the model can be determined. The Kondo temperature for this weakly magnetic case is an improvement on the effective Kondo temperature of the $\langle n_{f\downarrow} \rangle = 0$ case as expected.

From the analysis of the previous section the up and down spin densities of states are:

$$\rho_{ff\sigma}(E) = \frac{1}{\pi} \frac{(\Delta - \text{Im}\hat{\Sigma}_{ff\sigma}(E))}{(E - \varepsilon_{f\sigma} - U\langle n_{f-\sigma} \rangle - \text{Re}\hat{\Sigma}_{ff\sigma}(E))^2 + (\Delta - \text{Im}\hat{\Sigma}_{ff\sigma}(E))^2} \quad (4.3.21)$$

where $\text{Im}\hat{\Sigma}_{ff\sigma}(E)$ is the imaginary part of, and $\text{Re}\hat{\Sigma}_{ff\sigma}(E)$ the real parts of the self energy contribution $\hat{\Sigma}_{ff\sigma}(E)$ of equations (4.3.18) and (4.3.19) with, for this the symmetric Anderson model, $\varepsilon_f = -U/2$ and $\langle n_{f\uparrow} \rangle = (1 - \langle n_{f\downarrow} \rangle)$. For a completely self consistent calculation of the down spin self energy term $\hat{\Sigma}_{ff\downarrow}(E)$ we need the up spin density of states above the Fermi level (see equation (4.3.14)). However this function is only known below the Fermi level. Similarly to calculate the up spin self energy term $\hat{\Sigma}_{ff\uparrow}(E)$ we need the down spin density of the states below the Fermi level (see equation (4.3.15)). However this function is only known above the Fermi level. The contribution to $\hat{\Sigma}_{ff\sigma}(E)$ from these unknown densities of states is lost when we make the the spin flip pole approximation to the susceptibilities of equations (4.3.10) and (4.3.11).

The problem, then, is to find a reasonable approximation for the densities of states in the unknown energy regions. The information available about these unknown densities of states is that they must join continuously with the known densities of states at the Fermi level and also they must hold the correct f up and down spin electron weight as given by the Friedel sum rule. The

condition that the f densities of states are continuous at the Fermi level is written:

$$\rho_{ff\uparrow}(0^+) = \frac{1}{\pi} \frac{\Delta}{(-\epsilon_f + \mu_B H - U\langle n_{f\downarrow} \rangle - \hat{\Sigma}_{ff\uparrow}(0))^2 + \Delta^2}, \quad (4.3.22)$$

$$\rho_{ff\downarrow}(0^-) = \frac{1}{\pi} \frac{\Delta}{(-\epsilon_f - \mu_B H - U\langle n_{f\uparrow} \rangle - \hat{\Sigma}_{ff\downarrow}(0))^2 + \Delta^2}. \quad (4.3.23)$$

Also the Friedel sum rule (Luttinger (1960)) for an infinitely wide band can be expressed as:

$$\begin{aligned} \langle n_{f\uparrow} \rangle &= \int_0^{\tau_p} \rho_{ff\uparrow}(E) dE \\ &= \frac{1}{\pi} \cot^{-1} \left[\frac{\epsilon_f - \mu_B H + U\langle n_{f\downarrow} \rangle + \hat{\Sigma}_{ff\uparrow}(0)}{\Delta} \right], \end{aligned} \quad (4.3.24)$$

and

$$\begin{aligned} \langle n_{f\downarrow} \rangle &= \int_{Bt}^0 \rho_{ff\downarrow}(E) dE \\ &= \frac{1}{\pi} \cot^{-1} \left[\frac{\epsilon_f + \mu_B H + U\langle n_{f\uparrow} \rangle + \hat{\Sigma}_{ff\downarrow}(0)}{\Delta} \right] \end{aligned} \quad (4.3.25)$$

For energies close to zero we can expand the up and down spin self energies in a Taylor expansion around zero to find:

$$\rho_{ff\sigma}(E) \underset{E \approx 0}{=} \frac{\tilde{\Delta}_\sigma}{\pi\Delta} \frac{\tilde{\Delta}_\sigma}{(E - \tilde{E}_\sigma)^2 + \tilde{\Delta}_\sigma^2}, \quad (4.2.26)$$

where

$$\tilde{\Delta}_\sigma = \frac{\Delta}{\left(1 - \frac{d\hat{\Sigma}_{ff\sigma}(E)}{dE}\right) \Big|_{E=0}}, \quad (4.2.27)$$

and

$$\tilde{E}_\sigma = \Delta \frac{(\varepsilon_{f\sigma} + U\langle n_{f-\sigma} \rangle + \hat{\Sigma}_{ff\sigma}(0))}{\tilde{\Delta}_\sigma}. \quad (4.2.28)$$

If the density of states expansions of equation (4.2.26) are used for the form of the densities of states in the unknown energy regions then, from equations (4.3.18) and (4.3.19) for $\hat{\Sigma}_{ff\sigma}(0)$ in the symmetric case, where $\varepsilon_f = -U/2$ and $\langle n_{f\downarrow} \rangle = (1 - \langle n_{f\uparrow} \rangle)$, we find that

$$\tilde{\Delta}_\uparrow = \tilde{\Delta}_\downarrow \quad \text{and} \quad \tilde{E}_\uparrow = -\tilde{E}_\downarrow, \quad (4.2.29)$$

and hence from equation (4.2.26)

$$\rho_{ff\uparrow}(E) = \rho_{ff\downarrow}(-E), \quad (4.2.30)$$

as it must be, in this symmetric case. The original idea was to approximate the densities of states in the unknown energy regions by $\rho_{ff\sigma}(E)$ of equation (4.2.26). With this prescription the continuity condition is automatically satisfied and the up and down spin f densities of states in the unknown energy regions are the tails of some effective resonance in the known energy region. For the up spin f density of states the effective resonance is built from contributions from the up spin f resonance around $\varepsilon_f - \mu_B H + U\langle n_{f\downarrow} \rangle$ and the narrow resonance around $-2\mu_B H$. Similarly for the down spin density of states. Also when we allow the bandwidth to tend to infinity $\tilde{\Delta} \rightarrow \Delta$ and the Friedel sum is satisfied.

Unfortunately for this choice of up and down spin f densities of states in the unknown energy regions it was found that that $\tilde{\Delta}$ varied too rapidly with magnetic field. Therefore the assumption that the expansions around $E = 0$ of equation (4.2.26) are good for

all energies $E > 0$ for up spin and $E < 0$ for down spin is not valid.

In the following we retain the idea that for small hybridisations the densities of states in the unknown energy regions must be the tail of some effective resonance in the known energy region. The up and down spin densities of states in the unknown energy regions are chosen as:

$$\rho_{ff\uparrow}(E) \equiv \frac{1}{\pi} \frac{\Delta}{(E - \varepsilon_f + \mu_B H - U\langle n_{f\downarrow} \rangle - \hat{\Sigma}_{ff\uparrow}(0))^2 + \Delta^2} \quad E > E_F, \quad (4.3.31)$$

and

$$\rho_{ff\downarrow}(E) \equiv \frac{1}{\pi} \frac{\Delta}{(E - \varepsilon_f - \mu_B H - U\langle n_{f\uparrow} \rangle - \hat{\Sigma}_{ff\downarrow}(0))^2 + \Delta^2} \quad E \leq E_F, \quad (4.3.32)$$

which satisfy the continuity condition and the Friedel sum rule exactly. These forms reduce to the correct up and down spin densities of states within the Hartree Fock approximation and for the symmetric Anderson model where $\varepsilon_f = U/2$ and $\langle n_{f\uparrow} \rangle = 1 - \langle n_{f\downarrow} \rangle$ they give:

$$\text{Re}\hat{\Sigma}_{ff\uparrow}(-E) = -\text{Re}\hat{\Sigma}_{ff\downarrow}(E), \quad (4.3.33)$$

and hence

$$\rho_{ff\uparrow}(E) = \rho_{ff\downarrow}(-E), \quad (4.3.34)$$

as must be true for this the symmetric Anderson model.

To calculate the magnetisation for this the symmetric case $\varepsilon_f = -U/2$ we use

$$m = (1 - 2\langle n_{f\downarrow} \rangle), \quad (4.3.35)$$

where from equation (4.3.25)

$$\langle n_{f\downarrow} \rangle = \int_{Bt}^0 \frac{1}{\pi} \frac{\Delta}{(E - \varepsilon_f - \mu_B H - U\langle n_{f\uparrow} \rangle - \hat{\Sigma}_{ff\downarrow}^{\circ}(0))^2 + \Delta^2} dE. \quad (4.3.36)$$

From equation (4.3.36) for $\langle n_{f\downarrow} \rangle$, we see that $\langle n_{f\downarrow} \rangle$ is a function of $\hat{\Sigma}_{ff\downarrow}^{\circ}(0)$ and hence $\hat{\Sigma}_{ff\downarrow}^{\circ}(0)$. However from equation (4.3.14) with $(1 - \langle n_{f\downarrow} \rangle) = \langle n_{f\uparrow} \rangle$ and $d^{\downarrow}(\varepsilon) = \rho_{ff\uparrow}(E)$ of (4.3.31), then:

$$\hat{\Sigma}_{ff\downarrow}^{\circ}(0) = \frac{1}{\pi} \int_0^{\Gamma p} \left[\frac{\Delta(1 - \langle n_{f\downarrow} \rangle)^2}{(\varepsilon - \varepsilon_f + \mu_B H - U\langle n_{f\uparrow} \rangle - \hat{\Sigma}_{ff\uparrow}^{\circ}(0))^2 + \Delta^2} \frac{1}{(-\varepsilon - 2\mu_B H)} \right] d\varepsilon, \quad (4.3.37)$$

so that $\Sigma_{ff\downarrow}(E)$ is a function of $\Sigma_{ff\uparrow}(E)$ and vice versa. However in this the symmetric case we can decouple equation (4.3.37) using the relation:

$$\varepsilon_f - \mu_B H + U\langle n_{f\uparrow} \rangle + \hat{\Sigma}_{ff\downarrow}^{\circ}(0) = -(\varepsilon_f + \mu_B H + U\langle n_{f\downarrow} \rangle + \hat{\Sigma}_{ff\uparrow}^{\circ}(0)). \quad (4.3.38)$$

When equation (4.3.38) is used in equation (4.3.37) we can find $\hat{\Sigma}_{ff\downarrow}^{\circ}(E)$ as a function of $\langle n_{f\downarrow} \rangle$ and magnetic field. This relation is then used in equation (4.3.36) to find $\langle n_{f\downarrow} \rangle$.

Equation (4.3.36) cannot be solved analytically for $\langle n_{f\downarrow} \rangle$ instead it is solved computationally as a transcendental equation for $\langle n_{f\downarrow} \rangle$. To find the solution the computer evaluates both sides of the equation for several values of $\langle n_{f\downarrow} \rangle$ in a specified interval until it finds a value for $\langle n_{f\downarrow} \rangle$ for which both sides match to the required accuracy. For each $\langle n_{f\downarrow} \rangle$ in this interval a similar procedure is carried out to solve equation (4.3.37) as a transcendental equation for $\hat{\Sigma}_{ff\downarrow}^{\circ}(E)$.

The Bethe ansatz result of equation (4.3.20) can be re-expressed, assuming H and T_K are measured in units of eV, as:

$$\frac{1}{4\langle n_{f\downarrow} \rangle} = \ln|\hat{H}| - \ln|\hat{T}_k|, \quad (4.3.39)$$

where \hat{H} and \hat{T}_k are dimensionless. Therefore a plot of $1/4\langle n_{f\downarrow} \rangle$ versus $\ln|\hat{H}|$ should have a gradient of one and cut the $1/4\langle n_{f\downarrow} \rangle$ axis at $\ln|\hat{T}_k|$ for any hybridisation. Figures 4.6 to 4.9 are plots of the calculated $1/4\langle n_{f\downarrow} \rangle$ versus $\ln|\hat{H}|$ for various Δ . For each case the scaling is seen for $H/T_k > 10$ (assuming $T_k \approx 0.0007\text{eV}$) and $H < D$ where

$$T_k = D e^{-\frac{|\epsilon_f|\pi}{2\Delta}}, \quad (4.3.40)$$

(Andrei et al (1983)). For each of the figures the upper curve is the Hartree Fock result, where the exact self energy is approximated as:

$$\Sigma_{ff\sigma}(E)_{\text{ex}} = U\langle n_{f-\sigma} \rangle, \quad (4.3.41)$$

and the lower curve is the model result:

$$\Sigma_{ff\sigma}(E)_{\text{ex}} = U\langle n_{f-\sigma} \rangle + \hat{\Sigma}_{ff\sigma}(E). \quad (4.3.42)$$

The dotted line has the expected gradient of one for comparison with each of the curves. For each hybridisation the model gives better agreement with the Bethe ansatz behaviour (shown by the dotted line) than the Hartree Fock result. The bandwidth is chosen to be extremely large $W = 200\text{eV}$ in order to ensure the validity of the Friedel sum rule and $U = 7\text{eV}$. The hybridisations studied range from $V = 0.56$ ($\Delta = 0.005\text{eV}$) to $V = 1.69$ ($\Delta = 0.045\text{eV}$). For the smallest hybridisation, $\Delta = 0.005\text{eV}$, the Hartree Fock and model results are closest. For larger but still small hybridisations the model results show increased improvement over the Hartree Fock result.

To see how the extension of the model to $\langle n_{f\downarrow} \rangle \approx 0$ improves the Kondo temperature we substitute the Bethe ansatz expression for the

Kondo temperature of equation (4.3.40) in equation (4.3.39) so that

$$\frac{1}{4\langle n_{f\downarrow} \rangle} - \ln|\hat{H}| = -\ln|\hat{D}| + \frac{|\epsilon_f|\pi}{2\Delta} . \quad (4.3.43)$$

From equation (4.3.43) we see that a plot of $1/4\langle n_{f\downarrow} \rangle - \ln|\hat{H}|$ versus $|\epsilon_f|\pi/\Delta$ should have a gradient of 1/2 if the exponent in the Kondo temperature is correct. For the $\langle n_{f\downarrow} \rangle = 0$ model the exponent of the effective Kondo temperature is wrong by a factor of two so that in terms of the aforementioned plot the gradient is one rather than 1/2. Figures 4.9 and 4.10 show this same plot for the improved $\langle n_{f\downarrow} \rangle \approx 0$ model. These plots have a gradient of around 1/3 so that the Kondo temperature is indeed improved. In Figure 4.10 the magnetic field is taken to be 0.01eV ($H/T_k \approx 10$) while in Figure 4.11 it is 0.1eV ($H/T_k \approx 10^2$). For the larger field case of Figure 4.11 the Kondo temperature shows the best improvement.

4.3.3. Conclusion.

We identify the origin of the error in the exponent of the effective Kondo temperature of the strongly magnetic case to be the inconsistency introduced when we assume that the hybridisation is non zero and yet maintain that the down spin occupation is zero. When the model is extended to treat the fact that the down spin occupancy is never strictly zero, the weakly magnetic case, we see that although this occupation is still small it allows the build up of an up spin self energy. The up and down spin self energies for this weakly magnetic case are identified and are seen to be the origin of resonances in both the up and down spin densities of states near the Fermi energy.

A numerical calculation of the magnetisation as a function of magnetic field is made for the symmetric case where $\epsilon_f = -U/2$ and shows good agreement with Bethe ansatz results. Also via a comparison with the Bethe ansatz results we can identify a Kondo temperature. This Kondo temperature is shown to be an improvement over the effective Kondo temperature of the strongly magnetic case

in which the down spin occupation and the up spin self energy are assumed to be zero. Therefore when we treat the hybridisation of the down spin more self consistently we find that the magnetic ground state breaks down earlier with increasing hybridisation.

Similar reasoning can be applied for the analysis of the weakly ferromagnetic situation in the lattice. Up and down spin self energies analogous to those of the impurity calculation can be identified. Once again they are the origin of resonances in the up and down spin density of states near the Fermi level so that again we see how the inclusion of the up spin self energy leads to a quicker breakdown of the magnetic state with increasing hybridisation and hence an improved Kondo temperature. As in the impurity case the model does not yield expressions for the f electron density of states in certain energy regions once we make the magnon pole approximation to the susceptibility. In order to make any numerical calculations some form must be proposed for these missing densities of states. Unlike the impurity calculation there is no Friedel sum rule for guidance. Therefore we either have to introduce some inconsistency to the model by guessing at these densities of states or, perhaps relax the magnon pole approximation so that the susceptibility has some lorentzian form. This second possibility would of course bring in the complication of parameters which would then have to be fitted.

Figure 4.5.

$1/4\langle n_{f\downarrow} \rangle$ versus $\ln|\hat{H}|$ for $\Delta = 0.005\text{eV}$.

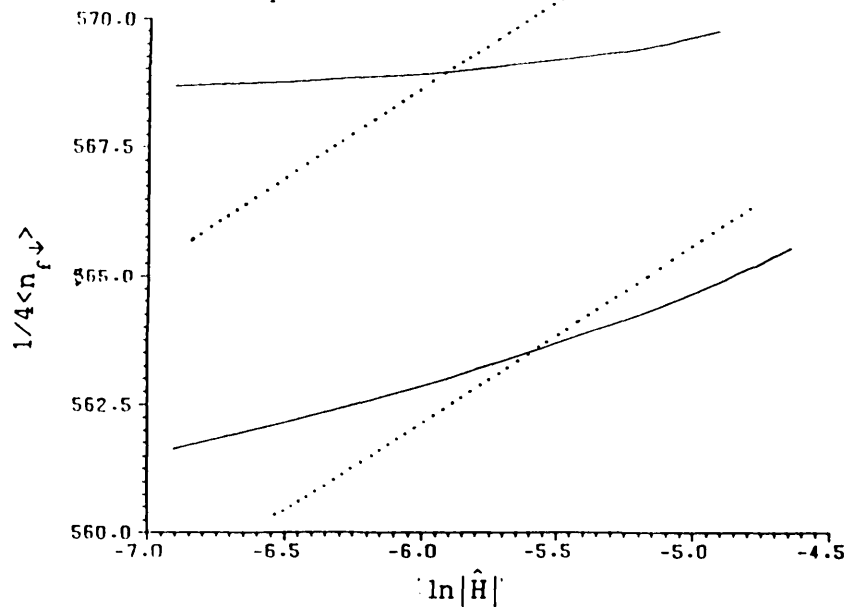


Figure 4.6.

$1/4\langle n_{f\downarrow} \rangle$ versus $\ln|\hat{H}|$ for $\Delta = 0.01\text{eV}$.

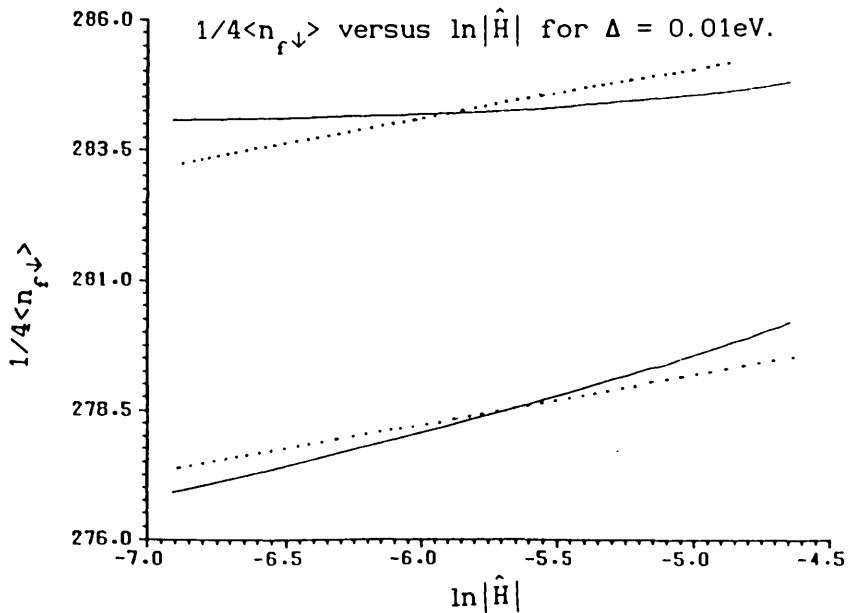


Figure 4.7.

$1/4\langle n_{f\downarrow} \rangle$ versus $\ln|\hat{H}|$ for $\Delta = 0.04\text{eV}$.

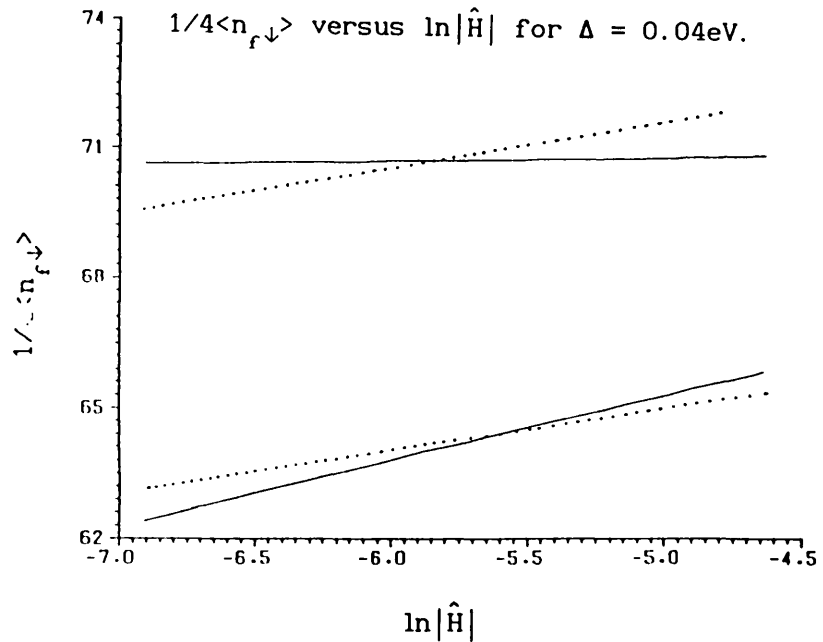


Figure 4.8.

$1/4\langle n_{f\downarrow} \rangle$ versus $\ln|\hat{H}|$ for $\Delta = 0.045\text{eV}$.

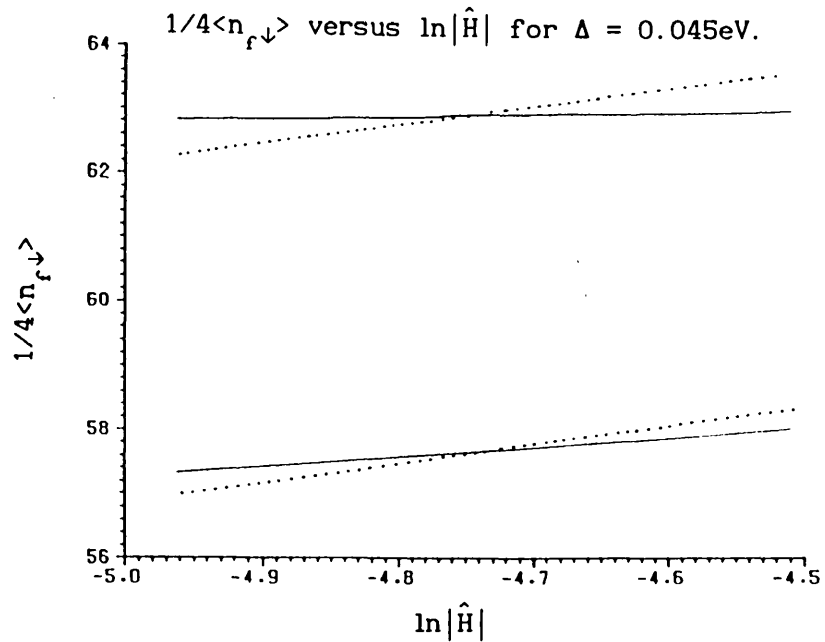


Figure 4.9. $1/4\langle n_{f\downarrow} \rangle - \ln|\hat{H}|$ versus $|\epsilon_f|\pi/\Delta$ for $\mu_B H = 0.01$ eV.

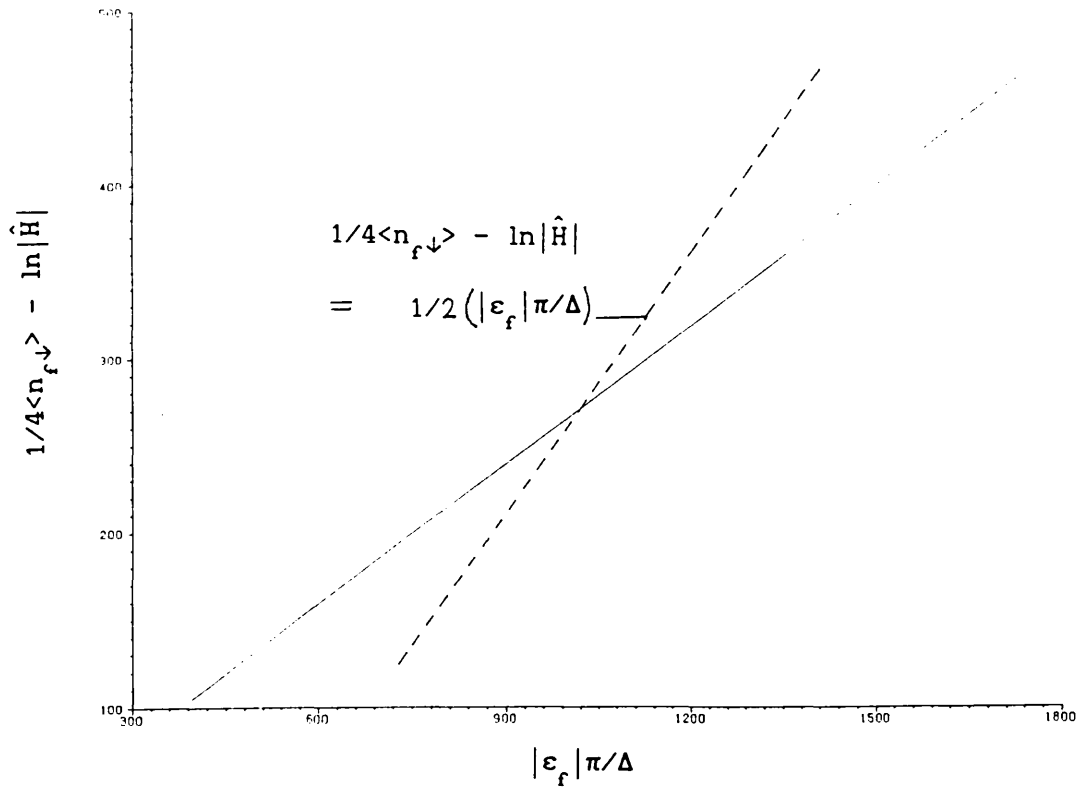
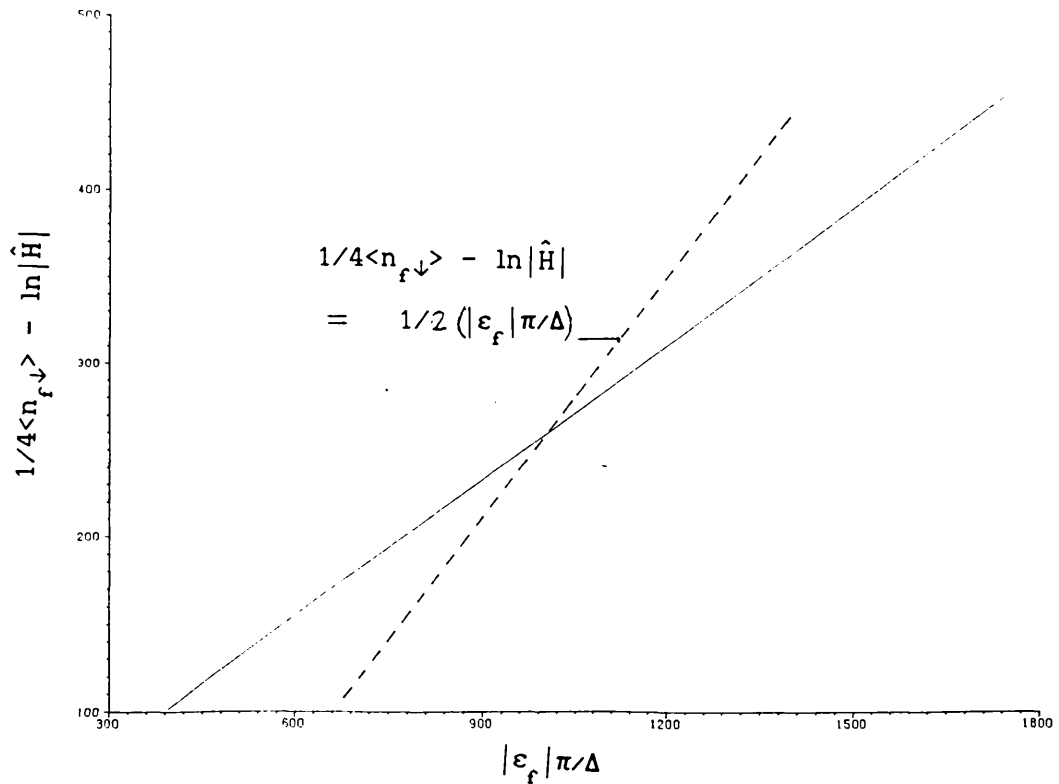


Figure 4.10. $1/4\langle n_{f\downarrow} \rangle - \ln|\hat{H}|$ versus $|\epsilon_f|\pi/\Delta$ for $\mu_B H = 0.1$ eV.



CHAPTER 5.

CRYSTAL FIELDS.

5.1. INTRODUCTION.

In most HF systems the degeneracy of the f level is treated as spin only, that is as two, rather than the full angular momentum degeneracy of fourteen. For many cerium systems this approximation is reasonable since crystal field effects and spin orbit coupling split the degeneracy and in the ground state the lowest level is a doublet. In treatments of HF systems account of the coulomb interaction and hybridisation is usually given first priority and the crystal field effects and spin orbit coupling are neglected. However it is through a combination of crystal fields and spin orbit coupling that the spin rotational symmetry of a system is broken, so that these effects are the origin of magnetic anisotropy in real systems. The existence of magnetic anisotropy means that it costs different energy to point the moment in different directions. In the spin only case of Chapter 3 the zero momentum magnon excitation corresponds to a rotation of total spin and costs no energy since the model does not care how the moment is orientated. However in the real systems the existence of magnetic anisotropy means that this rotation costs energy and thus the zero momentum magnon energy is finite as is seen in Figure 5.1.

Consider an improved model which takes account of crystal field effects, spin orbit splitting, hybridisation and coulomb correlation. If all these ingredients are present and are treated in a sensible way then a calculated magnon dispersion relation must permit comparison with the experimentally measured magnon energies. The ultimate aim, then, is to develop a model which contains magnetic anisotropy and then apply it to a particular system. Since any calculated magnon energy is necessarily a function of hybridisation, a comparison of the calculated and experimentally

measured magnon energies then gives a measure of the hybridisation of the system. Once the hybridisation is determined it can be used for a self consistent mass enhancement prediction. In the present work a model which can describe magnetic anisotropy is proposed and an analytical expression for the magnon energies is obtained. The actual calculation of the magnon energy and the comparison with experiment is left to future work.

A comparison of this sort is worthwhile since the hybridisation is very much an unknown quantity. The hybridisation is some measure of the overlap of conduction electron wavefunctions and the localised f electron wavefunctions, and is normally taken as momentum independent, which is a very crude approximation. Gunnarson and Schönhammer estimate $\Delta = \pi V^2 \rho_0$, where ρ_0 is the unhybridised conduction band density of states, to be of the order of 0.1eV for typical rare earth systems. They arrive at this value by fitting their calculated densities of states to XPS and BIS results.

The systems we aim to model are ferromagnetic systems in which the crystal field splitting is large and the lowest lying crystal field states form a Kramers doublet. In these systems the remainder of the crystal field states are at higher energies and can be considered to be unoccupied in the ground state. The ferromagnetic HF system CeSi_x , where $1.7 < x < 1.83$, falls into this category. In CeSi_x the lowest energy f states have $J = 5/2$ and form a low lying Γ_7 doublet as well as two other doublets up by 300K (Sato et al (Preprint) and Section 5.2.4). This system has a gap at $q = 0$ (see Figure 5.1) in the magnetic excitation spectrum due to the presence of magnetic anisotropy.

In normal local theories of rare earth metals the magnetic anisotropy is described assuming the full $J = 5/2$ is involved in the ground state. However in systems like HF CeSi_x , $1.7 < x < 2.0$, and CeAs where there is a large crystal field splitting, only the Γ_7 state has non negligible occupation in the ground state and therefore the anisotropy should result from interactions of the conduction band with the Γ_7 band alone. In fact Thayamballi and Cooper (1985) find magnetic anisotropy for just such a case, that is a two band model of a flat Γ_7 band and a conduction band. Therefore we expect that to obtain magnetic anisotropy it is sufficient to

consider only the Γ_7 band and conduction band in the model.

The system is treated here as a doubly degenerate f level which hybridises with a conduction band. The f electrons now occupy the crystal field states of the low lying doublet and are subject to coulomb repulsion when they occupy crystal field states on the same site. When the Anderson hamiltonian is written in this new basis of crystal field eigenstates the effects of crystal fields and spin orbit coupling are included in the model. The resulting hamiltonian is different to the spin only hamiltonian of Chapter 3 because now both the f doublet states hybridise with both the up and down spin conduction bands. The model therefore has a non spin only nature and thus we expect it to contain the magnetic anisotropy found by Thayamballi and Cooper (1985).

The new model, like the spin only model, also predicts the breakdown of the magnetic state with increasing hybridisation and so is ideally suited to description of the HF system CeSi_x which is discussed in Section 5.2.4. For $1.7 < x < 1.83$ CeSi_x is magnetic, while for $1.83 < x < 2.0$ it is non magnetic. From a tight binding picture we find that increasing the Si concentration increases the hybridisation (see Appendices B and C). Therefore in CeSi_x the magnetic state breaks down as the hybridisation increases so that this HF system is an ideal candidate for comparison with quantitative predictions of the model.

In the following sections we set up a general model in which it is recognised that for a particular case the model reduces to 'spin only'. When a model or a hamiltonian is labelled as 'spin only' we mean that the hamiltonian can be written within a new basis so that each of the two degenerate f doublet states hybridises with only one of the new orthogonal conduction states. Also the hybridisation between these two sets of f states and conduction band states is the same. Therefore we can easily identify a zero momentum pseudo magnon excitation which costs no energy. Any hamiltonian which is described as 'spin only' is analogous to the spin only model where the spin σ f's only hybridise with the spin σ conduction electrons, with the same hybridisation, and a simple zero momentum magnon excitation costs no energy. A 'spin only' hamiltonian does not describe magnetic anisotropy.

A similar variational calculation to that of Chapter 3 is made

and, since the findings of Thayamballi and Cooper (1985) indicate that the model should have magnetic anisotropy the mass enhancement is calculated, avoiding the choice of hybridisation for which the model reduces to 'spin only'. Later it is shown that the spin only condition is always satisfied when a Γ_7 doublet hybridises with a single s or p_x conduction band in any lattice with inversion symmetry. The implication is that the magnetic anisotropy calculated by Thayamballi and Cooper (1985) is due to some numerical error. In fact Thayamballi and Cooper remark that their calculated spin wave dispersion has the structure of 'spin only' which seems to vindicate the conclusion that their magnetic anisotropy is an error.

Finally it is shown that in order to obtain the magnetic anisotropy which we know to exist in real systems like CeSi_x and CeAs at least two conduction bands are needed.

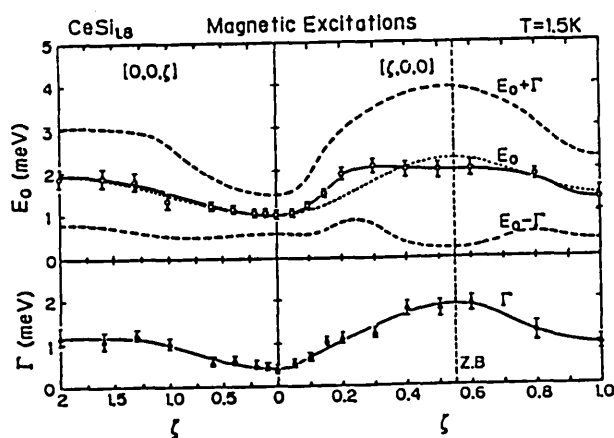


Figure 5.1. The magnetic excitation dispersion in CeSi_x (Kohgi et al (1987)).

5.2. A GENERAL THEORY.

5.2.1. The Hamiltonian.

Consider a system like HF CeSi_x or CeAs in which the crystal field is large so that in the ground state the lowest lying f states form a Kramers doublet. The remainder of the crystal field states are at much higher energies than the doublet and can be assumed to have negligible occupation in the ground state. We propose a Anderson lattice hamiltonian, for systems such as these, which describes a band of conduction electrons, a flat band of f electrons in the crystal field states of the low lying doublet, the hybridisation between the f electron states and the conduction electrons and the coulomb repulsion between f electrons in crystal field states on the same site:

$$H_{CF}^A = \sum_{k\sigma} \epsilon_k c_{k\sigma}^\dagger c_{k\sigma} + \sum_{ni} \epsilon_f f_{ni}^\dagger f_{ni} + \sum_{kn\sigma} (V_{\sigma n}(k) c_{k\sigma}^\dagger f_{kn} + h.c.) + \sum_i U f_{1i}^\dagger f_{1i} f_{2i}^\dagger f_{2i} \quad (5.2.1)$$

where

$$f_{in}^\dagger = \sum_k e^{-ik \cdot R_i} f_{kn}^\dagger \quad (5.2.2)$$

Here $c_{k\sigma}^\dagger$ creates a conduction electron in a state of momentum k and energy ϵ_k , while f_{in}^\dagger , $n = 1$ or 2 , creates an f electron in one of the degenerate crystal field states (labelled by n) on site i. The hybridisation term is chosen to allow mixing between f and conduction electrons of the same spin only. Since the crystal field states are a mixture of both up and down spin states this term hybridises both the up and down spin conduction states with both crystal field states to degrees dependent on the amplitude of up and down spin f's present in the crystal field states.

The various $V_{\sigma n}(k)$ are defined as:

$$V_{\sigma_n}(k) = \langle V | c_{k\sigma} H_{CF}^A f_{kn}^\dagger | V \rangle. \quad (5.2.3)$$

In general the hybridisation matrix, $V_{\sigma_n}(k)$ is treated as momentum independent and we adopt the same strategy later in this section. In Section 5.3.1 and 5.3.2 the full momentum dependent hybridisations, $V_{\sigma_n}(k)$, are calculated within the tight binding approximation. The calculation shows that for the present model with hamiltonian H_{CF}^A given by equation (5.2.1) the momentum dependence of the hybridisation must be considered to avoid the loss of important symmetry properties.

At this stage we notice that if we choose new basis states as linear combinations of the original up and down spin conduction states with creation operators:

$$c_{kn}^\dagger = \frac{\sum_{\sigma} V_{\sigma_n}(k) c_{k\sigma}^\dagger}{\sqrt{\sum_{\sigma} |V_{\sigma_n}(k)|^2}}, \quad (5.2.4)$$

where $n = 1$ or 2 labels the new basis states, then, within the new basis, c_{kn}^\dagger , c_{kn} , f_{kn}^\dagger , f_{kn} , $n = 1$ or 2 , the hybridisation term becomes:

$$\tilde{H}_{hyb} = \sum_{kn} (V_n(k) c_{kn}^\dagger f_{kn} + \text{h.c.}), \quad (5.2.5)$$

where

$$V_n(k) = \sqrt{\sum_{\sigma} |V_{\sigma_n}(k)|^2}. \quad (5.2.6)$$

The condition for the new basis states $c_{k_1}^\dagger |V\rangle$ and $c_{k_2}^\dagger |V\rangle$ to be orthogonal is:

$$[c_{kn}^\dagger, c_{km}] = \delta_{nm}, \quad (5.2.7)$$

or

$$V_{\alpha} = V_{\uparrow_1}(k) V_{\uparrow_2}^*(k) + V_{\downarrow_1}(k) V_{\downarrow_2}^*(k) = 0. \quad (5.2.8)$$

When $V_\alpha = 0$ we have a new orthogonal basis: $c_{kn}^\dagger, c_{kn}, f_{kn}^\dagger, f_{kn}$, $n = 1$ or 2 . Also if the hybridisations $V_{\sigma n}(k)$ are such that not only is the orthogonality condition, $V_\alpha = 0$, satisfied but also

$$V_1(k) = V_2(k), \quad (5.2.9)$$

then the hamiltonian H_{CF}^A reduces to a 'spin only' type hamiltonian in which the conduction electron states and the f electron states are characterised by a pseudo spin, $n = 1$ or 2 , instead of just a straightforward spin and we can identify a zero momentum magnetic excitation which costs no energy. This excitation is a zero momentum pseudo magnon which results in a pseudo spin flip analogous to the straight forward spin flip which results when the magnon of Chapter 3 is excited. Also in analogy with the original spin only case, the zero momentum pseudo magnon amounts to a uniform rotation of the pseudo moment and since this costs no energy the new model is insensitive to different orientations of the pseudo moment. Therefore when $V_\alpha = 0$, $V_1(k) = V_2(k)$, the model contains no magnetic anisotropy. Since Thayamballi and Cooper find magnetic anisotropy using a simple two band model it is assumed that for general hybridisation the criteria for the reduction to a 'spin only' problem are not satisfied. In the remainder of this section the model is treated for general hybridisations assuming that the conditions for the reduction to 'spin only' are not satisfied.

Once again a completely general diagrammatic derivation of the f electron Green function is useful. Suppose that the hybridisation and the coulomb interaction are treated as perturbations on the non interacting system of up and down spin conduction bands and two flat crystal field bands. An f electron now enters the system. It can either propagate without interacting as either a non interacting f_1 or f_2 propagator or it can interact with the system. If the interactions with the system are treated in two parts, namely, those in which the f electron emerges still as an f and those where it is changed to a conduction electron, then the propagator can be written as the solution of the self consistent equations:

$$\begin{aligned} \overline{\overline{G}}_{f_2}(k,E) &= \overline{G}_{f_2}^{\circ}(k,E) + \sum_{\sigma} \overline{G}_{f_2}^{\circ}(k,E) \overline{G}_{c_2}^{\circ}(k,E) \begin{array}{c} V_{\sigma 2}(k) \\ | \\ \hline \end{array} \\ & \quad (5.2.10) \end{aligned}$$

$$+ \overline{G}_{f_2}^{\circ}(k,E) \left(\sum_{22}(k,E) \right) \overline{\overline{G}}_{f_2}(k,E) + \overline{G}_{f_2}^{\circ}(k,E) \left(\sum_{21}(k,E) \right) \overline{\overline{G}}_{f_2}(k,E)$$

$$\begin{aligned} \overline{\overline{G}}_{c_2}(k,E) &= \overline{G}_{c_2}^{\circ}(k,E) \overline{\overline{G}}_{f_2}(k,E) \begin{array}{c} V_{\sigma 2}^*(k) \\ | \\ \hline \end{array} + \overline{G}_{c_2}^{\circ}(k,E) \overline{\overline{G}}_{f_2}(k,E) \begin{array}{c} V_{\sigma 1}^*(k) \\ | \\ \hline \end{array} \\ & \quad (5.2.11) \end{aligned}$$

$$\begin{aligned} \overline{\overline{G}}_{f_2}(k,E) &= \sum_{\sigma} \overline{G}_{f_1}^{\circ}(k,E) \overline{\overline{G}}_{c_2}^{\circ}(k,E) \begin{array}{c} V_{\sigma 1}(k) \\ | \\ \hline \end{array} + \overline{G}_{f_1}^{\circ}(k,E) \left(\sum_{12}(k,E) \right) \overline{\overline{G}}_{f_2}(k,E) \\ & \quad (5.2.12) \end{aligned}$$

$$+ \overline{G}_{f_1}^{\circ}(k,E) \left(\sum_{11}(k,E) \right) \overline{\overline{G}}_{f_2}(k,E)$$

so that

$$\begin{aligned}
G_{f_2 f_2}(k, E) &= G_{f_2 f_2}^{\circ}(k, E) + \sum_{\sigma} G_{f_2 f_2}^{\circ}(k, E) V_{\sigma 2}(k) G_{c_{\sigma} f_2}(k, E) \\
&\quad + G_{f_2 f_2}^{\circ}(k, E) \Sigma_{22}(k, E) G_{f_2 f_2}(k, E) \\
&\quad + G_{f_2 f_2}^{\circ}(k, E) \Sigma_{21}(k, E) G_{f_1 f_2}(k, E),
\end{aligned}
\tag{5.2.13}$$

$$\begin{aligned}
G_{c_{\sigma} f_2}(k, E) &= G_{c_{\sigma} c_{\sigma}}^{\circ}(k, E) V_{\sigma 2}^*(k) G_{f_2 f_2}(k, E) \\
&\quad + G_{c_{\sigma} c_{\sigma}}^{\circ}(k, E) V_{\sigma 1}^*(k) G_{f_1 f_2}(k, E),
\end{aligned}
\tag{5.2.14}$$

$$\begin{aligned}
G_{f_1 f_2}(k, E) &= \sum_{\sigma} G_{f_1 f_1}^{\circ}(k, E) V_{\sigma 1}(k) G_{c_{\sigma} f_2}(k, E) \\
&\quad + G_{f_1 f_1}^{\circ}(k, E) \Sigma_{12}(k, E) G_{f_2 f_2}(k, E) \\
&\quad + G_{f_1 f_1}^{\circ}(k, E) \Sigma_{11}(k, E) G_{f_1 f_2}(k, E),
\end{aligned}
\tag{5.2.15}$$

and the quasi particle energies E are the zeros of

$$\begin{vmatrix}
E - \varepsilon_k & 0 & -V_{1\uparrow}(k) & -V_{2\uparrow}(k) \\
0 & E - \varepsilon_k & -V_{1\downarrow}(k) & -V_{2\downarrow}(k) \\
-V_{1\uparrow}^*(k) & -V_{1\downarrow}^*(k) & E - \varepsilon_f - \Sigma_{11}(k, E)_{\text{ex}} & \Sigma_{12}(k, E)_{\text{ex}} \\
-V_{2\uparrow}^*(k) & -V_{2\downarrow}^*(k) & \Sigma_{21}(k, E)_{\text{ex}} & E - \varepsilon_f - \Sigma_{22}(k, E)_{\text{ex}}
\end{vmatrix} = 0
\tag{5.2.16}$$

All the unknown quantities have been assigned to the self energies $\Sigma_{nm}(k, E)_{\text{ex}}$ n, m one or two. The subscript, ex , is intended to indicate that these are the exact quantities. $\Sigma_{nn}(k, E)_{\text{ex}}$ contains

all processes or diagrams in which an f_n electron first interacts with the system via the coulomb interaction and after all subsequent interactions it emerges finally still as an f_n . $\Sigma_{12}(k, E)_{ex}$ is another proper self energy containing all processes or diagrams in which an f_1 first interacts with the system via the coulomb interaction and after all subsequent interactions it emerges as an f_2 . Similarly for $\Sigma_{21}(k, E)_{ex}$.

The following calculation involves postulating a reasonable variational wavefunction for an f electron in the system by including those processes which are considered to be the most important under the condition of large U and negligible occupation of one of the crystal field levels, that is strong ferromagnetism. The method yields determinantal equations for the quasi particle energies of the correct form derived above.

5.2.2. The Ground State For U Infinite.

As for the spin only case a variational wavefunction for an f electron in the system is proposed and a Dyson equation for the quasi particle energies results. The first task is to propose a ground state for the system and, once this is established, to calculate the f single particle Green function by postulating what happens when an f electron is added to the system.

The method is applied firstly to the U infinite or strongly ferromagnetic system. The description is of a ferromagnetic system where it is assumed that in the atomic limit the f_1 state of the low lying doublet is occupied, and coulomb repulsion renders the other crystal field state unoccupied at large energy. Therefore the starting point for $V \neq 0$ is a Hartree Fock ground state of f_1 states hybridising with both up and down conduction bands and an unoccupied and unhybridised crystal field band of f_2 states at energy $\epsilon_f + U\langle n_1 \rangle$, where $\langle n_1 \rangle$ is the occupation of crystal field f_1 states in the ground state.

In this $U \rightarrow \infty$ Hartree Fock ground state we assume that the off diagonal or Hartree Fock exchange terms are zero due to symmetry in the lattice (see Section 5.2.6) or are at least small for large enough U . Later in Section 5.2.6 when the Hartree Fock ground state

is examined more closely we find that this is indeed the case but only for a certain choice of hybridisations. These particular hybridisations satisfy one of the criteria for a 'spin only' hamiltonian, that is $V_\alpha = 0$ (see equation (5.2.8)). For general hybridisation, $V_\alpha \neq 0$ and these Hartree Fock exchange terms are non zero and must be included (see Section 5.2.6).

In the remainder of this section we assume that the Hartree Fock exchange terms are negligible. The hybridisation of the lower crystal field level with the conduction band results in new bands whose energies and wave functions are eigenstates of:

$$H_{CF}^o = \sum_{k\sigma} \epsilon_k c_{k\sigma}^\dagger c_{k\sigma} + \sum_i \epsilon_f f_{1i}^\dagger f_{1i} + \sum_{k\sigma} V_{\sigma 1} (c_{k\sigma}^\dagger f_{k1} + f_{k1}^\dagger c_{k\sigma}), \quad (5.2.17)$$

where the hybridisation matrix is assumed real and k independent as is usual in treatments of the Anderson hamiltonian. The operators a_{kb}^\dagger , a_{kb} which diagonalise the hamiltonian H_{cf}^o are:

$$a_{kb}^\dagger = A_{knb} f_{kn}^\dagger + \sum_{\sigma} B_{k\sigma b} c_{k\sigma}^\dagger, \quad (5.2.18)$$

where

$$H_{CF}^o a_{kb}^\dagger |V\rangle = \epsilon_{kb} a_{kb}^\dagger |V\rangle, \quad (5.2.19)$$

and the subscript b allows for the possibility of more than one band. As for the spin only case we solve for A_{knb} , the f_n amplitude in any eigenstate, $B_{k\sigma b}$, the spin σ conduction electron amplitude in any state, and new band energies ϵ_{kb} . The eigenstates of energy ϵ_{kb} are found to form three bands with energies satisfying

$$\begin{vmatrix} \epsilon_{kb} - \epsilon_k & 0 & -V_{\uparrow 1} \\ 0 & \epsilon_{kb} - \epsilon_k & -V_{\downarrow 1} \\ -V_{\uparrow 1} & -V_{\downarrow 1} & \epsilon_{kb} - \epsilon_f \end{vmatrix} = 0 \quad (5.2.20)$$

where the subscript b labels the possible multiple solutions, or bands, of equation (5.2.20). When equation (5.2.20) for the quasi particle energies is coupled with the with the final equation for the flat band at $\epsilon_f + U\langle n_1 \rangle$, that is

$$\epsilon_{kb} - \epsilon_f - U\langle n_1 \rangle = 0 \quad (5.2.21)$$

then the full equation for the quasi particle energies of the approximate ground state is identical in form to the general equation for the quasi particle energies determined from a general diagrammatic expansion (see equation (5.2.16)). In this approximate ground state the coulomb interaction is treated in the Hartree Fock approximation and the hybridisation of crystal field f_2 with the conduction bands is assumed to be zero so that $\Sigma_{22}^{ex}(E)$ is approximated by $U\langle n_1 \rangle$ and $V_{2\sigma}$ by zero in equation (5.2.16). From this Hartree Fock starting point we proceed to include more effects of the coulomb correlation. The improvements appear as corrections to the Hartree Fock self energy, as they must to agree with the prediction of the general diagrammatic expansion

The three hybridised bands of equation (5.2.20) are labelled by the band index $b = \alpha, \beta$ or γ and have energies ϵ_{kb} given by:

$$\epsilon_{k\alpha} = \epsilon_k, \quad (5.2.22)$$

$$\epsilon_{k\beta} = \frac{\epsilon_k + \epsilon_f \pm \sqrt{(\epsilon_f - \epsilon_k)^2 + 4V^2}}{2}, \quad (5.2.23)$$

where

$$V^2 = V_{\uparrow 1}^2 + V_{\downarrow 1}^2 \quad (5.2.24)$$

These energies, ϵ_{kb} , describe a quasi band labelled by α in which the quasi particle states are a mixture of up and down spin conduction states only, and have energies equal to the original conduction band energies. The other two bands contain a mixture of both up and down spin conduction states as well as some f weight. The f weights in the quasi particle states are A_{k1b}^2 where

$$A_{k1b} = \frac{V}{\sqrt{(\epsilon_{kb} - \epsilon_f)^2 + V^2}} \quad b = \beta, \gamma, \quad (5.2.25)$$

and

$$A_{k1\alpha} = 0, \quad (5.2.26)$$

and the up and down spin conduction weights are $B_{k\sigma b}^2$ where

$$B_{k\sigma b} = \frac{V_{\sigma 1} (\epsilon_{kb} - \epsilon_f)}{V \sqrt{(\epsilon_{kb} - \epsilon_f)^2 + V^2}} \quad b = \beta, \gamma \quad (5.2.27)$$

$$B_{k\sigma\alpha} = \sigma \frac{V_{-\sigma 1}}{V}. \quad (5.2.28)$$

In equation (5.2.28) $\sigma = 1$ when spin is up and $\sigma = -1$ when spin is down. Also the normalisation associated with equation (5.2.18) is:

$$\sum_{\sigma} B_{k\sigma b}^2 + A_{k1b}^2 = 1, \quad (5.2.29)$$

for any band b . The ground state is written in terms of the eigenstate creation operators as:

$$|0\rangle = \prod_{\substack{kb \\ occ}} a_{kb}^{\dagger} |V\rangle \quad (5.2.30)$$

It is correct in the atomic limit of no hybridisation and is considered to be a good basis for an improved treatment of coulomb interaction. In the postulated ground state $|0\rangle$ the band picture can be drawn schematically as in Figure 5.2

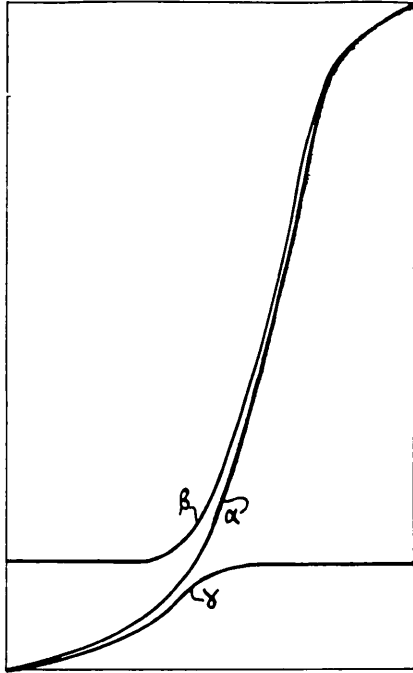


Figure 5.2. A schematic ground state band picture for the periodic Anderson model with crystal field and spin orbit effects included.

From equation (5.2.25) for the f weight in the β and γ bands we see that for ϵ_{kb} , $b = \beta$ or γ , near ϵ_f the states in these bands are of mainly f character whereas for ϵ_{kb} , $b = \beta$ or γ , away from ϵ_f they are mainly conduction in character. The initial assumption that the upper crystal field level is unoccupied and that its hybridisation may be neglected results in an α band of purely conduction character.

5.2.3. A Variational Wavefunction.

The next stage in the calculation is the proposal of a variational wavefunction for an f electron of momentum k in the presence of the interactions described by the periodic Anderson hamiltonian of equation (5.2.1). As in the spin only case of Chapter 3 the wavefunction is written as a linear combination of all the most likely processes which would occur if an f electron were put into the system. At zero temperature the lowest energy and most likely processes are considered to be the following: the f electron can occupy the upper crystal field state f_2 , it can, via hybridisation $V_{1\sigma}$, occupy the state $a_{k\beta}$ and via $V_{2\sigma}$ the state $a_{k\alpha}$ and also in analogy with the spin only case it can, via the coulomb interaction,

scatter into a state $a_{k\beta}'$ and excite a particle hole or magnon type excitation. The creation operator of the low energy particle hole excitation of this problem which is analogous to the magnon in the spin only case is approximated as:

$$A_{k-k'}^- = \sum_p f_{(p-k)2}^\dagger f_{(p-k)1} \quad (5.2.31)$$

This low energy excitation created by $A_{k-k'}^-$, is not actually a magnon but will be called by that name in what follows. The variational wavefunction is written as a linear combination of all these possible low energy excitations:

$$|\Psi\rangle = M f_{k_2}^\dagger |0\rangle + \sum_{b=\alpha\beta} N_{kb} a_{kb}^\dagger |0\rangle + \sum_{\substack{k' \\ k'\beta \text{ not occ}}} G_{k'\beta} a_{k'\beta}^\dagger A_{k-k'}^- |0\rangle, \quad (5.2.32)$$

where the sum over k' is such that states $k'\beta$ are not occupied. The third process in the wave function is mediated by the coulomb interaction and has the end result of adding a correction to the Hartree Fock self energy of the approximate ground state. The self energy diagrams which correspond to this third process in which the f electron scatters into an $a_{k'\beta}$ state and excites a magnon can be represented by Figure 3.3 where now the up spin f propagators are replaced by the f_1 propagators and the down spin f propagators by the f_2 propagators. The self energy diagrams of Figure 3.3 and hence the corresponding process in the variational wavefunction are considered to be the most important for inclusion in the calculation of this strongly ferromagnetic ground state in which the occupation of the f_1 state is close to one in analogy with the spin only case (see Section 3.2.3).

We solve for the coefficients of the variational wavefunction by left multiplying the Schrodinger equation:

$$H|\Psi\rangle = E|\Psi\rangle, \quad (5.2.33)$$

by f_{k_2} , $a_{k\beta}$ and $A_{k-k'}^+ a_{k''\beta}$. The result is equation (5.2.34) for the excitation energy $E = E - E_0$ where E_0 is the ground state energy and $E > 0$. Since the poles of the f electron Green function are by

definition these very excitation energies then equation (5.2.34) is a Dyson equation for the quasi particle energies E greater than the Fermi level:

$$\begin{vmatrix} E - \varepsilon_k & 0 & -M2_\alpha(k) \\ 0 & E - \varepsilon_{k\beta} & -M2_\beta(k) \\ -M2_\alpha(k) & -M2_\beta(k) & E - \varepsilon_f - \Sigma_{22}(k, E) \end{vmatrix} = 0, \quad (5.2.34)$$

where

$$M2_\alpha(k) = \left(\sum_{\sigma} V_{\sigma 2} B_{k\sigma\alpha} \right), \quad (5.2.35)$$

$$M2_\beta(k) = \left(\sum_{\sigma} V_{\sigma 2} B_{k\sigma\beta} \right), \quad (5.2.36)$$

and

$$\Sigma_{22}(k, E) = \frac{\sum_{\substack{k' \beta \\ \text{unocc}}} \frac{U^2 A_{k' 1 \beta}^2 \langle n_1 \rangle}{E - \varepsilon_{k' \beta} - \hbar \omega_{k-k'}}}{1 - \sum_{\substack{k' \beta \\ \text{unocc}}} \frac{U A_{k' 1 \beta}^2}{E - \varepsilon_{k' \beta} - \hbar \omega_{k-k'}}}} + U \langle n_1 \rangle. \quad (5.2.37)$$

The magnon energy in this approximation is defined by:

$$\hbar \omega_{k-k'} + E_0 = \frac{\langle 0 | A_{k-k'}^+ H_{CF}^A A_{k-k'}^- | 0 \rangle}{\langle 0 | A_{k-k'}^+ A_{k-k'}^- | 0 \rangle} \quad (5.2.38)$$

where E_0 is the energy of the approximate ground state.

The Dyson equation (5.2.34) can be expressed in the form

expected from the general diagrammatic expansion of (5.2.16). We rewrite the hamiltonian H_{CF}^A in the new basis of eigenstates $a_{kn}^\dagger|V\rangle$ and perform another general diagrammatic derivation, this time treating only the hybridisation of the f_2 level and the coulomb interaction as perturbations. The Dyson equation which results must describe the same quasi particle energies as equation (5.2.16). Since the variational wavefunction of equation (5.3.32) can only describe f electron states with $k > k_F$ and $E > E_F$ where k_F is the Fermi wavevector and E_F is the Fermi energy we write down this general diagrammatic expansion for an f_2 particle propagator, that is with $k > k_F$. The Dyson equation which results has exactly the form of equation (5.2.34) so that the calculated Dyson equation (5.2.34) is equivalent in form to that expected from the diagrammatic expansion of equation (5.2.16).

The spin only model of Chapter 3 does not describe magnetic anisotropy and thus does not support the definition of a realistic magnon. This limitation of the 'spin only' model means that in the spin only self energy of equation (3.2.18), which is analogous to the crystal field self energy of equation (5.2.37), we do not calculate the magnon dispersion self consistently but approximate it by a flat magnon dispersion. The approximation of a flat magnon dispersion is not unreasonable for $CeSi_x$ (see Figure 5.1). The new crystal field model however can describe magnetic anisotropy provided $V_\alpha \neq 0$ or $V_1(k) \neq V_2(k)$ (see equations (5.2.8) and (5.2.9)). Therefore at this stage we could define and calculate a more realistic magnon dispersion which could then be compared with the measured magnon dispersion for a particular system to determine the hybridisation in this system. However in Section 5.3.1 we show that when a Γ_7 doublet band hybridises with either an s or p_x conduction band in a lattice with inversion symmetry $V_\alpha = 0$ and $V_1(k) = V_2(k)$ so that the model reduces to 'spin only'. Therefore this simple two band model cannot describe the magnetic anisotropy observed in the large crystal field system CeAs. CeAs has a cubic lattice and therefore inversion symmetry. It is also likely that the two band model is not sufficient to describe the magnetic excitation spectrum in systems where the lattice does not have inversion symmetry. Therefore we continue to search for a model which does not reduce to 'spin only' and can describe magnetic

anisotropy.

In order to discuss the 'spin only' or non 'spin only' nature of a model the actual hybridisations between the Γ_7 doublet band and a conduction band must be calculated for a particular system. At this stage the prototype system CeSi_x is introduced.

5.2.4. The Prototype System CeSi_x

The model of the previous section is completely general in that it can be applied to any system in which the crystal field is large and the only f states which are occupied in the ground state form a doublet. As in the spin only case of Chapter 3 the model predicts the build up of HF behaviour as well as the breakdown of the magnetic state with increasing hybridisation. In order to make any quantitative comparison with experiment it is necessary to calculate the hybridisation for a particular system. The HF system CeSi_x is chosen for the calculation.

For $1.7 \leq x < 1.83$ the system CeSi_x is magnetic while for $1.83 \leq x \leq 2.0$ it is non magnetic at least down to 0.1K. The electronic specific heat of the non magnetic system is fairly large $\gamma = 0.1\text{J/molK}^2$ for $x = 2.0$ and $\gamma = 0.2\text{J/molK}^2$ for $x = 1.86$. From studies of the magnetic susceptibility and the magnetic part of the resistivity the system is judged to be a dense Kondo lattice system (M.Kohgi et al (1987)). The system undergoes a magnetic transition for $x < 1.83$ at $T_c = 10\text{K}$. The saturation moment is much reduced from the moment expected by considering the crystal field effects for a Ce^{3+} ion, as is the magnetic entropy. These measurements suggest that the ferromagnetic state is also strongly affected by the Kondo effect. The experimental facts indicate that CeSi_x is on the boundary of a ferromagnetic instability caused at least partly by the competition between the Kondo effect and the exchange interactions. The HF system CeSi_x is an ideal candidate for modelling since: it is heavy, it varies from magnetic, $1.7 \leq x < 1.83$, to non magnetic, $1.83 \leq x \leq 2.0$, with increasing silicon concentration or hybridisation and in the ground state the lowest lying crystal field states form a Γ_7 doublet.

In CeSi_x the multiplet $J = 5/2$, where J is the total angular

momentum, of the Ce^{3+} splits into three doublets in the tetragonal crystal field. These three doublets are the lowest lying crystal field states of the system and consist of a Γ_7 doublet and a split Γ_8 quartet at higher energies. The splitting between the Γ_7 doublet and the lowest of the higher energy states is 300K (Sato et al (Preprint)) so that only the Γ_7 has a non negligible occupation in the ground state. The states of the Γ_7 doublet are written:

$$\Gamma_7 = a|\pm\frac{5}{2}\rangle - b|\mp\frac{3}{2}\rangle, \quad (5.2.39)$$

where a and b are coefficients depending on the crystal field of the system. For $CeSi_x$ $x = 1.7$ (a magnetic system) these coefficients are calculated to be $a = 0.472$ and $b = 0.882$ (Sato et al (Preprint)). Also the same authors calculate $a = 0.454$ and $b = 0.981$ for the non magnetic system with $x = 1.86$. These values for a and b are not much different from the cubic crystal field values of $a = 0.408$ and $b = 0.913$.

The states $|\pm\frac{5}{2}\rangle$ and $|\pm\frac{3}{2}\rangle$ of the Γ_7 doublet all have total angular momentum $J = \frac{5}{2}$ and are quantised by their z components of angular momentum $J_z = \pm\frac{5}{2}$ and $J_z = \pm\frac{3}{2}$ respectively. The two states of the Γ_7 doublet are written:

$$\Gamma_{17} = f_{1i}^{\dagger}|V\rangle = a|\frac{5}{2}\rangle - b|-\frac{3}{2}\rangle, \quad (5.2.40)$$

$$\Gamma_{27} = f_{2i}^{\dagger}|V\rangle = a|-\frac{5}{2}\rangle - b|+\frac{3}{2}\rangle, \quad (5.2.41)$$

where $|V\rangle$ is the vacuum and i a site index. These states can be written as linear combinations of products of their orbital angular momentum and spin components weighted by Clebsch Gordan coefficients as:

$$\begin{aligned} |J_z\rangle &= |J = \frac{5}{2}, J_z\rangle \\ &= \sum_{m_L, m_S} \langle L=3, S = \frac{1}{2}, m_L, m_S | J = \frac{5}{2}, J_z \rangle |L=3, m_L\rangle |S = \frac{1}{2}, m_S\rangle, \\ &\quad \text{st. } m_L + m_S = J_z \end{aligned} \quad (5.2.42)$$

where L is the total orbital angular momentum which is three for f electrons, S the total spin of $1/2$, m_L the z component of orbital angular momentum and m_S the z component of spin either $\pm\frac{1}{2}$ for spin up or down. We write the Clebsch Gordan coefficients $\langle L=3, S=\frac{1}{2}, m_L, m_S | J=\frac{5}{2}, J_z \rangle$, as $C_{m_L \sigma}$ where σ now serves the purpose of m_S so that

$$f_{1i}^\dagger |V\rangle = a \sum_{\substack{m_L \sigma \\ m_L + \sigma = 5/2}} C_{m_L \sigma} f_{i m_L \sigma}^\dagger |V\rangle - b \sum_{\substack{m_L \sigma \\ m_L + \sigma = -3/2}} C_{m_L \sigma} f_{i m_L \sigma}^\dagger |V\rangle, \quad (5.2.43)$$

$$f_{2i}^\dagger |V\rangle = a \sum_{\substack{m_L \sigma \\ m_L + \sigma = -5/2}} C_{m_L \sigma} f_{i m_L \sigma}^\dagger |V\rangle - b \sum_{\substack{m_L \sigma \\ m_L + \sigma = 3/2}} C_{m_L \sigma} f_{i m_L \sigma}^\dagger |V\rangle, \quad (5.2.44)$$

where $f_{i m_L \sigma}^\dagger$ is an operator, obeying normal fermion anticommutation relations, which creates an f electron with z component of orbital angular momentum m_L and spin σ on site i . At this stage it is useful to calculate the magnetic moments, μ_n of the Γ_{n7} states. The magnetic moments are defined as:

$$\mu_n = \langle \Gamma_{n7} | \hat{J}_z + \hat{S}_z | \Gamma_{n7} \rangle \quad n=1 \text{ or } 2, \quad (5.2.45)$$

where \hat{J}_z is the usual operator which measures z component of angular momentum in a state so that

$$\hat{J}_z | J, J_z \rangle = J_z | J, J_z \rangle, \quad (5.2.46)$$

and \hat{S}_z measures the z component of spin

$$\hat{S}_z | S = \frac{1}{2}, \sigma \rangle = \sigma | S = \frac{1}{2}, \sigma \rangle. \quad (5.2.47)$$

Here J , J_z , S and m_S are as in equation (5.2.42). The magnetic moments for arbitrary a and b are therefore:

$$\mu_{\frac{1}{2}} = \pm a^2 \frac{15}{7} \mp b^2 \frac{9}{7}, \quad (5.2.48)$$

where we have substituted the values of the relevant Clebsch Gordan coefficients in equations (5.2.43) and (5.2.44). For the ferromagnetic ground state of $\text{CeSi}_{1.7}$ we expect that one or the other of the crystal field states is practically fully occupied. The magnetic moment expected by considering the crystal field effects is $\mu_1 = -0.523\mu_B$ if the Γ_{17} level is occupied or $\mu_2 = 0.523\mu_B$ if the Γ_{27} is occupied. However the measured magnetisation for $\text{CeSi}_{1.7}$ with $T_c = 13\text{K}$ is strongly anisotropic with a saturation moment for the Ce atom of around $0.45\mu_B$ along the a axis. The moment of the ferromagnetic ground state is therefore already much reduced from its expected value of $0.523\mu_B$ for the strongly ferromagnetic ground state of zero Γ_{17} occupation. The Kondo effect must be competing with exchange so that there is some Γ_{17} occupation in the ground state.

5.2.5. The Mass Enhancement.

The model and variational treatment of Sections 5.2.1 to 5.2.3 are only good in the limit $V_\alpha \rightarrow 0$ where V_α is defined in equation (5.2.8) since only in this limit are the Hartree Fock exchange terms negligible (see Section 5.2.6). In Section 5.3.1 we show that for a band of Γ_7 doublet states hybridising with a single conduction band in any lattice with inversion symmetry the criteria for a 'spin only' hamiltonian as defined in Section 5.2.1 are always satisfied. Therefore the magnetic anisotropy of the model is lost. However in real systems like CeSi_x there are deviations from complete inversion symmetry as the concentration of silicon is varied.

In the remainder of this section a brief mention is made of an initial mass enhancement calculation for $\text{CeSi}_{1.7}$ in which it is assumed that the off diagonal Hartree Fock terms are negligible but $V_\alpha \neq 0$. The hybridisation, $V_{\sigma n}$, of the crystal field state Γ_{n7} with the conduction band state of spin σ , is assumed to be proportional to the amplitude of the spin σ , f in the state Γ_{n7} . From equations

(5.2.43) and (5.2.44) we find:

$$V_{1\uparrow} \propto (a^2 C_{2\uparrow}^2 + b^2 C_{-2\uparrow}^2)^{1/2} \quad (5.2.49)$$

$$V_{1\downarrow} \propto (a^2 C_{3\uparrow}^2 + b^2 C_{-1\uparrow}^2)^{1/2} \quad (5.2.50)$$

$$V_{2\uparrow} = V_{1\downarrow} \quad \text{and} \quad V_{2\downarrow} = V_{1\uparrow} \quad (5.2.51)$$

As for the spin only model, the mass enhancement is defined as the ratio of quasi particle band density of states over the unperturbed conduction band density of states. The states in the quasi particle bands are a mixture of f electrons of both spins. The band picture can no longer be split into up and down spin band parts as was the situation in the spin only case. Therefore mass enhancement is given by:

$$\frac{m^*}{m} = \frac{\sum_b N_b(E)}{N_0(E)} \Big|_{E=0}, \quad (5.2.52)$$

where $N_b(E)$ is the density of states in quasi particle band b and $N_0(E)$ is now the sum of the up and down spin conduction band density of states.

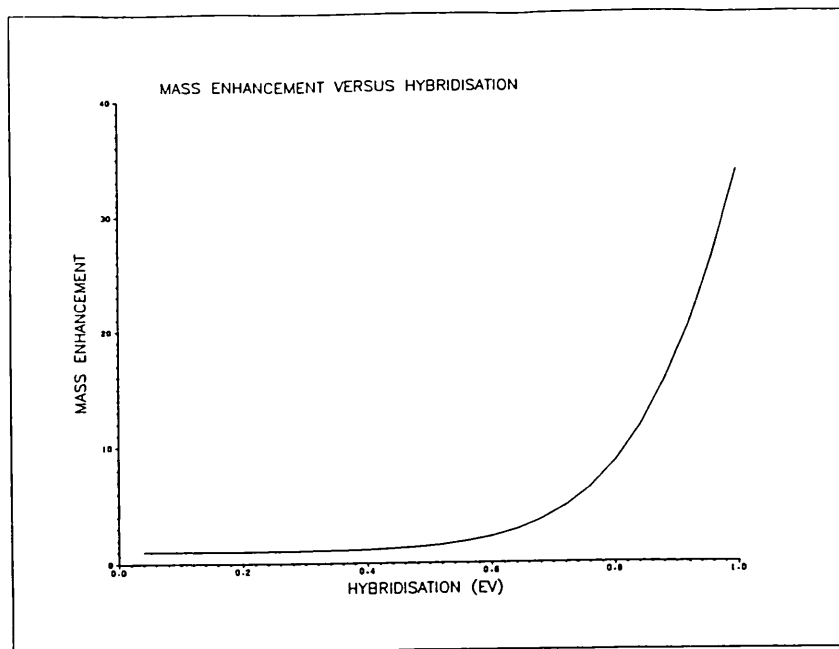


Figure 5.4. The mass enhancement versus hybridisation. The figure shows a plot of mass enhancement versus $V = (V_{1\uparrow}^2 + V_{1\downarrow}^2)^{1/2}$ for $\epsilon_f = -1.5\text{eV}$, $U = 7\text{eV}$ and unperturbed conduction band width $W = 10\text{eV}$. Also $a = 0.472$, $b = 0.882$ (Sato et al (Preprint)) and the magnon dispersion is taken to be flat with $\hbar\omega_{\mathbf{k}-\mathbf{k}'} = 0.002\text{eV}$ for all $\mathbf{k}-\mathbf{k}'$ (Kohgi et al (1987)).

5.2.6. The Hartree Fock Ground State For U Finite.

When the calculation is extended to U finite it becomes clear that the U infinite limit of Section (5.2.2) is only strictly correct when the condition $V_\alpha = 0$ is satisfied and not for general hybridisation as was assumed for the mass enhancement calculation. For general hybridisation the off diagonal Hartree Fock terms are non zero and, as the following calculation shows, are finite even for infinite U .

With U finite the operators which diagonalise the Hartree Fock hamiltonian are:

$$\hat{a}_{\mathbf{k}l}^\dagger = \left[\sum_n \hat{A}_{\mathbf{k}n1} f_{\mathbf{k}n}^\dagger + \sum_\sigma \hat{B}_{\mathbf{k}\sigma 1} c_{\mathbf{k}\sigma}^\dagger \right] |V\rangle, \quad (5.2.53)$$

where l is the band index and $n = 1$ or 2 labels the crystal field doublet states. The new Hartree Fock eigenstates are seen to be mixtures of both up and down conduction states as well as both f_1 and f_2 crystal field states. Also

$$\hat{H}_{CF}^{\circ} \hat{a}_{k1}^{\dagger} |V\rangle = \hat{\varepsilon}_{k1} \hat{a}_{k1}^{\dagger} |V\rangle, \quad (5.2.54)$$

where \hat{H}_{CF}° is the U finite Hartree Fock hamiltonian and $\hat{\varepsilon}_{k1}$ are the Hartree Fock eigenstate energies. To find \hat{H}_{CF}° and $\hat{\varepsilon}_{k1}$ we solve

$$[\hat{a}_{k1}^{\dagger}, \hat{H}_{CF}^A] \approx 0, \quad (5.2.55)$$

where the \approx is replaced by $=$ when the Hartree Fock approximation is made to the coulomb interaction. To make the Hartree Fock approximation groups of operators in the coulomb interaction contribution to equation (5.2.55) are replaced by the sum of the possible ways they can be written as number operators. The resulting Hartree Fock hamiltonian is:

$$\begin{aligned} \hat{H}_{CF}^{\circ} = & \sum_{k\sigma} \varepsilon_k c_{k\sigma}^{\dagger} c_{k\sigma} + \sum_{kn} \varepsilon_{fn} f_{nk}^{\dagger} f_{nk} + \sum_{nk\sigma} (V_{\sigma n}(k) c_{k\sigma}^{\dagger} f_{kn} + \text{h.c.}) \\ & - U \sum_{\kappa} [\langle n_{12} \rangle f_{k1}^{\dagger} f_{k2} + \text{h.c.}] , \end{aligned} \quad (5.2.56)$$

where

$$\begin{aligned} \varepsilon_{f1} &= \varepsilon_f + U \langle n_2 \rangle , \\ \varepsilon_{f2} &= \varepsilon_f + U \langle n_1 \rangle , \end{aligned} \quad (5.2.57)$$

and

$$\langle n_{12} \rangle = \sum_{k1 \text{ occ}} \hat{A}_{k11} \hat{A}_{k21}^* = \langle n_{21} \rangle^* \quad (5.2.58)$$

Here l labels the bands or the multiple solutions of equation (5.2.54) and $\langle n_{12} \rangle$ and $\langle n_{21} \rangle$ are the exchange terms of Hartree Fock. These terms reflect the fact that an f_1 state can hop into the conduction band and then back to an f_2 . In the previous sections this on-site hopping is assumed to be zero due to symmetry or at

least to be small for $U \rightarrow \infty$. When we solve the Hartree Fock problem for $\langle n_{12} \rangle$ we find:

$$\langle n_{12} \rangle = \frac{\sum_{\substack{k1 \\ occ}} \frac{|\hat{A}_{k21}|^2 V_\alpha}{\left[(\epsilon_{k1} - \epsilon_k)(\epsilon_{k1} - \epsilon_f - U\langle n_2 \rangle) - \sum_{\sigma} |V_{\sigma n}(k)|^2 \right]}}{1 + U \sum_{\substack{k1 \\ occ}} \frac{|\hat{A}_{k21}|^2 (\epsilon_{k1} - \epsilon_k)}{\left[(\epsilon_{k1} - \epsilon_k)(\epsilon_{k1} - \epsilon_f - U\langle n_2 \rangle) - \sum_{\sigma} |V_{\sigma n}(k)|^2 \right]}} \quad (5.2.59)$$

so that $\langle n_{12} \rangle$ and hence $\langle n_{21} \rangle$ are zero when the lattice has inversion symmetry and $V_\alpha = 0$. However when the lattice does not have inversion symmetry it is seen that even for large U $\langle n_{12} \rangle$ is finite. We let U to tend to infinity in equation (5.2.59) and retain terms to leading order in U so that

$$\langle n_{12} \rangle_{U \rightarrow \infty} = -\frac{1}{U} \left[\frac{\sum_{\substack{k1 \\ occ}} \frac{|\hat{A}_{k21}|^2 V_\alpha}{(\epsilon_{k1} - \epsilon_k) \langle n_2 \rangle}}{1 - \sum_{\substack{k1 \\ occ}} \frac{|\hat{A}_{k21}|^2}{\langle n_2 \rangle}} \right] \quad (5.2.60)$$

and since

$$\sum_{\substack{k1 \\ occ}} |\hat{A}_{k21}|^2 = \langle n_2 \rangle, \quad (5.2.61)$$

then as $U \rightarrow \infty$ the denominator in $\langle n_{12} \rangle$ tends to zero so that $\langle n_{12} \rangle$ is finite even for U tends to infinity.

5.3. MAGNETIC ANISOTROPY IN THE LARGE CRYSTAL FIELD LIMIT.

5.3.1. Symmetry Considerations.

In this section we study in more detail the symmetries of the momentum dependent hybridisation between a Γ_7 doublet and a single conduction band. We choose to study a Γ_7 doublet since this is the low lying doublet in CeSi_x , the prototype system. The hybridisation is calculated explicitly within tight binding to show that for any lattice with inversion symmetry the hybridisation between a band of Γ_7 doublets and an s or p_x conduction band always satisfies the criteria for reduction to a 'spin only' model (see Section 5.2.1). Therefore the two band model of the previous sections cannot describe the magnetic anisotropy seen in the large crystal field system CeAs which has a cubic lattice and hence inversion symmetry.

The system is modelled by the hamiltonian H_{CF}^b given by equation (5.2.1) but with the conduction state operators written as $c_{k\sigma}^{b\dagger}$, $c_{k\sigma}^b$ where the superscript b labels the type of conduction band, that is s or p_x and so on. The hybridisation term of the hamiltonian H_{CF}^b is written:

$$H_{\text{hyb}}^b = \sum_{kn\sigma} (V_{n\sigma}^{bf}(k) c_{k\sigma}^{b\dagger} f_{kn} + \text{h.c.}), \quad (5.3.1)$$

so that

$$V_{n\sigma}^{bf}(k) = \langle V | c_{k\sigma}^b H_{CF}^b f_{kn}^\dagger | V \rangle. \quad (5.3.2)$$

In order to remain in keeping with the notation of Slater and Koster (1954) the hybridisation is rewritten as:

$$V_{n\sigma}^{bf}(k) = \langle \psi_{k\sigma}^b | H_{CF}^b | \psi_{kn}^f \rangle, \quad (5.3.3)$$

where now $|\psi_{k\sigma}^b\rangle$ is a b conduction wavefunction of momentum k and spin σ equivalent to $c_{k\sigma}^{b\dagger} |V\rangle$ and $|\psi_{kn}^f\rangle$ is an f wavefunction of momentum k in equivalent to $f_{kn}^\dagger |V\rangle$. From the standard tight binding theory (Slater and Koster (1954)):

$$\langle \psi_{k\sigma}^b | H_{CF}^b | \psi_{kn}^f \rangle = \frac{1}{N} \sum_{R_i R_j} e^{ik \cdot (R_i - R_j)} \int \phi_{b\sigma}^*(r - R_i) H_{CF}^b \phi_{fn}(r - R_j) dv \quad (5.3.4)$$

where the sum is over the N unit cells of the system. R_i ranges over the positions on which the f orbitals, ϕ_{fn} , are located while R_j ranges over the positions of the atoms on which the conduction orbitals, $\phi_{b\sigma}$, are located. The orbitals ϕ_{fn} and $\phi_{b\sigma}$ are not atomic orbitals because Bloch sums of atomic orbitals are not orthogonal, rather they are orthogonal linear combinations of atomic orbitals called Lowdin functions. The Lowdin functions show similar symmetry to the atomic orbitals from which they are derived (Slater and Koster (1954)). In equation (5.3.4) the sum over R_j can be eliminated by letting R_j fix the position of a specific atom on which a ϕ_{fn} orbital is located. The sum over R_i then amounts to summing over all the neighbours, on which the orbitals $\phi_{b\sigma}$ exist, of this central atom. Therefore if the position of this central atom is taken as the origin then:

$$\langle \psi_{k\sigma}^b | H_{CF}^b | \psi_{kn}^f \rangle = \frac{1}{N} \sum_R e^{ik \cdot R} E_{b\sigma fn}(R), \quad (5.3.5)$$

(f to b)

where R is the vector to the b orbital sites and

$$E_{b\sigma fn}(R) = \int \phi_{b\sigma}^*(r-R) H_{CF}^b \phi_{fn}(r) dv. \quad (5.3.6)$$

In Appendix B it is shown that for any lattice in which a Γ_7 band hybridises with a single conduction band that

$$E_{b\uparrow f_1}(R) = - E_{b\downarrow f_2}^*(R), \quad (5.3.7)$$

$$E_{b\downarrow f_1}(R) = E_{b\uparrow f_2}^*(R). \quad (5.3.8)$$

Also for $b = s$ or p_x :

$$E_{s\sigma f_n}(R) = - E_{s\sigma f_n}(-R), \quad (5.3.9)$$

and

$$E_{p_x \sigma f_n}(R) = E_{p_x \sigma f_n}(-R), \quad (5.3.10)$$

so that it is easily shown (see Appendix B) that the hybridisations between a Γ_7 band and an s or p_x conduction band in a lattice with inversion symmetry satisfy the relations:

$$V_{\uparrow_1}^{sf}(k) = V_{\downarrow_2}^{sf*}(k), \quad (5.3.11)$$

$$V_{\downarrow_1}^{sf}(k) = - V_{\uparrow_2}^{sf*}(k), \quad (5.3.12)$$

and

$$V_{\uparrow_1}^{pf}(k) = - V_{\downarrow_2}^{pf*}(k), \quad (5.3.13)$$

$$V_{\downarrow_1}^{pf}(k) = V_{\uparrow_2}^{pf*}(k). \quad (5.3.14)$$

From the arguments of Section 5.2.1 these hybridisations satisfy the criterion for a 'spin only' hamiltonian namely:

$$V_{\alpha}^b = V_{\uparrow_1}^{bf}(k)V_{\uparrow_2}^{bf*}(k) + V_{\downarrow_1}^{bf}(k)V_{\downarrow_2}^{bf*}(k) = 0, \quad (5.3.15)$$

and

$$V_1^{bf}(k) = V_2^{bf}(k), \quad (5.3.16)$$

where

$$V_n^{bf}(k) = \sqrt{\sum_{\sigma} |V_{\sigma n}^{bf}(k)|^2}, \quad (5.3.17)$$

and $b = s$ or p_x (see equations 5.2.8 and 5.2.9). Therefore there exist linear combinations, $c_{kn}^{b\dagger} |V\rangle$, of the up and down conduction states such that within the new basis $c_{kn}^{b\dagger}$, c_{kn}^b , f_{kn}^{\dagger} , f_{kn} , $n = 1$ or

2, each of the crystal field states $f_{kn}^\dagger |V\rangle$ hybridises with only one of the conduction band states $c_{kn}^{b\dagger} |V\rangle$ where

$$c_{kn}^{b\dagger} = \frac{\sum_{\sigma} V_{\sigma n}^{bf}(k) c_{k\sigma}^{b\dagger}}{\sqrt{\sum_{\sigma} |V_{\sigma n}^{bf}(k)|^2}}, \quad (5.3.18)$$

We can easily remind ourselves of how the 'spin only' nature of the hamiltonian in the new basis comes about by transforming to the new basis where the hamiltonian H_{CF}^b becomes:

$$\begin{aligned} \tilde{H}_{CF}^b = & \sum_{\substack{kb \\ nn'}} \varepsilon_k^b \frac{\sum_{\sigma} V_{\sigma n}^{bf}(k) V_{\sigma n'}^{bf*}(k)}{\sqrt{\sum_{\sigma} |V_{\sigma n}^{bf}(k)|^2} \sqrt{\sum_{\sigma} |V_{\sigma n'}^{bf}(k)|^2}} c_{kn}^{b\dagger} c_{kn}^b \\ & + \sum_{\substack{kb \\ nn'}} \left[\frac{\sum_{\sigma} V_{\sigma n}^{bf}(k) V_{\sigma n'}^{bf*}(k)}{\sqrt{\sum_{\sigma} |V_{\sigma n'}^{bf}(k)|^2}} c_{kn',f}^{b\dagger} + \text{h.c.} \right] \\ & + \sum_{kn} \varepsilon_f f_{kn}^\dagger f_{kn} + \sum_i U f_{i1}^\dagger f_{i1} f_{i2}^\dagger f_{i2}, \end{aligned} \quad (5.3.19)$$

where $b = s$ or p_x and $n, n' = 1$ or 2 . Now since

$$\sum_{\sigma} V_{\sigma n}^{bf}(k) V_{\sigma n'}^{bf*}(k) = \begin{cases} V_{\alpha}^b & \text{for } n \neq n' \\ \sum_{\sigma} |V_{\sigma n}^{bf}(k)|^2 & \text{for } n = n' \end{cases} \quad (5.3.20)$$

then

$$\begin{aligned} \tilde{H}_{CF}^b = & \sum_{knb} \varepsilon_{kn}^b c_{kn}^{b\dagger} c_{kn}^b + \sum_{kn} \varepsilon_{fn} f_{nk}^\dagger f_{nk} + \sum_{knb} (V_n^{bf}(k) c_{kn}^{b\dagger} f_{kn} + \text{h.c.}) \\ & + \sum_i U f_{i1}^\dagger f_{i1} f_{i2}^\dagger f_{i2} , \end{aligned} \quad (5.3.21)$$

where

$$\varepsilon_{k1}^b = \varepsilon_{k2}^b = \varepsilon_k^b , \quad (5.3.22)$$

and $V_n^{bf}(k)$ are given by equation (5.3.17) with $b = s$ and p_x . Within the new basis we can easily identify a set of low energy collective magnetic excitations with creation operator:

$$\tilde{S}_{k-k'}^- = \sum_p c_{(p-k')_z}^{b\dagger} c_{(p-k)_z} + \sum_p f_{(p-k')_z}^\dagger f_{(p-k)_z} , \quad (5.3.23)$$

which result in a single 'pseudo' spin flip and which cost no energy when they have zero momentum since

$$\begin{aligned} [\tilde{H}_{CF}^b , \tilde{S}_{q=0}^-] = & \sum_k [\varepsilon_{k2}^b - \varepsilon_{k1}^b] c_{k2}^{b\dagger} c_{k1}^b + \\ & \sum_k \left[\left[V_2^{bf}(k) - V_1^{bf}(k) \right] c_{k2}^{b\dagger} f_{k1} + \left[V_2^{bf*}(k) - V_1^{bf*}(k) \right] f_{k2}^\dagger c_{k1}^b \right] \\ & = 0 . \end{aligned} \quad (5.3.24)$$

These 'pseudo' magnons are analogous to the magnon excitations of the spin only model. Therefore the observed gap in the magnetic excitation spectrum at $q = 0$ which indicates that the magnetic excitation with zero momentum has finite energy remains unexplained. The observed finite energy of the real zero momentum magnetic excitation is due to magnetic anisotropy which is not included in the two band model contrary to the results of Thayamballi and Cooper (1985).

The development of a model for systems like CeSi_x and CeAs which exhibit magnetic anisotropy and have a large crystal field, so that only the Γ_7 doublet has a non negligible occupation in the

ground state, remains a problem. The origin of the magnetic anisotropy in these systems is discussed in the following sections.

5.3.2. A Three Band Hamiltonian.

In the previous section it is shown that the two band periodic Anderson model of a flat f band of Γ_7 crystal field states hybridising with a single conduction band cannot describe the magnetic anisotropy seen in systems like CeSi_x and CeAl . The problem of building magnetic anisotropy into the Anderson model remains.

The rare earth systems are usually studied using localised models and assuming that all the crystal field states (not just the Γ_7 as is assumed in the previous sections) are involved in the ground state. However in systems like CeSi_x and CeAl where the crystal field is large it cannot be a bad approximation to assume that only the Γ_7 is involved in the ground state (see Section 5.2.4). In these large crystal field systems we propose that the magnetic anisotropy is due to the interaction of the f band with all of the conduction bands and cannot be described using an idealised two band model.

Consider now a first improvement over the two band model, that is a three band model of one f band, again a Γ_7 band, and two conduction bands. In the following it is shown that addition of a second conduction band introduces an extra degree of freedom which allows the system to respond in different ways to different moment orientations even when the lattice has inversion symmetry.

The three band hamiltonian is written:

$$\begin{aligned}
 H_{CF}^{spx} = & \sum_{k\sigma b} \epsilon_k^b c_{k\sigma}^{b\dagger} c_{k\sigma}^b + \sum_{kn} \epsilon_{fn} f_{kn}^\dagger f_{kn} + \sum_{kn\sigma b} (V_{\sigma n}^{bf}(k) c_{k\sigma}^{b\dagger} f_{kn} + \text{h.c.}) \\
 & + \sum_i U f_{i1}^\dagger f_{i1} f_{i2}^\dagger f_{i2} + \sum_{k\sigma} (V^{spx}(k) c_{k\sigma}^{s\dagger} c_{k\sigma}^p + \text{h.c.}) ,
 \end{aligned}
 \tag{5.3.25}$$

where the superscript b labels the type of conduction band orbitals, which are taken to be s and p_x . The conduction bands of the model

calculation are chosen as s and p_x since in CeSi_x , the prototype system, the basic structure is approximated as tetragonal (see Figure C.1) and in a tetragonal lattice the remaining four p bands may be at much higher energies than the p_x . Therefore restricting the conduction bands to just an s and p_x is not unreasonable for CeSi_x .

The Hamiltonian $H_{CF}^{sp_x}$ contains two conduction bands each hybridising with the f band of Γ_7 states and also with one another. Suppose now that we are modelling a system in which the lattice has inversion symmetry. As illustrated in Section 5.3.1. there exist linear combinations of the up and down conduction states in each of the two separate bands, $c_{kn}^{b\dagger}|0\rangle$ given by equation (5.3.18) with $b = s$ or p_x , which hybridise with only one of the degenerate f bands. Within the new basis $c_{kn}^{b\dagger}$, c_{kn}^b , f_{kn}^\dagger , f_{kn} , $b = s$ or p_x and $n = 1$ or 2 , the hamiltonian is written:

$$\begin{aligned} \tilde{H}_{CF}^{sp_x} = & \sum_{knb} \epsilon_{kn}^b c_{kn}^{b\dagger} c_{kn}^b + \sum_{kn} \epsilon_{fn} f_{nk}^\dagger f_{nk} + \sum_{knb} (V_n^{bf}(k) c_{kn}^{b\dagger} f_{kn} + \text{h.c.}) \\ & + \sum_i U f_{i1}^\dagger f_{i1} f_{i2}^\dagger f_{i2} + \sum_{nn'} (\tilde{V}_{nn'}^{sp_x}(k) c_{kn}^{s\dagger} c_{kn}^{p_x} + \text{h.c.}) , \end{aligned} \quad (5.3.26)$$

where $\epsilon_{kn}^b = \epsilon_{kn}^b = \epsilon_k^b$ (see equation (5.3.22)) and $V_1^{bf}(k) = V_2^{bf}(k)$ are given in equation (5.3.17) with $b = s$ or p_x . Also

$$\tilde{V}_{nn'}^{sp_x}(k) = V^{sp_x}(k) \frac{V_{\uparrow n}^{sf*}(k) V_{\uparrow n'}^{p_x f}(k) + V_{\downarrow n}^{sf*}(k) V_{\downarrow n'}^{p_x f}(k)}{\left[\sum_{\sigma} |V_{\sigma n}^{sf}(k)|^2 \right]^{1/2} \left[\sum_{\sigma} |V_{\sigma n'}^{p_x f}(k)|^2 \right]^{1/2}} . \quad (5.3.27)$$

Therefore provided the hybridisation matrix $\tilde{V}_{nn'}^{sp_x}(k)$ is non zero then there remains some interaction between the new conduction bands which destroys the 'spin only' nature of the model. It can be shown that because of the presence of this interaction between the two conduction bands, the three band model is sensitive to different orientations of the magnetic moment. In the following the existence

of magnetic anisotropy in the three band model is shown for the case of s and p_x conduction bands hybridising with an f band of Γ_7 states in a simple body centred cubic and tetragonal body centred lattice, both of which have inversion symmetry.

The new basis wavefunctions $c_{kn}^{b\dagger}|V\rangle$ and $f_{kn}^\dagger|V\rangle$ possess a pseudo spin analogous to the straightforward spin of the spin only case (see Chapter 3). As in the spin only case we can identify a set of low energy collective magnetic excitations which we term pseudo magnons and which are directly analogous to the magnons of the spin only case. As in the spin only case the zero momentum pseudo magnon with creation operator:

$$\hat{S}_{q=0}^- = \sum_{pb} c_{p^2}^{b\dagger} c_{p^1}^b + \sum_p f_{p^2}^\dagger f_{p^1}, \quad b = s \text{ or } p_x, \quad (5.3.28)$$

corresponds to a simple twisting of the pseudo moment and in the absence of magnetic anisotropy costs no energy.

In order, then, to illustrate the presence of magnetic anisotropy in the model it is sufficient to show that the zero momentum pseudo magnon has non zero energy or:

$$[\tilde{H}_{CF}^{sp^x}, \hat{S}_{q=0}^-] \neq 0. \quad (5.3.29)$$

where $\tilde{H}_{CF}^{sp^x}$ is given by equation (5.3.26). In the absence of the hybridisation $\tilde{V}_{nn}^{sp^x}(k)$ between the two conduction bands the hamiltonian $\tilde{H}_{CF}^{sp^x}$ reduces to 'spin only'. However when this hybridisation is non zero the 'spin only' nature of the model is destroyed. The new pseudo magnon creation operator, $\hat{S}_{q=0}^-$, commutes with the first four terms of $\tilde{H}_{CF}^{sp^x}$ since $\epsilon_{k1}^b = \epsilon_{k2}^b = \epsilon_k^b$ and $V_1^{bf}(k) = V_2^{bf}(k)$ (see equation (5.3.24)) so that

$$\begin{aligned} & [\tilde{H}_{CF}^{sp^x}, \hat{S}_{q=0}^-] = \\ & \sum_k \left[(\tilde{V}_{22}^{sp^x}(k) - \tilde{V}_{11}^{sp^x}(k)) c_{k2}^{s\dagger} c_{k1}^{p^x} + (\tilde{V}_{22}^{sp^x*}(k) - \tilde{V}_{11}^{sp^x*}(k)) c_{k2}^{p^x\dagger} c_{k1}^s \right] \\ & + \sum_k \tilde{V}_{12}^{sp^x}(k) \left[c_{k1}^{s\dagger} c_{k1}^{p^x} - c_{k2}^{s\dagger} c_{k2}^{p^x} + \text{h.c.} \right], \end{aligned} \quad (5.3.30)$$

where we have used the relation $\tilde{V}_{12}^{sp^*}(k) = \tilde{V}_{21}^{sp^*}(k)$ in a lattice with inversion symmetry. Therefore the model describes magnetic anisotropy provided

$$(\tilde{V}_{11}^{sp^*}(k) - \tilde{V}_{22}^{sp^*}(k)) \neq 0, \quad (5.3.31)$$

and, or

$$\tilde{V}_{12}^{sp^*}(k) \neq 0 \quad (5.3.32)$$

or when equations (5.3.31) and (5.3.32) are rewritten using the relations between the hybridisations for a lattice with inversion symmetry (see equations (5.3.11) to (5.3.14)) we say that for a lattice with inversion symmetry the three band hamiltonian contains magnetic anisotropy provided:

$$V^{sp^*}(k) \neq 0, \quad (5.3.33)$$

and

$$\sum_{\sigma} \left[(\sigma) V_{-\sigma 1}^{sf}(k) V_{\sigma 2}^{p^*f}(k) + c.c \right] \neq 0, \quad (5.3.34)$$

or

$$\sum_{\sigma} V_{\sigma 1}^{sf^*}(k) V_{\sigma 2}^{p^*f}(k) \neq 0, \quad (5.3.35)$$

where (\uparrow) = 1 and (\downarrow) = -1. In Appendix C we show that the criteria for magnetic anisotropy are satisfied for both the simple bcc and tetragonal lattices. Therefore we conclude that in systems with large crystal fields where only a low lying f doublet is occupied in the ground state the interaction of the low lying doublet states with all the different conduction bands of the system is the origin of magnetic anisotropy.

In a proper multiband treatment the three p bands should be included for completeness. However since the main advantage of a multiband model, magnetic anisotropy, is achieved by including just

the p_x band the rest can be neglected for a first round attempt at the problem. Also there is some justification for the inclusion of just an s and a p_x band since in a tetragonal lattice the remainder of the p bands can be at much higher energies than the p_x and can be assumed unoccupied in the ground state.

5.3.3. A Self Consistent Magnon Within the Three Band Hamiltonian.

In the spin only model of Chapter 3 and the impurity model of Chapter 4 as well as the preceding sections of the present chapter the magnon creation operators are approximations to the creation operator of the real low energy magnetic excitation. Therefore the magnon energies of the various models are also approximations. The success of these approximations and the accuracy of the calculated magnon energy depends on how close these creation operators and ground state are to the real situation. Within the three band model a variational wavefunction for the self consistent magnon is proposed:

$$\tilde{S}_{k-k'}^- |V\rangle = \sum_{p1\bar{1}} D_{p1\bar{1}} \tilde{a}_{(p-k')1}^+ \tilde{a}_{(p-k)\bar{1}}^- |V\rangle, \quad (5.3.36)$$

where $\tilde{a}_{(p-k')1}^+$ and $\tilde{a}_{(p-k)\bar{1}}^-$ are the creation and destruction operators of the one electron eigenfunctions in the Hartree Fock ground state. Equation (5.3.36) is a variational wavefunction for the magnon which has energy $\hbar\tilde{\omega}_{k-k'}$, given by:

$$(\hbar\tilde{\omega}_{k-k'} + \tilde{E}_0) \langle 0 | \tilde{S}_{k-k'}^+, \tilde{S}_{k-k'}^- | 0 \rangle = \langle 0 | \tilde{S}_{k-k'}^+, H_{CF}^{spx} \tilde{S}_{k-k'}^- | 0 \rangle, \quad (5.3.37)$$

Here \tilde{E}_0 is the energy of the new three band Hartree Fock ground state, $|0\rangle$. When the energy $\hbar\tilde{\omega}_{k-k'}$ is minimised with respect to the coefficients $D_{p1\bar{1}}$ in the variational wavefunction we arrive at an expression for the magnon energy which is in agreement with that of the R.P.A. calculation of Muniz and Edwards (1985).

Within the Hartree Fock approximation the H_{CF}^{spx} is approximated as \hat{H}_{CF}^{spx} which is diagonalised by the operators \tilde{a}_{k1}^+ where:

$$\hat{H}_{CF}^{spx} \tilde{a}_{k1}^\dagger |V\rangle = \tilde{\epsilon}_{k1} \tilde{a}_{k1}^\dagger |V\rangle, \quad (5.3.38)$$

and

$$\tilde{a}_{k1}^\dagger = \left[\sum_n \tilde{A}_{kn1} f_{kn}^\dagger + \sum_{b\sigma} \tilde{B}_{k\sigma 1}^b c_{k\sigma}^\dagger \right] |V\rangle, \quad (5.3.39)$$

Here the subscript, 1, labels the six bands of energy $\tilde{\epsilon}_{k1}$ of the Hartree Fock ground state, $b = s$ or p_x labels the type of conduction band and $n = 1$ or 2 the crystal field states. The Hartree Fock eigenstates are mixtures of both crystal field states and up and down spin conduction states from both the s and p_x bands. Within the Hartree Fock approximation the coulomb interaction term of the hamiltonian H_{CF}^{spx} is treated as follows:

$$\begin{aligned} U \sum_{k_1 k_2} f_{k_1 1}^\dagger f_{k_1 + q 1} f_{k_2 2}^\dagger f_{k_2 - q 2} \approx \\ \sum_k \langle \tilde{n}_2 \rangle f_{k1}^\dagger f_{k1} + \sum_k \langle \tilde{n}_1 \rangle f_{k2}^\dagger f_{k2} - \sum_k \left[U \langle \tilde{n}_{12} \rangle f_{k1}^\dagger f_{k2} + \text{h.c.} \right] \end{aligned} \quad (5.3.40)$$

with

$$\langle \tilde{n}_{12} \rangle = \sum_{k1 \text{ occ}} \tilde{A}_{k11} \tilde{A}_{k21}^* = \langle \tilde{n}_{21} \rangle^*, \quad (5.3.41)$$

so that the band energies $\tilde{\epsilon}_{k1}$ as well as the conduction state amplitudes $\tilde{B}_{k\sigma 1}^b$ and crystal field state amplitudes \tilde{A}_{kn1} in any eigenstate are given by:

$$\begin{bmatrix}
E - \epsilon_k^s & 0 & V^{sp^*}(k) & 0 & -V_{1\uparrow}^{sf}(k) & -V_{2\uparrow}^{sf}(k) \\
0 & E - \epsilon_k^s & 0 & V^{sp^*}(k) & -V_{1\downarrow}^{sf}(k) & -V_{2\downarrow}^{sf}(k) \\
V^{sp^*}(k) & 0 & E - \epsilon_k^{p^*} & 0 & -V_{1\uparrow}^{p^*f}(k) & -V_{2\uparrow}^{p^*f}(k) \\
0 & V^{sp^*}(k) & 0 & E - \epsilon_k^{p^*} & -V_{1\downarrow}^{p^*f}(k) & -V_{2\downarrow}^{p^*f}(k) \\
-V_{1\uparrow}^{sf^*}(k) & -V_{1\downarrow}^{sf^*}(k) & -V_{1\uparrow}^{p^*f^*}(k) & -V_{1\downarrow}^{p^*f^*}(k) & E - \epsilon_{f2} & \langle \tilde{n}_{12} \rangle \\
-V_{2\uparrow}^{sf^*}(k) & -V_{2\downarrow}^{sf^*}(k) & -V_{2\uparrow}^{p^*f^*}(k) & -V_{2\downarrow}^{p^*f^*}(k) & \langle \tilde{n}_{21} \rangle & E - \epsilon_{f1}
\end{bmatrix}
\times \begin{bmatrix}
\tilde{B}_{k\uparrow}^s & \tilde{B}_{k\downarrow}^s & \tilde{B}_{k\uparrow}^{p^*} & \tilde{B}_{k\downarrow}^{p^*} & \tilde{A}_{k1} & \tilde{A}_{k2}
\end{bmatrix}^T = 0$$

(5.3.42)

where ϵ_{fn} , $n = 1$ or 2 , are defined in equation (5.2.57). Once again even the Hartree Fock problem is non trivial because of the presence of the off diagonal Hartree Fock exchange terms. When equation (5.3.42) is solved for $\langle \tilde{n}_{12} \rangle$ we find that for any lattice with inversion symmetry these Hartree Fock exchange terms are zero provided:

$$V^{sp^*}(k) = -V^{sp^*}(k). \quad (5.3.43)$$

From standard tight binding ((Slater and Koster (1954)) and Appendix C) we find that for a lattice with inversion symmetry

$$V^{sp^*}(k) = \sum_{(s \text{ to } p^*)} e^{-ik \cdot R} (s\sigma)l = \sum_{(s \text{ to } p^*)} e^{ik \cdot R} (s\sigma)(-l) = -V^{sp^*}(k),$$

(5.3.44)

, where (l, m, n) are the direction cosines of the vectore R. Therefore the off diagonal Hartree Fock terms, $\langle \tilde{n}_{12} \rangle$ are zero and equation (5.3.42) can be easily solved.

After lengthy algebra to minimise the energy $\hbar\tilde{\omega}_{k-k'}$, we find:

$$\left[1 + \Gamma_{\rho\pi\xi\mu} (\hbar\tilde{\omega}_{k-k'}) W_{\xi\mu\nu\eta} \right]^{-1} = 0, \quad (5.3.45)$$

where

$$\Gamma_{\rho\pi\xi\mu} = \sum_{\hat{k}\Gamma} \frac{\tilde{A}_{(\hat{k}-\mathbf{k})\xi\bar{r}} \tilde{A}_{(\hat{k}-\mathbf{k}')\mu\bar{r}} \tilde{A}_{(\hat{k}-\mathbf{k}')\rho\bar{r}} \tilde{A}_{(\hat{k}-\mathbf{k})\pi\bar{r}}}{\hbar\tilde{\omega}_{\mathbf{k}-\mathbf{k}'} + \tilde{\epsilon}_{(\hat{k}-\mathbf{k})\bar{r}} - \tilde{\epsilon}_{(\hat{k}-\mathbf{k}')\bar{r}}}. \quad (5.3.46)$$

and all $W_{\xi\mu\nu\eta} = 0$ except for

$$W_{1122} = W_{2211} = -U, \quad (5.3.47)$$

$$W_{1212} = W_{2121} = U. \quad (5.3.48)$$

The next stage in the calculation is the solution of equation (5.3.45) for the magnetic excitation energies $\hbar\tilde{\omega}_{\mathbf{k}-\mathbf{k}'}$, and ultimately the comparison of these excitation energies with the magnetic excitation spectrum in CeSi_x . However this calculation must be left to future work.

5.3.4. Conclusions and Further Work.

It is found that the magnetic anisotropy observed in the large crystal field systems such as CeSi_x and CeAs cannot be described by a periodic Anderson model in which a Γ_7 doublet band hybridises with a single s or p_x conduction band. This result suggests that the magnetic anisotropy found by Thayamballi and Cooper (1985) is due to some numerical error. In fact, these authors remark that their calculated magnetic excitation dispersion is 'spin only'.

It is maintained that in these large crystal field systems only the low lying Γ_7 doublet has non negligible occupation and that the magnetic anisotropy is due to the hybridisation of this Γ_7 band with all of the conduction bands. The magnetic anisotropy is shown to exist for a periodic Anderson model in which a Γ_7 band hybridises with two conduction bands (s and p_x), even in a lattice with inversion symmetry.

Now that we have finally achieved a model which does not reduce

to 'spin only', the stage is set for a calculation of the magnetic excitation spectrum. It is proposed that the calculation be made computationally, including all p bands in order to make a realistic comparison with the observed magnetic excitation dispersion in CeSi_x .

It should be noted that the anisotropy discussed above is exchange anisotropy which causes the interaction between two atomic moments to depend on the direction of the line joining the moments. The possible anisotropy of the g tensor describing the coupling of the system to a magnetic field has not been discussed.

APPENDIX A.

The system is modelled by the spin degenerate periodic Anderson hamiltonian with added exchange interaction of equation (3.4.12). The variational wavefunction for a down spin f electron introduced into the system is proposed as:

$$|\psi \rangle^i = \left[D_k^i f_{k\downarrow}^\dagger + F_k^i c_{k\downarrow}^\dagger + \sum_{k' \uparrow > k_f} G_{k',i}^i a_{k',i\uparrow}^\dagger S_{k-k'}^- \right] |0\rangle, \quad (\text{A.1})$$

where the superscripts I distinguish this wavefunction from that of the spin only calculation without the exchange interaction. Here $f_{k\downarrow}^\dagger$ creates an f electron in a state of momentum k and energy ϵ_f , $c_{k\downarrow}^\dagger$ creates a conduction electron in a state of momentum k and energy $\epsilon_{k\downarrow}$ of equation (3.4.25) and $a_{k',i}^\dagger$ creates an electron in the up spin eigenstate of momentum k' and energy $\epsilon_{k',i}^\uparrow$ of equation (3.2.6) with ϵ_k replaced by $\epsilon_{k\uparrow}$ and ϵ_f by $\epsilon_{f\uparrow}$.

To solve for the coefficients D_k^i , F_k^i , $G_{k',i}^i$ we left multiply the Schrodinger equation:

$$H_{\text{latt}}^A |\psi \rangle^i = \epsilon |\psi \rangle^i, \quad (\text{A.2})$$

by each of the constituent elements of the variational wavefunction to find three equations for the three coefficients. The equations are written:

$$D_k^i M1 + F_k^i M2 + \sum_{k' \uparrow > k_f} G_{k',i}^i M3(k,k') = \epsilon D_k^i, \quad (\text{A.3})$$

$$D_k^i M2 + F_k^i M4(k) + \sum_{k' \uparrow > k_f} G_{k',i}^i M5(k') = \epsilon F_k^i, \quad (\text{A.4})$$

$$\begin{aligned}
D_k^I M3(k'k'') + F_k^I M5(k'') + G_{k'',i}^I M6_{diag}(k'') \\
+ \sum_{k',i>k_f} G_{k',i}^I \overline{M6}(k,k',k'') = \varepsilon G_{k'',i}^I \langle 0 | S_{k-k''}^+ S_{k-k''}^- | 0 \rangle,
\end{aligned} \tag{A.5}$$

and

$$M1 = E_o + \varepsilon_f + U \langle n_{f\uparrow} \rangle + \frac{J_{ex}}{2} \sum_{\sigma} \langle n_{c\sigma} \rangle, \tag{A.6}$$

$$M2 = V + J_{ex} C, \tag{A.7}$$

$$\begin{aligned}
M3(k,k') = -U \langle n_{f\uparrow} \rangle A_{k',i}^I - J_{ex} C (1 - A_{k',i}^{I2}) B_{k',i}^I \\
- J_{ex} \sum_p B_{(p-k),r}^{I2} A_{k',i}^I \langle 0 | n_{(p-k),r} (1 - n_{(p-k',\downarrow)}) | 0 \rangle,
\end{aligned} \tag{A.8}$$

$$M4(k) = E_o + \varepsilon_{k\downarrow}, \tag{A.9}$$

$$M5(k') = -J_{ex} \langle n_{f\uparrow} \rangle B_{k',i}^I - J_{ex} C A_{k',i}^I B_{k',z}^{I2}, \tag{A.10}$$

$$M6(k,k',k'') = M6_{diag}(k,k'') \delta_{k',k''} + \overline{M6}(k,k',k''), \tag{A.11}$$

$$M6_{diag}(k,k'') = (E_o + \hbar\omega_{k-k''} + \varepsilon_{k'',i}) \langle 0 | S_{k-k''}^+ S_{k-k''}^- | 0 \rangle, \tag{A.12}$$

$$\begin{aligned}
\overline{M}(k, k', k'') &= U A_{k', i}^{\uparrow} A_{k'', i}^{\uparrow} \langle n_{f \uparrow} \rangle + \frac{J_{ex}}{2} B_{k', i}^{\uparrow} B_{k'', i}^{\uparrow} \langle n_{f \uparrow} \rangle \\
&+ \frac{J_{ex}}{2} \sum_{rps} \left[A_{k', i}^{\uparrow} A_{k'', i}^{\uparrow} B_{(p-k), s}^{2\uparrow} \right] \cdot \\
&\quad \langle 0 | n_{(p-k), s} (1 - n_{(p-k'), c \downarrow}) (1 - n_{(p-k''), c \downarrow}) | 0 \rangle \\
-\frac{J_{ex}}{2} \sum_{puv} &\left[B_{k', i}^{\uparrow} A_{k'', i}^{\uparrow} B_{(p-k), v}^{\uparrow} A_{(p-k'+k''-k), u}^{\uparrow} \right. \\
&\quad + A_{k', i}^{\uparrow} B_{k'', i}^{\uparrow} A_{(p-k), v}^{\uparrow} B_{(p-k'+k''-k), u}^{\uparrow} \\
&\quad - B_{k', i}^{\uparrow} B_{k'', i}^{\uparrow} A_{(p-k), v}^{\uparrow} A_{(p-k'+k''-k), u}^{\uparrow} \\
&\quad \left. - A_{k', i}^{\uparrow} A_{k'', i}^{\uparrow} B_{(p-k), v}^{\uparrow} B_{(p-k'+k''-k), u}^{\uparrow} \right] \cdot \\
&\quad \left[B_{(p-k'+k''-k), u}^{\uparrow} B_{(p-k), v}^{\uparrow} \langle 0 | (1 - n_{(p-k'), c \downarrow}) | 0 \rangle \right. \\
&\quad \left. + A_{(p-k'+k''-k), u}^{\uparrow} A_{(p-k), v}^{\uparrow} \right] \cdot \\
&\quad \langle 0 | n_{(p-k'+k''-k), u} n_{(p-k), v} | 0 \rangle \\
&+ \frac{J_{ex}}{2} \sum_{ps} \left[B_{k', i}^{\uparrow} A_{k'', i}^{\uparrow} B_{(p-k), s}^{\uparrow} A_{(p-k), s}^{\uparrow} + A_{k', i}^{\uparrow} B_{k'', i}^{\uparrow} A_{(p-k), s}^{\uparrow} B_{(p-k), s}^{\uparrow} \right] \cdot \\
&\quad \langle 0 | n_{(p-k), s} (1 - n_{(p-k''), c \downarrow}) | 0 \rangle.
\end{aligned} \tag{A.13}$$

where E_0 is the ground state energy, $\hbar\omega_{k-k''}$, the magnon energy defined by:

$$E_o + \hbar\omega_{k-k''} = \frac{\langle 0 | S_{k-k''}^+ H_{lattice}^A S_{k-k''}^- | 0 \rangle}{\langle 0 | S_{k-k''}^+ S_{k-k''}^- | 0 \rangle}, \quad (A.14)$$

and $\langle n_{f\uparrow} \rangle$ and $\langle n_{c\sigma} \rangle$ are the up spin f occupation and spin σ conduction occupation in the ground state respectively. Also

$$\langle 0 | S_{k-k''}^+ S_{k-k''}^- | 0 \rangle = \langle n_{f\uparrow} \rangle + \sum_p \langle 0 | n_{(p-k)\uparrow} (1 - n_{(p-k'')\downarrow}) | 0 \rangle, \quad (A.15)$$

where

$$n_{(p-k)\downarrow} = c_{(p-k)\sigma}^\dagger c_{(p-k)\sigma}, \quad (A.16)$$

and

$$C = \sum_{k_r \text{ occ.}} A_{k_r}^i B_{k_r}^i \langle 0 | n_{k_r} | 0 \rangle, \quad (A.17)$$

so that C is of the order of the up spin f amplitude in the states of band 1 at the Fermi wavevector. To arrive at equation (3.4.29) of the main text we take the limit of small hybridisation and work to order $V^2/|\epsilon_{f\uparrow}|^2$ (the f weight in band 1 at the Fermi level). Also since we want to study the competition between exchange and hybridisation when J_{ex} is of the order of $2V^2/|\epsilon_{f\uparrow}|$ we work to order $J_{ex}/|\epsilon_{f\uparrow}|$. In this limit of small hybridisation the up spin f weight above the Fermi level is approximated by its value at the Fermi level for both bands 1 and 2 so that:

$$A_{k > k_F}^i \approx \frac{V}{|\epsilon_{f\uparrow}|} \quad (A.18)$$

$$A_{k > k_F}^i \approx 1 - \frac{V^2}{2|\epsilon_{f\uparrow}|^2} \quad (A.19)$$

$$B_{k > k_F}^I \approx 1 - \frac{V^2}{2|\epsilon_{f\uparrow}|^2} \quad (\text{A.20})$$

$$B_{k > k_F}^I \approx - \frac{V}{|\epsilon_{f\uparrow}|} \quad (\text{A.21})$$

and also

$$\langle n_{f\uparrow} \rangle = 1 - \frac{V^2 T_{p\uparrow}}{W|\epsilon_{f\uparrow}|(|\epsilon_{f\uparrow}| + T_{p\uparrow})} \quad T_{p\uparrow} = T_p - \frac{J_{ex}}{2} \langle n_{f\uparrow} \rangle \quad (\text{A.22})$$

and T_p is the top of the conduction band. Also

$$\sum_{\sigma} \sigma \langle n_{c\sigma} \rangle = \frac{1}{W} \left[-\frac{J_{ex}}{2} \langle n_{f\uparrow} \rangle + \frac{V^2 T_{p\uparrow}}{W|\epsilon_{f\uparrow}|(|\epsilon_{f\uparrow}| + T_{p\uparrow})} \right] \quad (\text{A.23})$$

and

$$C \approx - \sum_{k > k_F} A_{k_F, i}^I B_{k_F, i}^I = - \frac{T_{p\uparrow} V}{W|\epsilon_{f\uparrow}|} \quad (\text{A.24})$$

Within these approximations, equations (A.3) to (A.5) can be solved for the Dyson equation:

$$\begin{aligned}
E - \varepsilon_f - U \langle n_{f\downarrow} \rangle - \frac{J_{\alpha}}{2} \sum_{\sigma} \langle n_{c\sigma} \rangle - \hat{\Sigma}_{ff\downarrow}(k, E) - \frac{\left[V - \frac{J_{\alpha} \hat{\Sigma}_{ff\downarrow}(k, E)}{U A_{k_F}^i} \right]^2}{E - \varepsilon_{k\downarrow} - \frac{J_{\alpha}^2 \hat{\Sigma}_{ff\downarrow}(k, E)}{U A_{k_F}^{i2}}} \\
= 0
\end{aligned}
\tag{A.25}$$

where

$$\begin{aligned}
\hat{\Sigma}_{ff\downarrow}(k, E) = \frac{\sum_{k' : > k_F} \frac{U^2 A_{k_F}^{i2} \langle n_{f\uparrow} \rangle}{(E - \varepsilon_{k', i} - \hbar\omega_{k-k'})}}{1 - \sum_{k' : > k_F} \frac{U A_{k_F}^{i2} + J_{\alpha} B_{k_F}^{i2}}{(E - \varepsilon_{k', i} - \hbar\omega_{k-k'})}}
\end{aligned}
\tag{A.26}$$

APPENDIX B.

The systems under investigation are those in which the crystal field splitting is large and the lowest lying f electron states form a Γ_7 doublet. It is assumed that in the ground state only the Γ_7 crystal field states are occupied so that others do not feature in the hamiltonian. The hamiltonian is given by

$$H_{CF}^b = \sum_{k\sigma} \epsilon_{kc}^b c_{k\sigma}^\dagger c_{k\sigma}^b + \sum_{kn} \epsilon_{fn} f_{kn}^\dagger f_{kn} + \sum_{k\sigma n} (V_{\sigma n}^{bf}(k) c_{k\sigma}^\dagger f_{kn} + h.c.) + \sum_i U f_{i1}^\dagger f_{i1} f_{i2}^\dagger f_{i2}, \quad (B.1)$$

where $n = 1$ or 2 labels the states of the Γ_7 doublet, as in the main text, and b labels the type of conduction band, that is, s, p, d and so on. In the following, the possibility of an s or p_x conduction band is considered. From standard tight binding theory the hybridisation is written:

$$V_{\sigma n}^{bf}(k) = \sum_{\substack{R \\ (f \text{ to } b)}} e^{ik \cdot R} E_{b\sigma f_n}(R), \quad (B.2)$$

where the superscript b labels the type of conduction band, either s or p_x , R is the vector from the f orbital site to the b orbital site and

$$E_{b\sigma f_n}(R) = \int \phi_{b\sigma}^*(r-R) H_{CF}^b \phi_{f_n}(r) dv, \quad (B.3)$$

where $\phi_{f_n}(r)$, $n = 1$ or 2 , is the wavefunction of the crystal field orbital Γ_{n7} on a site at the origin and $\phi_{b\sigma}(r-R)$ is the product of a conduction band b orbital and spin function σ on a site at R. Therefore

$$\phi_{f_n}(r) = f_{i_n}^\dagger |V\rangle, \quad (\text{B.4})$$

where site i is at the origin. To evaluate the energy integrals $E_{b\sigma f_n}(R)$ we express the wavefunctions $\phi_{f_n}(r)$ as products of spherical harmonics and spin functions and use the Slater and Koster tables of f energy integrals (Takegahara et al (1980)). We use the mapping

$$f_{m_L \sigma}^\dagger |V\rangle = Y_{3m_L} |\sigma\rangle, \quad (\text{B.5})$$

where Y_{3m_L} is the spherical harmonic of orbital angular momentum three and z component of orbital angular momentum m_L and $|\sigma\rangle$ is the spin function, to rewrite the Γ_7 doublet states of equations (5.2.43) and (5.2.44) as

$$\begin{aligned} \phi_{f_1}(r) = a & \left[C_{3\downarrow} Y_{33\beta} + C_{2\uparrow} Y_{32\alpha} \right] \\ & - b \left[C_{-2\uparrow} Y_{3-2\alpha} + C_{-1\downarrow} Y_{3-1\beta} \right], \end{aligned} \quad (\text{B.6})$$

and

$$\begin{aligned} \phi_{f_2}(r) = a & \left[C_{-3\uparrow} Y_{3-3\alpha} + C_{-2\downarrow} Y_{3-2\beta} \right] \\ & - b \left[C_{-2\downarrow} Y_{32\beta} + C_{2\uparrow} Y_{31\alpha} \right], \end{aligned} \quad (\text{B.7})$$

where $C_{m_L \sigma}$ are the Clebsch Gordan coefficients, α and β are the up and down spin functions respectively and a and b are coefficients which depend on the crystal field of the system (see equations 5.2.43 and 5.2.44). When we substitute equation (B.6) and (B.7) into equation (B.3) and remember that the energy integrals and hence the hybridisation is only non zero between states of the same spin we find:

$$E_{b_{\uparrow f_1}}(R) = \frac{1}{\sqrt{7}} \left[-a E_{b_{Y_{32}}}(R) + b\sqrt{5} E_{b_{Y_{3-2}}}(R) \right], \quad (B.8)$$

$$E_{b_{\downarrow f_1}}(R) = \frac{1}{\sqrt{7}} \left[a\sqrt{6} E_{b_{Y_{33}}}(R) - b\sqrt{2} E_{b_{Y_{3-1}}}(R) \right], \quad (B.9)$$

$$E_{b_{\uparrow f_2}}(R) = \frac{1}{\sqrt{7}} \left[-a\sqrt{6} E_{b_{Y_{3-3}}}(R) + b\sqrt{2} E_{b_{Y_{31}}}(R) \right], \quad (B.10)$$

$$E_{b_{\downarrow f_2}}(R) = \frac{1}{\sqrt{7}} \left[a E_{b_{Y_{3-2}}}(R) - b\sqrt{5} E_{b_{Y_{32}}}(R) \right], \quad (B.11)$$

where we have inserted the relevant Clebsch Gordan coefficients and

$$E_{b_{Y_{3m_L}}}(R) = \int \phi_b^*(r-R) H_{CF}^b \phi_{f_{m_L}}(r) d\nu, \quad (B.12)$$

In equation (B.12) $\phi_{f_{m_L}}(r)$ is an f orbital with z component of angular momentum m_L on the f electron site at the origin and $\phi_b(r-R)$ is a conduction electron b orbital function on the site at R .

In order to use the Slater and Koster tables of f energy integrals (Takegahara et al (1980)) we must express the spherical harmonics in terms of the cartesian coordinate functions xyz , $x(5x^2 - 3r^2)$ and $x(y^2 - z^2)$. So that

$$Y_{3\pm 1} = C_f \left[\mp \frac{1}{2} \sqrt{3} (5z^2 - r^2)(x \pm iy) \right], \quad (B.13)$$

$$Y_{3\pm 2} = C_f \left[\sqrt{15/2} (x \pm iy)^2 z \right], \quad (B.14)$$

$$Y_{3\pm 3} = C_f \left[\mp \frac{1}{2} \sqrt{5} (x \pm iy)^3 \right], \quad (B.15)$$

(Lendi (1980)) and in terms of the functions xyz , $x(5x^2 - 3r^2)$, $x(y^2 - z^2)$ and all those new functions achieved by cyclic permutation of x , y and z ,

$$Y_{3\pm 1} = \pm \frac{C_f}{4} \left[\begin{aligned} &\sqrt{3} (x(5x^2 - 3r^2) \pm iy(5y^2 - 3r^2)) \\ &+ \sqrt{5} (\sqrt{15}x(y^2 - z^2) \mp i\sqrt{15}y(z^2 - x^2)) \end{aligned} \right],$$

(B.16)

$$Y_{3\pm 2} = \frac{C_f}{\sqrt{2}} \left[\sqrt{15}z(x^2 - y^2) \pm i2\sqrt{15}xyz \right], \quad (\text{B.17})$$

$$Y_{3\pm 3} = \mp \frac{C_f}{4} \left[\sqrt{5} (x(5x^2 - 3r^2) \mp iy(5y^2 - 3r^2)) \right. \\ \left. - \sqrt{3} (\sqrt{15}x(y^2 - z^2) \pm i\sqrt{15}y(z^2 - x^2)) \right]. \quad (\text{B.18})$$

When we substitute equations (B.16) to (B.18) into equation (B.12) we find:

$$E_{bY_{3\pm 1}}(R) = \pm \frac{1}{4} \left[\sqrt{3} (E_{b x(5x^2 - 3r^2)}(R) \pm i E_{b y(5y^2 - 3r^2)}(R)) \right. \\ \left. + \sqrt{5} (E_{b x(y^2 - z^2)}(R) \mp i E_{b y(z^2 - x^2)}(R)) \right], \quad (\text{B.19})$$

$$E_{bY_{3\pm 2}}(R) = \frac{1}{\sqrt{2}} \left[E_{b z(x^2 - y^2)}(R) \pm i E_{b xyz}(R) \right], \quad (\text{B.20})$$

$$E_{bY_{3\pm 3}}(R) = \mp \frac{1}{4} \left[\sqrt{5} (E_{b x(5x^2 - 3r^2)}(R) \mp i E_{b y(5y^2 - 3r^2)}(R)) \right. \\ \left. + \sqrt{3} (E_{b x(y^2 - z^2)}(R) \pm i E_{b y(z^2 - x^2)}(R)) \right], \quad (\text{B.21})$$

so that in general

$$E_{bY_{3,1}}(R) = - E_{bY_{3,-1}}^*(R), \quad (\text{B.22})$$

$$E_{bY_{3,2}}(R) = E_{bY_{3,-2}}^*(R), \quad (\text{B.23})$$

$$E_{bY_{3,3}}(R) = - E_{bY_{3,-3}}^*(R). \quad (\text{B.24})$$

Also when equations (B.22) to (B.24) are used in equations (B.8) to (B.11) we find that for the case of a Γ_7 band hybridising with a single conduction band that:

$$E_{b\uparrow f_1}(R) = - E_{b\downarrow f_2}^*(R), \quad (\text{B.25})$$

$$E_{b\downarrow f_1}(R) = E_{b\uparrow f_2}^*(R). \quad (\text{B.26})$$

The relationships between the f energy integrals in equations (B.25) and (B.26) are true for the case of a Γ_7 band hybridization with any type of conduction band. The actual values of the energy integrals $E_{b\sigma f_n}(R)$ depend on the type of conduction band and the type of lattice in the system.

For an s conduction band (Takegahara et al (1980))

$$E_{sY_3\pm_1}(R) = \pm \frac{1}{4} \left[\sqrt{3} \left(\frac{1}{2}l(5l^2 - 3) \pm \frac{i}{2}m(5m^2 - 3) \right) + \sqrt{5} \left(\frac{\sqrt{15}}{2}l(m^2 - n^2) \mp i \frac{\sqrt{15}}{2}m(n^2 - l^2) \right) \right] (sf\sigma), \quad (\text{B.27})$$

$$E_{sY_3\pm_2}(R) = \frac{1}{\sqrt{2}} \left[\frac{\sqrt{15}}{2}n(l^2 - m^2) \pm i\sqrt{15}lmn \right] (sf\sigma), \quad (\text{B.28})$$

$$E_{sY_3\pm_3}(R) = \mp \frac{1}{4} \left[\sqrt{3} \left(\frac{1}{2}l(5l^2 - 3) \mp \frac{i}{2}m(5m^2 - 3) \right) - \sqrt{3} \left(\frac{\sqrt{15}}{2}l(m^2 - n^2) \pm i \frac{\sqrt{15}}{2}m(n^2 - l^2) \right) \right] (sf\sigma), \quad (\text{B.29})$$

where (l, m, n) are the direction cosines of the vector R . It is seen that each of the functions $E_{sY_3\pm_l}(R)$ of equations (B.27) to (B.29) is an odd function of R :

$$E_{sY_3\pm_l}(-R) = - E_{sY_3\pm_l}(R), \quad (\text{B.30})$$

and on substituting equation (B.30) into equation (B.8) to (B.11)

with $b = s$ for this s conduction band it is found that

$$E_{s\sigma f_n}(-R) = -E_{s\sigma f_n}(R). \quad (\text{B.31})$$

Also from equation (B.2)

$$V_{\uparrow_1}^{sf}(k) = \sum_{\substack{R \\ (f \text{ to } s)}} e^{ik \cdot R} E_{s\uparrow_{f_1}}(R) \quad (\text{B.32})$$

so that using equation (B.25)

$$\begin{aligned} V_{\uparrow_1}^{sf}(k) &= - \sum_{\substack{R \\ (f \text{ to } s)}} e^{ik \cdot R} E_{s\downarrow_{f_2}}^*(R) \\ &= - \left[\sum_{\substack{R \\ (f \text{ to } s)}} e^{-ik \cdot R} E_{s\downarrow_{f_2}}(R) \right]^* \\ &= - \left[\sum_{\substack{R \\ (f \text{ to } s)}} e^{ik \cdot R} E_{s\downarrow_{f_2}}(-R) \right]^*, \end{aligned} \quad (\text{B.33})$$

and provided the lattice has inversion symmetry we can use equation (B.31) to show that

$$- \left[\sum_{\substack{R \\ (f \text{ to } s)}} e^{ik \cdot R} E_{s\downarrow_{f_2}}(-R) \right]^* = V_{\downarrow_2}^{sf*}(k). \quad (\text{B.34})$$

Therefore when a Γ_7 doublet state, labelled by $n = 1$ or 2 , hybridises with a spin σ , s conduction state in a lattice with inversion symmetry then

$$V_{\uparrow_1}^{sf}(k) = V_{\downarrow_2}^{sf*}(k), \quad (\text{B.35})$$

and similarly

$$V_{\downarrow_1}^{sf}(k) = -V_{\uparrow_2}^{sf*}(k). \quad (\text{B.36})$$

Similar relations exist between the hybridisation of a Γ_7 doublet band and a p_x conduction band. The f energy integrals for this p_x conduction band are (Takegahara et al (1980)):

$$E_{p_x \text{ } xyz} (R) = \sqrt{15} l^2 mn (pf\sigma) - \frac{\sqrt{5}}{\sqrt{2}} (3l^2 - 1) mn (pf\pi), \quad (B.37)$$

$$E_{p_x \text{ } x(5x^2 - 3r^2)} (R) = \frac{1}{2} l^2 (5l^2 - 3) (pf\sigma) - \frac{\sqrt{3}}{\sqrt{8}} (5l^2 - 1) (l^2 - 1) (pf\pi) \quad (B.38)$$

$$E_{p_x \text{ } x(y^2 - z^2)} (R) = \frac{1}{2} \sqrt{15} l^2 (m^2 - n^2) (pf\sigma) - \frac{\sqrt{5}}{\sqrt{8}} (3l^2 - 1) (m^2 - n^2) (pf\pi). \quad (B.39)$$

where (l, m, n) are the direction cosines of R. All the other energy integrals which appear in equations (B.19) with $b = p_x$ to (B.21) can be obtained by cyclically permuting x, y, z and l, m, n of equations (B.37) to (B.39). We can easily see that each of these energy integrals is an even function of R so that:

$$E_{p_x \text{ } yz \text{ } x} (R) = E_{p_x \text{ } yz \text{ } x} (-R), \quad (B.40)$$

and on substituting equation (B.40) in equations (B.8) to (B.11) with $b = p_x$ for this p_x conduction band, then

$$E_{p_x \text{ } \sigma f \text{ } n} (-R) = E_{p_x \text{ } \sigma f \text{ } n} (R). \quad (B.41)$$

Therefore when the steps used to get from equation (B.32) to (B.35) are repeated it is found that in a lattice with inversion symmetry the hybridisations between the band of Γ_7 doublets and a p_x conduction band in a lattice with inversion symmetry satisfy:

$$V_{\uparrow 1}^{p \times f} (k) = - V_{\downarrow 2}^{p \times f^*} (k), \quad (B.42)$$

$$V_{\downarrow 1}^{p \times f} (k) = V_{\uparrow 2}^{p \times f^*} (k). \quad (B.43)$$

APPENDIX C.

In the main text it is shown that the hamiltonian $H_{CF}^{sp^x}$ of equation (5.3.25) can describe magnetic anistropy provided

$$V_{\sigma}^{sp^x}(k) \neq 0, \quad (C.1)$$

and

$$\left(\sum_{\sigma} (\sigma) V_{-\sigma_1}^{sf}(k) V_{\sigma_2}^{p^x f}(k) + c.c \right) \neq 0, \quad (C.2)$$

or

$$\sum_{\sigma} V_{\sigma_1}^{sf^*}(k) V_{\sigma_2}^{p^x f}(k) \neq 0 \quad (C.3)$$

where

$$V_{\sigma_n}^{sf}(k) = \sum_R e^{ik \cdot R} E_{s\sigma f_n}(R), \quad (C.4)$$

(f to s)

and R is the vector form the f orbital site at the origin to the s orbital sites. Also

$$V_{\sigma_n}^{p^x f}(k) = \sum_R e^{ik \cdot R} E_{p^x \sigma f_n}(R), \quad (C.5)$$

(f to p_x)

where R is the vector from the f orbital at the origin to the p_x orbital sites and

$$V^{sp^x}(k) = \sum_R e^{ik \cdot R} E_{s p^x}(R), \quad (C.6)$$

(s to p_x)

where R is now the vector from a particular s orbital site to all p orbital sites. The energy integrals $E_{s\sigma f_n}(R)$ and $E_{p^x \sigma f_n}(R)$ are given in equations (B.8) to (B.11) with b = s or p_x and

$$E_{\text{sp}^x}(\mathbf{R}) = \int \phi_s^*(\mathbf{r}) H_{\text{CF}}^{\text{sp}^x} \phi_{p_x}(\mathbf{r}-\mathbf{R}) d\nu. \quad (\text{C.7})$$

where \mathbf{R} is again the vector connecting the site on which the s orbital, $\phi_s(\mathbf{r})$, is located and the site on which the p_x orbital, $\phi_{p_x}(\mathbf{r})$, is located. From the tables of tight binding energy integrals (Slater and Koster (1954)) we find:

$$V^{\text{sp}^x}(\mathbf{k}) = \sum_{\mathbf{R}} e^{i\mathbf{k}\cdot\mathbf{R}} (sp\sigma)l, \quad (\text{C.8})$$

(s to p_x)

where (l, m, n) are the direction cosines of the vector \mathbf{R} which locates the positions of all p_x orbital sites relative to a single s orbital site.

In the following the functions $V_{\sigma_n}^{\text{sf}}(\mathbf{k})$, $V_{\sigma_n}^{\text{p}^x\text{f}}(\mathbf{k})$ and $V^{\text{sp}^x}(\mathbf{k})$ are evaluated within the nearest neighbour approximation for a bcc and tetragonal lattice. The conditions for magnetic anisotropy are shown to be satisfied for both cases.

A Model Tetragonal Lattice.

In CeSi_x the f orbitals are located on the cerium atoms while the conduction s and p_x orbitals are located on the silicon atoms. The nearest neighbours of any cerium atom are shown in Figure C.1 for a simplified CeSi_x structure.

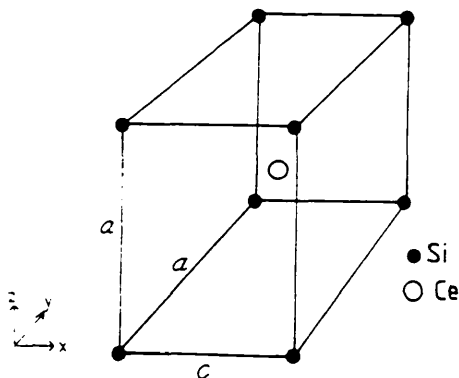


Figure C.1. The nearest neighbour silicon atoms of a cerium atom in a model tetragonal lattice.

The z direction is taken along one of the a axis since the moment is quantised in the z direction and is known from experiment to lie

along an a axis in CeSi_x .

To evaluate equations (C.4) and (C.5) for $V_{\sigma_n}^{sf}(k)$ and $V_{\sigma_n}^{p \times f}(k)$ in the nearest neighbour approximation we sum over the vectors $\{ R \}$ where

$$\{ R \} = \left\{ \left(\pm \frac{c}{2}, \pm \frac{a}{2}, \pm \frac{a}{2} \right) \right\}, \quad (\text{C.9})$$

locate the eight nearest neighbour silicon atoms. The vectors $\{ R \}$ have direction cosines $\{ (l, m, n) \}$, where

$$\{ R \} = \{ |R|(l, m, n) \}, \quad (\text{C.10})$$

so that for each of the eight vectors $\{ R \}$ locating the nearest neighbour sites the direction cosines satisfy:

$$m^2 = n^2 = \frac{1}{2}(1-l^2). \quad (\text{C.11})$$

When we use equation (C.11) in equations (B.8) to (B.11) for $E_{s\sigma f n}(R)$ and $E_{p \times \sigma f n}(R)$ we find that for a tetragonal lattice:

$$E_{s \uparrow f_1}(R) = - \frac{\sqrt{15}}{2 \sqrt{14}} (sf\sigma) n \left[(a - \sqrt{5}b) \left(\frac{3}{2} l^2 - \frac{1}{2} \right) + i2(a + \sqrt{5}b)lm \right], \quad (\text{C.12})$$

$$E_{s \downarrow f_1}(R) = \frac{\sqrt{6}}{8 \sqrt{7}} (sf\sigma) \left\{ (b - \sqrt{5}a)(5l^2 - 3)l + im \left[a\sqrt{5}(1 - 7l^2) - b(-3 + 5l^2) \right] \right\}. \quad (\text{C.13})$$

and from equations (B.25) and (B.26)

$$E_{s \uparrow f_2}(R) = E_{s \downarrow f_1}^*(R), \quad (\text{C.14})$$

$$E_{s \downarrow f_2}(R) = -E_{s \uparrow f_1}^*(R), \quad (C. 15)$$

Also

$$E_{p \times \uparrow f_1}(R) = \frac{\sqrt{15}}{2} \left\{ \begin{aligned} &(-a + b\sqrt{5}^-) \ln \times \\ &\left[\frac{\sqrt{15}}{2} \left(\frac{3}{2} l^2 - \frac{1}{2} \right) (pf\sigma) - \frac{\sqrt{5}^-}{\sqrt{8}} \left(\frac{9}{2} l^2 - \frac{7}{2} \right) (pf\pi) \right] \\ &- i (a + b\sqrt{5}^-) mn \times \\ &\left[\sqrt{15} l^2 (pf\sigma) - \frac{\sqrt{5}^-}{\sqrt{2}} (3l^2 - 1) (pf\pi) \right] \end{aligned} \right\} \quad (C. 16)$$

$$E_{p \times \downarrow f_1}(R) = \frac{1}{4\sqrt{7}} \left\{ \begin{aligned} &(-a\sqrt{6}\sqrt{5}^- + b\sqrt{6}^-) \times \\ &\left[\frac{l^2}{2} (5l^2 - 3) (pf\sigma) - \frac{\sqrt{3}^-}{\sqrt{8}} (5l^2 - 1) (l^2 - 1) (pf\pi) \right] \\ &- i \left[\frac{1}{2} \left(-\frac{1}{2} - \frac{5}{2} l^2 \right) (pf\sigma) - \frac{\sqrt{3}^-}{\sqrt{8}} \left(\frac{3}{2} - \frac{5}{2} l^2 \right) (pf\pi) \right] lm \end{aligned} \right\} \\ + i (a\sqrt{6}\sqrt{3}^- + b\sqrt{2}\sqrt{15}^-) \ln \times \\ \left[\frac{\sqrt{15}}{2} \left(\frac{1}{2} - \frac{3}{2} l^2 \right) (pf\sigma) - \frac{\sqrt{5}^-}{\sqrt{8}} \left(3 \left(\frac{1}{2} - \frac{3}{2} l^2 \right) + 2 \right) (pf\pi) \right] \right\} \quad (C. 17)$$

and from equations (B.26) and (B.25)

$$E_{p \times \uparrow f_2}(R) = E_{p \times \downarrow f_1}^*(R), \quad (C. 18)$$

$$E_{p_x \downarrow f_2}(R) = -E_{p_x \uparrow f_1}^*(R), \quad (C.19)$$

When we substitute equations (C.12) and (C.13) into equation and (C.4) and sum over the eight nearest neighbours using the relation:

$$\sum_{\substack{(f \text{ to } s \\ \text{n.n. only})}} e^{ik \cdot R} = \sum_{l=1}^{|l|} \sum_{m=1}^{|m|} \sum_{n=1}^{|n|} e^{i|R|(k_x l + k_y m + k_z n)}, \quad (C.20)$$

where

$$|l| = \frac{c/2}{|R|}, \quad |m| = \frac{a/2}{|R|}, \quad |n| = \frac{a/2}{|R|}. \quad (C.21)$$

we find that, in a tetragonal lattice

$$V_{\uparrow 1}^{sf}(k) = -4 \frac{\sqrt{15}}{\sqrt{14}} (sf\sigma) |n|$$

$$\left[i(a - \sqrt{5}b) \left(\frac{3}{2} l^2 - \frac{1}{2} \right) \cos(kx \frac{c}{2}) \cos(ky \frac{a}{2}) \cos(kz \frac{a}{2}) \right. \\ \left. + 2(a + \sqrt{5}b) |l| |m| |n| \sin(kx \frac{c}{2}) \sin(ky \frac{a}{2}) \sin(kz \frac{a}{2}) \right] \quad (C.22)$$

$$V_{\downarrow 1}^{sf}(k) = \frac{\sqrt{6}}{\sqrt{7}} (sf\sigma) \left\{ \begin{aligned} & i(b - \sqrt{5}a)(5l^2 - 3) |l| \sin(kx \frac{c}{2}) \cos(ky \frac{a}{2}) \cos(kz \frac{a}{2}) \\ & - |m| \left[a\sqrt{5} (1 - 7l^2) - b(-3 + 5l^2) \right] \cos(kx \frac{c}{2}) \sin(ky \frac{a}{2}) \cos(kz \frac{a}{2}) \end{aligned} \right\}. \quad (C.23)$$

$$V_{2\uparrow}^{sf}(k) = -V_{1\downarrow}^{sf*}(k), \quad (C.24)$$

$$V_{2\downarrow}^{sf}(k) = V_{1\uparrow}^{sf*}(k), \quad (C.25)$$

Similarly when we use equation (C.16) and (C.17) in equation (C.5) we find that in a tetragonal lattice:

$$V_{1\uparrow}^{p \times f}(k) = 4\sqrt{15} \left\{ \begin{aligned} & - (-a + b\sqrt{5}) \left[\frac{\sqrt{15}}{2} \left(\frac{3}{2} l^2 - \frac{1}{2} \right) (pf\sigma) - \frac{\sqrt{5}}{\sqrt{8}} \left(\frac{9}{2} l^2 - \frac{7}{2} \right) (pf\pi) \right] \\ & \quad |l||n| \sin(kx_{\frac{c}{2}}) \cos(ky_{\frac{a}{2}}) \sin(kz_{\frac{a}{2}}) \\ & \\ & i(a+b\sqrt{5}) \left[\sqrt{15} l^2 (pf\sigma) - \frac{\sqrt{5}}{\sqrt{2}} (3l^2 - 1) (pf\pi) \right] \\ & \quad |m||n| \cos(kx_{\frac{c}{2}}) \sin(ky_{\frac{a}{2}}) \sin(kz_{\frac{a}{2}}) \end{aligned} \right\} \quad (C.26)$$

$$\begin{aligned}
V_{1\downarrow}^{sp^*}(k) = & \frac{2}{\sqrt{7}} \left\{ (-a\sqrt{6}\sqrt{5} + b\sqrt{6}) \times \left[\right. \right. \\
& \left. \left. \left[\frac{I^2}{2} (5I^2 - 3)(pf\sigma) - \frac{\sqrt{3}}{\sqrt{8}} (5I^2 - 1)(I^2 - 1)(pf\pi) \right] \times \right. \right. \\
& \left. \left. \cos(kx\frac{c}{2}) \cos(ky\frac{a}{2}) \cos(kz\frac{a}{2}) \right. \right. \\
& + i \left[\frac{1}{2} \left(-\frac{1}{2} - \frac{5}{2} I^2 \right) (pf\sigma) - \frac{\sqrt{3}}{\sqrt{8}} \left(\frac{3}{2} - \frac{5}{2} I^2 \right) (pf\pi) \right] |l||m| \\
& \left. \left. \left. \sin(kx\frac{c}{2}) \sin(ky\frac{a}{2}) \cos(kz\frac{a}{2}) \right] \right. \right. \\
& - i (a\sqrt{6}\sqrt{3} + b\sqrt{2}\sqrt{15}) |l||n| \times \\
& \left. \left. \left. \left[\frac{\sqrt{15}}{2} \left(\frac{1}{2} - \frac{3}{2} I^2 \right) (pf\sigma) - \frac{\sqrt{5}}{\sqrt{8}} \left(3 \left(\frac{1}{2} - \frac{3}{2} I^2 \right) + 2 \right) (pf\pi) \right] \right. \right. \right. \\
& \left. \left. \left. \sin(kx\frac{c}{2}) \cos(ky\frac{a}{2}) \sin(kz\frac{a}{2}) \right] \right. \right. \left. \right\}, \tag{C.27}
\end{aligned}$$

$$V_{2\uparrow}^{p^*f}(k) = V_{1\downarrow}^{p^*f^*}(k), \tag{C.28}$$

$$V_{2\downarrow}^{p^*f}(k) = -V_{1\uparrow}^{p^*f^*}(k), \tag{C.29}$$

To investigate the criteria for magnetic anisotropy we consider the particular case of a body centred cubic lattice where the hybridisation expressions are simpler.

The Body Centred Cubic Lattice.

For the particular case of a body centred cubic lattice the relations of the previous section are simplified by the fact that $a = c$ so that the direction cosines of the eight nearest neighbour silicon atoms of a cerium atom are:

$$\{ (l, m, n) \} = \left\{ \frac{1}{\sqrt{3}} (\pm 1, \pm 1, \pm 1) \right\}. \quad (\text{C.30})$$

The hybridisations $V_{\sigma_n}^{sf}(k)$ and $V_{\sigma_n}^{p*sf}(k)$ for a bcc lattice are obtained from equations (C.22) to (C.25) and (C.26) to (C.29) respectively by substituting $l^2 = 1/3$. Also we use the values of a and b for a cubic lattice (Sato et al (Preprint)):

$$a = \frac{1}{\sqrt{6}} \quad \text{and} \quad b = \frac{\sqrt{5}}{\sqrt{6}}, \quad (\text{C.31})$$

to show that in a bcc lattice

$$V_{\uparrow 1}^{sf}(k) = -48 \frac{\sqrt{15}}{\sqrt{64}} (sf\sigma) |l|^2 \sin(kx_{\frac{a}{2}}) \sin(ky_{\frac{a}{2}}) \sin(kz_{\frac{a}{2}}) \quad (\text{C.32})$$

$$V_{\downarrow 1}^{sf}(k) = 0 \quad (\text{C.33})$$

$$V_{\uparrow 2}^{sf}(k) = 0 \quad (\text{C.34})$$

$$V_{\downarrow 2}^{sf}(k) = V_{\uparrow 1}^{sf*}(k) \quad (\text{C.35})$$

and

$$V_{\uparrow 1}^{p*sf}(k) = 4\sqrt{15} \left[-\frac{\sqrt{5}}{\sqrt{6}\sqrt{8}} 8 (pf\sigma) |l|^2 \sin(kx_{\frac{a}{2}}) \cos(ky_{\frac{a}{2}}) \sin(kz_{\frac{a}{2}}) + i \frac{8\sqrt{15}}{\sqrt{6}} (pf\sigma) |l|^2 \cos(kx_{\frac{a}{2}}) \sin(ky_{\frac{a}{2}}) \sin(kz_{\frac{a}{2}}) \right]. \quad (\text{C.36})$$

$$V_{\downarrow 1}^{p*sf}(k) = i4 \frac{\sqrt{5}}{\sqrt{56}} |l|^2 (\sqrt{3} + \sqrt{5}) (pf\pi) \sin(kx_{\frac{a}{2}}) \cos(ky_{\frac{a}{2}}) \sin(kz_{\frac{a}{2}}) \quad (\text{C.37})$$

$$V_{\uparrow 2}^{p*sf}(k) = V_{\downarrow 1}^{p*sf*}(k), \quad (\text{C.38})$$

$$V_{2\downarrow}^{p \times f}(k) = - V_{1\uparrow}^{p \times f^*}(k). \quad (C.39)$$

Also to calculate $V^{sp \times}(k)$ from equation (C.8) we sum over the nearest neighbour silicon atoms of a silicon atom to find

$$V^{sp \times}(k) = i 2 a \sin(k_x a)(sp\sigma), \quad (C.40)$$

therefore the first of the criteria for magnetic anisotropy, that is $V^{sp \times}(k) \neq 0$ (see equation (C.1)) is satisfied. Also when we use equations (C.33) and (C.34) in equations (C.2) and (C.3), which give the second of the criteria for magnetic anisotropy, we find that in this bcc lattice the second criterion becomes:

$$V_{\uparrow 1}^{sf}(k)V_{\downarrow 2}^{p \times f}(k) + V_{\uparrow 1}^{sf^*}(k)V_{\downarrow 2}^{p \times f^*}(k) \neq 0, \quad (C.41)$$

(from equation (C.2)) or

$$V_{\uparrow 1}^{sf^*}(k)V_{\uparrow 2}^{p \times f}(k) \neq 0, \quad (C.42)$$

(from equation (C.3)). Also in a bcc lattice

$$V_{\uparrow 1}^{sf}(k) = V_{\uparrow 1}^{sf^*}(k) \neq 0, \quad (C.43)$$

(see equation (C.32)) so that the criterion for magnetic anisotropy of equation (C.41) becomes

$$V_{\downarrow 2}^{p \times f}(k) \neq - V_{\downarrow 2}^{p \times f^*}(k) \neq 0, \quad (C.44)$$

which from equation (C.39) is obviously satisfied. Finally from equations (C.32) and (C.38) we see that the criterion for magnetic anisotropy of equation (C.42) is also satisfied.

REFERENCES.

P.W. Anderson, Phys. Rev. **124**, 41 (1961).

N. Andrei, Phys. Rev. Lett. **45**, 379 (1980).

N. Andrei, K. Furuya and J.H. Lowenstein, Rev. Mod. Phys. **55**, 331 (1983).

K. Andres, J.E. Graebner and H.R. Ott, Phys. Rev. Lett. **35**, 1779 (1975).

A. Benoit, A. Berton, J. Chaussey, J. Flouquet, J.C. Lasjaunias, J. Odin, J. Palleau, J. Peynard and M. Ribault, in Valence Fluctuations in Solids edited by L.M. Falicov, W. Hanke and M.B. Maple, 283 (1981).

A. Berton, T. Chaussey, G. Chouteau, B. Cornut, J. Peynard and R. Tournier, in Valence Instabilities and Related Narrow-band Phenomena, edited by R.D. Parks 471 (1977).

W.F. Brinkman and S. Engelsberg, Phys. Rev. **169**, 417 (1968).

W.F. Brinkman and T.M. Rice, Phys. Rev. B. **2**, 4302 (1970).

P. Coleman, Phys. Rev. B **29**, 3035 (1984).

P. Coleman, Phys. Rev. B **28**, 5255 (1983).

B.R. Cooper, R. Siemann, D. Yang, P. Thayambali and A. Banerjea, Handbook on the Physics and Chemistry of the Actinides, edited by A.J. Freeman and G.H. Lander copyright Elsevier Science Publishers B.V. , 435 (1985).

B. Coqblin and J.R. Shrieffer, Phys. Rev. **185**, 847 (1969).

G. Czycholl, Phys. Rev. B 25, 3413 (1982).

G. Czycholl and H.J. Leder, Z. Phys. B. Condensed matter 44, 59 (1981).

G. Czycholl and H.J. Leder, Z. Phys. B. Condensed matter 48, 67 (1982).

S. Doniach, Physica 91B, 231 (1977).

S. Doniach and S. Engelsberg, Phys. Rev. Lett. 17, 750 (1966).

A.S. Edelstein, C.J. Tranchita, O.D. McMasters and R.A. Gschnerder, Solid State Commun. 15, 81 (1974).

D.M. Edwards, J. App. Phys. 39, 481 (1968).

D.M. Edwards, Theoretical and Experimental Aspects of Valence Fluctuations and Heavy Fermions, Plenum Publishing Corporation, 585 (1987).

D.M. Edwards and R. B. Muniz, J. Phys. F: Met Phys. 15, 2339 (1985).

Valence Fluctuations in Solids edited by L.M. Falicov, W.Hanke, M.B. Maple. North Holland Amsterdam (1981).

Z. Fisk, G.R. Stewart, J.O. Willis, H.R. Ott and F. Hulliger, Phys. Rev. B. 30, 6360 (1984)

P.H. Frings, J.J.M. Franse, F.R. de Boer and A. Menovsky, J. Magn. Mater. 31-34, 240 (1983).

G. Gunnarson and K. Schönhammer, Phys. Rev. B.28, 4315 (1983).

M.C. Gutzwiller, Phys. Rev. 137, A1726 (1965).

J.A. Hertz and D.M. Edwards, J. Phys. F: Metal Phys. 3, (1973)

- B. Horvatić and V. Zlatic, Solid State Commun. **541**, 957 (1985).
- B. Horvatić and V. Zlatic, Phys. Stat. Col. (b) **99**, 251 (1980).
- B. Horvatić and V. Zlatic, Pys. Stat. Sol. (b) **111**, 65 (1982).
- J. Hubbard, Proc. Roy. Soc. (London), **281**, 401 (1964).
- J. Hubbard, Proc. Roy. Soc. (London), **A276**, 238 (1963).
- B. Hulg, A. Furrer, J.K. Kjems and O. Vogt, Phys. Rev. Lett. **50**, 1085 (1983).
- T. Jarlborg, H.F. Braun and M. Peter, Z. Phys. B **52**, 295 (1983).
- Theory of Heavy Fermions and Valence Fluctuations, Springer Series in Solid State Science **62**. Editors T.Kasuya and T Sasa.
- N. Kawakami and A. Okiji, Phys. Rev. Lett. **86A** 483 (1981).
- D.D. Koelling, Solid State Commun. **43**, 247 (1982).
- M. Kohgi, F. Hippert, L.P. Reynault, J. Rossat-Mignod, B. Hennion, T. Satoh, F.L. Chui, T. Miura and H. Takei, Jap. J. App. Phys. **26**, suppl 26-3, 559 (1987).
- J. Kondo, Prog. Theo. Phys. **32**, 37 (1964).
- H.R. Krishnamurthy, J.W. Wilkins and K.G. Wilson, Phys. Rev. B **21**, 1003 (1980).
- H.R. Krishnamurthy, J.W. Wilkins and K.G. Wilson, Phys. Rev. B **21**, 1043 (1980).
- D.C. Langreth, Phys. Rev. **150**, 516 (1966).
- J.M. Lawrence, P.S. Riseborourgh and R.D. Parks, Rep. Prog. Phys.

44, 1 (1981).

H.J. Leder and G. Czycholl, Z. Physik B 35, 7 (1979)

P.A. Lee, T.M. Rice, J.W. Serene, L.J. Sham and J.W. Wilkins, Comm. Cond. Mat. Phys. 12, 99 (1986).

W. Lieke, U. Rauschwalbe, C.D. Bredl, F. Sleglich, J. Aarts and F.R. de Boer, J. Appl. Phys. 53, 2111 (1982).

J.M. Luttinger, Phys. Rev. 119, 1153 (1960).

W.C.M. Mattens, F.R. de Boer, A.P. Murani and G.H. Lander, J. Magn. Magn. Mater 15-18, 973 (1980).

V.V. Moshchalkov, O.V. Petrenko, and O.I. Babich and I. Ciric, Preprint.

D.M. Newns and A.C. Hewson, J. Phys. F. Metal Phys. 10, 2429 (1980).

P. Nozieres, J. Low Temp. Phys. 17, 31 (1974).

H.R. Ott, Ann. Rev. Mater. Sci. 17, 13 (1987).

H.R. Ott, H. Rudigier, P. Delsing and Z. Fisk, Phys. Rev. Lett. 52, 1551 (1984a).

H.R. Ott, H. Rudigier, Z. Fisk and J.L. Smith in Moment Formation in Solids edited by W.J.L. Buyers, p.305 (1984b).

H.R. Ott, H. Rudigier, Z. Fisk and J.L. Smith, Physica B. (1984c)

H.R. Ott, H. Rudigier, Z. Fisk and J.L. Smith, Phys. Rev. Lett. 50, 1595 (1983).

N. Read and D.M. Newns, J. Phys. C 16, 3273 (1983).

N. Read, D.M. Newns, and S. Doniach, Phys. Rev. B. 30, 3841 (1984).

- N. Read and D.M. Newns, Solid State Commun. 52, 993 (1984).
- T.M. Rice and K.Ueda, Phys. Rev. Lett. 55, 995 (1985).
- B.C. Sales and R. Viswanathan, J. Low Temp. Phys. 23, 449 (1976)
- N. Sato, H. Mori, T. Satoh, T. Taira and H. Takei (preprint).
- N. Sato, M. Sera, K. Torizuka, M. Kohgi, A. Sawada, and T. Satoh
Jap. J. App. Phys. 26 suppl. 26-3, 557 (1987).
- J.R. Schrieffer and P.A. Wolff, Phys. Rev. 149, 491 (1966).
- S. Seki, Prog. Theo Phys. 63, 759 (1980).
- J.C. Slater and G.F. Koster, Phys. Rev. 94, 1498 (1954).
- J.L. Smith and Z. Fisk, J. Appl. Phys. 53, 7783 (1982).
- F. Steglich, J. Aarts, C.D. Bredl, W. Lieke, D. Meschede, W. Franz
and J. Schafer, Phys. Rev. Lett. 43, 1892 (1979).
- G.R. Stewart. Rev. Mod. Phys. 56, 755 (1984a).
- G.R. Stewart, Z. Fisk and J.O. Willis, Phys. Rev. B. 28, 172 (1983).
- G.R. Stewart, Z. Fisk, J.L. Smith, H.R. Ott and F.M. Mueller,
presented at the 17th International Conference on Low Temperature
Physics, University of Karlsruhe (1984b)
- G.R. Stewart, Z. Fisk, J.L. Smith, J.O. Willis and M.S. Wire, Phys.
Rev. B. 30, 1249 (1984c).
- G.R. Stewart, Z. Fisk and M.S. Wire, Phys. Rev. B. 30, 482 (1984d)
- G.R. Stewart, Z. Fisk, J.O. Willis and J.L. Smith, Phys Rev. Lett.
52, 679 (1984e).

K. Takegahara, Y. Aoki and A. Yunuse, J. Phys. C: Solid St. Phys., **13**, 583 (1980).

K. Takegahara, H. Harima and T. Kasuya, J. Magn. Magn. Mat. **47 & 48**, 263 (1985).

P. Thayamballi and B.R. Cooper, Phys. Rev. B. **31**, 5911 (1985).

R.J. Trainor, M.B. Brodsky and H.V. Culbert, Phys. Rev. Lett. **34**, 1019 (1975).

R. Troc, N. Trzebiatowski and K. Piprek, Bull. Acad. Pol. Ser. Chim. **19**, 427 (1971).

A.M. Tselick and P.B. Wiegmann, Phys. Lett. A (Netherlands) **89A**, 368 (1982).

A.M. Tselick and P.B. Wiegmann, Adv. Phys. **32**, 453 (1983).

D. Vollhart, Rev. Mod. Phys. **56**, 99 (1984).

K. Yamada, Prog Theo. Phys. (Kyoto) **54**, 316 (1975b).

K. Yamada, Prog. Theo. Phys. (Kyoto) **55**, 1345 (1976).

K. Yamada, Prog Theo. Phys. **53**, 970 (1985).

K. Yosida and K. Yamada, Supp. Prog. Theo. Phys. **46**, 244 (1970).

K. Yosida and K. Yamada, Prog. Theo. Phys. **53**, 1286 (1975).

H. Yu and H.C. Ku, Jap. J. App. Phys. **26**, Supplement 26-3 (1987).

V. Zlatic', B. Horvatic', and D. Šokčević', Z. Physik B. Condensed matter **59**, 151 (1985).

V. Zlatic' and B. Horvatic', Phys. Rev. B **28**, 6904 (1983).